ÉCOLE CENTRALE LYON

THÈSE
Présentée devant:
ÉCOLE CENTRALE DE LYON
Pour obtenir le grade de:

DOCTEUR

De l'école doctorale :

Électronique, électrotechnique, automatique

UNIVERSITÉ DE LYON

Spécialité : Ingénierie Du Vivant

Par

Christoph Keuschnig

Implication des champignons et des bactéries dans le cycle de l'azote et la production de N_2O dans le sol

soutenue le 6 Décembre 2016 devant le jury composé de:

Pr. Leif Klemedtsson: Professeur, Département des Sciences de la Terre – Université de Göteborg – Göteborg (SUÈDE)	Examinateur
Pr. Sophie Zechmeister-Boltenstern: Professeur, Département des Sciences du Sol - Université des Ressources Naturelles et des Sciences de la Vie – Vienne (AUTRICHE)	Examinateur
Dr. Télesphore Sime-Ngando: Directeur de Recherche, Laboratoire Microorganismes : Génome et Environnement – Université Blaise Pascal – Clermont-Ferrand (FRANCE)	Examinateur
Pr. Timothy M. Vogel: Professeur, Groupe Génomique Microbienne Environnementale – Université Claude Bernard Lyon 1 – Lyon (FRANCE)	Examinateur
Pr. Wietse de Boer: Professeur, Département de la Qualité des Sols – Université de Wageningen – Wageningen (PAYS-BAS)	Rapporteur
Dr. Kirsten S. Hofmockel: Chercheur, Laboratoire des Sciences Moléculaires Environnementales, Pacific Northwest National Laboratory (USA)	Rapporteur
Dr. Pascal Simonet: Directeur de Recherche, Groupe Génomique Microbienne Environnementale - Ecole Centrale de Lyon - Lyon (FRANCE)	Directeur de thèse
Dr. Catherine Larose: Chargée de Recherche, Groupe Génomique Microbienne Environnementale – Ecole Centrale de Lyon – Lyon (FRANCE)	Co-directrice de thèse

N° d'ordre NNT : 2016LYSEC5

Résumé

L'objectif principal de cette thèse est de déterminer le rôle des communautés microbiennes dans les émissions de N_2O du sol, et plus précisément de définir dans quelle mesure les champignons sont impliqués. Par conséquent, leur structure communautaire à l'échelle micro, leur comportement dans la réduction de l'azote et la production de N_2O, et leur interaction avec les communautés microbiennes impliquées dans le cycle de l'azote en tant que décomposeurs de matière organique dans le sol ont été étudiés. L'analyse des fractions de sol du parc Rothamsted a montré que les communautés fongiques changent au sein de fractions isolées, contrairement aux communautés bactériennes. De plus, des potentiels de nitrification, de dénitrification et de réduction de N_2O ont été détectés dans toutes les fractions et se sont révélés liés à la chimie du carbone et de l'azote. Des expériences quantifiant la production de NO et N_2O à partir de nitrite sur 24 souches de champignons de culture pure ont montré que les espèces de *Fusarium* sont de véritables producteurs de N_2O parmi les champignons. Le suivit de NO a révélé que le milieu de nitrite est instable dans des conditions anoxiques et produit du NO abiotiquement, ce qui implique que des souches produisant du N_2O à de faibles taux détoxifient ce NO plutôt que de le respirer, comme précédemment supposé. L'absence d'un nirK - p450nor dans la plupart des champignons a étayé cette hypothèse. Les relations interspécifiques entre champignons et bactéries ont été étudiées après l'addition de matière organique. Différentes modifications organiques ont déclenché des réponses distinctes en termes d'activité bactérienne et fongique sein d'une même communauté de sol. Les signatures fonctionnelles identifiées dans cette étude corroborent notre hypothèse selon laquelle les champignons sont impliqués dans la production de N_2O en influençant les bactéries impliquées dans le cycle N par des processus de dégradation de glucides. Les résultats de cette thèse fournissent une base pour explorer les relations interspécifiques dans le cycle

biogéochimique de l’azote dans le sol et marque une étape vers l'intégration de tous les membres de la communauté dans la recherche sur les écosystèmes du sol.

Abstract

The main objective of this thesis is to determine the role of microbial communities in N_2O emissions from soil, and more specifically to define to what extent fungi are involved. Therefore, their community structure at the micro scale, their behavior in reducing nitrogen and producing N_2O, and their impact on nitrogen cycling communities as decomposers in soil were investigated. Analysis of soil fractions of unmanaged, pristine Rothamsted Park Grass soil showed that fungal communities change within isolated fractions in contrast to bacterial communities. Also, nitrifying, denitrifying and N_2O reducing potentials were detected in all fractions and found to be linked to carbon and nitrogen chemistry. Pure culture experiments on 24 fungal strains quantifying NO and N_2O production from nitrite showed that *Fusarium* species are true N_2O producers among fungi. Monitoring NO revealed that nitrite medium is unstable under anoxic conditions and produces NO abiotically, which implies that low N_2O producing strains are actually detoxifying this NO rather than respiring it, as previously assumed. The lack of a nirK - p450nor in most fungi supported this hypothesis. Interspecies relationships between fungi and bacteria were studied following community development after organic matter addition. Different organic amendments triggered distinct responses of a soil community with respect to bacterial and fungal activity. Functional signatures identified in this study corroborated our hypothesis that fungi are involved in N_2O production by influencing a N-cycling bacterial community via carbohydrate degradation processes. The results from this thesis provide a basis for exploring interspecies relationships in nitrogen cycling processes in soil and mark a step towards integrating all members of the community in soil ecosystem research.

Table of contents

List of figures and tables

General introduction

Chapter 1

Chapter 2

Chapter 3

Introduction générale

Cycle biogéochimique et changements climatiques

La nutrition humaine est basée sur la production végétale. Les plantes fixent le carbone de l'atmosphère et prennent l'azote des sols pour former la biomasse (Zelitch, 1975; Krapp, 2015). Cela marque le flux d'entrée de carbone et d'azote dans notre réseau alimentaire. L'azote est un nutriment essentiel pour toutes les formes de vie. Il permet aux organismes de synthétiser des acides nucléiques, des acides aminés et par conséquent des protéines.

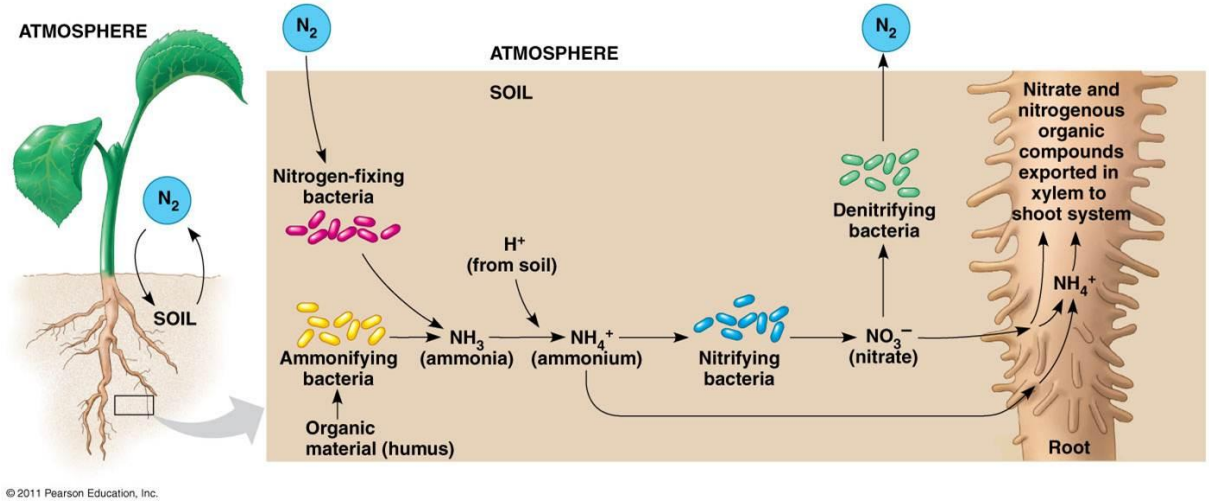

Figure 1: Vue macroscopique et microscopique des processus du cycle de l'azote dans le sol entraînant l'absorption d'azote par les plantes. Figure adaptée de Pearson Education Inc.

Les plantes, ainsi que la plupart des organismes, ne peuvent pas utiliser directement les fortes concentrations de gaz nitrique (N_2) présents dans l'atmosphère. Ils reposent sur la disponibilité de nitrate (NO_3^-) ou d'ammonium (NH_4^+) dans les sols qui peuvent être absorbés par les racines de la plante et sont finalement incorporés dans la biomasse (Figure 1) (Loque and Wiren, 2004; O'Brien *et al.*, 2016). On trouve donc dans la littérature le terme «azote réactif» (N_r), qui désigne des formes oxydées ou réduites d'atomes d'azote (Galloway *et al.*, 2003). L'étape initiale de transformation de l'azote non réactif en des formes réactives nécessite la rupture de la triple liaison entre les deux atomes d'azote dans le gaz N_2. Cela se produit dans

la nature par deux processus: la foudre et la fixation biologique de l'azote (BNF) (Galloway *et al.*, 2003). L'utilisation de combustibles fossiles, les pratiques agricoles intenses et la fixation technique de l'azote atmosphérique pour produire de l'azote augmentent BNF.

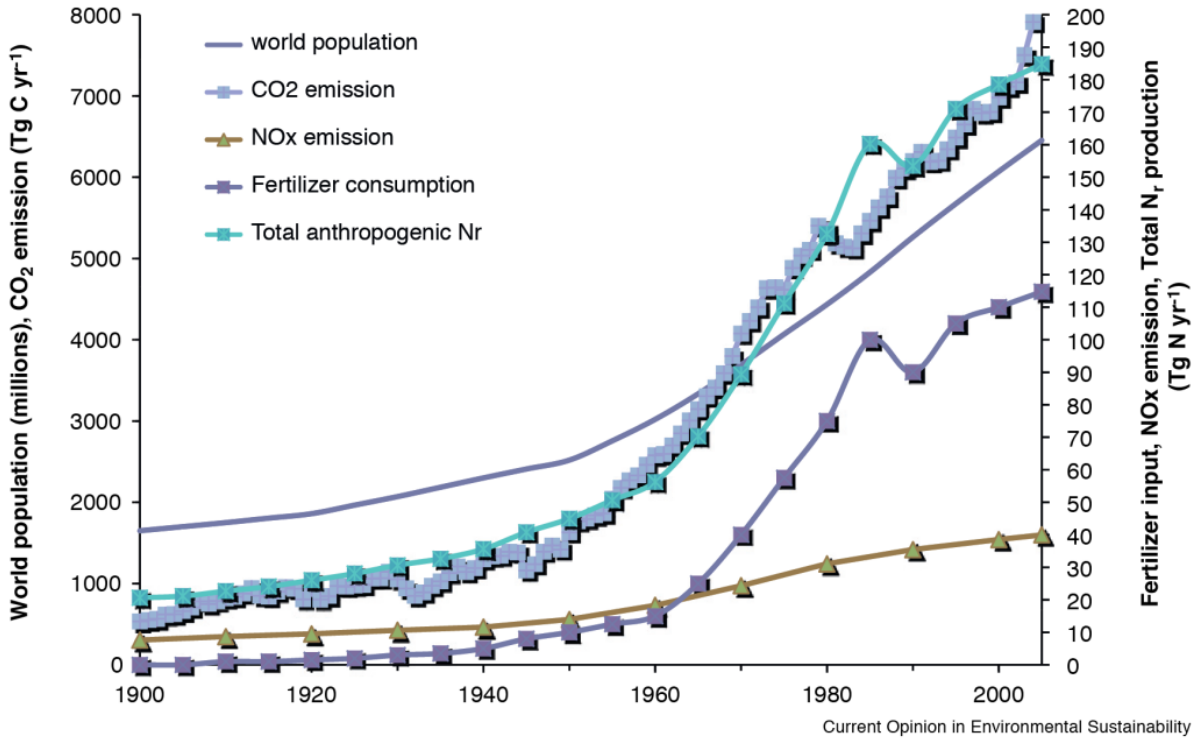

Figure 2: Développement de la population mondiale au cours du dernier siècle, consommation anthropique de N_r et engrais au cours des 110 dernières années. Figure adaptée de (Erisman *et al.*, 2011).

Les engrais sont des flux d'intrants pour le budget global de l'azote causés par des actions anthropiques. On estime que la quantité de N_r mondiale créée est passée de 241 Tg N an-1 en 1890 à 353 Tg N an-1 en 1990 (Galloway, 2003). La principale cause de cette augmentation spectaculaire réside dans une population en croissance rapide depuis le début du siècle dernier, ce qui a créé des demandes croissantes pour une production et des rendements plus élevés des systèmes agricoles (Figure 2) (Erisman *et al.*, 2011). Avec l'invention du procédé de Haber-Bosch au début du 20ème siècle, il fut possible de synthétiser NH_4^+ artificiellement par la réduction du gaz nitrique (N_2) de l'atmosphère par l'hydrogène pour former NH_4^+ (Haber and Le Rossignol, 1913). Ce procédé technique nécessite des pressions et températures élevées et une source d'hydrogène, qui est aujourd'hui principalement le

méthane à partir du gaz naturel. Conjuguée à une révolution technologique dans l'agriculture et à l'amélioration des cultures, l'utilisation d'engrais artificiels ou parfois chimiques dans les systèmes de production agricole a augmenté de façon le rendement agricole (Tilman, 1999). Les budgets globaux d'azote de cette décennie estiment que les humains fixent actuellement 51% de l'azote total dans le monde (210 de 413 Tg N an-1) (Fowler *et al.*, 2013). Grâce à cette contribution supplémentaire, nous alimentons les voies biochimiques dans le cycle de l'azote et nous faisons maintenant face à des impacts croissants sur l'environnement.

La lixiviation des excès de nitrate dans les sols a conduit à la pollution des eaux souterraines et à l'eutrophisation des rivières et les côtes dans les années 1950, mettant en lumière pour la première fois les impacts environnementaux dus aux actions agricoles. De plus, des concentrations croissantes d'oxyde nitreux (N_2O) ont été mesurées dans l'atmosphère au cours de la deuxième moitié du XXe siècle (Figure 3). Lorsque ce gaz d'azote atteint la stratosphère, environ 10% est décomposé par photolyse en radicaux NO qui réagissent dans une réaction catalytique avec l'ozone et le réduisent à dioxygène (Portmann *et al.*, 2012).

Le NO est recyclé plusieurs fois (~ 103-105 fois) dans cette réaction avant qu'il ne soit converti en une molécule moins réactive (Lary, 1997). Au total, la durée de vie globale du N_2O a été déterminée comme étant d'environ 114 ans et, dans une comparaison par molécule, elle contribue 300 fois plus qu'une molécule de CO_2 au réchauffement planétaire (Stocker *et al.*, 2013; Prather *et al.*, 2015). Les modèles prédisent que le N_2O sera le gaz d'appauvrissement de la couche d'ozone qui domine au XXIe siècle (Ravishankara *et al.*, 2009). Sa longue durée de vie, combinée à l'augmentation prévue de l'atmosphère, en fait un gaz à effet de serre important à côté du méthane (CH_4) et du dioxyde de carbone (CO_2) malgré ses concentrations comparativement faibles.

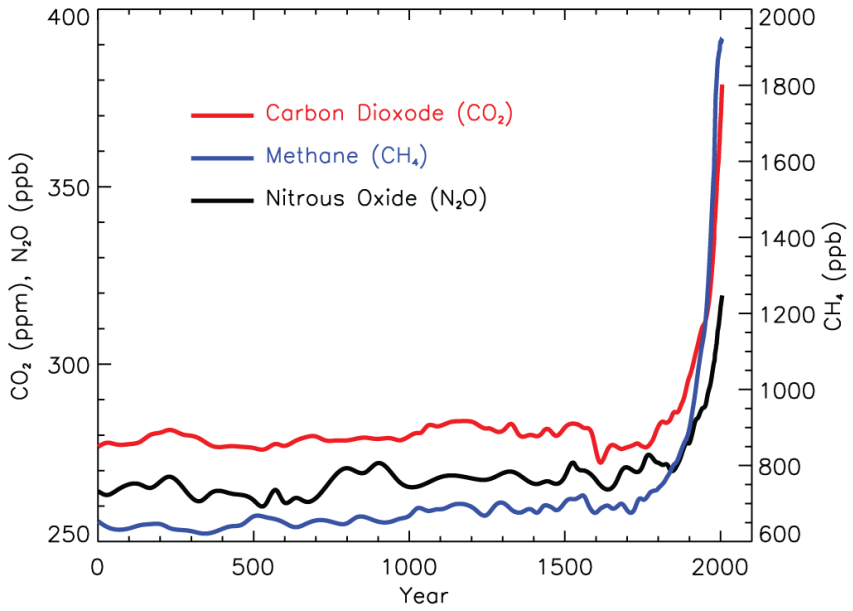

Figure 3: Concentration des principaux gaz à effet de serre de l'année 0 à 2005. Figure adaptée de (Forster *et al.*, 2007).

Les études sur les signatures isotopiques de N_2O dans l'atmosphère ont confirmé que l'action anthropogénique est responsable de ce développement et que la majorité du N_2O est émise par les sols (Park *et al.*, 2012; Snider *et al.*, 2015). Dans un scénario optimal, l'azote que nous mettons sur les champs serait absorbé à 100% par la plante et serait disponible comme nutriment dans nos aliments. En réalité, comme les communautés des écosystèmes naturels ont appris à concurrencer cette ressource rare, l'azote appliqué est également absorbé par les microbes, où il entre dans le cycle de l'azote microbien. Ici, de nombreuses voies biochimiques effectuées par des microbes produisent potentiellement du N_2O, qui est la source réelle d'émissions élevées de N_2O dans les systèmes agricoles (Mosier *et al.*, 1998; Smith and Conen, 2004). La quantité de N_2O émise par les sols et l'agriculture a été estimée à 13 Tg N yr-1 et plus de la moitié (7 Tg N yr-1) est attribuée à l'action anthropique (Fowler *et al.*, 2013). Bien que l'effet négatif des apports anthropiques d'azote sur les écosystèmes du sol sur notre climat ait été reconnu, l'application de stratégies appropriées pour atténuer ces

impacts ont eu peu de succès. Ceux-ci incluent l'application d'inhibiteurs de nitrification, la variation dans le dosage et le temps d'application des engrais et la variation des formes d'azote appliquées aux champs (Mosier *et al.*, 1998; Bell *et al.*, 2015).

Par conséquent, il est essentiel d'améliorer notre compréhension fondamentale du cycle de l'azote, des voies biogéochimiques et des acteurs concernés si nous voulons prédire et réduire avec précision la contamination des écosystèmes par les processus industriels et agricoles.

Écosystèmes du sol et cycle des nutriments

Le sol forme une couche mince sur la surface de la Terre, où il sert de réservoir de nutriments et d'eau pour les plantes, et est donc essentiel pour la nutrition des formes de vie supérieures. L'assemblage finement structuré du sol crée des microhabitats avec des conditions polyvalentes pour la vie, construisant un écosystème considéré comme le plus divers parmi tous les habitats de la planète (Dance, 2008). On a estimé à 1 milliard de cellules bactériennes et entre 100 à 1 km d'hyphes fongiques dans 1 g de sol (Elmholt and Kjøller, 1987; Gans *et al.*, 2005; Bardgett *et al.*, 2005; Roesch *et al.*, 2007). Par exemple, on a constaté que les eaux de surface dans les océans abritaient jusqu'à 105 cellules par mL, ce qui correspond à un volume comparable à 1 g de sol (Sogin *et al.*, 2006). Cela montre que la densité de la vie dans le sol est étonnante, et cela est en partie lié à la structure du sol. En plus de la partie microbiologique du biome du sol, on trouve des organismes comme les protozoaires, les nématodes et les biotes supérieurs. Les plantes sont également une partie importante de ces écosystèmes, car leurs racines constituent une source nutritive majeure pour les communautés souterraines en fournissant des exsudats de racine ou de matériel végétal mort pour des processus de décomposition (Henry *et al.*, 2008; Rennenberg *et al.*, 2009). Au total, ces organismes forment une chaîne alimentaire, où la matière organique et l'énergie sont transformées et cyclées (Figure 4). En regardant l'immense nombre de microorganismes

retrouvés dans le sol, il n'est pas surprenant que diverses interactions se produisent. Par exemple, on a constaté que les bactéries se développaient dans le voisinage immédiat des champignons mycorhiziens, qui sécrètent des molécules de carbone facilement accessibles qui servent de nutriments pour ces bactéries (Warmink and van Elsas, 2008; Warmink *et al.*, 2009; Nazir *et al.*, 2010).

Un facteur clé pour le fonctionnement des écosystèmes du sol est sa structure. Généralement, le sol peut être défini comme un assemblage de particules d'origine organique et inorganique. On a trouvé que cet assemblage n'était pas aléatoire, plutôt consistant en des réarrangements constants effectués par l'activité microbienne et végétale (Six *et al.*, 2004; Bronick and Lal, 2005).

Ce réarrangement est lié au cycle du carbone, puisque la matière organique du sol entraîne la structuration du sol. La matière organique qui pénètre dans le sol est décomposée et la

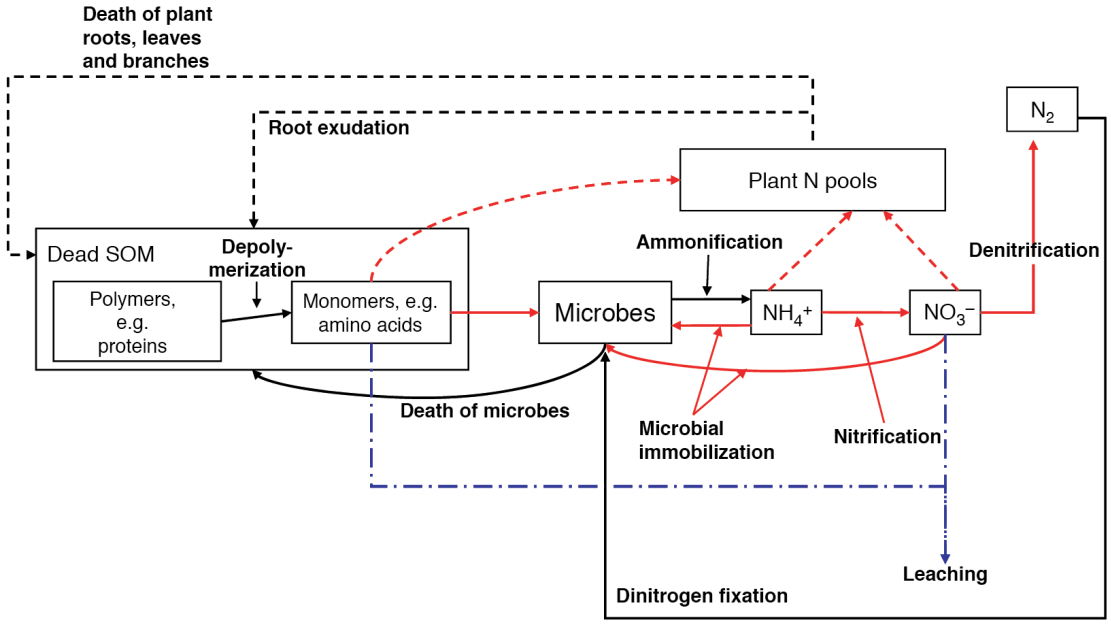

Figure 4: Cycle des éléments nutritifs dans le sol montrant le recycle de la matière organique des piscines N de la plante. SOM, matière organique du sol; Lignes pointillées: procédés végétaux; Lignes pleines: processus microbiens; Lignes en pointillés rouges et pleins: processus compétitifs entre les plantes et les microbes; Lignes bleues en pointillés: voies de transport hydrologiques. Adapté de (Rennenberg *et al.*, 2009).

formation d'agrégats a lieu là où des blocs de construction simples comme le sable, le limon et l'argile se stabilisent autour de matière organique incrustée de produits microbiens et de mucus de vers de terre. L'activité microbienne est la clé dans ce processus puisque les hyphes fongiques et les exopolysaccharides excrétés par les microbes fonctionnent comme colle dans la stabilisation des agrégats (Figure 5). En même temps, alors qu'ils forment leur propre micro-environnement, les micro-organismes utilisent la matière organique comme source nutritive. Lorsque les nutriments sont épuisés, l'agrégat finit par être perturber. Des perturbations telles que le labourage améliorent le roulement des agrégats et réduisent la formation de nouveaux agrégats (Six *et al.*, 2000). Ainsi, la capacité du sol à lier la matière organique, également appelée séquestration du carbone, est réduite. Dans l'ensemble, un système complexe et poreux est formé où l'eau et l'air peuvent coexister. Puisque la structure du sol change avec le temps, elle est parfois appelée la quatrième dimension du sol (Bardgett *et al.*, 2005).

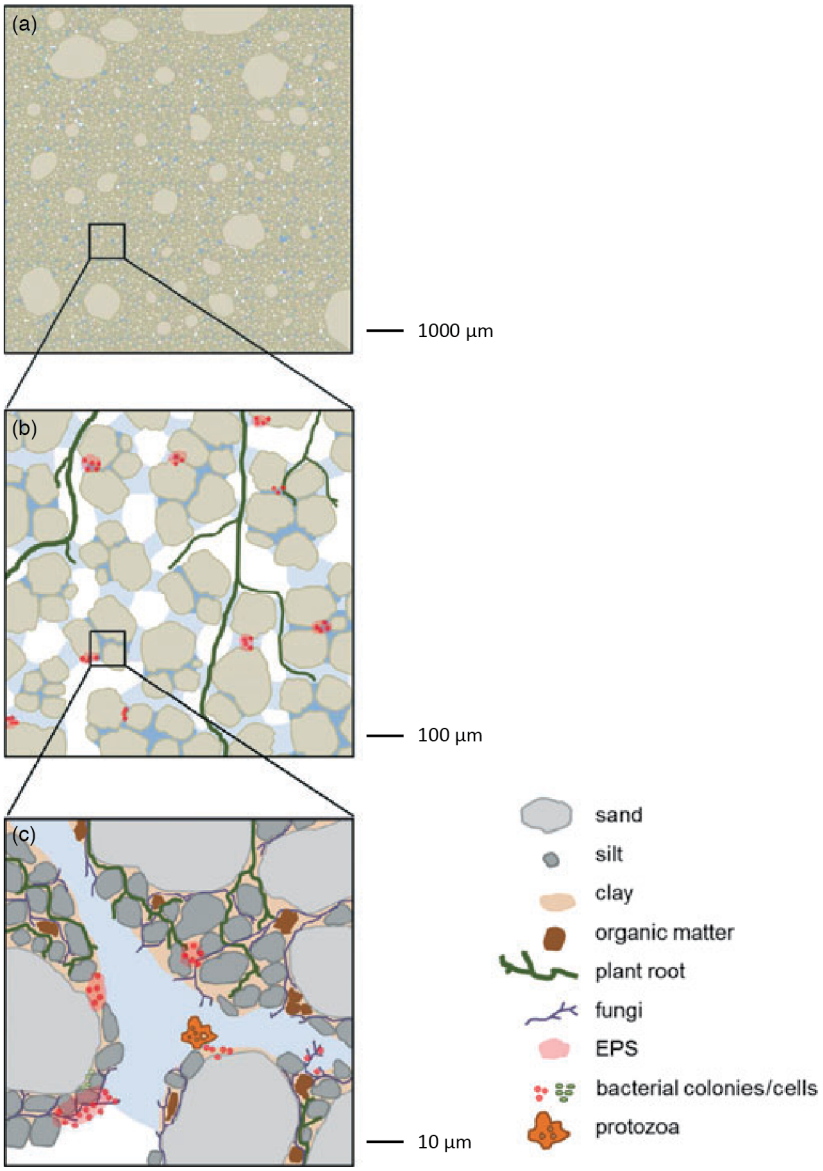

Figure 5: Disposition spatiale des particules de sol sur l'échelle du millimètre (a) au micromètre (b, c). EPS: exopolysaccharide. Figure adaptée de (Vos *et al.*, 2013).

On peut imaginer qu'en raison de la structure complexe d'une matrice de sol, les paramètres environnementaux (comme la concentration d'oxygène, la disponibilité en eau et en nutriments et le pH) qui impactent les communautés microbiennes pourraient changer à petite échelle. On a estimé qu'un gramme de sol fournit 20 m^2 de surface et que seulement 1% de cette région est réellement couverte par des microbes (Bardgett *et al.*, 2005). Cela suggère que les micro-organismes ne sont pas distribués au hasard dans le sol, mais qu'ils prolifèrent dans les micro-habitats où ils trouvent les conditions les plus adaptées à leur mode de vie. Les communautés de sols ont été étudiées sur différentes échelles allant de kilomètres à mètres et

à centimètres (Green and Bohannan, 2006; Vos and Velicer, 2006; Enwall *et al.*, 2010; Bru *et al.*, 2011). Jusqu'à présent, peu de travaux se sont concentrés sur la différenciation des communautés fonctionnelles à l'échelle micrométrique, l'échelle de taille réelle des microbes. C'est un aspect critique, car si nous voulons acquérir des connaissances fondamentales sur les voies impliquées dans la production de N_2O, nous devons étudier les processus à l'échelle à auxquels ils se produisent, à savoir la micro-échelle.

Le cycle microbien de l'azote

La composante microbienne de ces communautés complexes du sol effectue plusieurs étapes cruciales dans les processus de transformation de nutriments. Ils jouent des rôles clés dans le cycle du carbone, où ils agissent principalement comme décomposeurs en décomposant la matière organique, la rendant ainsi biodisponible pour d'autres microbes ou plantes (Nielsen *et al.*, 2011; Schimel and Schaeffer, 2012). Dans le cycle de l'azote, le rôle des microbes semble encore plus critique, puisque certaines transformations biochimiques de l'azote ont été trouvées exclusivement chez ces organismes (Hayatsu *et al.*, 2008).

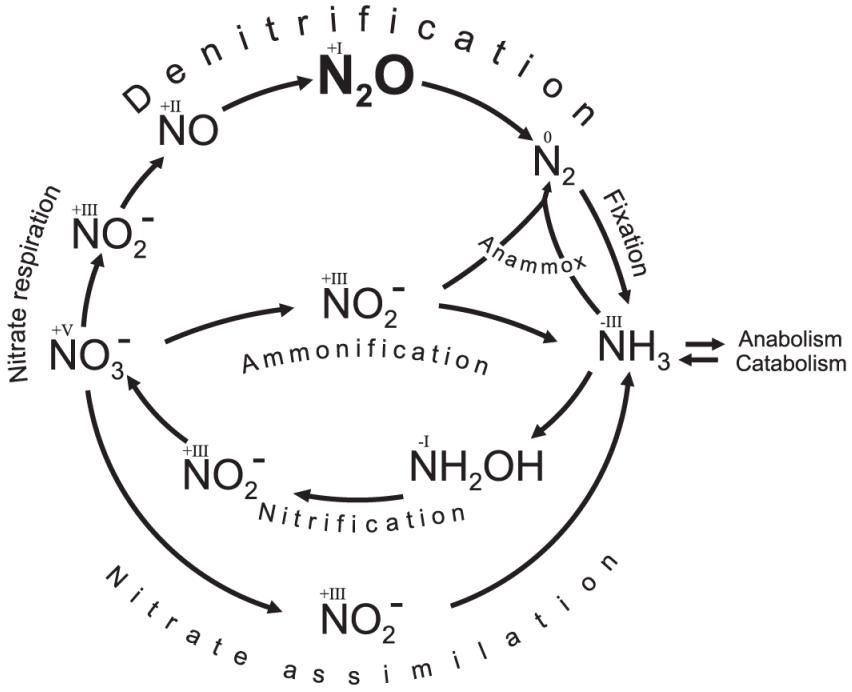

Figure 6: Processus biochimiques dans le cycle N et les formes azotées présentes. Les chiffres romains indiquent l'état d'oxydation de l'atome d'azote dans le composé chimique. Figure adaptée de (Zumft and Kroneck, 2007).

La plupart des organismes assimile l'azote sous forme réduite (NH_4^+) ou oxydée (NO_3^-), et ces nutriments sont limités dans les environnements naturels. L'azote est donc constamment réduit ou oxydé, car les microbes trouvent des moyens de produire de l'énergie à partir des processus de conversion, ce qui ferme complètement le cycle de l'azote (Figure 6). Deux courants d'entrée dans le cycle d'azote microbien peuvent être identifiés. L'un est la fixation de l'azote de l'atmosphère par la vie libre et les bactéries symbiotiques et les archées (Réaction 1) (Zehr *et al.*, 2003). Ces organismes possèdent des nitrogénases hautement conservées (NIF) qui peuvent catalyser la rupture de la triple liaison du gaz nitrure (N_2) et générer du NH_3 dans des environnements anaérobies après l'équation suivante:

$$2N_2 + 6H_2O \xrightarrow{NIF} 4NH_3 + 3O_2$$

Réaction 1: Fixation biologique de l'azote (BNF). NIF, nitrogenase.

Une autre entrée d'azote dans le cycle est le recyclage de la matière organique, lorsque l'azote anaboliquement incorporé dans la biomasse est relâché par des processus de décomposition, également appelé minéralisation d'azote.

Lorsque l'oxygène est présent, NH_4^+ peut être oxydé en NO_3^- par nitrification (Réaction 2) (Klotz and Stein, 2008). Des groupes spécifiques de bactéries et d'archées effectuent ces réactions biochimiques. On a considéré que l'oxydation de l'ammonium en nitrite et l'oxydation ultérieure en nitrate sont effectuées par des groupes distincts d'organismes, à savoir les bactéries oxydantes de l'ammoniac (AOB) ou les archées (AOA) et les bactéries oxydant les nitrites (NOB). Au cours de la nitrification, NH_4^+ est d'abord oxydé en hydroxylamine (NH_2OH) par une ammoniac monooxygénase (AMO), qui est ensuite oxydée en nitrite par l'hydroxylamine oxydoréductase (HAO). Enfin, le nitrite est oxydé en nitrate par une nitrite oxydoréductase (NXR).

$$NH_3 + O_2 + 2H^+ + 2e^- \xrightarrow{AMO} NH_2OH + H_2O$$

$$NH_2OH + H_2O \xrightarrow{HAO} NO_2^- + 5H^+ + 4e^-$$

$$NO_2^- + 0.5O_2 \xrightarrow{NXR} NO_3^- + H_2O$$

Réaction 2: Nitrification montrant les enzymes impliquées dans chaque étape. AMO, ammoniac monooxygénase; HAO, hydroxylamine oxydoréductase; NXR, nitrite oxydoréductase. Les abréviations désignent toute enzyme capable de catalyser la réaction respective.

Récemment, une souche de Nitrospira capable de catalyser l'oxydation complète de l'ammonium en nitrate a été découverte (Daims *et al.*, 2015).

Si l'oxygène devient limité, NO_3^- ou NO_2^- peuvent être de nouveau réduits à NH_4^+ par la réduction dissimilatoire du nitrate en ammonium (DNRA), parfois aussi appelée nitration-ammonification (Réaction 3) (Simon, 2002).

$$NO_3^- \xrightarrow{NAR} NO_2^- \xrightarrow{NIR} NH_4^+$$

Réaction 3: Dissimilation de la réduction du nitrate en ammonium (DNRA) montrant les enzymes impliquées dans chaque étape. NAR, nitrate réductase; NIR, production de nitrite réductase-ammonium. Les abréviations désignent toute enzyme capable de catalyser la réaction respective (Mohan and Cole, 2007).

La réduction de NO_3^- en NO_2^- est réalisée par les mêmes réductases que celles trouvées chez les dénitrifiants. Deux enzymes distinctes ont été trouvées pour réduire le NO_2^- à NH_4^+. Une réductase NADH-dépendante NirB ou une cytochrome c réductase NrfA (Darwin *et al.*, 1993; Cole, 1996; Einsle *et al.*, 1999).

Une autre voie réductrice importante se terminant par la production de N_2 gazeux via NO et N_2O est appelée dénitrification et sera décrite plus loin en détail (Réaction 6). Cette voie est caractérisée par l'utilisation d'une nitrate réductase dissimilatoire (dNAR) pour la réduction du NO_3^- en NO_2^-, contrairement à la réduction du nitrate en ammonium à des fins anaboliques,

où une nitrate réductase assimilatrice catalyse cette réaction (Guerrero *et al.*, 1981; Crawford and Arst, 1993; Mahne and Tiedje, 1995; Zumft, 1997).

La voie d'oxydation anaérobie de l'ammoniac (Anammox) décrit un mécanisme alternatif pour la réduction de NH_4^+ en N_2 (Réaction 4) (Strous *et al.*, 1999). Le NO_2^- est tout d'abord réduit en NO et NH_4^+ sert d'accepteur terminal d'électrons dans les autres réactions:

$$NO_2^- \xrightarrow{NIR} NO + NH_4^+ \xrightarrow{HH} N_2H_2 \xrightarrow{HZO/HAO} N_2$$

Réaction 4: Oxydation anaérobie de l'ammoniac (ANAMMOX) montrant les enzymes impliquées dans chaque étape. NIR, nitrite réductase; HH, hydrazine hydrolase; HZO / HAO hydrazine / hydroxylamine oxydoréductase. Les abréviations désignent toutes les enzymes qui catalysent la réaction respective (Kraft *et al.*, 2011).

On a constaté que les bactéries Anammox vivaient dans des écosystèmes marins et terrestres et qu'elles effectuaient de la DNRA lorsque l'ammonium devenait limitant (Penton *et al.*, 2006; Kartal *et al.*, 2007; Humbert *et al.*, 2009). En outre, l'application technique de ces organismes dans le traitement des eaux usées promet une réduction des coûts et des émissions de N_2O (Ali and Okabe, 2015).

L'oxyde nitreux comme produit intermédiaire dans le cycle N ne se produit que dans la dénitrification. Cependant, des dénitrifiants complets, des dénitrifiants incomplets, des réducteurs de nitrate, des microbes effectuant de la DNRA et des nitrifiants ont été montrés comme pouvant contribuer à la production biologique de N_2O (Wrage *et al.*, 2001; Megonigal *et al.*, 2003; Stremińska *et al.*, 2011). En outre, un processus abiotique pourrait également conduire à la formation de N_2O par la réduction de NO_2^-. En raison de son équivalent biologique, ce processus a été appelé chemodenitrification (Réaction 5) (Nelson and Bremner, 1969; 1970a). Le nitrite est chimiquement réduit en NO et plus loin en N_2O à pH bas et quand des ions métalliques sont présents (Nelson and Bremner, 1970b; Kampschreur *et al.*, 2011).

$$NO_2^- + Fe^{2+} + 2H^+ \longrightarrow Fe^{3+} + NO + H_2O$$

$$NO + Fe^{2+} + 1H^+ \longrightarrow Fe^{3+} + 0.5N_2O + 0.5H_2O$$

Réaction 5: Réduction chimique du nitrite en N_2O via NO (Van Cleemput and Samater, 1995).

On a montré, par exemple, que le fer ferreux produit par les bactéries réduisant les ions ferriques a catalysé la réduction chimique du nitrite présent à N_2O (D. C. Cooper and Picardal, 2003; Coby and Picardal, 2005).

Quantifier la contribution de diverses voies du cycle de l'azote aux émissions de N_2O est une tâche difficile. La distinction entre la dénitrification et la production de N_2O médiée par la nitrification pourrait être obtenue par une approche isotopique stable et l'utilisation d'inhibiteurs (Bateman and Baggs, 2005). Des modèles plus complexes ont été développés récemment, mais des travaux supplémentaires doivent être effectués pour pouvoir distinguer les processus de conversion de l'azote unique se produisant lors des événements d'émission de N_2O (Müller *et al.*, 2014).

La dénitrification est souvent considérée comme le principal processus impliqué dans les émissions de N_2O des sols agricoles en conditions anoxiques (Webster and Hopkins, 1996; Pihlatie *et al.*, 2004; Li *et al.*, 2016). En outre, les enzymes dénitrifiantes sont répandues dans les bactéries et aussi quelques archées et champignons (Zumft, 1997; Philippot, 2002; Shoun *et al.*, 2012). Une compréhension plus large des interactions écologiques entre ces microbes pourrait aider à élaborer des stratégies ciblées d'atténuation des émissions de N_2O des sols agricoles.

Dénitrification dans les bactéries

La génération d'énergie dans chaque forme de vie est basée sur l'exploitation des différences de potentiel redox. Ceci est soit réalisé par l'accumulation d'une force motrice du proton (pmf) à travers les membranes par des réactions en chaîne de transport d'électrons ou par la phosphorylation au niveau du substrat dans les voies fermentatives (Simon *et al.*, 2008). Dans les deux cas, l'énergie est stockée dans l'adénosine triphosphate (ATP) et peut être utilisée plus tard par la cellule.

Les microorganismes peuvent utiliser divers accepteurs terminaux d'électrons dans les chaînes respiratoires. L'oxygène est le plus efficace, suivi du nitrate, du manganèse, du fer, du soufre et du dioxyde de carbone. Contrairement à la réduction de l'O_2 à H_2O, la réduction complète de NO_3^- à N_2 est un processus par étapes appelé dénitrification (Réaction 6).

$$NO_3^- \xrightarrow{NAR} NO_2^- \xrightarrow{NIR} NO \xrightarrow{NOR} N_2O \xrightarrow{N_2OR} N_2$$

Réaction 6: dénitrification montrant les enzymes impliquées dans chaque étape. NAR, nitrate réductase; NIR, nitrite réductase; NOR, oxyde nitrique réductase; N_2O R, oxyde nitreux réductase. Les abréviations désignent toutes les enzymes capables de catalyser la réaction respective (Zumft, 1997).

Toutes les étapes de ce processus sont catalysées par des métalloenzymes multisites (van Spanning *et al.*, 2007). Les nitrates réductases (NAR) réduisent le NO_3^- en NO_2^- et se sont révélés être liés à la membrane (NarG) ou situés dans le périplasme (NapA) (Blasco *et al.*, 2001; Simon *et al.*, 2003; Ellington *et al.*, 2005). Le nitrite est réduit par les nitrites réductases (NIR) en oxyde nitrique (NO). En tant que première étape de production d'une molécule de gaz, il est considéré comme une caractéristique clé de la dénitrification. L'enzyme contenant du cuivre NirK ainsi que le cytochrome cd1 contenant de l'hème NirS sont capables de réduire les nitrites (Tavares *et al.*, 2006). Jusqu'à présent, aucun organisme contenant les deux types de NIR a été trouvé. Le NO produit est ensuite réduit en N_2O par l'oxyde nitrique reductases (NOR). On a trouvé trois enzymes catalysant cette réaction dans les bactéries, à savoir un

qNOR à longue chaîne ou un cNOR à chaîne courte dans des bactéries Gram-négatives, et un qCuANOR dans des bactéries Gram-positives (Hendriks *et al.*, 2000; Suharti and S. de Vries, 2005; Tavares *et al.*, 2006). Enfin, la dernière étape de la dénitrification est la réduction du N_2O en gaz N_2 qui est catalysée par les oxydes nitrés réductases (N2OR). Deux variantes sont connues pour les N2OR, un N2OR de type z ainsi qu'un N2OR de type c nouvellement découvert (Sanford *et al.*, 2012; Jones *et al.*, 2013). Les deux types d'enzymes se trouvent dans des groupes phylogénétiquement distincts de bactéries et la possibilité d'une spécialisation de niche dans la réduction de N_2O parmi ces groupes est actuellement à l'étude (Jones *et al.*, 2014).

La terminologie décrivant les organismes réduisant les nitrates s'est diversifiée. On considère généralement que les dénitrifiants sont capables de réduire le nitrate jusqu'au gaz N_2. En revanche, de nombreux organismes se sont avérés être des dénitrificateurs incomplets, possédant diverses combinaisons d'enzymes impliquées qui ne permettent pas une réduction complète. De plus, les microbes qui utilisent la réduction la plus économe en énergie de NO_3^- à NO_2^- sont définis comme des réducteurs de nitrate ou des respirateurs à nitrate. La réduction des nitrites a également été observée dans les bactéries oxydantes de l'ammoniac, connues sous le nom de dénitrification nitrifiante (Wrage *et al.*, 2001).

La dénitrification est, contrairement à la nitrification, phylogénétiquement répandue et aucun modèle des enzymes sur l'arbre bactérien de la vie n'a pu être trouvé (Philippot, 2002). Cela rend plus difficile l'étude de cette fonction par les écologistes microbiens, puisque les marqueurs phylogénétiques purs comme les séquences d'ARN ribosomique sont difficiles à interpréter par rapport à une communauté dénitrifiante.

Réduction de l'azote dans les champignons

Les chaînes de transport d'électrons dans les champignons sont situées dans les mitochondries, comme c'est le cas pour tous les organismes eucaryotes, où l'on a également trouvé des enzymes pour la réduction dissimilatoire de l'azote (Kobayashi *et al.*, 1996). Puisque l'oxyde nitreux a été mesuré dans le gaz des cultures fongiques, l'implication de ces derniers en tant que producteurs de gaz à effet de serre a été supposé (Bleakley and Tiedje, 1982). Plus tard, la production de N_2O dans les champignons a été liée à un processus de réduction de nitrate dissimilatoire dans *Fusarium oxysporum* qui a été par conséquent nommé dénitrification fongique (Shoun and Tanimoto, 1991). La réduction des nitrites dans les champignons est catalysée par un nitrite réductase contenant du cuivre nirK (Long *et al.*, 2015). La comparaison des séquences d'acides aminés des nitrites réductases des eucaryotes, des bactéries et des archées suggère que le nirK de ces domaines a la même origine (S.-W. Kim *et al.*, 2009). La distribution aléatoire de nirK parmi les protéobactéries pourrait être due au transfert horizontal de gènes entre ces bactéries, alors que les nirK eucaryotes ont été trouvés systématiquement distribués.

L'enzyme catalysant la réduction de l'oxyde nitrique en N_2O dans les champignons s'est révélée être un cytochrome P450 monooxygénase qui était par conséquent appelée P450nor. Cette classe d'enzymes est abondante chez les champignons et exerce des rôles essentiels dans différents processus cellulaires (Črešnar and Petrič, 2011). Bien que l'on trouve généralement que les enzymes P450 eucaryotes sont liées à la membrane, le P450nor est soluble et se trouve donc dans le cytosol (Takaya, 2002).

L'analyse de structure de P450nor a montré une similarité plus élevée avec des enzymes bactériennes dérivées de P450, cependant, un P450nor n'a pas encore été trouvé dans les bactéries (Shoun *et al.*, 2012). En raison de sa fonction spéciale parmi les enzymes P450, l'attention a été attirée vers elle. Des résultats contradictoires sur le comportement de la

réduction du NO des champignons alimentent les discussions quant à savoir si elle contribue à la production d'énergie pour l'organisme, soit un processus respiratoire, ou simplement une fonction détoxifiante pour éviter de fortes concentrations de NO réactif dans la cellule. Par exemple, même dans l'organisme modèle *Fusarium oxysporum*, on a observé l'expression simultanée dans des conditions dénitrifiantes de flavohémoglobine (Fhb), qui est exprimée chez les bactéries pour neutraliser le NO (S.-W. Kim *et al.*, 2009; Forrester and Foster, 2012). Plus tard, ces résultats ont été confirmés par les mêmes chercheurs dans un autre organisme modèle pour la dénitrification fongique, *Fusarium lichenicola* (ancien *Cylindrocarpon tonkinense*), et l'expression de Fhb a été liée à la dénitrification dans ce champignon (S.-W. Kim *et al.*, 2010). En outre P450nor a été trouvé pour avoir la fonction de détoxification pure de NO dans le pathogène humain *Histoplasma capsulatum* (Nittler *et al.*, 2005).

Le nitrate semble être le substrat préféré pour la dénitrification fongique, puisque le N_2O peut être détecté après culture dans des milieux contenant des nitrites (Mothapo *et al.*, 2015). Le développement d'outils moléculaires pour des études sur la contribution de la dénitrification fongique aux processus de transformation de N est en cours en ce moment et les amorces pour le nitrite fongique et les réductases oxyde nitrique ont été récemment publiées (Long *et al.*, 2015; Wei *et al.*, 2015; Higgins *et al.*, 2016). Des similitudes élevées avec les enzymes du cytochrome P450 ou le nirK bactérien rendent difficile la détection distincte de ces gènes à partir d'échantillons environnementaux. Afin d'identifier l'importance écologique de ces gènes, nous devons davantage étudier les profils d'expression de champignons dans des conditions anaérobies ou hypoxiques. Les approches métatranscriptomiques dans des expériences de laboratoire contrôlées pourraient être la première étape pour améliorer l'image que nous avons d'une communauté fongique réduisant l'azote. Le séquençage du génome complet des espèces candidates fournirait des informations sur le potentiel génétique général de ces organismes en ce qui concerne le cycle de l'azote, en particulier la présence ou

l'absence de séquences de globine active P450nor versus NO-active et pourrait marquer une étape importante dans ce domaine de recherche.

Décomposition de la matière organique et ses implications dans le cycle N

L'ajout d'engrais chimiques provoque des émissions élevées de N_2O provenant des écosystèmes du sol, mais l'application de la matière organique comme engrais a également été démontrée pour initier ce processus (McSwiney and Robertson, 2005; Shcherbak, Millar, and Robertson, 2014b; Zhu-Barker *et al.*, 2015). Dans les milieux naturels, l'azote doit être recyclé à partir de la biomasse ou fixé de l'atmosphère par des microbes (Figure 4). Lorsque la matière organique morte pénètre dans le sol, un processus de dépolymérisation décompose ces structures polymères en molécules qui peuvent à nouveau être réutilisées par les microbes. Les mécanismes sous-jacents de la dégradation de la matière organique dans le sol sont actuellement à l'étude. Les méthodes d'analyse modernes soutiennent l'hypothèse selon laquelle la matière organique du sol est continuellement dégradée de plus grands à plus petits polymères plutôt que le modèle largement accepté d'humification, ce qui n'a pas pu être confirmé par la chimie carbonée du sol (Lehmann and Kleber, 2015).

Le matériel végétal mort se compose principalement de composés lignocellulosiques. Ces composites de structures polysaccharidiques telles que la cellulose, l'hémicellulose, la lignine et la pectine sont des éléments constitutifs des parois des cellules végétales et fournissent ainsi de l'azote sous la forme de protéines de la paroi cellulaire. Cette étape marque également une interconnexion du cycle de l'azote avec le cycle du carbone, puisqu'il fournit non seulement de l'azote, mais aussi le carbone nécessaire à une communauté hétérotrophe du cycle de l'azote.

Lorsque les activités du cycle du carbone et de l'azote ont été couplées dans des modèles de prédiction de l'absorption mondiale de carbone terrestre suite à des niveaux élevés de CO_2

dans l'atmosphère, les valeurs prédites ont été réduites de 74% par rapport à un modèle de carbone unique (Thornton *et al.*, 2007).

Les organismes et les enzymes qui effectuent ces processus de dégradation ont été étudiés de façon intensive, car la capacité à dégrader les polysaccharides récalcitrants à partir de structures en carbone est également intéressante pour des procédés industriels tels que la production de composés sucres à partir de matériel végétal pour la fermentation ultérieure en biocarburants (Voloshin and Rodionova, 2016).

Un ensemble complexe d'enzymes est impliqué dans la déconstruction des composés lignocellulosiques (Figure 7). Par exemple, la dégradation complète d'un polymère structuré relativement simple comme la cellulose nécessite trois classes d'enzymes, ß-1,4-endoglucanases, cellobiohydrolases et ß-glucosidases. Ces enzymes font partie des enzymes dites glucides actives qui comprennent des enzymes dégradant et générant des glycosides (base de données des Enzymes Actives de Carbohydrate; http://www.cazy.org/) (Lombard *et al.*, 2013).

Le plus grand groupe d'enzymes de clivage de liaisons glycosidiques sont les glycosides hydrolases (GH) (Henrissat, 1991). Cette classe d'enzymes actives en hydrates de carbone est actuellement divisée en 131 familles sur la base des séquences d'acides aminés des modules catalytiques apparentés structurellement et catalyse l'hydrolyse de glycosides liés à O, N et S (Davis and Sinnott, 2008). Les hydrolases glycosidiques exo et endo sont distinguées en raison de la localisation de leur site c'activité, à l'intérieur de la chaîne polysaccharidique (endo) ou à la fin de ces chaînes (exo), clivant des molécules de sucre unique de la chaîne comme les ß-galactosidases.

Un autre groupe d'enzymes clivant les liaisons glycosidiques sont les polysaccharides lyases (PL). Ces enzymes clivent les polysaccharides contenant de l'acide uronique qui se produise en diverses quantités dans les hémicelluloses et les pectines de plantes supérieures (Figure 7

(b), (c)) (Willför *et al.*, 2009). Le troisième groupe d'enzymes dégradant les glucides est classé dans les familles d'activités auxiliaires (AA) dans le système de classification CAZy (Levasseur *et al.*, 2013). Ces familles comprennent généralement des enzymes qui ont une fonction d'assistance pour les GH et les PL. Par exemple, la famille AA9 inclue des polysaccharides monooxygénases lytiques (LPMO) qui peuvent attaquer divers polysaccharides et fournir de nouvelles extrémités de chaîne pour une dégradation ultérieure (Kracher *et al.*, 2016; Johansen, 2016).

L'application récente d'approches omiques à la dégradation des glucides a transformé le paradigme des processus de décomposition qui ont été considérés comme étant exclusivement

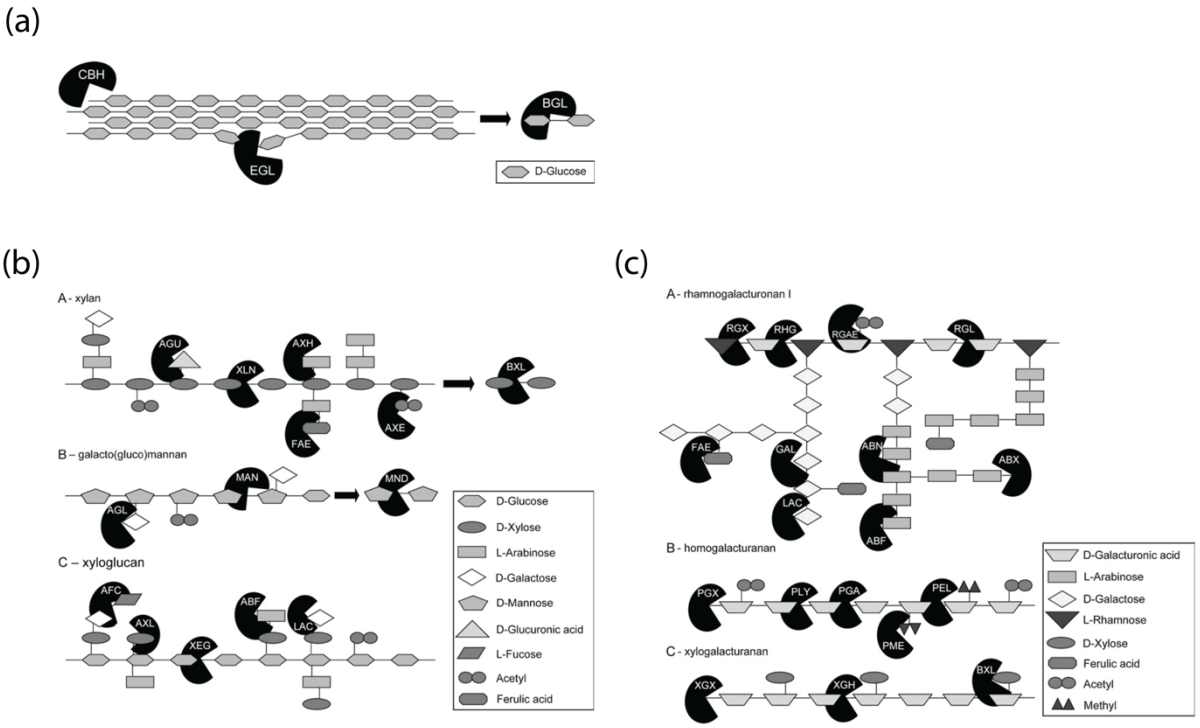

Figure 7: Enzymes impliquées dans le clivage de liaisons glycosidiques dans (a) cellulose et diverses formes de (b) hémicellulose et (c) pectine. Différentes formes correspondent à des résidus de glycoside distincts du polysaccharide. ABF, -arabinofuranosidase; ABN endoarabinanase, ABX exoarabinanase, AFC α-fucosidase, AGL α-1,4-galactosidase, AGU α-glucuronidase, AX acétyle (xylan) estérase, AXH arabinoxylan α-arabinofuranohydrolase, AXL α-xylosidase, BGL ß-glucosidase, BXL β -1,4-xylosidase, CBH cellobiohydrolase, EGL ß-1,4-endoglucanase, FAE feruloyl esterase, GAL β-1,4-endogalactanase, LAC β-1,4-galactosidase, MAN β-1,4-endomannanase, La MND β-1,4-mannosidase, la pectine lyase PEL, la PLYpectate lyase, l'endopoly-galacturonase PGA, l'exo-polygalacturonase PGX, la pectine méthyl esterase RGAE, l'acétyl-estérase rhamnogalacturonane RGL, l'endorhamnogalacturonase RGX, l'exorhamnogalacturonase RGX, la XEG xyloglucane active B-1,4-endoglucanase, XGH endoxylogalacturonase, XGX exoxylogalacturonase XLN β-1, 4-endoxylanase. Figure adaptée de (van den Brink and R. P. de Vries, 2011a).

fongiques, vers celui d'une communauté combinée responsable de la dégradation complète de la matière organique (Bugg *et al.*, 2011; Cragg *et al.*, 2015; de Gonzalo *et al.*, 2016). Cependant, les champignons sont encore considérés comme des acteurs clés dans ces processus puisqu'ils effectuent efficacement les premières attaques sur les polymères récalcitrants, fournissant l'accès plus facile à d'autres substrats (Eastwood *et al.*, 2011; Payne *et al.*, 2015; Kracher *et al.*, 2016). En outre, leur croissance dans les hyphes leur permet d'accéder à des zones avec des concentrations d'OM élevées contrairement aux bactéries immobiles. Ainsi, ils sont capables de transporter des composés carbonés sur de plus longues distances et de surmonter les sites pauvres en éléments nutritifs dans le sol (Jennings, 1987).

L'apparition d'enzymes dégradant les glucides codés dans des génomes fongiques pourrait être liée à l'habitat naturel des organismes respectifs (van den Brink and R. P. de Vries, 2011b). Par exemple, on a trouvé un faible nombre d'enzymes actives en hydrates de carbone dans les génomes des levures de Saccharomyces naturellement présentes à la surface des champignons pourris ou dans l'intestin des termites (Jeffries *et al.*, 2007; Liti *et al.*, 2009). Les champignons filamenteux présentaient un nombre beaucoup plus élevé de gènes encodant ces enzymes dans leurs génomes (Coutinho *et al.*, 2009; Rileya *et al.*, 2014). Les champignons décomposeurs semblent également développer une spécificité vis-à-vis de la nature chimique du substrat à attaquer. Des génomes complets de champignons dégradant le bois ont révélé que des espèces distinctes possèdent des mécanismes complètement différents pour la dégradation des glucides, soulignant la spécialisation du substrat de ces organismes (Ohm *et al.*, 2014). Par exemple, les *Aspergilli* présentaient de multiples enzymes codant pour la dégradation de la pectine, contrairement à d'autres champignons filamenteux caractérisés comme spécialistes de la cellulose ou dégradants de la lignine comme *T.reesei* ou *Phanerochaet chrysosporium* respectivement, ou *Zygomycota* qui se sont souvent avérés spécialisés dans l'utilisation de facilement accessibles et digestibles (Richardson, 2009a; Battaglia *et al.*, 2011; van den Brink and R. P. de Vries, 2011b).

Il est peu probable que deux groupes de microorganismes partageant un habitat aussi diversifié que le sol soient complètement indépendants l'un de l'autre. En fait, de nombreuses interactions ont été observées dans les écosystèmes du sol (Wardle, 2006; Faust and Raes, 2012; Bakker *et al.*, 2014) dans les organismes végétaux, végétaux, microbiens et microbes.

Un exemple bien connu pour les interactions mutualistes dans le sol est la symbiose entre les racines des plantes et les champignons mycorhiziens arbusculaires (AMF) où l'absorption d'azote par le champignon bénéfique pour la plante se produit en échange de substrats de carbone fixes pour le champignon (Lang *et al.*, 2010; Tisserant *et al.*, 2013; van der Heijden, de Bruin, *et al.*, 2015). Cette relation s'est diversifiée après l'observation des bactéries colonisant l'AMF (Garbaye, 1994; Frey-Klett *et al.*, 2007). Ces communautés bactériennes influencent le fonctionnement de ces écosystèmes (Johansson *et al.*, 2004; Frey-Klett *et al.*, 2011). Par exemple, une interaction antagoniste entre l'AMF et les bactéries a été trouvée pour la compétition des produits de décomposition (Leigh *et al.*, 2011). En outre, la colonisation des bactéries sur les hyphes mycorhiziens semble dépendre des espèces fongiques présentes, suggérant une interaction étroite entre des membres spécifiques des bactéries et des champignons (Toljander *et al.*, 2006). En plus de la symbiose des plantes AMF, on a constaté récemment que des bactéries ont participé à la symbiose étroite des champignons et des algues vertes chez les lichens, ce qui confirme l'hypothèse selon laquelle les interactions interdomaines sont probablement plus fréquentes que nous ne le pensions (Aschenbrenner *et al.*, 2016).

Des interactions de champignons vivants avec des bactéries ont également été observées (Boer *et al.*, 2005; Warmink *et al.*, 2009). Les interactions peuvent être antagonistes, comme la concurrence pour une ressource limite ou une interférence directe. La compétition trophique entre les champignons et les bactéries pour des nutriments comme le carbone est bien documentée dans de nombreux environnements et peut avoir un impact sur le cycle

biogéochimique (Schmidt *et al.*, 2012). Par exemple, des études ont montré que les interactions compétitives entre les champignons et les bactéries peuvent être importantes lors de la dégradation fongique de la matière organique récalcitrante telle que la lignine (Bugg *et al.*, 2011). Les interactions peuvent également être coopératives, comme le transfert de métabolites complémentaires ou la détection de quorum (Berry and Widder, 2014). Des données récentes suggèrent un rôle des consortiums champignons-bactériens dans la dégradation et la transformation des HAP environnementales (Folwell *et al.*, 2016). Cependant, le rôle et l'importance des consortiums bactériens-champignons dans le cycle des nutriments environnementaux ont été largement négligés et doivent être clarifiés si nous voulons bien comprendre et prédire comment les communautés vont réagir à l'évolution des milieux.

L'abondance des AMF dans une expérience en serre a été reliée aux émissions de N_2O, puisque les émissions ont augmenté lorsque des mutants de plantes sans AMF ont été cultivés (Bender *et al.*, 2013). Le nombre de copies des gènes codant pour nitrite réductase et oxyde nitreux réductase de la communauté bactérienne co-habitante est corrélé négativement et positivement avec l'abondance des AMF, qui décrit la première observation d'un effet indirect des champignons sur les émissions de N_2O par leur influence sur le cycle de l'azote bactérien. Jusqu'à présent, la recherche sur les émissions de N_2O s'est concentrée sur des processus spécifiques dans le cycle N et a essayé principalement de lier l'occurrence de la production de N_2O à l'activité des groupes d'organismes. Dans le cas de la dénitrification fongique, des études sur les environnements du sol ont été réalisées à l'aide d'inhibiteurs procaryotes et / ou eucaryotes pour identifier les différences d'émission de N_2O ou de potentiel de production (Crenshaw *et al.*, 2007; Laughlin *et al.*, 2009; Marusenko *et al.*, 2013; Wei *et al.*, 2014; H. Chen, Mothapo, and Shi, 2014a; 2014b). Puisque la production de N_2O a diminué de façon significative après l'ajout de fongicides, les champignons étaient souvent considérés comme les principaux producteurs de N_2O dans ces environnements. Cependant, bien que les

champignons aient été trouvés posséder une base enzymatique leur permettant d'effectuer la réduction d'azote à N_2O, nous observons actuellement une contradiction entre les données obtenues à partir des études de microcosme de sol et de cultures de champignons pures. On a trouvé que les taux de production de N_2O dans les cultures pures de champignons étaient de 3 à 6 ordres de grandeur inférieurs à ceux des bactéries dénitrifiantes (Betlach and Tiedje, 1981; I. C. Anderson and Levine, 1986; Jirout *et al.*, 2012; Mothapo *et al.*, 2013; Wei *et al.*, 2014; Maeda *et al.*, 2015). Bien qu'il soit difficile de comparer les résultats de deux configurations expérimentales distinctes, la diminution de la production de N_2O après l'ajout de fongicide dans le sol ne peut être expliquée par les taux observés dans les cultures fongiques.

C'est notre hypothèse que la réduction des émissions de N_2O dans les expériences d'inhibition des champignons montre la perturbation d'une relation étroite entre les champignons libres et une communauté bactérienne produisant du N_2O potentiel. Par l'inhibition des champignons, une perturbation involontaire de la dégradation du carbone pourrait se produire, ce qui ralentirait l’apport du substrat de carbone pour les bactéries. La communauté bactérienne impliquée dans cycle d'azote pourrait ainsi être indirectement affectée. Pour clarifier ce lien possible entre les microbes du carbone et de l'azote, nous devons étudier la dégradation de la matière organique par rapport à la production de N_2O dans les sols et l'activité des communautés fongiques et bactériennes impliquées dans ces processus.

Objectifs de cette thèse

Cette thèse est divisée en trois chapitres qui traitent chacun des hypothèses différentes développées au cours de ma thèse. Dans le premier chapitre, nous avons cherché à localiser spatialement les sites du cycle de l'azote dans le sol au niveau de la micro-échelle en utilisant une approche de fractionnement physique. Nous avons émis l'hypothèse que les potentiels dénitrifiants sont situés à l'intérieur des agrégats de sol où des microsites anaérobies sont présents. On a mesuré les changements dans les communautés fongiques et bactériennes dans les fractions granulométriques d'un sol de prairie vierge, ainsi que les abondances des gènes marqueurs du cycle de l'azote.

Le manque d'outils moléculaires pour étudier l'apparition et l'activité des membres réduisant l'azote des champignons dans les extraits d'ADN du sol nous a conduit à une approche de dépistage des champignons du sol afin de recueillir des données sur leur potentiel de production d'azote et de N_2O. Les résultats sont présentés et discutés dans le deuxième chapitre. Nous avons émis l'hypothèse que les champignons utilisent des nitrates réductases assimilatrices de manière dissimilatoire lorsqu'ils sont exposés à des conditions anoxiques. Vingt-deux isolats fongiques de sols agricoles capables d'assimiler les nitrates ont été incubés dans un système d'échantillonnage de gaz robotisé où nous pourrions suivre la production de NO et de N_2O à partir de nitrite par les cultures pures.

Dans le troisième chapitre, un lien potentiel entre la dégradation du carbone et le cycle de l'azote a été étudié à l'aide d'approches metatranscriptomiques et métagénomiques. Ici, nous avons émis l'hypothèse que la dégradation du carbone causée par les champignons affecte une communauté bactérienne cycle de l'azote et donc la production potentielle de N_2O. Le sol agricole a été incubé pendant 30 jours dans des microcosmes et des matériaux organiques avec des chimies de carbone variables ont été ajoutés. Des échantillons de sol ont été prélevés huit fois au cours de cette incubation et des métatranscriptomes, des métagénomes ainsi que

des chimies d'azote dans le sol et des gaz à effet de serre émis ont été analysés pour suivre l'évolution des communautés après addition du substrat.

General introduction

Biogeochemical cycling and climate change

Human nutrition is based on plant production. Plants fix carbon from the atmosphere and take nitrogen from soils to form biomass (Zelitch, 1975; Krapp, 2015). This marks the input stream of carbon and nitrogen to our food web. Nitrogen is an essential nutrient for all life forms. It allows organisms to synthesize nucleic acids, amino acids and consequently proteins.

Plants, together with most organisms, cannot directly use high concentrations of dinitrogen gas (N_2) present in the atmosphere. They rely on the availability of nitrate (NO_3^-) or ammonium (NH_4^+) in soils that can be taken up by plant roots and are ultimately incorporated in biomass (Figure 1) (Loque and Wiren, 2004; O'Brien *et al.*, 2016). Therefore we find the

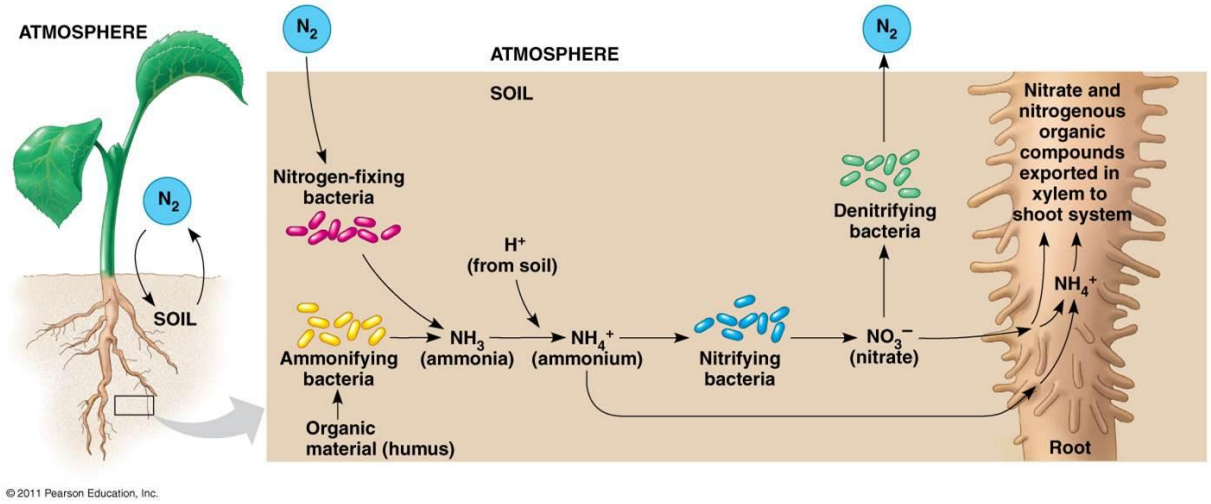

Figure 1: Macroscopic and microscopic view of nitrogen cycling processes in soil leading to uptake of nitrogen by plants. Figure adapted from Pearson Education Inc.

term 'reactive nitrogen' (N_r) in literature, which refers to oxidized or reduced forms of nitrogen atoms (Galloway *et al.*, 2003). The initial transformation step of changing non-reactive nitrogen to reactive forms requires the break-up of the triple bond between the two nitrogen atoms in N_2 gas. This happens in nature by two processes: lightning and biological nitrogen fixation (BNF) (Galloway *et al.*, 2003). Fossil fuel combustion, the cultivation of crops increasing BNF and the technical fixation of atmospheric nitrogen to produce nitrogen

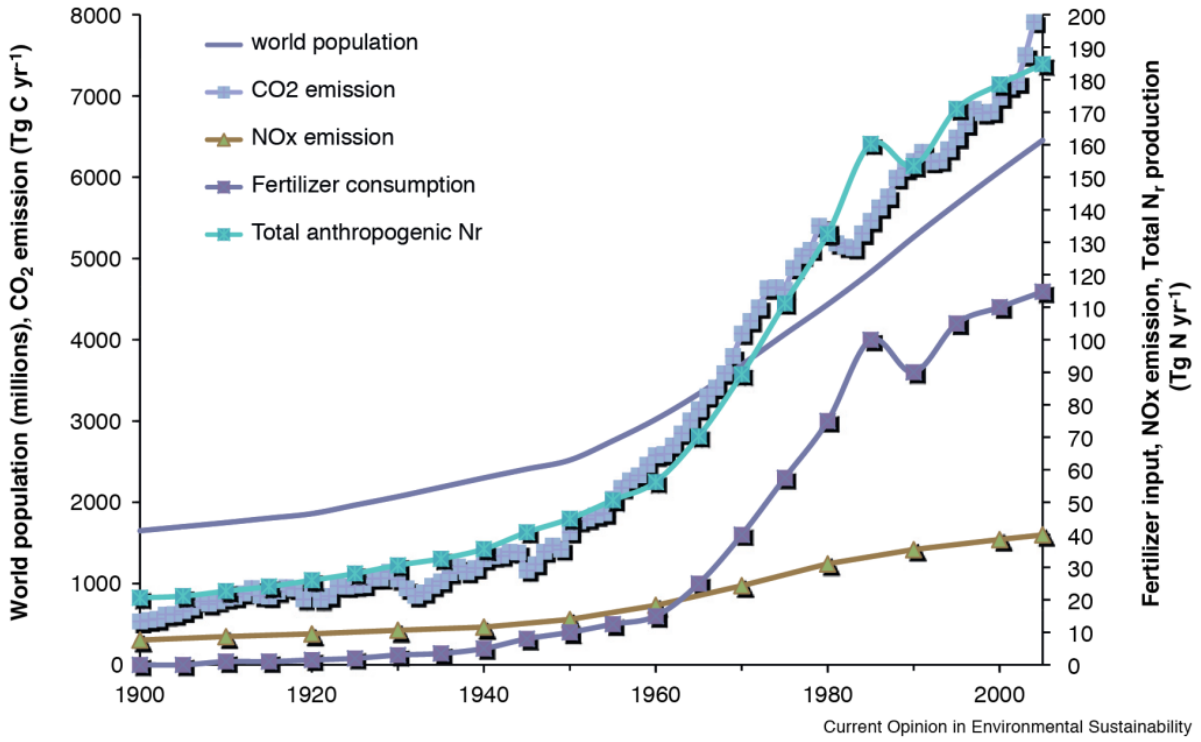

Figure 2: Development of world population in the last 20th century, anthropogenic produced Nr and fertilizer consumption over the last 110 year. Figure adapted from (Erisman *et al.*, 2011)

fertilizers are input streams for the global nitrogen budget caused by anthropogenic actions. It is estimated that the amount of global Nr created increased from 241 Tg N yr^{-1} in 1890 to 353 Tg N yr^{-1} in 1990 (Galloway, 2003). The main cause for this dramatic increase lies in a rapidly growing population since the beginning of the last century, which created increasing demands for higher production and yields from agricultural systems (Figure 2) (Erisman *et al.*, 2011). With the invention of the Haber-Bosch process at the beginning of the 20th century, it was possible to synthesize NH_4^+ artificially through the reduction of dinitrogen gas (N_2) from the atmosphere by hydrogen to form NH_4^+ (Haber and Le Rossignol, 1913). This technical process requires high pressures and temperatures and a source of hydrogen, which is nowadays mainly methane from natural gas. Together with a technological revolution in agriculture and improved crop breeding programs, the use of artificial, or sometimes called chemical, fertilizers in crop production systems increased the yield in agriculture dramatically (Tilman, 1999). Global nitrogen budgets from this decade estimate that humans currently fix 51 % of the total nitrogen worldwide (210 of 413 Tg N yr^{-1}) (Fowler *et al.*, 2013). Due to this

additional input, we fuel biochemical pathways within the nitrogen cycle and now face growing impacts on the environment.

Leaching of excess nitrate in soil led to pollution of groundwater and eutrophication in rivers and coasts in the 1950s, casting light on environmental impacts due to agricultural actions for the first time (Howarth, 2008). Furthermore, increasing concentrations of nitrous oxide (N_2O) were measured in the atmosphere in the second half of the 20th century (Figure 3). When this nitrogen gas reaches the stratosphere, approximately 10 % is broken down by photolysis to NO radicals that react in a catalytic reaction with ozone and reduce it to

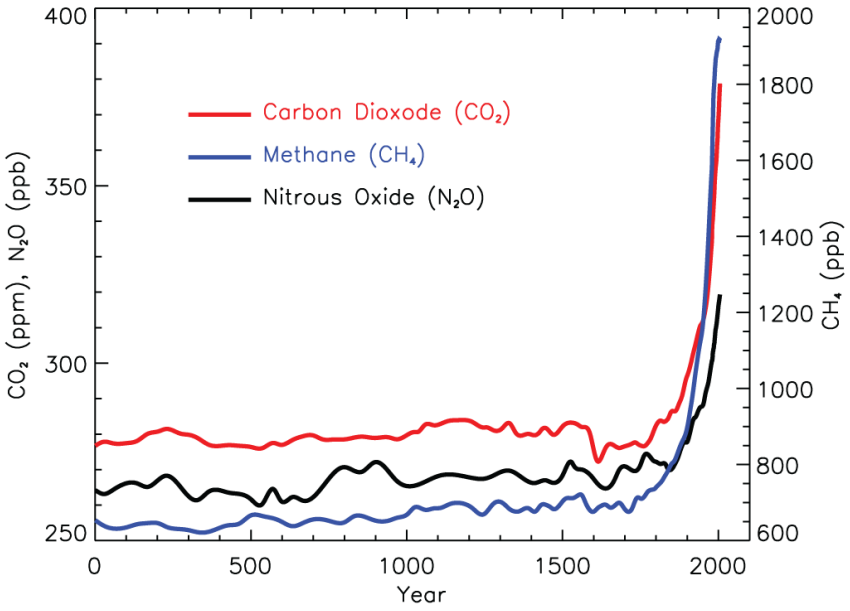

Figure 3: Concentration of major greenhouse gases from year 0 to 2005. Figure adapted from (Forster *et al.*, 2007).

dioxygen (Portmann *et al.*, 2012). NO is recycled multiple times (~10^3 – 10^5 times) in this reaction before it is converted to a less reactive molecule (Lary, 1997). Altogether, the global lifetime of N_2O was determined to be approximately 114 years and in a per molecule comparison it contributes to global warming 300 times more than one molecule of CO_2 (Stocker *et al.*, 2013; Prather *et al.*, 2015). Models predict N_2O to be the dominating ozone depleting gas emitted in the 21st century (Ravishankara *et al.*, 2009). Its long lifetime, in

combination with the predicted further increase in the atmosphere, makes it an important greenhouse gas next to methane (CH_4) and carbon dioxide (CO_2) despite its comparably low concentrations.

Studies on isotopic signatures of N_2O in the atmosphere confirmed that anthropogenic action is responsible for this development and the majority of N_2O is emitted by soils (Park *et al.*, 2012; Snider *et al.*, 2015). In an optimal scenario, the nitrogen we put on fields would be 100 % taken up by the plant and be available as a nutrient in our food. In reality, since communities in natural ecosystems learned to compete for this scarce resource, the applied nitrogen is also taken up by microbes, where it enters the microbial nitrogen cycle. Here, many biochemical pathways carried out by microbes are potentially producing N_2O, which is the actual source of elevated N_2O emissions in agricultural systems (Mosier *et al.*, 1998; Smith and Conen, 2004). The amount of N_2O emitted from soils and agriculture was estimated to be 13 Tg N yr^{-1} and more than half of it (7 Tg N yr^{-1}) is attributed to anthropogenic action (Fowler *et al.*, 2013). Although the negative effect of anthropogenic nitrogen inputs to soil ecosystems on our climate has been recognized, applying suitable strategies to mitigate these impacts has had little success. These include application of nitrification inhibitors, variation in dosing and time of application of fertilizers and variation in nitrogen forms applied to fields (Mosier *et al.*, 1998; Bell *et al.*, 2015).

Therefore, it is critical to improve our fundamental understanding of the nitrogen cycle, the biogeochemical pathways and players involved, if we are to accurately predict and reduce ecosystem contamination related to industrial/agricultural processes.

Soil ecosystems and nutrient cycling

Soil forms a thin layer on the Earth's surface, where it serves as a nutrient and water reservoir for plants, and is thus essential for the nutrition of higher life forms. The fine structured assembly of soil creates microhabitats with versatile conditions for life, constructing an ecosystem considered to be the most diverse among all habitats on the planet (Dance, 2008). Up to 1 billion bacterial cells and between 100 m to 1 km of fungal hyphae were estimated in 1 g of soil (Elmholt and Kjøller, 1987; Gans *et al.*, 2005; Bardgett *et al.*, 2005; Roesch *et al.*, 2007). These numbers cannot be matched by other ecosystems. For example, surface waters in oceans were found to harbor up to 10^5 cells per mL, which is a comparable volume to 1 g of soil (Sogin *et al.*, 2006). This shows that the density of life in soil is astonishing, and this is partially related in part to the fine structured environment of soil. In addition to the microbiological portion of the soil biome, we find organisms like protozoans, nematodes and higher biota. Plants are also an important part of these ecosystems, since their roots are a major nutrient source for belowground communities by provision of root exudates or dead plant material for decomposition processes when the plant dies (Henry *et al.*, 2008; Rennenberg *et al.*, 2009). Altogether, these organisms form a food web, where organic matter and energy are transformed and cycled (Figure 4). Looking at the immense number of microbes found in soil, it is not surprising that various interactive relationships occur. For example, bacteria were found to grow in the immediate surroundings of mycorrhizal and free-living fungi called the mycosphere, where they secrete easily accessible carbon molecules that serve as nutrients for these bacteria (Warmink and van Elsas, 2008; Warmink *et al.*, 2009; Nazir *et al.*, 2010).

A key factor for the functioning of soil ecosystems is its structure. Generally, soil can be defined as an assembly of particles of organic and inorganic origin. This assembly was found to be not random, rather consisting in constant rearrangements carried out by microbial and plant activity (Six *et al.*, 2004; Bronick and Lal, 2005).

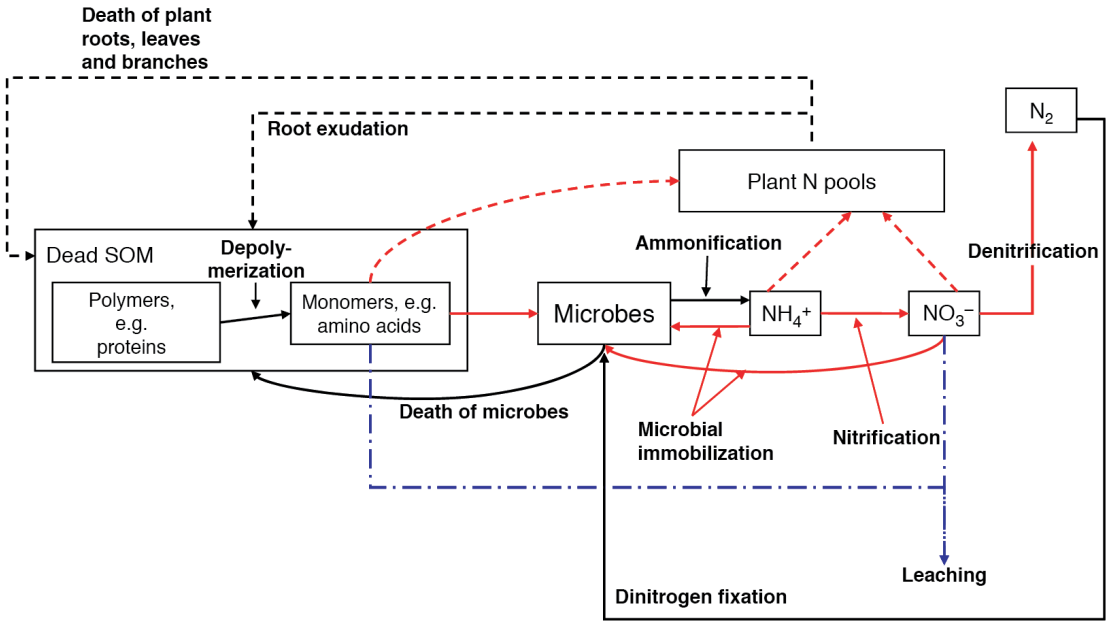

Figure 4: Nutrient cycling in soil showing recycling of organic matter from plant N pools. SOM, soil organic matter; dashed lines: plant processes; solid lines: microbial processes; red dashed and solid lines: competitive processes between plants and microbes; Blue dashed lines: hydrological transport pathways. Adapted from (Rennenberg *et al.*, 2009).

This rearrangement is linked to the carbon cycle, since soil organic matter drives the structuring of soil. Organic matter entering the soil is broken down and aggregate formation takes place where single building blocks like sand, silt and clay stabilize around organic matter encrusted with microbial products and earthworm mucus. Microbial activity is the key in this process as fungal hyphae and exopolysaccharides excreted by microbes function as glue in the stabilization of aggregates (Figure 5). At the same time, while they form their own micro environment, microorganisms use the organic matter as nutrient source. When nutrients are exhausted, the aggregate eventually disrupts. Disturbances such as tillage enhance the turnover of aggregates and reduce the formation of new aggregates (Six *et al.*, 2000). Thus the capacity of soil in binding organic matter, also called carbon sequestration, is reduced. Altogether, a complex and porous system is formed where water content and air can coexist. Since soil structure changes over time, it is sometimes called the fourth dimension of soil (Bardgett *et al.*, 2005).

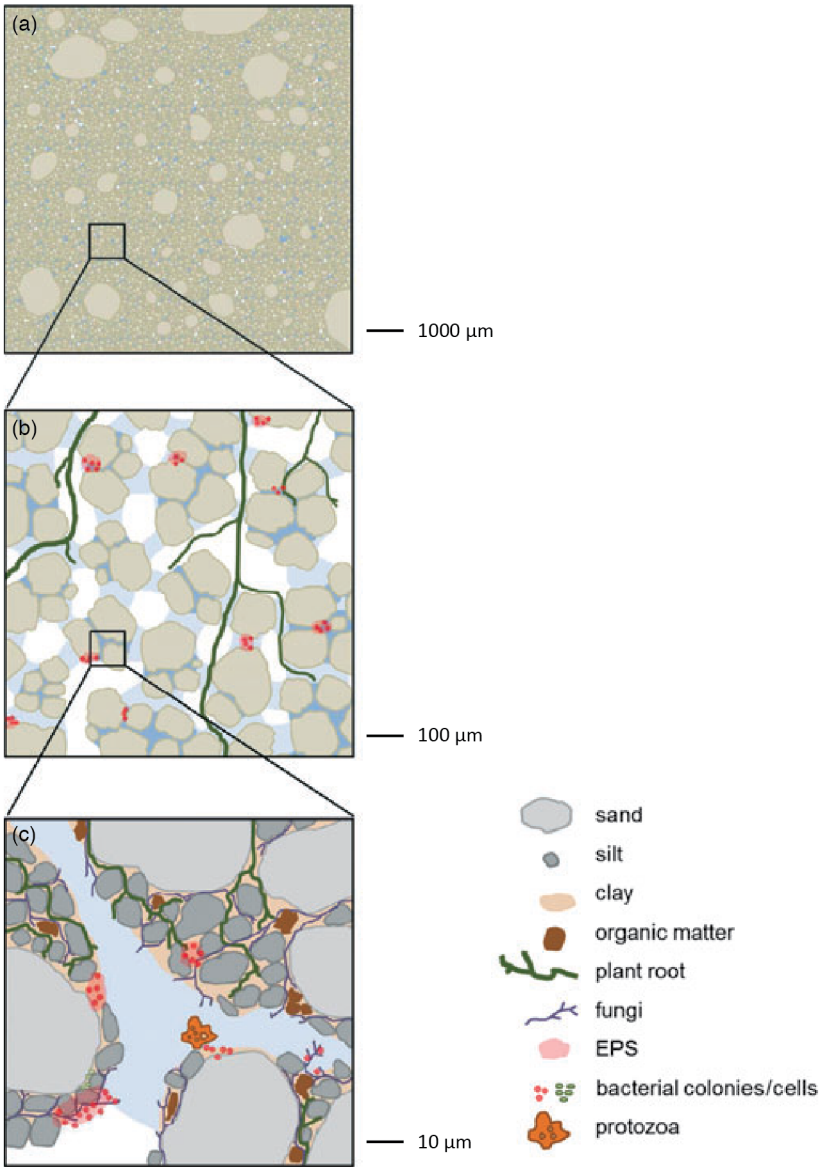

Figure 5: Spatial arrangement of soil particles on millimeter (a) to micrometer (b, c) scale. EPS: exopolysaccharide. Figure adapted from (Vos *et al.*, 2013).

One can imagine that due to the complex structure of a soil matrix, the environmental parameters (like oxygen concentration, water and nutrient availability and pH) that shape microbial communities might change on small scales. It has been estimated that one gram of soil provides 20 m^2 of surface area and that just 1 % of this area is actually covered by microbes (Bardgett *et al.*, 2005). This suggests that microorganisms are not randomly distributed in soil, but that they proliferate in micro-habitats where they find the most suitable conditions for their lifestyle. Soil communities have been studied over various scales from

kilometers to meters to centimeters (Green and Bohannan, 2006; Vos and Velicer, 2006; Enwall *et al.*, 2010; Bru *et al.*, 2011). So far, only little work has focused on differentiating functional communities at the micrometer scale, the actual size scale of microbes. This is a critical aspect, because if we are to gain fundamental knowledge on the pathways leading to N_2O production, we need to study the processes at the scale at which they occur, i.e. the microscale.

The microbial Nitrogen Cycle

The microbial component of these complex soil communities carries out several crucial steps in nutrient cycling processes. They play key roles in the carbon cycle, where they mainly act as decomposers by breaking down organic matter, thus making it bioavailable again for other microbes or plants (Nielsen *et al.*, 2011; Schimel and Schaeffer, 2012). Within the nitrogen cycle, the role of microbes seems even more critical, since certain biochemical transformations of nitrogen were found to be carried out exclusively by these organisms (Hayatsu *et al.*, 2008).

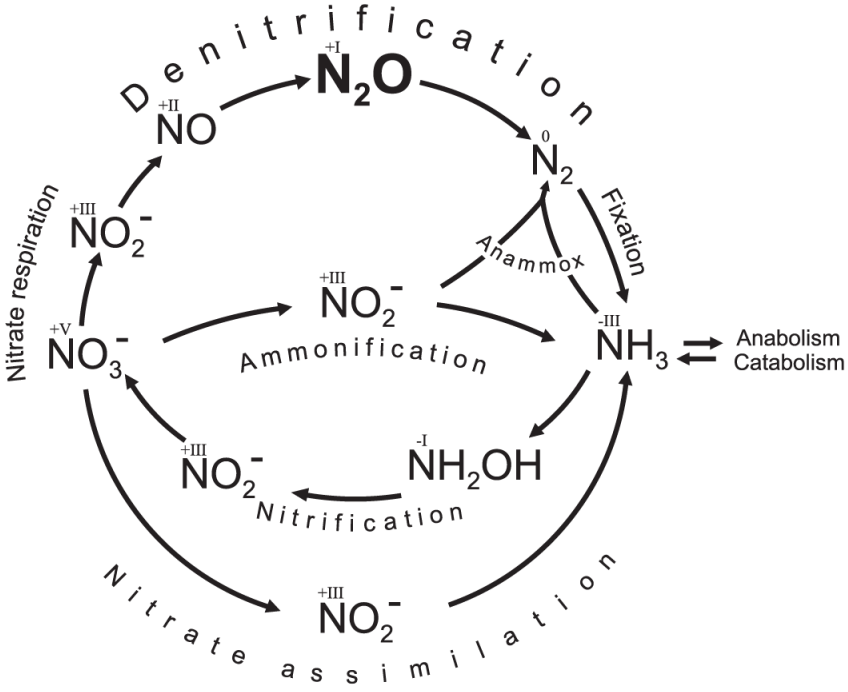

Figure 6: Biochemical processes within the N-cycle and occurring nitrogen forms. Roman numerals indicate the oxidation state of the nitrogen atom in the chemical compound. Figure adapted from (Zumft and Kroneck, 2007).

Most organisms have to take up nitrogen in a reduced (NH_4^+) or oxidized state (NO_3^-), which makes it a nutrient that is competed for in natural environments. Nitrogen is therefore constantly being reduced or oxidized, since microbes find ways to generate energy from manifold conversion processes, which altogether close the nitrogen cycle (Figure 6).

Two input streams in the microbial nitrogen cycle can be identified. One is the fixation of nitrogen from the atmosphere by free-living and symbiotic bacteria and archaea (Reaction 1) (Zehr *et al.*, 2003). These organisms possess highly conserved nitrogenases (NIF) that can catalyze the break-up of the triple bond of dinitrogen gas (N_2) and generate NH_3 in anaerobic environments after the following equation:

$$2N_2 + 6H_2O \xrightarrow{NIF} 4NH_3 + 3O_2$$

Reaction 1: Biological nitrogen fixation (BNF). NIF, nitrogenase.

Another input of nitrogen in the cycle is the recycling of organic matter, where formerly anabolically incorporated nitrogen in biomass is released again by decomposition processes, also called nitrogen mineralization.

When oxygen is present, NH_4^+ can be oxidized to NO_3^- by nitrification (Reaction 2) (Klotz and Stein, 2008). Specific groups of bacteria and archaea perform these biochemical reactions. It was considered that the oxidation of ammonium to nitrite and the further oxidation to nitrate is carried out by distinct groups of organisms, namely ammonia oxidizing bacteria (AOB) or archaea (AOA) and nitrite oxidizing bacteria (NOB). During nitrification, NH_4^+ is first oxidized to hydroxylamine (NH_2OH) by an ammonia monooxygenase (AMO), which is then further oxidized to nitrite by hydroxylamine oxidoreductase (HAO). Finally, nitrite is oxidized to nitrate by a nitrite oxidoreductase (NXR).

$$NH_3 + O_2 + 2H^+ + 2e^- \xrightarrow{AMO} NH_2OH + H_2O$$

$$NH_2OH + H_2O \xrightarrow{HAO} NO_2^- + 5H^+ + 4e^-$$

$$NO_2^- + 0.5O_2 \xrightarrow{NXR} NO_3^- + H_2O$$

Reaction 2: Nitrification showing enzymes involved in each step. AMO, ammonia monooxygenase; HAO, hydroxylamine oxidoreductase; NXR, nitrite oxidoreductase. Abbreviations stand for any enzyme capable to catalyze the respective reaction.

Recently, a *Nitrospira* strain able to catalyze the complete oxidation from ammonium to nitrate was discovered (Daims *et al.*, 2015).

If oxygen becomes limited, NO_3^- or NO_2^- might be reduced again to either NH_4^+ by dissimilatory nitrate reduction to ammonium (DNRA), sometimes also called nitrate-ammonification (Reaction 3) (Simon, 2002).

$$NO_3^- \xrightarrow{NAR} NO_2^- \xrightarrow{NIR} NH_4^+$$

Reaction 3: Dissimilatory nitrate reduction to ammonium (DNRA) showing enzymes involved in each step. NAR, nitrate reductase; NIR, nitrite reductase- ammonium producing. Abbreviations stand for any enzyme capable to catalyze the respective reaction (Mohan and Cole, 2007).

Reduction of NO_3^- to NO_2^- is carried out by the same reductases as those found in denitrifiers. Two distinct enzymes were found to reduce the NO_2^- to NH_4^+. A NADH-dependent reductase NirB or a cytochrome c reductase NrfA (Darwin *et al.*, 1993; Cole, 1996; Einsle *et al.*, 1999). Another important reductive pathway ending in the production of N_2 gas via NO and N_2O is called denitrification and will be described later in more detail (Reaction 6). This pathway is characterized by the use of a dissimilatory nitrate reductase (dNAR) for the reduction of NO_3^- to NO_2^- in contrast to the reduction of nitrate to ammonium for anabolic purposes, where an assimilatory nitrate reductase catalyzes this reaction (Guerrero *et al.*, 1981; Crawford and Arst, 1993; Mahne and Tiedje, 1995; Zumft, 1997).

The anaerobic ammonia oxidation (Anammox) pathway describes an alternative mechanism for the reduction of NH_4^+ to N_2 (Reaction 4) (Strous *et al.*, 1999). The NO_2^- is first reduced to NO and NH_4^+ serves as a terminal electron acceptor in the further reactions:

$$NO_2^- \xrightarrow{NIR} NO + NH_4^+ \xrightarrow{HH} N_2H_2 \xrightarrow{HZO/HAO} N_2$$

Reaction 4: Anaerobic ammonia oxidation (ANAMMOX) showing enzymes involved in each step. NIR, nitrite reductase; HH, hydrazine hydrolase; HZO/HAO hydrazin/hydroxylamine oxidoreductase. Abbreviations stand for any enzymes that catalyze the respective reaction (Kraft *et al.*, 2011).

Anammox bacteria were found to inhabit marine and terrestrial ecosystems and were also shown to perform DNRA when ammonium becomes limiting (Penton *et al.*, 2006; Kartal *et al.*, 2007; Humbert *et al.*, 2009). Also, the technical application of these organisms in wasterwater treatment promises a reduction in costs and N_2O emissions (Ali and Okabe, 2015).

Nitrous oxide as an intermediate product within the N-cycle only occurs in denitrification. However, complete denitrifiers, incomplete denitrifiers, nitrate reducers, microbes performing DNRA and nitrifiers were shown to potentially contribute to biological N_2O production (Wrage *et al.*, 2001; Megonigal *et al.*, 2003; Stremińska *et al.*, 2011). Additionally, an abiotic process might also lead to the formation of N_2O by the reduction of NO_2^-. Due to its biological counterpart, this process was called chemodenitrification (Reaction 5) (Nelson and Bremner, 1969; 1970a). Nitrite is chemically reduced to NO and further to N_2O at low pH and when metal ions are present (Nelson and Bremner, 1970b; Kampschreur *et al.*, 2011).

$$NO_2^- + Fe^{2+} + 2H^+ \longrightarrow Fe^{3+} + NO + H_2O$$

$$NO + Fe^{2+} + 1H^+ \longrightarrow Fe^{3+} + 0.5N_2O + 0.5H_2O$$

Reaction 5: Chemical reduction of nitrite to N_2O via NO (Van Cleemput and Samater, 1995).

It was shown, for example, that ferrous-iron produced by ferric-ion reducing bacteria catalyzed the chemical reduction of present nitrite to N_2O (D. C. Cooper and Picardal, 2003; Coby and Picardal, 2005).

Quantifying the contribution of various pathways in the nitrogen cycle to N_2O emissions is a difficult task. Distinction between denitrification and nitrification mediated N_2O production could be achieved by a stable isotope approach and use of inhibitors (Bateman and Baggs, 2005). More complex models were developed recently, but further work has to be carried out to be able to distinguish single nitrogen conversion processes occurring at N_2O emission events (Müller *et al.*, 2014).

Denitrification is often considered to be the main process involved in N_2O emissions from agricultural soil under anoxic conditions (Webster and Hopkins, 1996; Pihlatie *et al.*, 2004; Li *et al.*, 2016). Furthermore, denitrifying enzymes are widespread in bacteria and also some archaea and fungi (Zumft, 1997; Philippot, 2002; Shoun *et al.*, 2012). A broader understanding of the ecological interactions among these microbes might help to develop targeted mitigation strategies for N_2O emissions from agricultural soil.

Denitrification in bacteria

Energy generation in every lifeform is based on exploitation of redox potential differences. This is either achieved by the build up of a proton motive force (pmf) across membranes by electron transport chain reactions or by substrate level phosphorylation in fermentative pathways (Simon *et al.*, 2008). In both cases, energy is stored in adenosine triphosphate (ATP) and can be used later by the cell.

Microorganisms can use various terminal electron acceptors in respiratory chains. Oxygen is the most effective, followed by nitrate, manganese, iron, sulfur and carbon dioxide. In contrast to the reduction of O_2 to H_2O, the complete reduction of NO_3^- to N_2 is a stepwise process called denitrification (Reaction 6).

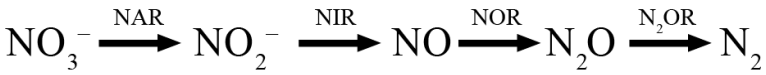

Reaction 6: Denitrification showing enzymes involved in each step. NAR, nitrate reductase; NIR, nitrite reducatase; NOR, nitric oxide reductase; N_2OR, nitrous oxide reductase. Abbreviations stand for any enzymes capable of catalyzing the respective reaction (Zumft, 1997).

All steps in this process are catalyzed by multisite metalloenzymes (van Spanning *et al.*, 2007). Nitrate reductases (NAR) reduce NO_3^- to NO_2^- and were found to be membrane bound (NarG) or located within the periplasm (NapA) (Blasco *et al.*, 2001; Simon *et al.*, 2003; Ellington *et al.*, 2005). Nitrite is reduced by nitrite reductases (NIR) to nitric oxide (NO). As the first step producing a gas molecule, it is considered a key feature of denitrification. The copper-containing enzyme NirK as well as a heme-containing cytochrome cd_1 NirS were both found to carry out nitrite reduction (Tavares *et al.*, 2006). So far, no organism where both NIR-types are encoded has been found. The NO produced is further reduced to N_2O by nitric oxide reductases (NOR). Three enzymes were found to catalyze this reaction in bacteria, namely a long chain qNOR or a short chain cNOR in Gram-negative bacteria, and a qCu_ANOR in Gram-positive bacteria (Hendriks *et al.*, 2000; Suharti and S. de Vries, 2005; Tavares *et al.*, 2006). Finally, the last step in denitrification is the reduction of N_2O to N_2 gas that is catalyzed by nitrous-oxide reductases (N_2OR). Two variants are known for N_2ORs, a z-type N_2OR as well as a newly discovered c-type N_2OR (Sanford *et al.*, 2012; Jones *et al.*, 2013). The two types of enzymes are found in phylogenetically distinct groups of bacteria and the possibility of a niche specialization in N_2O reduction among these groups is currently under discussion (Jones *et al.*, 2014).

Terminology describing nitrate reducing organisms has diversified. Denitrifiers are generally considered to be able to reduce nitrate all the way to N_2 gas. In contrast, many organisms were found to be so called incomplete denitrifiers, possessing various combinations of the involved enzymes that do not allow for complete reduction. Furthermore, microbes just using the most energy yielding reduction of NO_3^- to NO_2^- are defined as nitrate reducers or nitrate

respirers. Nitrite reduction was also found in ammonia oxidizing bacteria, known as nitrifier denitrification (Wrage *et al.*, 2001).

Denitrification is, in contrast to nitrification, phylogenetically widespread and no pattern of the enzymes over the bacterial tree of life could be found (Philippot, 2002). This makes it additionally challenging for microbial ecologists to study this function, since pure phylogenetical markers like ribosomal RNA sequences are difficult to interpret with respect to a denitrifying community.

Nitrogen reduction in fungi

Electron transport chains in fungi are located in mitochondria, as is the case for all eukaryotic organisms, where enzymes for dissimilatory nitrogen reduction were also found (Kobayashi *et al.*, 1996). Since nitrous oxide was measured in gas of fungal cultures, their potential role as producers of this greenhouse gas was hypothesized (Bleakley and Tiedje, 1982). Later, the production of N_2O in fungi was linked to a dissimilatory nitrate reduction process in *Fusarium oxysporum* which was consequently named fungal denitrification (Shoun and Tanimoto, 1991). Nitrite reduction in fungi is catalyzed by a copper containing nitrite reductase nirK (Long *et al.*, 2015). Comparison of amino acid sequences from nitrite reductases of eukaryotes, bacteria and archaea suggested that nirK from these domains had the same origin (S.-W. Kim *et al.*, 2009). The random distribution of nirK among proteobacteria might be due to horizontal gene transfer between these bacteria, whereas eukaryotic nirKs were found to be systematically distributed.

The enzyme catalyzing the reduction of nitric oxide to N_2O in fungi was found to be a cytochrome P450 monooxygenase that was consequently called P450nor. This class of enzymes is abundant in fungi and carries out essential roles in various cellular processes (Črešnar and Petrič, 2011). Although eukaryotic P450 enzymes are generally found to be membrane bound, P450nor was found to be soluble and thus located in the cytosol (Takaya, 2002). Structure analysis of P450nor showed a higher similarity with bacterial derived P450-

like enzymes, however, a P450nor has yet to be found in bacteria (Shoun *et al.*, 2012). Due to its special function among P450 enzymes, attention was drawn to it. Contradicting results on the NO reduction behavior of fungi fueled discussions as to whether it contributes to energy generation for the organism, thus being a respiratory process, or simply has a detoxifying function to avoid high concentrations of reactive NO in the cell. For example, even in the model organism *Fusarium oxysporum,* the simultaneous expression under denitrifying conditions of flavohemoglobin (Fhb), which is expressed in bacteria to counteract NO stress, was observed (S.-W. Kim *et al.*, 2009; Forrester and Foster, 2012). Later, these findings were confirmed by the same researchers in another model organism for fungal denitrification, *Fusarium lichenicola* (former *Cylindrocarpon tonkinense*), and the expression of Fhb was linked to denitrification in this fungus (S.-W. Kim *et al.*, 2010). Furthermore P450nor was found to have a pure NO-detoxifying function in the human pathogen *Histoplasma capsulatum* (Nittler *et al.*, 2005).

Nitrite seems to be the preferred substrate in fungal denitrification, since N_2O could be detected after cultivation in nitrite containing media (Mothapo *et al.*, 2015). Development of molecular tools for studies on contribution of fungal denitrification to N-cycling processes is ongoing at the moment and primers for fungal nitrite and nitric-oxide reductases were just recently published (Long *et al.*, 2015; Wei *et al.*, 2015; Higgins *et al.*, 2016). High similarities to cytochrome P450 like enzymes or bacterial nirK makes the distinct detection of these genes from environmental samples difficult. In order to identify ecological significance of these genes, we need to study more expression profiles of fungi under anaerobic or hypoxic conditions. Metatranscriptomic appoaches in controlled laboratory experiments could be first steps to improve the picture we have of a nitrogen reducing fungal community. Whole genome sequencing of candidate species would provide information on the general genetic potential of these organisms with respect to nitrogen cycling, especially the presence or

absence of P450nor versus NO-active globin sequences, and could mark an important next step in this research field.

Organic matter decomposition and its implications in the N-cycle

Chemical fertilizer addition causes elevated N_2O emissions from soil ecosystems, but the application of organic matter as fertilizer was also shown to initiate this process (McSwiney and Robertson, 2005; Shcherbak, Millar, and Robertson, 2014a; Zhu-Barker *et al.*, 2015). In natural environments, nitrogen has to be recycled from biomass or fixed from the atmosphere by microbes (Figure 4). When dead organic material enters soil, a depolymerisation process breaks down these polymeric structures to molecules that can be reused by microbes. The underlying mechanisms of organic matter degradation in soil are currently under discussion. Modern analytical methods support the hypothesis that soil organic matter is continuously degraded from bigger to smaller polymers rather than the widely accepted model of humification, which could not be confirmed by carbon chemistries found in soil (Lehmann and Kleber, 2015).

Dead plant material mainly consists of lignocellulosic compounds. These composites of polysaccharide structures like cellulose, hemi-cellulose, lignin and pectin are building blocks of plant cell walls and thus provide nitrogen in the form of cell wall proteins. This step also marks an interconnection of the nitrogen cycle with the carbon cycle, since it not only provides nitrogen, but also the necessary carbon for a heterotrophic nitrogen cycling community.

When carbon and nitrogen cycling activities were coupled in prediction models for global terrestrial carbon uptake following elevated CO_2 levels in the atmosphere, predicted values were reduced by 74 % in comparison to a sole carbon model, underlining the interconnection of these nutrient cycles (Thornton *et al.*, 2007).

Organisms and enzymes performing these degradation processes have been studied intensively, since the ability to degrade recalcitrant polysaccharides from plant fixed carbon structures is also of interest for industrial processes like the provision of sugar compounds from plant material for the further fermentation to biofuels (Voloshin and Rodionova, 2016).

A complex set of enzymes is involved in the deconstruction of lignocellulosic compounds (Figure 7). For example, the complete degradation of a relatively simple structured polymer like cellulose requires three classes of enzymes, ß- 1,4-endoglucanases, cellobiohydrolases and ß-glucosidases. These enzymes are part of the so called carbohydrate active enzymes which comprise glycoside degrading and generating enzymes (Carbohydrate Active Enzymes database; http://www.cazy.org/) (Lombard *et al.*, 2013).

The biggest group of glycoside bond cleaving enzymes are glycoside hydrolases (GH) (Henrissat, 1991). This class of carbohydrate active enzymes is currently divided in 131 families based on amino acid sequences of the structurally related catalytic modules and catalyze the hydrolysis of O-, N- and S-linked glycosides (Davis and Sinnott, 2008). Exo and endo acting glycoside hydrolases are distinguished due to their location of activity within the polysaccharide chain (endo) or at the end of these chains (exo), cleaving single sugar molecules from the chain like ß-galactosidases.

Another group of glycoside bond cleaving enzymes are polysaccharide lyases (PL). These enzymes cleave uronic-acid containing polysaccharides that occur in various amounts in hemicelluloses and pectins of higher plants (Figure 7 (b), (c)) (Willför *et al.*, 2009). The third group of carbohydrate degrading enzymes are classified in auxiliary activity families (AA) in the CAZy classification system (Levasseur *et al.*, 2013). These families generally include enzymes that have an assisting function for GHs and PLs. For example, family AA9 includes

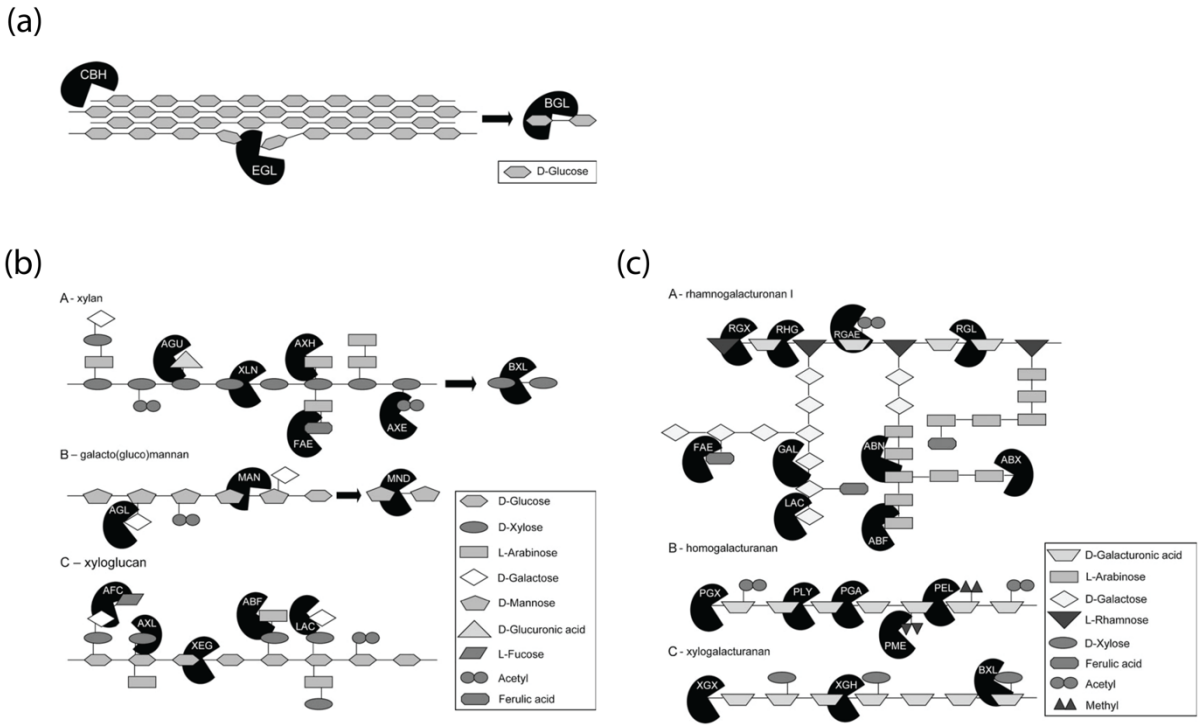

Figure 7: Enzymes involved in cleavage of glycosidic bonds within (a) cellulose and various forms of (b) hemicellulose and (c) pectin. Different shapes correspond to distinct glycoside residues of the polysaccharide. *ABF, α-arabinofuranosidase;* ABN endoarabinanase, ABX exoarabinanase, AFC α-fucosidase, AGL α-1,4-galactosidase, AGU α- glucuronidase, AXE acetyl (xylan) esterase, AXH arabinoxylan α-arabinofuranohydrolase, AXL α-xylosidase, *BGL β- glucosidase,* BXL β-1,4- xylosidase, *CBH cellobiohydrolase, EGL β-1,4-endoglucanase,* FAE feruloyl esterase, GAL β- 1,4-endogalactanase, LAC β-1,4-galactosidase, MAN β-1,4-endomannanase, MND β-1,4-mannosidase, PEL pectin lyase, PLYpectate lyase, PGA endopoly-galacturonase, PGX exo-polygalacturonase, PME pectin methyl esterase, RGAE rhamnogalacturonan acetyl esterase, RGL rhamnogalacturonan lyase, RHG endorhamnogalacturonase, RGX exorhamnogalacturonase, XEG xyloglucan-active β-1,4- endoglucanase, XGH endoxylogalacturonase, XGX exoxylogalacturonase XLN β-1, 4-endoxylanase. Figure adapted from (van den Brink and R. P. de Vries, 2011a).

lytic polysaccharide monooxygenases (LPMO) that can attack various polysaccharides and provide new chain ends for further degradation (Kracher *et al.*, 2016; Johansen, 2016).

The application of omic-approaches recently revealed that carbohydrate degradation is widespread over the tree of life including fungi, bacteria and higher eukaryotes (Bugg *et al.*, 2011; Cragg *et al.*, 2015; de Gonzalo *et al.*, 2016). This led to a shift in the paradigm of solely fungal decomposition processes towards that of a combined community responsible for the complete deconstruction of organic material. However, fungi are still considered key players in these processes since they efficiently perform the first attacks on recalcitrant polymers, providing access to easier substrates to possible beneficiaries (Eastwood *et al.*, 2011; Payne *et*

al., 2015; Kracher *et al.*, 2016). In addition, their growth in hyphae allows them to access zones with high OM concentrations in contrast to immobile bacteria. Thus, they are able to transport carbon compounds over longer distances and to overcome nutrient poor sites in soil (Jennings, 1987).

The occurrence of carbohydrate degrading enzymes encoded in fungal genomes could be linked to the natural habitat of the respective organisms (van den Brink and R. P. de Vries, 2011a). For example, in Saccharomyces yeasts naturally occurring on the surface of rotting fungi or in the gut of termites, low numbers of carbohydrate active enzymes were found in the genomes (Jeffries *et al.*, 2007; Liti *et al.*, 2009). Filamentous fungi were found to have much higher numbers of these enzymes encoded in their genomes (Coutinho *et al.*, 2009; Rileya *et al.*, 2014). Fungi having decomposing lifestyles also seem to develop specificity towards the chemical nature of the substrate to attack. Full genomes of wood-degrading fungi revealed that distinct species possess completely different mechanisms for carbohydrate degradation, underlining the substrate specialization of this organisms (Ohm *et al.*, 2014). For example, Aspergilli were found to have multiple enzymes encoded pectin degradation, in contrast to other filamentous fungi characterized as cellulose or lignin- degrading specialists like *T.reesei* or *Phanerochaet chrysosporium* respectively, or Zygomycota which are often found to be specialized in the use of easily accessible and digestible substrates (Richardson, 2009a; Battaglia *et al.*, 2011; van den Brink and R. P. de Vries, 2011a).

It is unlikely that two groups of microorganisms sharing a diverse habitat like soil are completely independent from one another. In fact, manifold interactions in plant-plant, plant-microbe, microbe-higher organisms and microbe-microbe relations have been observed and studied in soil ecosystems (Wardle, 2006; Faust and Raes, 2012; Bakker *et al.*, 2014).

A well know example for mutualistic interactions in soil is the symbiosis between plant roots and arbuscular mycorrhizal fungi (AMF) where nitrogen uptake by the fungus beneficial for the plant happens in exchange for plant fixed carbon substrates for the fungus (Lang *et al.*,

2010; Tisserant *et al.*, 2013; van der Heijden, Martin, *et al.*, 2015). This relationship has been diversified after the observation of bacteria colonizing AMF (Garbaye, 1994; Frey-Klett *et al.*, 2007). These bacterial communities were meanwhile found to influence the functioning of these ecosystems (Johansson *et al.*, 2004; Frey-Klett *et al.*, 2011). For example, an antagonistic interaction between AMF and bacteria was found for the competition of decomposition products (Leigh *et al.*, 2011). Furthermore, the colonization of bacteria on mycorrhizal hyphae seems to depend on the fungal species present, suggesting a close interaction between specific members of bacteria and fungi (Toljander *et al.*, 2006). In addition to the AMF-plant symbiosis, bacteria were recently found to take part in the close symbiosis of fungi and green algae in lichens, which further supports the hypothesis that interdomain interactions are probably more likely than we thought (Aschenbrenner *et al.*, 2016).

Free living fungi interactions with bacteria have also been observed (Boer *et al.*, 2005; Warmink *et al.*, 2009). Interactions can be antagonistic, such as competition for a limiting resource or direct interference. Trophic competition between fungi and bacteria for nutrients such as carbon is well documented in many environments and can impact biogeochemical cycling (Schmidt *et al.*, 2012). For example, studies have shown that competitive interactions between fungi and bacteria can be important during the fungal degradation of recalcitrant organic matter such as lignin (Bugg *et al.*, 2011). Interactions can also be cooperative, such as the transfer of complementary metabolites or quorum sensing(Berry and Widder, 2014). Recent evidence suggests a role of fungal-bacterial consortia in the degradation and transformation of environmental PAHs (Folwell *et al.*, 2016). However, the role and importance of bacterial-fungal consortia in environmental nutrient cycling have been largely overlooked and need to be clarified if we are to fully comprehend and predict how communities will respond to changing environments.

The abundance of AMFs in a greenhouse experiment has been connected to N_2O emissions, since emissions increased when AMF reduced mutants of plants were cultivated (Bender *et al.*, 2013). Nitrite reductase and nitrous oxide reductase copy numbers of the co-inhabiting bacterial community correlated negatively and positively, respectively, with the abundance of AMFs, which describes the first observation of an indirect effect of fungi on N_2O emissions through their influence on the bacterial nitrogen cycling community. So far, research on N_2O emissions has focused on specific processes in the N-cycle and tried mainly to link occurrence of N_2O production to activity of groups of organisms. In the case of fungal denitrification, studies on soil environments were carried out using prokaryotic and eukaryotic inhibitors to identify differences in N_2O emission or production potential (Crenshaw *et al.*, 2007; Laughlin *et al.*, 2009; Marusenko *et al.*, 2013; Wei *et al.*, 2014; H. Chen, Mothapo, and Shi, 2014a; 2014b). Since N_2O production decreased significantly after the addition of fungicides, fungi were often considered to be the prime N_2O producers in these environments. However, although fungi were found to possess an enzymatic base allowing them to perform nitrogen reduction to N_2O, we currently observe a contradiction between data obtained from soil microcosm studies and from fungal pure cultures. N_2O production rates in pure cultures of fungi were found to be 3 to 6 orders of magnitude lower than those of denitrifying bacteria (Betlach and Tiedje, 1981; I. C. Anderson and Levine, 1986; Jirout *et al.*, 2012; Mothapo *et al.*, 2013; Wei *et al.*, 2014; Maeda *et al.*, 2015). Although it is difficult to compare the results from two distinct experimental setups, the decrease of N_2O production after fungicide addition in soil cannot be explained by rates observed in fungal cultures.

It is our hypothesis that the behavior in N_2O emission reduction in fungal inhibition experiments point to the disturbance of a close relation between free living fungi and a potential N_2O producing bacterial community. By the inhibition of fungi, an unintended disturbance of carbon breakdown might happen, which slows down carbon substrate support for bacteria. A nitrogen cycling bacterial community could thus be indirectly affected. To

clarify this possible connection between carbon and nitrogen cycling microbes, we need to investigate organic matter degradation with respect to N_2O production in soils and the activity of fungal and bacterial communities involved in these processes.

Objectives of this thesis

This thesis is divided into three chapters that each address different hypotheses developed during my PhD. In the first chapter, we intended to localize nitrogen-cycling potentials of soil communities on a micro-scale level using a physical fractionation approach. We hypothesized that denitrifying potentials are located on the inside of soil aggregates where anaerobic microsites are present. Changes in fungal and bacterial communities in size fractions of a pristine grassland soil were measured, as well as the abundances of nitrogen cycling marker genes.

The lack of molecular tools to investigate the occurrence and activity of fungal nitrogen reducing members in DNA extracts from soil led us to a screening approach on soil fungi to collect data on their nitrogen reducing and N_2O production potential. The results are presented and discussed in the second chapter. We hypothesized that fungi use assimilatory nitrate reductases in a dissimilatory manner when exposed to anoxic conditions. Twenty-two fungal isolates from agricultural soil capable of assimilating nitrate were incubated in a robotized gas sampling system where we could follow the production of NO and N_2O from nitrite by the pure cultures.

In the third chapter, a potential link between carbon degradation and nitrogen cycling was studied using metatranscriptomic and metagenomic approaches. Here, we hypothesized that fungal driven carbon degradation affects a nitrogen cycling bacterial community and thus potential N_2O production. Agricultural soil was incubated for 30 days in microcosms and organic materials with varying carbon chemistries were added. Soil samples were taken eight times during this incubation and metatranscriptomes, metagenomes as well as nitrogen chemistries in the soil and emitted greenhouse gases were analyzed to follow the evolution of communities after substrate addition.

Chapter 1: Microbial Community Changes and N-cycling potential in Rothamsted Park Grass Soil Fractions

Abstract

Soil ecosystems constitute the basis of human life as they are crop production environments and drive major nutrient cycles on our planet. Increased nitrogen inputs in agricultural systems cause severe environmental impacts like leaching of nitrate in groundwater and nitrous oxide emissions to the atmosphere. Although research has identified enzymes and organisms potentially contributing to an elevated production of N_2O in soil, we still lack a fundamental understanding of how these processes are controlled in soils. Determining the spatial localization of biogeochemical processes within soil could help us improve models for nutrient usage of soil communities. We were interested in the compartmentalization of bacterial and fungal communities and nitrogen cycling potentials in a pristine soil environment and hypothesized that nitrogen reductive and oxidative processes are linked to inner aggregate and surface derived communities, respectively. Community fingerprints and abundance of nitrogen cycling marker genes as well as chemical signatures of particle size fractions of Rothamsted Park Grass soil were analyzed. Results indicated distinct communities in the inside of soil aggregates as compared to surface derived soil compartments, where a higher diversity of bacteria was found. Dominance of *Agaricales* and *Mucorales* in fungal communities in inside and outside fractions, respectively, suggested a compartmentalization of fungi due to their distinct carbon usage strategies. Abundance of nitrogen cycling genes was found to be comparable in all isolated fractions and could be linked to organic carbon and nitrogen concentrations, which did not support our hypothesis.

Introduction

As we have seen in the general introduction, soil harbors an immense diversity of life and its structure exposes microorganisms to many environmental conditions at a micrometer scale. At the same time, this makes it difficult to study these environments. In this chapter, we seeked to dissect bulk soil in order to isolate microenvironments that might be relevant to nitrogen cycling activities. We were also interested as to whether or not distinct bacterial and fungal communities were linked to these soil compartments.

A critical point in studying soil ecosystem functioning is related to scaling: changes are measured on a global scale with meter-sized samples or larger, but the underlying processes occur at micro-scales, i.e. at the scale where microorganisms live. For example, it was shown that loss of biodiversity impaired soil ecosystem functions like plant diversity, decomposition, nutrient retention and nutrient cycling (Wagg *et al.*, 2014). These findings suggest that a specific function carried out by specific members could be altered or influenced by the presence or absence of various soil inhabiting organisms.

Soils are complex mixtures of minerals, water, air and organic matter, and the porous structure of soil in combination with a fluctuating water content leads to the formation of microenvironments with various nutrient qualities and oxygen concentrations. Therefore, when trying to understand biogeochemical processing, it is important to study these microenvironments, which are difficult to access. Micro-scale fractionation of soil in particle size fractions (PSFs) has been used to attempt to isolate functional soil compartments (Chotte *et al.*, 1993; Moni *et al.*, 2012). Usually, this is achieved by an initially soil dispersion step with or without use of mechanical force and a subsequent size separation step by sieving, settling or centrifugation of soil particles (Vos *et al.*, 2013). From a microbiological point of view, each fraction can be considered as an isolated microenvironment where organisms find similar physico-chemical conditions. Activity measurements of individual aggregates

supported the hypothesis of the presence of microenvironments determined by soil structure (Bailey *et al.*, 2012; 2013). In addition, PSFs provide information about the maximal and minimal spatial distance of particle-inhabiting microbes within their natural environment.

Various studies focused on the compartmentalization of chemical parameters like soil organic matter (SOM) or elements of interest (Elliott and Cambardella, 1991; Navel and Martins, 2014; Six and Paustian, 2014), but less work has been carried out on microbial communities specific to PSFs. Microbial biomass and bacterial communities and nematodes were shown to vary between aggregate size classes (Monrozier *et al.*, 1990; Mummey *et al.*, 2006; Briar *et al.*, 2011; Davinic *et al.*, 2012). For fungal communities, research has mainly focused on their role in aggregate stabilization (Beare *et al.*, 1996; Caesar-TonThat and Cochran, 2001). The incorporation of carbon in microbial biomass has been investigated in soil aggregates (Kong *et al.*, 2011). High carbon concentrations and fungal biomass were correlated to microaggregates and it was suggested that this might be a specific environment for fungi. If carbon cycling differs within PSFs, it is likely that the biogeochemical transformations of other elements, especially those that are tightly coupled to C cycling such as nitrogen (N), are also occurring in soil microenvironments. Nitrification and denitrification represent the two major oxidative and reductive braches of the N-cycle, respectively. Each process is carried out by several groups of microorganisms that operate within different ranges of oxic conditions and might, therefore, be located in distinct soil compartments.

Using a PSFs approach, we wanted to study the spatial organization of bacterial and fungal communities of a pristine soil environment in order to determine the localization of N-cycling potentials. We hypothesized that isolated PSFs of a pristine soil environment represent microhabitats that can be distinguished by soil chemical properties as well as distinct bacterial and fungal communities. Furthermore we expected an increase in denitrification potential within aggregate particles (>250 and 250–63 μm) where zones limited in oxygen are

potentially created. In contrast, we hypothesized that nitrification potentials are localized in smaller fractions which might be drained first in soil and thus represent more oxic soil environments.

Rothamsted Park Grass soil was fractionated in 6 particle size fractions (>250, 250–63, 63–20, 20–2, <2 µm) by a gentle wet fractionation approach including sieving, settling and centrifugation of soil. Used water was collected for analysis of washed-off and not settled organisms during the process, which is further named "supernatant" (SN) fraction. Additionally, bulk soil samples were analyzed for comparison. We confirmed the isolation of targeted particle size ranges by laser-granulometry and performed soil chemical analysis of macro and micro elements. Community structure of bacteria and fungi inhabiting PSFs were determined by RISA analysis and SSU rRNA amplicon sequencing. Abundances of marker genes for denitrification (nitrite reductases nirK; nirS), nitrification (ammonium monooxigenases (amoA) of bacteria and archaea) and N_2O reduction (nitrous oxide reductases (nosZ) clade1 and clade 2) as well as SSU rRNA gene copies of bacteria, archaea and fungi were quantified by qPCR to localize N-cycling potentials within the isolated PSFs.

Material and Methods

Soil sampling and physical fractionation

Six fractions of the Rothamsted Park Grass soil (sampled October 2013, sieved at 2 mm), were obtained by dispersion and physical fractionation. A 'soft' particle size fractionation procedure was adapted from Jocteur Monrozier (Monrozier *et al.*, 1990) to optimize the preservation of soil micro-aggregation (agate marbles were not used in the macro-aggregate disruption step). Autoclaved and sterilized material and solutions were used to avoid contamination of samples. Ultra-pure water (200 mL) was added to 8 replicates (6 for biological, 2 for physical and chemical analysis) of 30 g bulk soil in 500 mL Duran® bottles and subsequently put on an orbital shaker for 1h at 250 rpm. This gentle soil dispersion was repeated 3 times. Subsequent fractionation steps were carried out as described previously and consisted in sequential i) wet sieving of dispersed soils to separate fractions of particle sizes >250 µm and 250-63 µm, ii) settlement of 63-20 µm diameter particles at 1 g (about 10 min), iii) sedimentation of 20-2 µm diameter particles at 1g (5 to 6h) and iv) centrifugation at 11000 g to collect dispersed particles of <2 µm diameter (Monrozier *et al.*, 1990). Supernatant of the centrifugation step was included in further analysis and represented all organisms washed of the soil matrix during the procedure and not settled during centrifugation (further called "supernatant" (SN) fraction). Soil fractions and SN were frozen at -80 °C for subsequent DNA extraction and chemical analysis. Soil physical analysis was carried out directly after the completed fractionation procedure.

Soil physical analysis

Particle size distributions of bulk soil and solid fractions were determined by laser granulometry with a Mastersize 2000 laser granulometer (Malvern Instruments Ltd, United Kingdom). A refractive index of 1.55 was used as a model parameter.

Soil chemical analysis

Total organic C and N concentrations of bulk soil and PSFs were determined in duplicate samples on approximately 15 mg of blended soil samples with a FlashEA1112/FLASH 2000 Elemental Analyzer equipped with a thermal conductivity detector. For ammonium and nitrate measurements, 1 g dry weight of bulk soil or PSF was extracted with 1 M KCL solution (1:5) for 30 min on a spinning wheel, subsequently spinned down and the supernatant used for quantification. Colorimetric measurements were carried out as described in (Hood-Nowotny *et al.*, 2010).

Total mineral elements (major and trace) were quantified in duplicate with 0.2 g of air-dried bulk soil and PSFs samples after microwave-assisted acid digestion. Samples were suspended in a mixed solution of HF/HNO_3 (6/2, v/v) in a pressurized closed-vessel microwave system (NovaWAVE, SCP SCIENCE). The digestion program consisted of a 10 min gradual increase to 180°C, a 10 min step at 180°C and then a cooling stage. In parallel to the total content of mineral elements, total available (soluble) mineral element concentrations were measured in bulk soil and PSFs. Three g of fresh bulk soil sample were suspended in 15 mL of ultra-pure water and shaken at 250 rpm for 30 min on a rotational shaker. The soil suspension was centrifuged at 9000 g for 15 min and supernatant was recovered, filtered at 0.45 µm and acidified with HNO_3 (2% final). Analyses of available mineral element concentrations in PSFs, supernatants were collected during the according fractionation step. Total and soluble mineral elements were quantified by ICP-AES (Perkin Elmer; Optima 3000 DV). Anion concentrations were determined in duplicate with supernatants of bulk soil and fractions before acidification by ion chromatography (Metrohm IC Net 2.3).

DNA extraction

Six replicates of homogenized bulk soil and PSF samples (40–800 mg wet soil representing 30 – 500 mg dry soil) were used for extraction of DNA (UltraClean Soil DNA Isolation Kit;

MO BIO Laboratories, Inc.; Carlsbad, CA). Water content for each sample was determined gravimetrically by drying 1 g of sample at 60°C for 24 h. Liquid samples collected after centrifugation of <2 µm PSF were filtered on sterile cellulose membranes (MF-Millipore™ membrane filters; pore size 0.45 µm) with a sterile fitration unit and DNA was subsequently extracted from the membranes (UltraClean Water Isolation Kit; MO BIO Laboratories, Inc.; Carlsbad, CA). Isolated DNA was quantified with Qubit® dsDNA HS Assay Kit on a Qubit® Fluorometer (Invitrogen™, Life Technologies) and stored at -20°C for further analysis.

Ribosomal Intergenic Spacer Analysis (RISA)

Internal transcribed spacer regions (ITS) of bacterial and fungal communities were amplified from isolated DNA samples using Illustra Hot Start Mix RTG Kit (Illustra, GE-Healthcare) with primer pairs FGPL 132-38 / FGPS 1490-72 (specific to bacterial ITS) and fITS7 / ITS4 (specific to fungal ITS2)(Ranjard *et al.*, 2000; Bokulich *et al.*, 2013). Each 25 µL reaction contained 12.5 pmol of the primers and 2 ng of template DNA. Cycling conditions for bacterial ITS amplification were: 94°C for 10 min; 29 cycles of 94 °C for 20 s, 55 °C for 30 s and 72 °C for 1.5 min; final elongation step at 72 °C for 10 min. Cycling conditions for fungal ITS2 amplification were: 94°C for 10 min, 35 cycles at 94 °C for 20 s, 57 °C for 30 s and 72 °C for 1.5 min; final elongation step at 72 °C for 10 min. One µL of PCR products was run on an Agilent 2100 Bioanalyzer (Agilent Technologies, Inc.) to obtain data tables of fluorescence intensity over time, which were extracted to comma separated text files. Data was scaled and centered for principal component analysis (PCA) using the FactomineR package (Lê *et al.*, 2008) within R (undefined author, 2015).

Pyrosequencing of bacterial and fungal communities

Fungal V7-V8 region of the 18S rRNA gene as well as V1-V3 region of the bacterial 16S rRNA gene were amplified with bar-coded primer pairs FR1/FF390 and 27F/519R respectively (Titanium-Taq-Kit; Clontech Laboratories, Inc) (Chemidlin Prévost-Bouré *et al.*,

2011; Marti *et al.*, 2013). Each reaction mix (50 µL) contained 10 pmol of each primer, 40 nmol of dNTPs, 1 x reaction buffer, 100 ng of template DNA and 1 x Titanium Taq DNA Polymerase. Cycling conditions were: 95°C for 1 min; 35 cycles of 95 °C for 30 sec and 68 °C for 1 min; final elongation step at 68 °C for 3 min. Subsequently reactions were loaded on an agarose gel and amplicon bands were purified (Gfx – DNA Purification Kit;GE Healthcare). Concentrations of DNA was quantified with Qubit® dsDNA HS Assay Kit on a Qubit® Fluorometer (Invitrogen™, Life Technologies). An equimolar pool of amplicon samples (60 ng DNA of each sample) was sent for 454-pyrosequencing (Beckman Coulter Genomics). Amplicon sequences were quality filtered, clustered by 97% sequence identity and annotated versus SILVA ribosomal database in QIIME(Caporaso *et al.*, 2010; Quast *et al.*, 2013). OTU-tables were imported into MEGAN for further analysis (Huson *et al.*, 2016).

Quantitative PCR

Standard curves of all reactions were derived from serial dilutions of linearized pGEM-T plasmids with the target sequences inserted (Bru *et al.*, 2011). All standard curves were linear and showed comparable efficiency values (R^2 = 0.96 to 0.99; E = 0.85 to 1.05). Quantitative PCR was performed on a Corbett Rotor-Gene 6000 realtime PCR cycler and QuantiTect SYBR® Green PCR Kit (Quiagen). Each reaction (25 µL) contained 12.5 µL 2x QuantiTect SYBR® Green Mix; 0.3 to 1.8 µL of each primer (10 µM); 100 ng of T4 gene protein 32 (Thermo Fisher Scientific Inc.); 2 to 5 ng of template DNA and PCR grade water. Primer sequences and cycling conditions used are summarized in Table S1. In each run 3 non-template control reactions were included to test for contamination of the master mix. Melting curve analysis was used as quality control of qPCR runs. Results from runs with no amplification in non-template controls and showing only one melting peak overlapping peaks from standards were considered for further analysis. Different groups were tested on significant differences by ANOVA in R (undefined author, 2015).

Results

Fractionation of bulk soil

Particle size distributions of isolated fractions were analyzed to ensure that targeted size ranges were captured within the defined fractions. Distribution curves (Figure 8) and the observed parameters of determined median diameter and coefficient of uniformity (Table 1) confirm a sufficient separation due to particle size following fractionation. Ultrasonication on PSFs caused a shift towards smaller particles in the >250 and 250–63 µm fractions but not in smaller size classes (Figure S 1). This confirmed the isolation of stable soil aggregates within the >250 and 250-63 µm fraction.

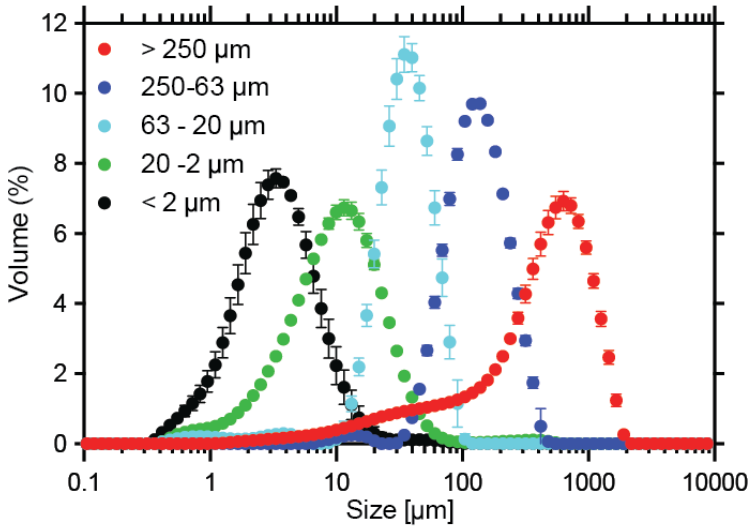

Figure 8: Particle size distribution of Rothamsted Park Grass soil fractions obtained by laser granulometry (Mastersizer 2000, Malvern) without ultra-sonication. Colours indicated different fractions, point represent the mean, error bars the standard deviation of the mean (n=3).

Chemical characteristics of isolated fractions

For comparison of soil chemical properties of different PSFs and bulk soil, total organic C, total organic N, major and trace elements were quantified in samples (Table 1; Table S 2). Values from single fractions were multiplied by their mass fraction and summed for comparison with values obtained in bulk soil samples (acceptable range was 90-110 %

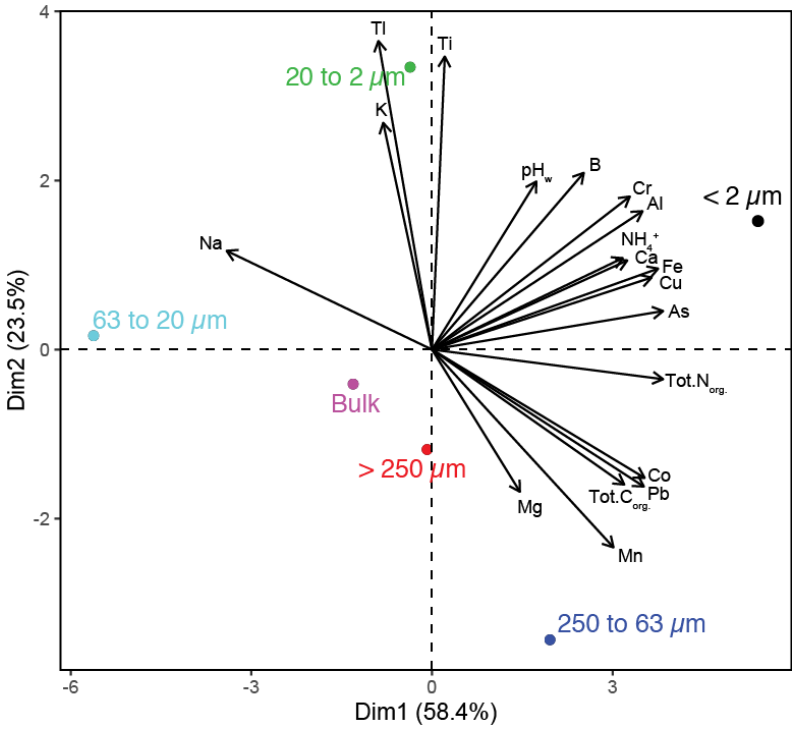

Figure 9: PCA-plot of soil fractions and bulk soil calculated from the chemical data obtained (Table S2). Coloured points indicate individuals (fractions), black arrows variables (chemical parameters) of the analysis. Percentage values on axes indicate the proportion of the total variance represented in the data set explained by the axis.

recovery). Similar levels of analyte suggested no loss during fractionation and consistent quantification within all samples. Of 23 analytes quantified, 18 were found to have sufficient recovery to be included in further analysis, however Ba, Ni, Sn, Sr and Zn had to be excluded. In general, available cations could not be detected in supernatants of PSFs but in supernatants of bulk soil. Available anions were detected in some of the PFSs and bulk soil samples (Table S 3).

Principal components based on chemical data in Table S 2 were calculated and plotted on a PCA graph to identify groups of samples with a comparable chemical signature (Figure 9). Axes shown in the graph represent 82 % of the total variance in the dataset. Generally, we observed the highest values of nutrients, cations and trace elements in the <2 µm fraction followed by the 250-63 µm fraction. The fraction found to be lowest in measured elements

Table 1: Summary of main physical and chemical parameters of soil fractions and bulk sample of Rothamsted Park Grass soil. pH_w was measured in supernatants of fractions and bulk soil after fractionation with distilled water. Ammonium and nitrate concentrations were measured after extraction with 1 M KCl solution.

Soil fraction	Mass[1] [%]	pH_w	d_{50} [µm]	C_u	Tot. C_{org} [g C kg^{-1}_{dw}]	Tot. N_{org} [g N kg^{-1}_{dw}]	Ammonium [mg N kg^{-1}_{dw}]	Nitrate [mg N kg^{-1}_{dw}]
>250 µm	46.03	5.84 ± 0.11	425.6	13.3	64.9 ± 3.5	4.77 ± 0.2	19.5 ± 3.2	0.01 ± 0.03
250-63 µm	9.50	5.85 ± 0.13	119.7	2.3	86.5 ± 11.5	6.40 ± 0.8	35.7 ± 10.2	0.11 ± 0.21
63-20 µm	25.87	5.95 ± 0.02	32.8	2.2	15.6 ± 0.8	1.19 ± 0.1	7.9 ± 1.7	0.00 ± 0.00
20-2 µm	16.21	6.01 ± 0.08	9.5	4.3	53.5 ± 1.8	4.73 ± 0.0	32.8 ± 1.8	0.47 ± 0.95
<2 µm	2.39	6.21 ± 0.15	3.1	3.3	67.1 ± 0.7	7.30 ± 0.0	224.6 ± 127.0	0.16 ± 0.31
Sum fractions [a]	-	5.91 ± -	-	-	52.4 ± -	4.05 ± -	25.1 ± -	0.10 ± -
Bulk soil	100.00	5.59 ± 0.01	285.7	16.7	52.2 ± 0.7	4.10 ± 0.1	25.6 ± 1.3	4.60 ± 0.74

1: gravimetric portion of fraction to bulk soil
a: Sum of all fractions (> 250, 250-63, 63-20, 20-2 and < 2 µm) according to their mass contribution of bulk soil (1)
C_u: coefficient of uniformity - d_{60}/d_{10}

was 63-20 µm with exception of sodium, which was highest in this fraction. The >250 µm fraction was found to be the most similar to bulk soil.

DNA extraction and SSU rRNA gene abundances

The highest amounts of DNA per gram of dry soil were extracted from the <2 µm fraction, while the lowest quantities were obtained from the 63-20 µm and SN fractions (Figure S 2). Abundance of SSU rRNA genes (g^{-1} dry soil) of bacteria, fungi and archaea was found to be significantly higher for all three domains in the <2 µm fraction, as compared to all other fractions and bulk soil (Figure 10). The 63-20 µm PSF and SN fraction showed the lowest values for rRNA genes and no archaeal 16S rRNA genes could be detected in the supernatant fraction.

Community structure in fractionated soil

Community structure of distinct fractions based on RISA of bacterial and fungal communities are shown in Figure 11. For both communities, replicates of >250, 250-63 and 63-20 µm fraction cluster together on a PCA plot indicating a similar microbial community. Fractions containing smaller particles (20-2 and <2 µm) as well as samples from the SN fraction also

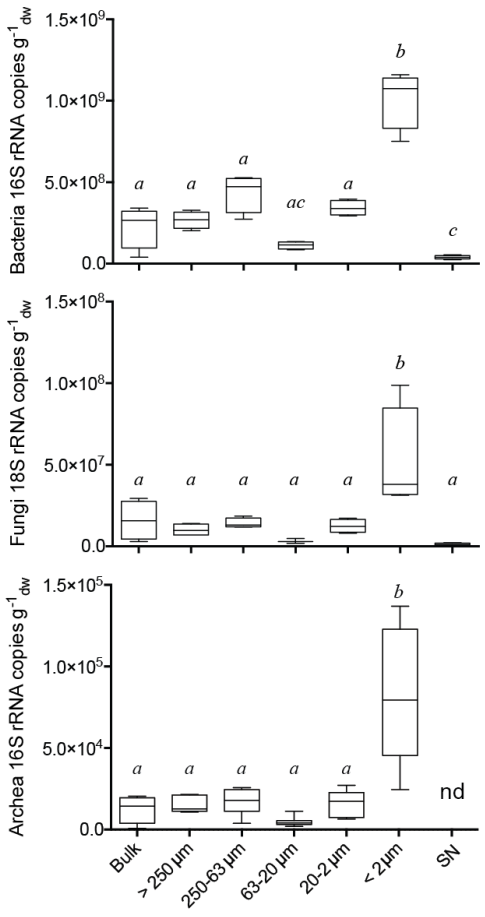

Figure 10: Copy numbers of small subunit ribosomal RNA coding sequences in DNA extracts of PSFs, bulk soil and supernatant (SN) of fractioned Rothamsted Park Grass soil for bacteria, fungi and archea. Boxplots show the median and 5-95% percentile, whiskers the highest and lowest observation of the dataset (n=12). Significant differences between means of groups were tested by one-way ANOVA and Tukey correction for multiple comparison after confirmation of normality and variance homogeneity of datasets. Significance levels (alpha = 0.05) are indicated in the graphs by letters *a*,*b* and *c*.

clustered together on a PCA plot, but showed a distinct band profile to all other PSFs and bulk soil for both bacterial and fungal communities. Bulk soil samples could not be clearly distinguished from bigger size fractions for fungal communities. In contrast, bacterial RISA profiles of DNA isolated from bulk soil appeared to be distinct form all other fractions included in the analysis.

We sequenced amplicons of bacterial 16S and fungal 18S rRNA coding genes for additional community structure information and identification of taxa contributing to differences observed with RISA analysis (Figure 12).

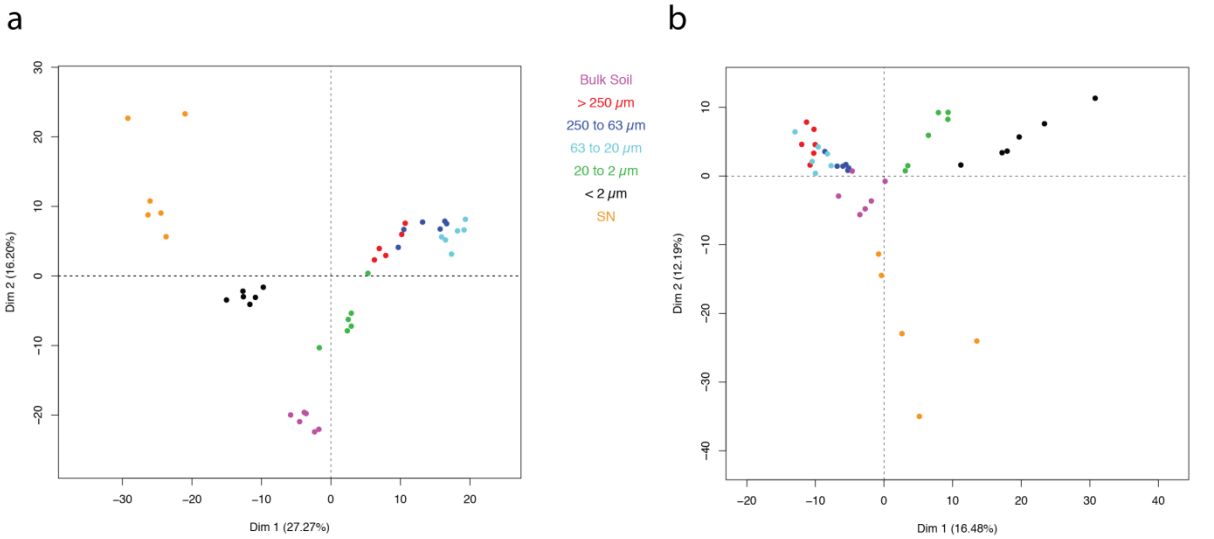

Figure 11: Comparison of bacterial and fungal community structures among fractions and bulk soil samples of Rothamsted Park Grass soil based on RISA-band profiles for bacteria (a) and fungi (b). Each point in PCA-plots represents one replicate (n=6) of soil fraction, bulk or supernatant (SN) fraction sample. Percentage values on axes indicate the proportion of the total inertia represented in the data set explained by the axis.

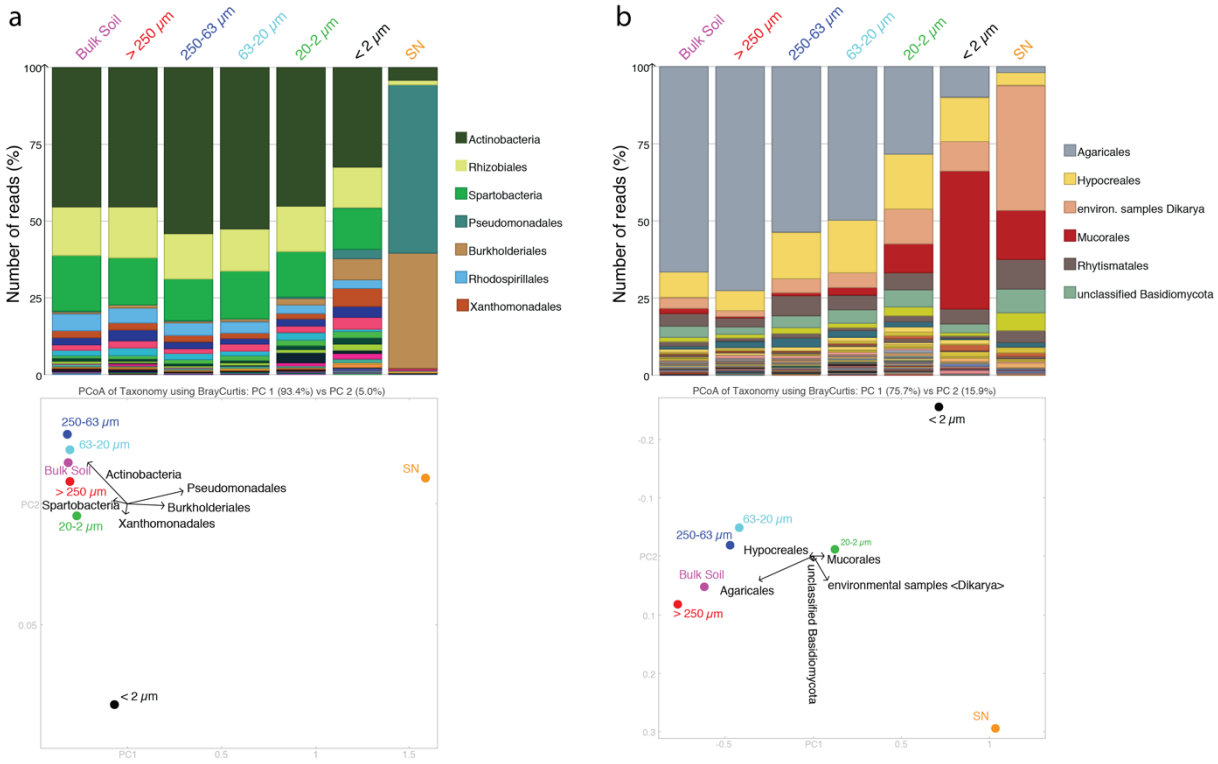

Figure 12: Bacterial (a) and fungal (b) community structures derived from PSFs, bulk soil and supernatant (SN) samples of Rothamsted Park grass soil based on 454-pyrotag sequenced SSU rRNA gene amplicons. Bar graphs indicate relative abundance of annotated OTUs at order level for bacteria (a) and fungi (b) respectively. Bi-plots based on relative abundances on order level of annotated OTUs respectively show position of PSFs bulk soil and SN groups and top 5 variables contributing to the total inertia represented in the graph. Percentage values on top of the graph indicate the proportion of the total inertia represented in the data set explained by the axis.

Data of annotated bacterial 16S amplicons on order level confirmed a distinct community in the SN fraction with a lower diversity compared to all other samples (Figure 12 a). Particle size fractions and bulk soil samples showed comparable community structures for bacteria, although more taxa were detected in the 20-2 and <2 µm fraction. A PCA analysis of annotated bacterial amplicons showed discriminating orders among PSF, bulk soil and SN samples. *Actinobacteria* were found to be more prominent in >250, 250-63, 63-20 µm fractions and bulk soil than in other samples. *Pseudomonadales* and *Burkholderiales* accounted for 90 % of the bacterial community found in the SN samples. These orders were only found to be 1-2 % in relative abundance in >250, 250-63, 63-20 µm fractions and bulk soil, and increased to 10 % towards the <2 µm fraction. *Xanthomonadales* were found to be higher in relative abundance in the <2 µm fraction. *Rhizobiales* and *Spartobacteria* were equally abundant in communities of all PSFs and bulk soil but not in the SN fraction.

Fungal community structure based on annotated 18S rRNA amplicons annotated at the order level supported findings based on RISA profiles (Figure 12 b). We observed a shift in community structure with particle size from bigger to smaller particles. For example, the relative abundance of *Basidiomycota* (order *Agaricales*) accounted for 75 % of the fungal community in the >250 µm fraction and gradually decreased to 10 % in the <2 µm fraction, while *Zygomycota* (order *Mucorales*) represented approximately 50 % of the relative abundance of annotated sequences and only 1 % in the >250 µm fraction. In contrast to results from bacteria, almost all orders found in PSFs could also be detected in SN samples. Here the biggest group was annotated to sequences derived from *Dikarya*.

Nitrogen cycling potential in fractionated soils

To determine denitrification, nitrification and N_2O reduction potentials of isolated communities based on particle size fractionation, we quantified marker genes encoding key enzymes in the targeted pathways by qPCR (Figure 13).

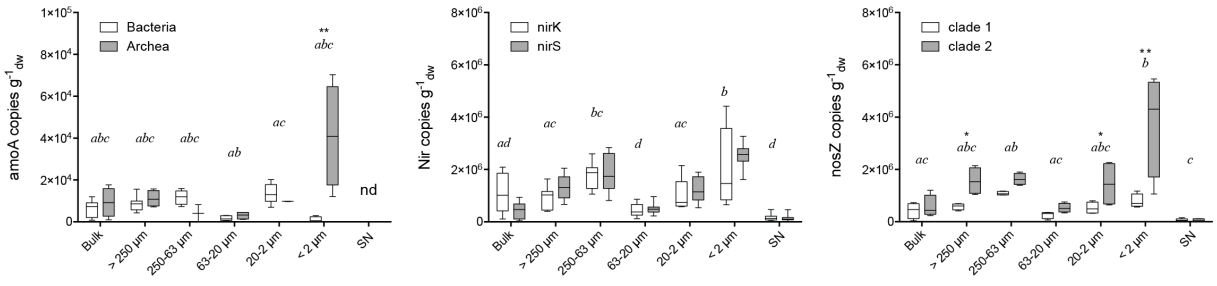

Figure 13: Comparison of nitrogen cycling gene abundance of PSFs, bulk soil and supernatant (SN) of fractionated Rothamsted Park Grass soil. Within each fraction abundance of distinct genes contributing to the same function in the N-cycle are show by distinct coloured box plots (nitrification – amoA of bacteria vs. amoA of archea; denitrification nirK vs. nirS; N_2O reduction – nosZ clade 1 vs. nosZ clade 2). Boxplots show the median and 5-95% percentile, whiskers the highest and lowest observation of the dataset (n=12). Data was tested for normal distribution and varinace homogeneity and significant differences between means of fractions were tested by one-way ANOVA (Tukey corrected for multiple comparisons) calculated with the sum of both genes of one fraction. Significance levels (alpha = 0.05) are indicated in the graphs by letters *a*,*b* and *c*. Significant differences of means within each fraction tested by Student's T-test are indicated by * and ** for alpha levels of 0.05 and 0.01 respectively.

Copy numbers of copper-containing (nirK) and cytochrome cd1 type nitrite reductase (nirS) were detected at comparable levels in isolated fractions and bulk soil. The highest copy numbers (1-4*10^6 copies g^{-1}_{dw}) were found in 250-63 and <2 µm fractions and lowest copy numbers (1-9*10^5 copies g^{-1}_{dw}) in the 63-20 µm and SN fraction. Comparison of nirK and nirS abundances within single fractions and bulk soil resulted in no significant difference in any of the analyzed groups. Nitrous oxide reductase genes (nosZ clade 1 and 2) were found in all PSFs and bulk soil samples, whereas copy numbers in the SN fraction were negligible (Figure 13). Genes derived from clade 2 of the nosZ gene were higher than those of clade 1 in all PSFs and bulk soil samples. Significant differences between the two genes were found in the >250, 20-2 and <2 µm fractions. Comparing copy numbers of denitrifying marker genes with chemical soil parameter showed a relationship between organic cabon and nitrogen concentrations (Figure 14). When organic C and N were high we also found higher copy numbers of NIR and NOSZ related genes.

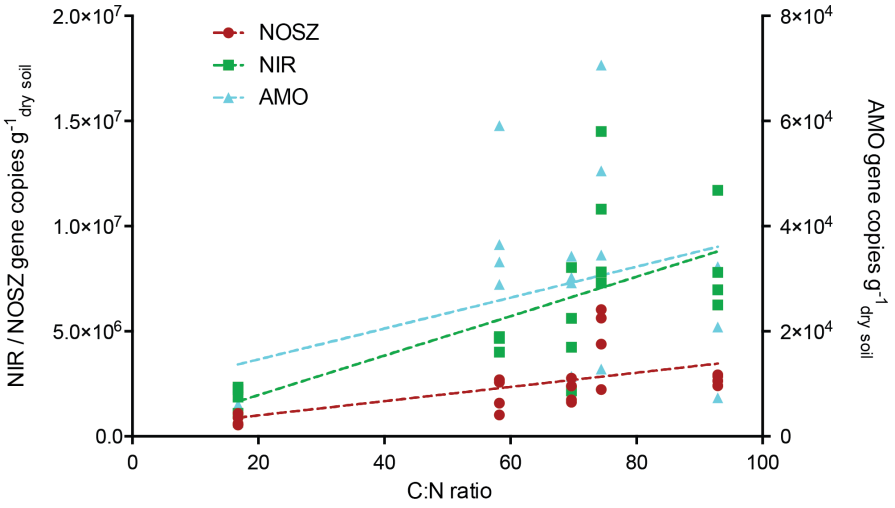

Figure 14: Organic carbon and nitrogen concentrations found in isolated fractions plotted against copy numbers of denitrification and nitrification marker genes. NIR nitrite reductase derived from nirK and nirS copies; NOSZ nitrous oxide reductase derived from nosZ clade 1 and clade 2 copies; AMO ammonia monoxigenase derived from bacterial and archaeal amoA copies.

Bacterial and archaeal amoAs were quantified to determine potential of nitrification in bulk soil sample PSFs and SN. Generally, this gene was found in low abundance (~1*10^4 copies g^{-1}_{dw}) and could not be detected in communities washed off the soil matrix (Figure 13). The highest gene copy numbers, up to 7*10^4 copies g^{-1}_{dw}, were detected in the < 2 µm fraction. Almost all amoA genes in this fraction were of archaeal origin, whereas bacterial amoA copies were found to be negligible. As for NIR and NOSZ copy numbers, we found AMO genes increasing in abundance when organic carbon and nitrogen concentrations increased in fractions (Figure 14).

Discussion

Connection of PSFs with soil micro-habitats

The spatial interpretation of microbial community data based on physical fractionation requires knowledge on where particles collected in single fractions are situated in the studied soil and what environmental conditions can be linked to them. Soil structure is determined by aggregate turnover, where clay particles with organic matter form aggregates that are bound together by fungal hyphae, plant roots and sticky organic polymers (Oades, 1984; Six *et al.*, 2004). The widely accepted size boundary separating macro- from microaggregates is 250 µm and by adjusting both the time and mechanical force of dispersion steps in fractionation protocols, soil structures can be broken down to compartments of different sizes (Chotte *et al.*, 1993). The fractionation protocol we chose was found to be suitable for isolating macro- (>250 µm) as well as mirco-aggregates (250-63 µm) since distributions in both fractions shifted to smaller sizes under ultrasonication treatment (Figure 8, Figure S 1). This confirms the existence of aggregates that were dispersed in single particles under treatment. Within these micro-porous soil compartments, conditions with respect to water availability are likely more stable, but there might also be a limitation to nutrients and oxygen availability (Sexstone and Revsbech, 1985; Vos *et al.*, 2013). Loosely attached particles on the surface of these aggregates would be washed off and collected in smaller PSFs. Rothamsted Park Grass soil control plots represent untreated pristine environments, thus we expected to find a well aggregated soil structure. We found aggregate fractions (>250 and 250-63 µm) accounting for about 50 % the total soil mass after fractionation, confirming the existence of a well aggregated soil environment (Table 1). In managed soil these fractions accounted between 10 and 30 % of the total mass which is in agreement with mechanical impacts on soil aggregation (Six *et al.*, 2000; Navel and Martins, 2014).

Based on the concept of the sequential build up and the hierarchical structure of soil aggregates, we would expect to collect loose soil particles and primary structures of microaggregates within the 63-20 (sand and silt) and 20-2 µm fractions (Tisdall and Oades, 1982; Oades, 1984; Oades and Waters, 1991). For these size classes, the tracking to a specific soil compartment is more challenging than for the inner part of aggregate structures. They might have been loosely bound to the outside regions of bigger particles before being washed off or constitute single particles situated in macro pores. We think that the inhabiting microbial community is exposed to changes in water availability, but have easier access to nutrients.

The <2 µm fraction represents clay particles at the scale of the size of microbes. They possess negative surface charges and are responsible for the binding of important nutrients to the soil matrix beside organic substances. This fraction is collected by centrifugation (11000 g) during the last step of fractionation. In addition to clay particles and the microbes attached to them, free cells that were washed off during the previous fractionation steps were also pelleted by this treatment, as previously shown (Bakken, 1985). Thus this fraction also contains information on all microbes loosely attached to soil, mainly situated on the surface. A further separation between cells still attached to clay particles and detached ones was not possible by this approach. Organisms detected in the SN fraction represent ones that could not be settled by centrifugation.

Distribution of microbial communities among PSFs

Normalized results to the dry mass of the respective PSF or bulk soil showed that highest amounts of DNA yielded after extraction as well as copy numbers of ribosomal SSU rRNA for bacteria, archaea and fungi were found in the <2 µm fraction followed by the 250-63 µm fraction (Figure 10, Figure S 2). Thus, the highest density of microorganisms was found to be washed off of surfaces and colonizing clay particles. One explanation for this might be the

smaller particle-surface ratio in the <2 µm fraction, although a connection between particle size and microbial abundance could not be found. A big part of the soil community seems to be situated on surfaces. In studies gradually dispersing soils and collecting washed off bacteria, the highest amount of cells was counted in the first washing step and decreasing with the following ones (Bakken, 1985). Also, results from several studies found the highest copy numbers or biomass in clay fractions (Monrozier *et al.*, 1990; Neumann *et al.*, 2013). This supports our findings of microbes being highly abundant on surfaces of soil. This is crucial when we seek to interpret biochemical processes carried out by microbes in soil. Generally, it seems that microbes find preferred conditions on surface oriented soil compartments.

Comparable copy numbers of all three domains in the >250, 250-63 and 20-2 µm fractions showed that these do not likely represent a favored habitat. Only bacteria 16S rRNA gene copies were higher in the 250-63 µm fraction, although the differences were not significant. However, microaggregates are considered to be created by microbial activity around organic matter particles entering the soil and elevated bacterial abundance in these compartments support this hypothesis (Six *et al.*, 2000; 2004).

The SN and 63-20 µm fraction showed both the lowest amounts of extracted DNA and the lowest SSU rRNA abundances. Sand and silt is mainly collected within the 63-20 µm fraction and these particles possess no or very little surface charges to bind nutrients or water as compared to clay or organic matter (Turpault *et al.*, 1996; Peinemann *et al.*, 2000).Thus, it is likely that this fraction represents no favorable conditions for microbial activity. The SN fraction was included in the analysis to account for organisms that could not be settled during centrifugation. The values were normalized and represent abundances washed off 1 gram of dry soil. Low copy numbers for bacteria and fungi and no copies for archaea indicate that most cells were collected during centrifugation and surface-based microbes were indeed collected in the <2 µm fraction.

Chemical analysis of PSFs

Except Ba, Ni, Sn, Sr and Zn, summed values found in PSFs were comparable to bulk soil, which was defined by a 90 – 110 % recovery. This mass balance check is crucial in a fractionation study, since an undetected loss of analyte during fractionation can lead to a bias in further analysis. We only used quantified elements with a recovery percentage close to 100 % to ensure a representative elemental profile of the single fractions.

Ammonium, as a positively charged ion, binds to negatively charged groups of organic matter and clay particles, thus immobilizing it within soils. In contrast, negatively charged nitrate is easily leached when excess water is available (Fowler *et al.*, 2013; Billen *et al.*, 2013). This behavior explains why nitrate could not be further extracted with KCl solution after fractionation and why the added values were lower than nitrate measured in bulk soil (Table 1).

Generally, the highest concentrations of measured chemical parameters were found in the small size fractions (20-2, 2 µm) followed by the big aggregate containing fractions (> 250, 250-63 µm) and lowest values were found in the 63-20 µm size fraction (Figure 9). It has been hypothesized that soil organic matter (SOM) is protected from microbial activity due to two factors: i) the localization of SOM within aggregates, which restricts access to it to a few microorganisms, and ii) sorption processes to mineral surfaces and metal ions (Stockmann *et al.*, 2013). This goes along with the proposed soil continuum model (SCM) for carbon (Lehmann and Kleber, 2015). Here, SOM is seen as consisting of biopolymer structures that are constantly being degraded to smaller structures and ultimately monomers and CO_2, rather than the buildup of a stable 'humified' carbon pool. Furthermore, all sizes of SOM are then included in the formation and destruction processes of aggregates and ad- and de-sorption processes on mineral surfaces. This model is supported by the findings of our study, where carbon and nitrogen were found in aggregate size fractions as well as clay fractions, but not in the sand and silt fraction. The chemical properties of sand and silt are less effective in

sorption processes, which would explain the difference between this fraction and smaller fractions (Pulford, 2007). Following a flowing nutrient model in soil, it is not surprising that concentrations of major and trace elements are also high in high C and N fractions. Microbes would preferentially find energy sources in these compartments and accumulate these elements through biological activities and organic matter contributes to the cation exchange capacity of soil. Copper, manganese and iron are at the core of biochemical reactions in active centers of enzymes, thus essential for microbial life (Vallee and Williams, 1968; Waldron and Robinson, 2009).High concentrations of these elements found in the <2 μm might be an artifact resulting from the analysis of the chemical composition of the washed off microbial cells from the surface of particles that were collected and concentrated in this fraction. Additionally, free metal ions would be included in adsorption processes to mineral surfaces, which is reflected in high concentrations in the 20-2 μm fraction.

Community structure in isolated PSFs

Bacterial communities: RISA based community fingerprinting as well as analysis of the sequenced SSU rRNA amplicons showed that bacterial communities changed among the isolated fractions, bulk soil and SN samples. The slightly different results between the two methods might derive from known shortcomings in amplicon sequencing approaches. It was shown that amplicons of the V3 hypervariable region aligned to two or more sequences in the database and that identical ribotypes do not translate to identical genetic potential (Vos and Velicer, 2006; Huse *et al.*, 2008). RISA analysis is based on band patterns derived from the amplification of ITS regions, which vary in length among distinct organisms. Studies showed that this fingerprinting method has the same sensitivity as amplicon sequencing based approaches in detecting ecological patterns of microbial communities (van Dorst *et al.*, 2014). Thus our results based on RISA fingerprinting can be considered to be derived from distinct signatures of the communities from isolated fractions.

In smaller PSFs (20-2, < 2 µm), groups of bacteria appear that could not be detected in other PSFs and bulk soil samples. We expected a higher microbial diversity in fractions where surface communities accumulated. Indeed, more orders of bacteria were annotated in the 20-2 and <2 µm fraction. Signatures from <2 µm particles representing mainly surface communities might be exposed to rapid changes in their physico-chemical environment. Thus they are likely the first ones to react to changes. Following this hypothesis, the 20-2 µm fraction might collect communities from more protected environments, but also communities from surfaces since they shared orders of bacteria with the <2 µm fraction. These fine particles might have been situated inside less stable aggregates and disrupted during fractionation, or were loosely attached to surfaces of bigger aggregates and detached from them. This is also supported in PCA plots of community fingerprints where 20-2 µm samples are situated between surface communities of <2 µm and inside communities from >250, 250-63 and 63-20 µm fractions (Figure 11; Figure 12).

Supernatant samples represent surface organisms that could not be settled during the final centrifugation step. Interestingly, only a few prominent groups of bacteria could be found in these samples, mainly *Pseudomonadales* and *Burkholderiales,* which together accounted for approximately 90 % of the annotated reads in this sample.

Fungal communities: Community structure bases on RISA profiles and 18S amplicons of fungi were found to discriminate more between all isolated PSFs, bulk soil and SN samples than those for bacteria (Figure 11; Figure 12). In contrast to bacterial amplicons, almost all fungal groups detected in the PSFs could also be found in the SN fraction. Although fungi are not easily washed off soil particles due to their morphology, this could be an indication that parts of them end up in the SN fraction due to disruption of hyphae during the fractionation procedure.

Fungi are often mentioned as key players in the formation and stabilization of aggregates, as well as their advantage in exploring a soil environment by hyphal growth as compared to unicellular organisms (Beare *et al.*, 1996; Caesar-TonThat and Cochran, 2001). Linking taxonomic data to morphological appearance is a difficult task, since many groups of fungi are dimorphic, thus able to grow as a hyphal multicelled organism or as a unicellular yeast form although, no members of *Agaricales* were found to produce a yeast-like stage (Walther *et al.*, 2005). This order was prominent in the aggregate-containing fractions and decreased with decreasing particle size, thus confirming our hypothesis that fungal communities discriminate in PSFs. The relative abundance of members of the *Mucorales* order increased in smaller PSFs and represented up to 45 % of the < 2 µm fraction. However, these organisms are also mainly hyphae forming, which does not support the hypothesis that soil particle selection is selective for fungal species based on their morphology. Aggregate formation and turnover was found to be driven by microbial activity degrading organic matter and accumulate organic and inorganic soil particles (Oades and Waters, 1991; Tisdall, 1994; Six *et al.*, 2000; 2004; Six and Paustian, 2014). The dominance of *Agaricales* in inside fractions of aggregates corroborates this hypothesis, since these fungi exhibit a mainly wood and plant biomass degrading lifestyle (Ohm *et al.*, 2014). Furthermore, fungal activity in carbon degradation was linked in a study using stable isotopes to the micro-aggregate fraction (250-63 µm) (Kong *et al.*, 2011). In contrast, *Mucorales*, dominating surface communities, were described as 'sugar fungi' as they are known to primary use substrates rich in simple carbohydrates, but lack an enzymatic set to degrade recalcitrant biomass (Richardson, 2009b; van den Brink and R. P. de Vries, 2011a; Pawłowska *et al.*, 2016). Together, these findings could point to a spatial separation of carbon substrate usage starting from the inside of aggregates and ends with the consummation of simple carbon compounds at the surface of soil. Co-inhabiting bacterial and archaeal communities might benefit from this substrate stream as well.

Localization of nitrogen cycling communities

A shift in community structure of bacteria and fungi was observed when we compared inner-aggregate fractions (>250, 250-63 μm) with fractions representing surface communities. This suggests that there is also a distinct localization of N-cycling potential within the different fractions of Rothamsted Park Grass soil.

Nitrification potential in Rothamsted Park Grass soil fractions: In most studies on nitrification in soil, amoA gene abundances were analyzed after addition of ammonium (Nicol *et al.*, 2008; Glaser *et al.*, 2010; Verhamme *et al.*, 2011; Levičnik-Höfferle *et al.*, 2012). In our study, we wanted to know if spatial differences in nitrification potential within a pristine soil environment develop over time. Generally, we found amoA copies of bacteria and archaea low as compared to other studies (Figure 13) (Leininger *et al.*, 2006; Hallin *et al.*, 2009), but abundances comparable to our study were also reported in unfertilized soil (Zhifeng Zhou *et al.*, 2014). We ruled out potential biases caused by primer mismatch since amoA copies of archaea were in good agreement with the archaeal 16S copies quantified. Archaeal amoA copies were only significantly higher in the <2 μm fraction as compared to other PSFs, whereas bacterial amoA genes were negligible within this fraction. In pristine soil environments, where no ammonium is added artificially, the only nitrogen source for organisms is derived from nitrogen fixation and mineralization of organic material. It has been shown that AOA respond faster to additions of organic based nitrogen than AOB , which led to the hypothesis that archaea utilize ammonia at the site of N mineralization (Levičnik-Höfferle *et al.*, 2012). Although nitrifying bacteria were detected in aggregate fractions, our results suggest a localization of nitrification potential in surface communities driven by ammonia-oxidizing archaea.

Denitrification potential: Denitrification potential in PSFs, bulk soil and SN samples was determined by quantification of nitrite reductase genes in extracted DNA (Figure 13). We

initially hypothesized that communities in stable aggregates would be more likely to carry out this pathway given the anoxic conditions, but this could not be corroborated with our dataset, since we could not find significant differences among analyzed samples. One explanation could simply be that all communities isolated from fractions have the potential to denitrify. For denitrifyers, no phylogenetically pattern exists given that this metabolic tool is distributed over a wide range of bacterial groups (Zumft, 1997; Philippot, 2002). Thus even a community with a high copy number of denitrifying genes might not actually carry out nitrogen reduction all the time. Based on our data, we suggest that denitrification potential is not specific to spatial location in soil.

Habitat selection between nirS and nirK type denitrifyers was observed on a meter and kilometer scale (Bru *et al.*, 2011; Keil *et al.*, 2011). Also abundance of copper containing nirK copies were found to be correlated to copper concentrations on a meter scale (Enwall *et al.*, 2005). However, we could neither find differences in abundance in the two nir classes in any of the isolated fractions, nor a correlation of copper concentrations to nirK.

N_2O reduction potential: Two clades of nitrous oxide reductase were discovered and have been detected at comparable abundances in various ecosystems, although a niche separation based on environmental factors was suggested (Jones *et al.*, 2013). We found similar abundances of nosZ copies as compared to previous work carried out on untreated soils (Hallin *et al.*, 2009; Cuhel *et al.*, 2010; Bru *et al.*, 2011; Di *et al.*, 2014). Results from both clade copy numbers showed a similar pattern as nir abundances and copies of nosZ clade 2 genes were generally higher than those of clade 1 in our soil (Figure 13). We hypothesized that N_2O reduction potential is localized in zones of depleted oxygen, thus on bigger aggregates. As was the case for nitrite reduction, this hypothesis could not be corroborated, since based on our data, a potentially N_2O reducing community seems to also be situated on the surface of soils.

Conclusions

Particle site fractionation intends to isolate compartments within soil that provide similar conditions for microbial communities. We found the biggest differences in community structures between fractions linked to inner aggregate communities and fractions where surface communities were collected. Bacterial communities on surfaces were found to be more diverse than the inside of aggregates. Fungal communities in aggregates were dominated by *Agaricales*, a group of filamentous fungi that is often found to degrade complex carbohydrate structures. In contrast, fungi on surfaces were dominated by *Mucorales*, also filamentous, but linked to a distinct strategy of carbon nutrition, as they are efficient users of easily consumed carbohydrates. Together these results suggest that I) bacterial surface communities might need to be more reactive to environmental changes and are thus more diverse and II) surface communities might be dependent on carbon cycling inside of aggregates, which is driven by a fungal community. We found nitrogen cycling potentials in all isolated fractions, but could not corroborate our hypothesis that denitrifying communities are linked to more anaerobic environments inside of aggregates. However, we found higher abundances of nitrogen cycling genes in fractions with high concentrations of organic carbon and nitrogen, suggesting a link between the carbon and nitrogen cycle. This might point to a dependence of bacterial and archaeal nitrogen cycling organisms on carbon degradation processes. Degradation of carbohydrates is driven by fungal community members, thus they might influence nitrogen cycling via organic matter decomposition.

Chapter 2: NO Release from sterile Nitrite Medium leads to Detection of False Positives in Screening for Denitrifying, N_2O Producing Fungi

Abstract

The potential roles for denitrifying fungi as big players in nitrous oxide (N_2O) emissions from soil has been discussed for years, although many questions remain about fungal N-cycling processes in anoxic environments and their related ecological significance. This study investigates the N_2O production capacity of 24 nitrate-reducing fungal strains isolated from soil. Incubations were carried out in an automated gas sampling unit that allowed the continuous measurement of NO, N_2O, O_2 and CO_2, providing high quality gas data through oxic and anoxic phases of culturing. Gas monitoring showed production of NO in sterile medium controls under anoxic conditions. This NO production could potentially distort outcomes from screening experiments on N_2O producing fungi by leading to the detection of false positives among low N_2O producers. When comparing N_2O endpoint levels, 17 out of the 24 tested strains were found to produce more N_2O than controls. However, this number decreased to 4 (all *Fusarium* related strains) when we corrected our data for estimated NO produced by the medium. Non-*Fusarium* strains increased N_2O concentrations following the injection of NO into the culture vials, which confirmed that biological activity of fungi reduced NO. Based on our results, it is possible that many fungi that have been characterized as low N_2O producers discovered by culturing in nitrite media might actually have been reducing NO derived from a chemical reduction of nitrite. In conclusion, we might have overestimated the number of denitrifying, N_2O producing fungi by testing in culture conditions that are not suitable.

Introduction

In chapter 1 we observed that fungal communities change when isolated from particle size fractions, suggesting a distinct ecological function in these compartments. We lack molecular tools to investigate whether fungi participate directly in nitrogen conversion processes in soil, which makes it difficult to include them in nitrogen cycling related studies. More data on fungi exposed to nitrogen and identification of nitrogen transforming organisms can help us to develop these tools and interpret data collected from environmental samples. In this chapter, we investigated nitrate assimilating fungal strains and their behavior when exposed to denitrifying conditions.

Apart from the oxidative pathway of nitrification, N_2O emissions from soil are linked to denitrification under oxygen limited conditions (Saggar *et al.*, 2013; Németh *et al.*, 2014; Z. Chen *et al.*, 2015). Denitrification in bacteria is defined as the sequential reduction of nitrate (NO_3^-) to nitrite (NO_2^-), nitric oxide (NO), nitrous oxide (N_2O) to dinitrogen gas (N_2) and has been extensively studied (Mahne and Tiedje, 1995; Bakken *et al.*, 2012). Current knowledge on fungal denitrification is mainly based on studies of *Fusarium oxysporum* (Shoun and Tanimoto, 1991; Zhemin Zhou *et al.*, 2001; Shoun *et al.*, 2012). So far, no nitrous-oxide reducing activity has been observed in fungi, supporting speculations on the significance of fungi in N_2O emissions.

To determine the relative contribution of either bacteria or fungi to N_2O emissions, addition of antibiotics inhibiting either the one or the other in soil microcosms was used (Joergensen and Wichern, 2008). When cycloheximide, a eukaryotic protein synthesis inhibitor, was added to soil samples with various characteristics, a decrease in N_2O production of over 50% was observed, suggesting a dominance of fungal activity in N_2O production in these studies (Crenshaw *et al.*, 2007; Laughlin *et al.*, 2009; Marusenko *et al.*, 2013; Wei *et al.*, 2014; H.

Chen, Mothapo, and Shi, 2014a; 2014b). However, a direct or indirect contribution of fungi to N_2O production and emission from soil is still under discussion.

In an effort to identify denitrifying fungi, pure cultures are undergoing screening by measurement of N_2O gas production (Jirout *et al.*, 2012; Mothapo *et al.*, 2013; Wei *et al.*, 2014; Maeda *et al.*, 2015). Although the fungal N_2O production rates reported are difficult to compare due to the use of different culture conditions and media, findings show that they are higher when nitrite is used as a terminal electron acceptor in contrast to nitrate (0.04 - 500 vs. 0.002 - 14 μmol N_2O-N d^{-1} gDW^{-1} respectively). In addition, the number of positive, N_2O producing strains identified is higher in nitrite relative to nitrate medium. This led to the common practice of using high concentrations of nitrite in culture media (up to 10 mM) when screening for fungal denitrification (Mothapo *et al.*, 2015).

Nitrite is also involved in another, physiologically distinct process of nitrogen reduction. During nitrate assimilation, nitrate is reduced by an assimilatory nitrate reductase (aNar) to nitrite which is further reduced by an assimilatory nitrite reductase (aNir) to ammonium and ultimately incorporated in the amino acid pool of the cell via glutamate biosynthesis (Crawford and Arst, 1993; Caddick *et al.*, 1994). Organisms have to invest considerable amounts of energy to carry out this pathway, which is therefore tightly regulated (Berger *et al.*, 2008). Dissimilatory nitrite reductases (dNir) and nitric oxide reductase (P450nor) associated with denitrification in fungi are localized in mitochondria were they are linked to ATP production (Kobayashi *et al.*, 1996). In *Fusarium oxysporum,* a dissimilatory nitrate reductase (dNar) is additionally active in mitochondria and allows the organism to generate energy from nitrate, but this enzyme is rarely found among fungi. A distinct denitrification pathway was found and described for *Fusarium lichenicola* (former *Cylindrocarpon tonkinense*) (Watsuji *et al.*, 2003). Here, an assimilatory type nitrate reductase, located in the cytosol, was producing nitrite as a substrate for dNir and P450nor in mitochondria, showing

for the first time, that the two pathways might interact under certain conditions. Surprisingly the presence of ammonium, nitrate and a fermentable sugar was key for N_2O production, whereas ammonium normally represses assimilatory nitrate reduction (Caddick *et al.*, 1994; Marzluf, 1997).

Assimilating nitrate is essential for plants and microbes in the competition for nitrogen in soils (Inselsbacher *et al.*, 2008). In the fungal kingdom, nitrate reductases were found throughout members of *Dikarya* (*Ascomycota* and *Basidiomycota*) which represent the majority of terrestrial fungi (Slot and Hibbett, 2007; Gorfer *et al.*, 2011) We speculated that a crossover of the assimilatory and dissimilatory nitrogen reduction system might be responsible for the preferred use of nitrite over nitrate observed for N_2O production in fungi. A pool of nitrite produced by aNar could be used by dNir and P450nor for energy generation when oxygen levels decline. Thus we hypothesized that nitrate assimilating fungi show N_2O production under anoxic conditions when nitrite and ammonium are present. We tested 22 nitrate assimilating fungal cultures isolated from agricultural soils in Czapeck-Dox broth amended with nitrite. An incubation system performing automated headspace gas sampling and subsequent quantification was used to monitor concentrations of NO, N_2O and O_2 throughout incubation. Measuring NO levels in cultures is crucial since it is a substrate for P450nor producing N_2O, resulting in information about nitrite and NO reduction behaviour of the different strains. Monitoring of oxygen allowed us to determine time points when the cultures become anoxic and a production of NO and N_2O can be expected.

Material and Methods

Strain selection and pre-cultures

Twenty-two fungal strains, 20 representing various classes within the *Ascomycota* and 2 within *Basidiomycota* (Table 2, Figure S 4) were selected from the culture collection of the Fungal Genomics Group (University of Life Sciences Vienna, Tulln - Austria). Selection was based on phylogenetic variety and ability to assimilate nitrate. *Fusarium oxysporum f.sp. lupini* and *Fusarium lichenicola* (CBS number: 483.96 and 100.97 respectively) were included in the study as positive controls for N_2O production from nitrite (Shoun and Tanimoto, 1991; Watsuji *et al.*, 2003). Strains were pre-cultured in Erlenmeyer flasks containing a teflon coated stirring bar and 100 mL of Czapeck-Dox broth (30 g L^{-1} Succrose; 0.85 g L^{-1} $NaNO_3$; 1 g L^{-1} K_2HPO_4; 0.5 g L^{-1} $MgSO_4$; 0.5 g L^{-1} KCl; 0.01 g L^{-1} $FeSO_4$)) inoculated with agar plugs from the culture collection and incubated at room temperature on a magnetic stirring unit (500 rpm).

Screening for N_2O production of fungi

Medical flasks (120 mL) were filled with 50 mL of phosphate buffered (pH 7) Czapeck-Dox broth (30 g L^{-1} Succrose; 4.15 g L^{-1} Na_2HPO_4; 2.9 g L^{-1} NaH_2PO_4; 1 g L^{-1} K_2HPO_4; 0.5 g L^{-1} $MgSO_4$; 0.5 g L^{-1} KCl; 0.16 g L^{-1} NH_4Cl; 0.01 g L^{-1} $FeSO_4$) and crimp-sealed with a gas tight butyl-rubber septum. Vials were autoclaved (120°C for 15 min) and He-washed with an alternated application of He-gas overpressure and vacuum (360 seconds vacuum followed by 30 seconds of He-gas filling for 6 cycles) after cooling down. Before starting the screening incubations, He-overpressure was released from the vials and 2 mL O_2 were injected (3% O_2 in headspace) followed by the injection of 500 µL of a sterile filtered, He-washed 1 M $NaNO_2$ solution (10 mM $NaNO_2$ in vials). Culture vials containing oxygen and nitrite were inoculated in triplicate with 1 mL of pre-cultures containing mycelium flocks of the fungi. After overpressure release to ensure same conditions for gas sampling, culture vials were incubated at 27°C for 270 hours in an incubation system with automated gas sampling (Molstad *et al.*,

2007) allowing for the continuous monitoring of headspace gas concentrations of O_2, NO and N_2O throughout the incubation. Cultures were stirred by teflon-coated stirring bars at 500 rpm to favour non-aggregated growth of mycelium and ensure proper gas exchange between the liquid and gas phase. Gas standards (25 ppm NO, 150 ppm N_2O, air for O_2, N_2 and CO_2) for calibration were run simultaneous with the cultures.

Inhibition experiment

To confirm that fungal activity caused a reduction of NO concentrations in non-*Fusarium* cultures, an inhibition experiment was designed where we injected cycloheximide (10 µg mL^{-1} medium) at the moment when vials turned anoxic. Protocols for the preparation of vials, medium used and measurements are the same as those described above for the screening experiment.

NO reduction experiment

To determine the NO reduction behaviour of fungi, a NO injection experiment was set up. Culture flasks were prepared as described above, with the exception of an injection of 100 µL of a sterile filtered, He-washed 1M $NaNO_2$ solution resulting in a nitrite concentration of 2 mM. At this nitrite concentration, no abiotic production of NO was observed in sterile medium. The NO injected in the vials was produced in He-washed vials containing acetic acid and NaI solution where KNO_2 was added, which is reduced to NO. The reaction was stopped by injection of 1 M NaOH (for details see (Hassan *et al.*, 2015)). Small doses were injected in vials containing fungi when anoxic conditions were reached. He-washed sterile medium vials were also injected with NO and monitored for autoxidation. Since the NO reaction occurs in liquid, but we are measuring headspace concentrations of the gas, we calculated NO concentrations in the liquid ($[NO]_{liquid}$) according to Molstad et al. (Molstad *et al.*, 2007). K_m and v_{max} was estimated by a Michalist-Menten curve fit in GraphPad Prism© 6.0e.

Detection of nirK and P450nor sequences

Two primer sets amplifying fungal nirK and one set specific to P450nor coding sequences were used to detect nitrogen reducing genes in tested strains. DNA of pure cultures was extracted from mycelia taken from cultures grown on malt extract agar plates using Quaigen DNeasy Plant Mini Kit. Primers and conditions for PCR reactions used were described previously (Wei *et al.*, 2015; Long *et al.*, 2015; Higgins *et al.*, 2016). PCR products were run on an agarose gel and bands in the expected size ranges were cut out, purified (illustra GFX PCR DNA and Gel Band Purification Kit; GE Healthcare Life Sciences) and sent for Sanger sequencing (GATC-Biotech AG, Cologne-Germany).

Chemical analyses

For measuring nitrite and ammonium concentrations, culture medium was sampled (~500 µL) by hand using sterile syringes and needles avoiding gas exchange between vials and the atmosphere. Samples were injected into a saturated triiodide solution in acetic acid where nitrite is reduced to NO, which is subsequently quantified in a NOx-analyzer (Sievers 280i, GE Analytical Instruments) (Cox, 1980; MacArthur *et al.*, 2007). For ammonium measurements, liquid samples were stored at -20°C and quantified colorimetrically in 96-well plates (Thermoscientific; Multiscan^{TM} FC Microplate Photometer) based on the Berthelot reaction (Hood-Nowotny *et al.*, 2010). To exclude chemodenitrification at low pH caused by organic acid production of fermenting strains, pH was measured at the end of experiment using a standard pH meter.

Biomass quantification and quality control

To estimate biomass of fungi in the screening experiment, medium with mycelium was spun down in 50 mL tubes, clear supernatant discarded and remaining mycelium dried at 80°C. In the NO-injection experiment, mycelium or cells were filtered (Merck Millipore Ltd; Isopore^{TM} Membrane Filters 0.2 µm) and weighed after drying. To estimate the amount of

nitrogen incorporated in biomass, we used average elemental stoichiometry determined for various fungal species (Mouginot *et al.*, 2014). At the end of the incubation periods, we sampled 2 mL of culture broth for DNA extractions (PowerWater® DNA isolation kit, Mo Bio Laboratories, Inc.) in order exclude bacterial contamination of cultures. Amplification of bacterial 16S rRNA gene sequences via PCR (primers used: 341f/534r (Watanabe *et al.*, 2001)) resulted in no bands on agarose gel for all fungal strains tested, with the exception of E.coli that was used as a positive control DNA.

Calculations and statistical analysis

MS Excel was used for calculations, for statistical analysis MS Excel and GraphPad Prism© 6.0e were used. Gas data were corrected for sample dilutions and concentrations were calculated based on peak areas from standards. We analysed N_2O production from fungi by comparing endpoint N_2O values as well as using the following formula to take also the potential N_2O derived from reduction of abiotically produced NO into account:

$$[N_2O]_{producing\ strain} > [N_2O]_{control} + ([NO]_{control} - [NO]_{left\ in\ culture\ vials})$$

Results

Abiotic NO production

Sterile Czapeck-Dox broth (10 mM nitrite, 3 mM ammonium) was monitored over 300 h for production of NO and N_2O under oxic (3% O_2 in headspace) and anoxic conditions (He-washed) (Figure 15). An increase in N_2O could be measured in both conditions, but it was slightly higher in anoxic than oxic conditions (2.5 nmol h^{-1} $vial^{-1}$, R^2 = 0.947 and 1.3 nmol h^{-1} $vial^{-1}$, R^2 = 0.915 respectively). NO, in contrast, was not detected when oxygen was present, but a NO production of 12 nmol h^{-1} $vial^{-1}$ (R^2= 0.988; measured over 300 h) could be measured under anoxia.

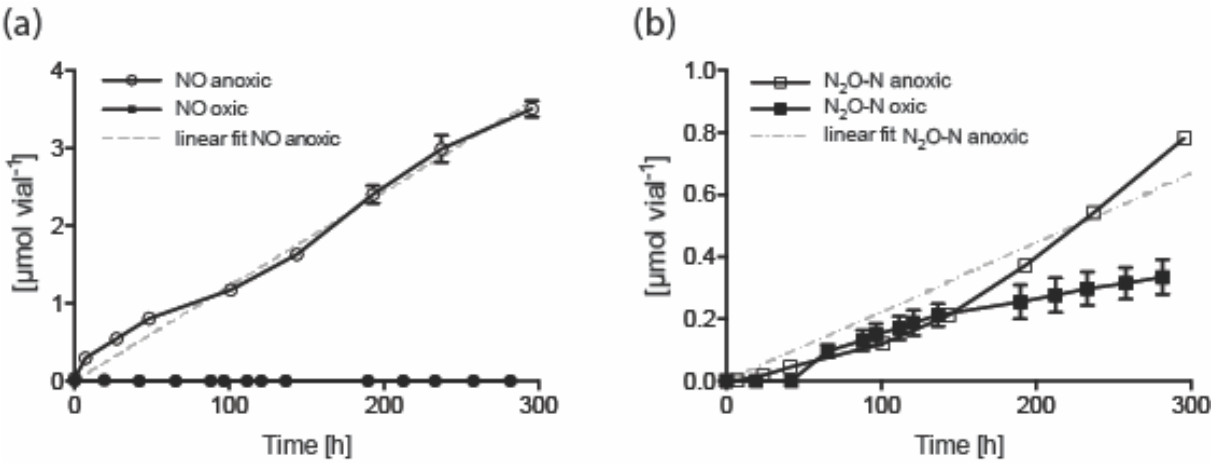

Figure 15: Abiotic NO (a) and N_2O-N (b) production from sterile Czapeck-Dox medium controls in oxic and anoxic conditions. Butyl-rubber sealed vials (120 mL) containing 50 mL sterile, He-washed Czapeck-Dox medium (3mM ammonium; 10mM nitrite; 50 mM phosphate buffer (pH 7); 3 % O_2 in headspace for oxic vials, anoxic vials just He-washed) were incubated at 27°C for 270 h for headspace gas sampling. Open symbols show gas concentrations in anoxic, closed symbols in oxic vials. Grey dotted lines show linear regression used to estimate abiotic NO (12 nmol h^{-1} $vial^{-1}$) and N_2O-N (2.5 nmol h^{-1} $vial^{-1}$) production in anoxic fungal cultures. Data points show mean, error bars the standard deviation (n=3).

Conditions for abiotic NO production

In order to correct for abiotically produced NO in our screening analysis, we estimated the NO increase from the medium in the culture vials during the anoxic phase of culturing. Tested fungi consumed the O_2 initially present in vials, thus turning conditions from oxic to anoxic during incubation. Using cultures that consumed O_2 at low rates, we defined an oxygen

Table 2: Endpoint gas concentration in headspace of tested strains for N_2O-N, NO and estimated abiotic NO produced by medium. Butyl-rubber sealed vials (120 mL) containing 50 mL sterile, He-washed Czapeck-Dox medium (3mM ammonium; 10mM nitrite; 50 mM phosphate buffer (pH 7); 3 % O_2 in headspace of vials, 10mM nitrite) were inoculated with 1 mL of pre-cultures and subsequently incubated at 27°C for 270 h for headspace gas sampling. Values show the mean and standard deviation (n=3) - T.test (alpha = 0.05) with Welch correction for unequal standard deviation was used to test for significant differences.

	Endpoint N_2O-N [µmol vial^{-1}]	Endpoint NO [µmol vial^{-1}]	Time abiotic NO production[a] [h]	estimated abiotic NO [µmol vial^{-1}]	abiotic NO reduced by fungi[b] [µmol vial^{-1}]	nirK[c]	P450nor[c]
01_*Cladosporium cladosporioides*	0.6 ± 0.07	0.35 ± 0.09	210	2.52	2.17 - (0.86)		
02_*Aspergillus creber*	1.1 ± 0.01*	0.84 ± 0.01	201	2.41	1.57 - (0.65)	+	
03_*Coniothyrium carteri*	0.6 ± 0.08	1.02 ± 0.15	170	2.04	1.02 - (0.50)		
05_*Solicoccozyma terricola*	0.2 ± 0.05	0.25 ± 0.18	108	1.30	1.05 - (0.80)		
08_*Chaetomiaceae*	2.1 ± 0.59*	0.17 ± 0.03	220	2.64	2.47 - (0.93)		
10_*Gibellulopsis nigrescens*	0.1 ± 0.01	0.00 ± 0.00	-	-	-		
14_*Fusarium oxysporum f.sp. lupini* CBS 100.97)	**73.2 ± 26.9***	0.19 ± 0.01	220	-	-	+	+
15_*Fusarium lichenicola* (CBS 483.96)	**382.5 ± 71.0***	0.02 ± 0.03	217	-	-	+	+
18_*Paraphoma chrysanthemicola*	1.4 ± 0.29*	0.50 ± 0.10	172	2.06	1.56 - (0.75)		+
23_*Talaromyces purpurogenus*	1.1 ± 0.14*	0.17 ± 0.06	215	2.58	2.41 - (0.93)	+	
26_*Clavicipitaceae*	1.1 ± 0.02*	0.01 ± 0.00	215	2.58	2.57 - (0.99)	+	
27_*Penicillium canescens*	1.3 ± 0.17*	0.44 ± 0.13	213	2.56	2.11 - (0.82)		
28_*Talaromyces rugulosus* related	0.7 ± 0.05	0.63 ± 0.10	200	2.41	1.78 - (0.74)		
30_*Pyrenochaeta cava*	1.8 ± 0.33*	0.03 ± 0.01	215	2.58	2.55 - (0.98)		+
31_*Hypocreales*	2.2 ± 0.40*	0.06 ± 0.02	215	2.58	2.53 - (0.97)		
32_*Talaromyces purpurogenus* related	2.2 ± 0.48*	0.13 ± 0.12	213	2.56	2.43 - (0.95)		
33_*Penicillium sp*.	1.2 ± 0.17*	0.94 ± 0.49	224	2.69	1.74 - (0.64)		
35_*Clavicipitaceae*	0.6 ± 0.05	0.01 ± 0.00	213	2.55	2.54 - (0.99)		
36_*Cordyceps bassiana*	0.9 ± 0.14*	0.29 ± 0.10	212	2.55	2.25 - (0.88)		
37_*Solicoccozyma aeria*	0.9 ± 0.15*	0.05 ± 0.02	213	2.55	2.50 - (0.98)		
38_*Oidiodendron cerealis*	0.1 ± 0.02	0.00 ± 0.00	-	-	-		
40_*Fusarium solani* species complex	0.9 ± 0.07*	0.20 ± 0.05	218	2.62	2.42 - (0.92)		
41_*Fusarium solani* species complex	**93.0 ± 29.6***	0.06 ± 0.02	221	-	-		
43_*Fusarium solani* species complex	**249.3 ± 82.4***	0.04 ± 0.01	230	-	-		
Sterile Medium Control	0.68 ± 0.15	3.24 ± --	270	3.24	-		

* significant higher N_2O production at the end of incubation compared to N_2O in sterile medium

Bold names: significantly higher N_2O production compared to N_2O in sterile medium plus estimated amount of abiotic NO reduced by fungi

[a] calculated at time when O_2 falls below 5 µmol vial^{-1} for the first time until end of experiment

[b] endpoint values NO measured substracted from estimated abiotic NO production – values in brackets estimate the ratio of reduced abiotic NO

[c] positive cultures were nirK or P450nor amplicons matched with sequences form the database (bit score > 100; blast searches vs. Ncbi NT/NR); primers: (Long *et al.*, 2015; Wei *et al.*, 2015; Higgins *et al.*, 2016)

threshold for abiotic NO production. We compared O_2 and NO data from two slow growing strains (38_*Oidiodendron cerealis, 05_Solicoccozyma terricola),* which also showed a high variability in oxygen consumption among their replicates (n=3) (Figure S 3). Only in vials where O_2 concentrations dropped below 5 µmol vial^{-1} could we also measure NO in headspace. Consequently, we assumed NO production in all other culture vials when O_2 dropped below that threshold. Estimated abiotic NO increases throughout the incubation were 2 – 2.6 µmol vial^{-1} (Table 2). Knowing the NO left in vials at end of incubations, we could estimate the amount of NO that was potentially reduced to N_2O by the fungus (1 - 2.6 µmol vial^{-1}).

N_2O production from fungi: endpoint vs. abiotic NO-corrected

By comparing endpoint N_2O values, we found 17 strains that produced significantly higher amounts of N_2O than the control vials (Table 2; strains marked with an asterisk*). When these data are corrected for abiotic NO production, only 4 tested *Fusarium* strains showed significantly higher N_2O concentrations as calculated by the addition of N_2O from controls and the NO reduced by the culture which potentially ends up as N_2O as well (bold names in Table 2). NO and N_2O-N concentrations throughout incubation are shown for two *Fusarium* and two non-*Fusarium* strains in Figure 16. N_2O production was observed for most *Fusarium* cultures (culture 14, 15, 41 and 43) and NO concentrations never exceeded 0.3 µmol vial^{-1}. In non-*Fusarium* cultures, a different behaviour in NO reduction was observed. NO increased at similar rates (12 nmol h^{-1} vial^{-1}) as those observed for the anoxic controls initially when O_2 concentrations dropped below 5 µmol vial^{-1}. This initial increase in NO was followed by a decrease in cultures and NO concentration in headspace never exceeded 1 µmol vial^{-1} (Figure S 5). Cultures 40_*Fusarium solani* species complex and 33_*Penicillium* sp. allowed higher NO concentrations in the headspace (up to 3 µmol vial^{-1}).

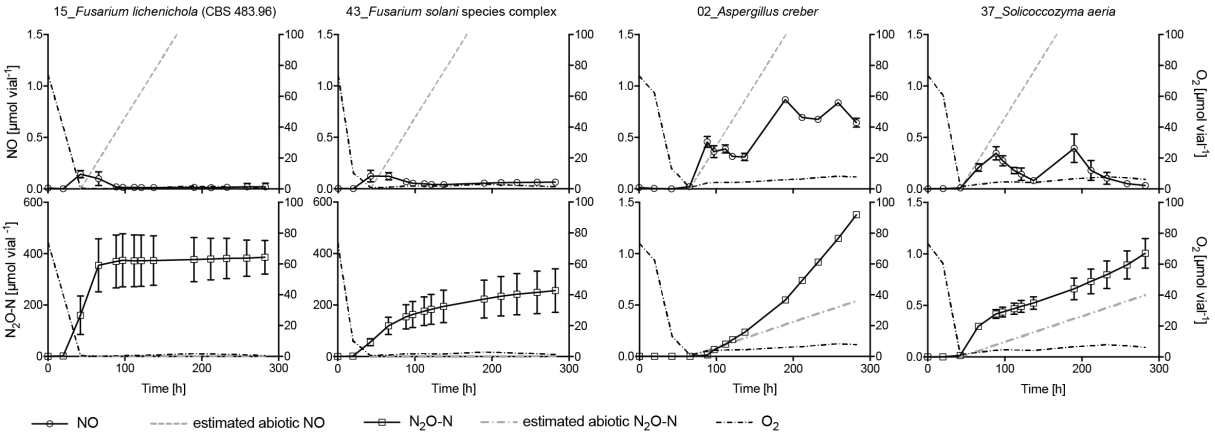

Figure 16: NO, N_2O-N and O_2 concentrations in headspace of *Fusarium* and non-*Fusarium* cultures. Butyl-rubber sealed vials (120 mL) containing 50 mL sterile, He-washed Czapeck-Dox medium (3mM ammonium; 10mM nitrite; 50 mM phosphate buffer (pH 7); 3 % O_2 in headspace of vials) were inoculated with 1 mL of pre-cultures and subsequently incubated at 27°C for 270 h for headspace gas sampling. Grey dotted lines show estimated abiotic NO (12 nmol h^{-1} $vial^{-1}$) and N_2O-N (2.5 mol h^{-1} $vial^{-1}$) production when vials get anoxic (O_2 < 5 µmol $vial^{-1}$); black dotted line indicates O_2 concentrations in headspace of vials. Data points show mean, error bars the standard deviation (n=3).

N_2O curves in vials could also be clearly distinguished between *Fusarium* and non-*Fusarium* strains. In *Fusarium* cultures, N_2O was found to increase earlier in the transition from oxic to anoxic conditions than in non-*Fusarium* cultures (Figure S 6).

Use of nitrite and ammonium and biomass increase

Fusarium strains were able to reduce nitrite efficiently and produce significant amounts of N_2O, unlike the other tested strains in the screening. Whereas nitrite dropped between 257 and 469 µmol $vial^{-1}$in *Fusarium* vials, non-*Fusarium* strains only used between 23 and 60 µmol $vial^{-1}$ (50 - 96 % and 4 - 16 % of initially present nitrite, respectively). Figure 17 shows decrease of nitrite concentrations in the cultures versus N_2O-N production in the headspace. Ammonium decreased between 91 and 120 µmol $vial^{-1}$ (60 – 90 % of initial present ammonium) in the cultures of *Fusarium* strains. Non-*Fusarium* strains used ammonium with a broad range of efficiency (0 – 109 µmol $vial^{-1}$ representing 0 – 75 % of initial present ammonium). Fungal biomass increase during cultivation was estimated to be between 7 and 17 mg dry weight. We estimated the amount of nitrogen incorporated in biomass between 27 and 70 µmol N $vial^{-1}$ for tested strains.

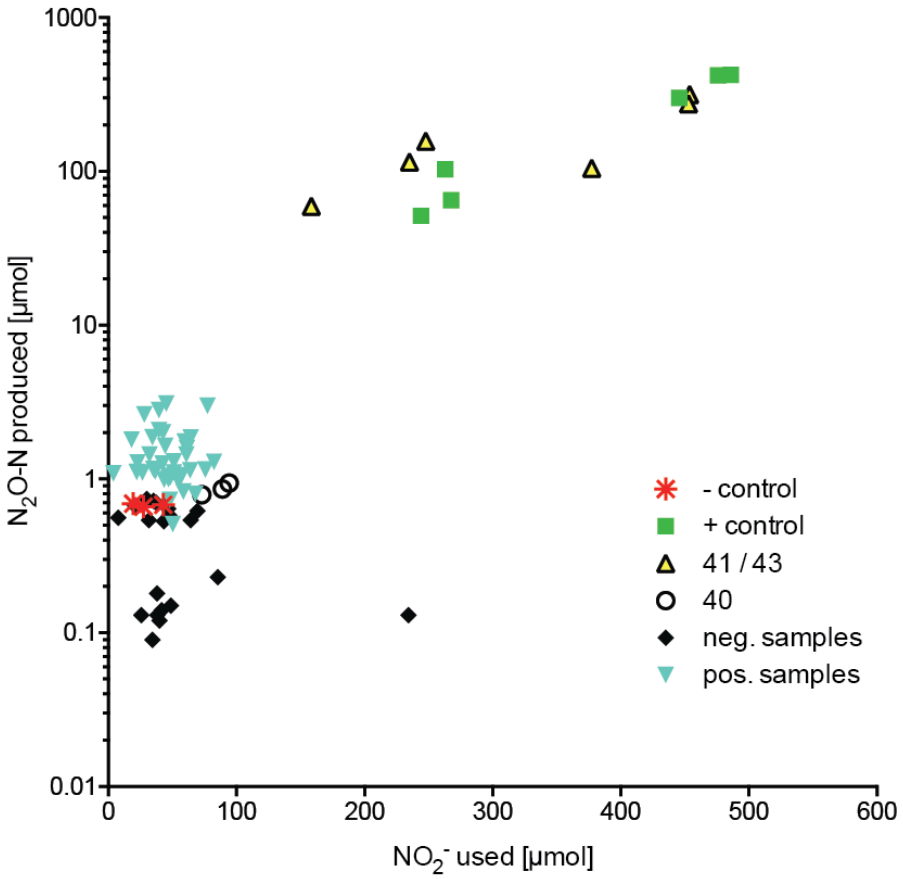

Figure 17: Decrease in nitrite vs. increase in N_2O-N for cultures and sterile nitrite medium vials. – control: sterile nitirite medium controls; + control: 14_*Fusarium oxysporum f.sp. lupini* (CBS 100.97), 15 *Fusarium lichenicola* (CBS 483.96); 41/43: 41_ and 43_*Fusarium solani* species complex; 40: 40_*Fusarium solani* species complex; neg. samples: data from cultures found to prodcuce not significantly more N_2O than sterile nitrite medium (Table 2); pos. samples: data from cultures found to produces significantly more N_2O-N than sterile nitrite medium without consideration of abiotic produced NO (Table 2). Data points show values from single vials.

Inhibition experiment

To confirm that NO curves were derived from biologically active fungi and not due to chemical reactions with fungal biomass, we repeated the experiment with *Solicoccozyma aeria* cultures, but injected cycloheximide in the culture vials at the beginning of anoxic conditions to inhibit fungal activity. In vials containing cycloheximide, NO concentration increased as expected from data of anoxic controls with an approximate rate of 12 nmol h^{-1} $vial^{-1}$ (Figure 18).

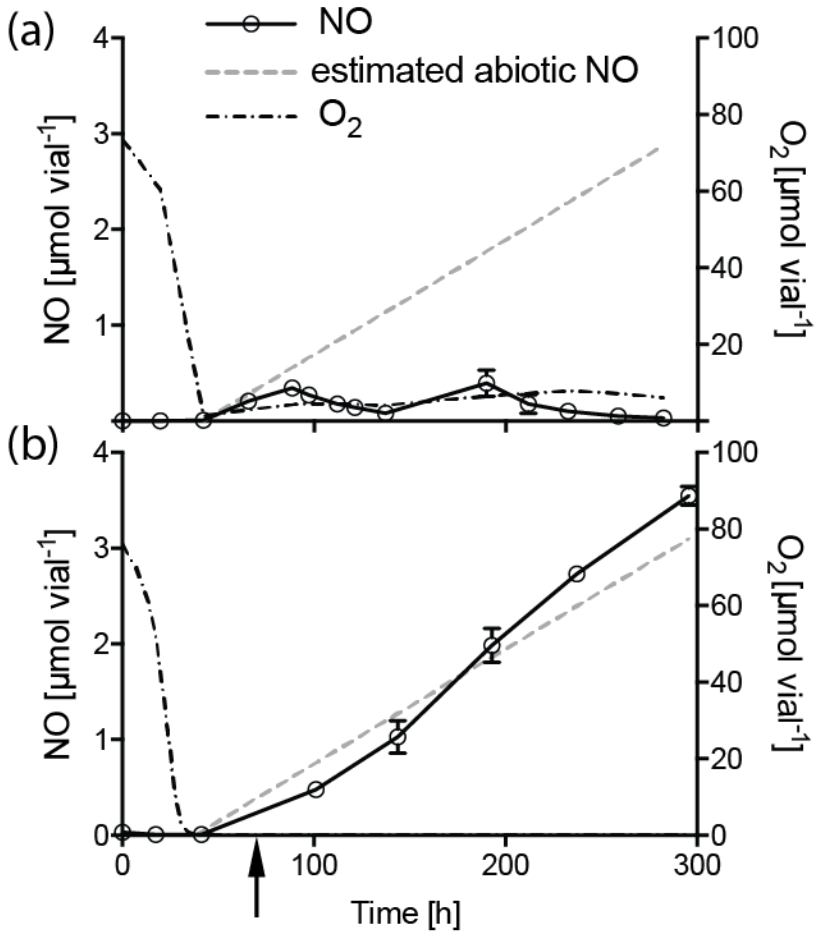

Figure 18: NO concentrations in headspace of *Solicoccozyma aeria* cultures without (a) and with (b) injection of cycloheximide into vials throughout incubation. Butyl-rubber sealed vials (120 mL) containing 50 mL sterile, He-washed Czapeck-Dox medium (3mM ammonium; 10mM nitrite; 50 mM phosphate buffer (pH 7); 3 % O_2 in headspace of vials, 10mM nitrite) were inoculated with 1 mL of pre-culture of *Solicoccozyma aeria* and subsequently incubated at 27°C for 270 (a) and 300 (b) hours for headspace gas sampling. Grey dotted lines show estimated abiotic NO (12 nmol h^{-1} $vial^{-1}$) production when vials get anoxic (O_2 < 5 µmol $vial^{-1}$); black dotted line indicates O_2 concentrations in headspace of vials; open symbols show NO concentrations in headspace. Arrow indicates time point of cycloheximide (10 µg mL^{-1} medium) injection in (b). Data points show the mean, error bars standard deviation (n=3).

NO reduction experiment

No increases in NO concentrations were observed in fungal culture vials, in contrast to the sterile medium control (Table 2, Figure S 5). To determine if these cultures could reduce this abiotic NO to N_2O, we injected NO gas in increasing concentrations into *Fusarium lichenicola* (CBS 483.96) (positive control), *Solicoccozyma aeria* cultures and sterile medium controls and monitored NO and N_2O concentrations in the headspace of vials. The results shown in Figure 19 confirmed the capability of *Fusarium lichenicola* (CBS 483.96) (a) to

convert NO to N_2O. Injection of NO in *Solicoccozyma aeria* cultures was also followed by an immediate increase in N_2O concentrations (b). We calculated NO reduction rates in liquid phase after NO injections and estimated v_{max} and K_m values for both organisms under culture conditions (Figure 19 (c) and (d); Table 3). Estimated v_{max} of *Fusarium lichenicola* (CBS 483.96) was two orders of magnitude higher than for *Solicoccozyma aeria* and three orders of magnitude higher than v_{max} estimated for sterile medium controls.

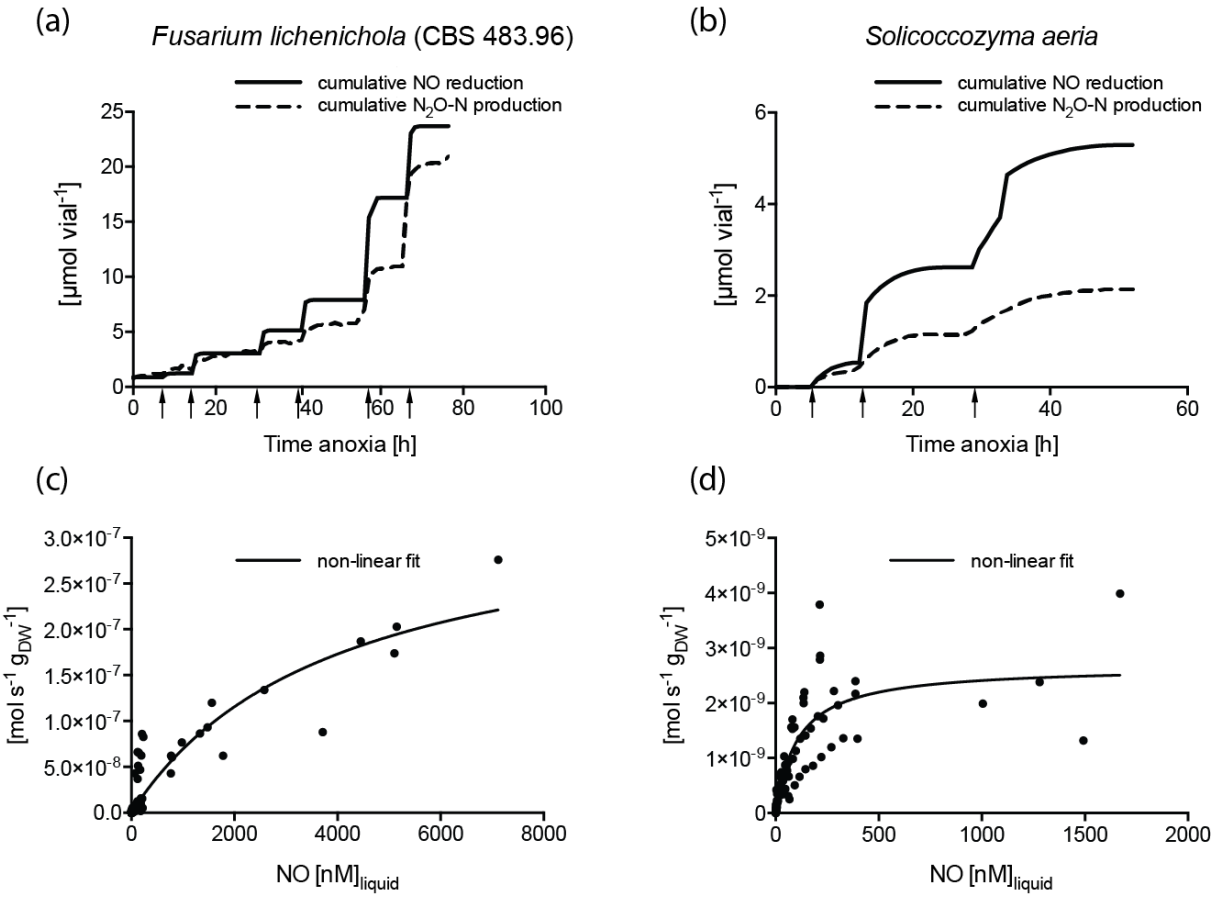

Figure 19: Cumulative NO reduction vs. N_2O-N production and NO reduction rates of *Fusarium lichenicola* (CBS 483.96) (a, c) and *Solicoccozyma aeria* (b, d) cultures in anoxia after NO injection. Butyl-rubber sealed vials (120 mL) containing 50 mL sterile, He-washed Czapeck-Dox medium (3 mM ammonium; 2 mM nitrite; 50 mM phosphate buffer (pH 7); 3 % O_2 in headspace of vials, 10mM nitrite) were inoculated with 1 mL of pre-culture of tested strain and subsequently incubated at 27°C for for 50 (a,c) and 80 (b,d) hours for headspace gas sampling. (a) and (b) show NO to N_2O-N concentrations in headspace plotted as cumulative reduction of NO and cumulative production of N_2O-N in vials. Arrows indicate time points of NO injections of increasing concentrations. Data points show values of a single vial out of 3 replicates. (c) and (d) show Michaelis-Menten curve fit to NO reduction rates calculated from NO injections in same vials as (a) and (b). NO concentrations in liquid phase were calculated based on measured headspace concentrations.

Table 3: NO reduction after NO injection kinetic parameters for *Fusarium lichenicola, Solicoccozyma aeria* and sterile medium control. Values derived from Michaelis-Menten curve fitting over NO reduction rates in liquid calculated by measured NO in headspace (n=3). T.tests with Welch correction for unequal standard deviation were performed on K_m and v_{max} values of single vial data. Letters in the table indicate a significant difference (alpha = 0.05) of the group.

	v_{max}[mol s^{-1}vial^{-1}]	v_{max}[mol $s^{-1}g_{DW}^{-1}$]	K_m[nM]	R^2
Fusarium lichenicola (CBS 483.96)	$1.7*10^{-9}$ [a]	$2.2*10^{-7}$	1878 [a]	0.855
Solicoccozyma aeria	$4.5*10^{-11}$ [b]	$2.7*10^{-9}$	116 [b]	0.763
Sterile medium control	$4.5*10^{-12}$ [c]	-	7.9 [c]	0.535

Nitrite and nitric oxide reductases

Sanger sequencing of nirK and P450nor amplicons was used to detect presence of key enzymes of the investigated nitrogen reduction processes encoded in the genomes fungal cultures. Tested strains where targeted genes were found are indicated in Table 2. The two sets of nirK specific primers used resulted in distinct bands for most cultures (Figure S 8). Presence of a nitrite and nitric oxide reductase could only be confirmed for the two positives control strains (14_*Fusarium oxysporum f.sp lupini* (CBS 100.97); 15_*Fusarium lichenicola* (CBS 483.96)). Furthermore, nirK could be amplified from culture 2, 23 and 26 and P450nor from culture 18 and 30. Surprisingly, we could not find any of the two sequences by this approach in the two *Fusarium solani* cultures (41 and 43) which showed high nitrite reduction and N_2O-N production.

Discussion

Fungal denitrification came into focus over the last two decades as a potent and important source for N_2O production in soil environments. Screenings on fungal cultures for N_2O production led to an agreement that denitrifying fungi prefer nitrite over nitrate in their dissimilatory nitrogen reduction system, since higher N_2O concentrations (up to one order of magnitude) were produced in nitrite media (Jirout *et al.*, 2012; Wei *et al.*, 2014; Maeda *et al.*, 2015). Consequently, the majority of N_2O producing fungi were identified in studies using culture media amended with nitrite (Mothapo *et al.*, 2015). In the attempt to compare our results to previous studies, we decided to use a chemically defined culture medium (Czapeck-Dox) amended with high concentrations of nitrite (10 mM) to test nitrate assimilating strains on the ability to denitrify and produce N_2O. The greenhouse gas was detected in all tested cultures and two main groups could be distinguished by the amount of N_2O produced: *Fusarium* related strains, where one to two orders of magnitude more N_2O was measured than in non-*Fusarium* strains (Table 2).

To identify fungi that are capable of producing N_2O by the sequential reduction of nitrite and NO, N_2O concentrations measured at the end of incubation experiments were compared to values reached in controls and tested for significance. In our study, we monitored NO and N_2O throughout the entire cultivation of fungal strains while the cultures underwent a transition from oxic to anoxic conditions. Anoxic sterile media controls showed an unexpected NO production (Figure 15). NO was also produced at the same rates when the oxygen was consumed by fungal cultures and biological activity was inhibited by the addition of cycloheximide once anoxia was reached (Figure 16). This supported our hypothesis that all tested cultures were disturbed and affected under anoxia by an abiotic NO production from the medium, a condition which might have been overlooked in culture studies using nitrite media. As a precursor molecule, abiotically produced NO could be potentially reduced to

non-toxic N_2O by fungi, thus leading to false positives in N_2O endpoint comparisons, especially if low N_2O concentrations are measured, as was the case for non-*Fusarium* stains in our study.

Fifteen studies were published so far investigating N_2O production from fungal isolates and results from 14 studies were recently reviewed (Maeda *et al.*, 2015; Mothapo *et al.*, 2015). Twelve of these 15 studies used nitrite media and over 120 different fungal species were identified as N_2O producing. In order to compare production rates from the studies, Mothapo et al. converted results to a comparable unit (nmol N_2O-N mL^{-1} medium day^{-1}), due to differences in protocols and data representation. The range of production rates reported in the review is < 0.1 - 2476 nmol N_2O mL^{-1} medium day^{-1}, which is comparable to our data (0.1 - 1.9 and 65 -330 nmol N_2O mL^{-1} medium day^{-1} for non-*Fusarium* and *Fusarium* strains respectively). About 25 % of reported species show similar values as we found for non-*Fusarium* strains, although exact comparison is difficult due to major differences or no data on fungal biomass in culture vials. Nevertheless, as all studies, including ours, found comparable values of N_2O production, our findings on an abiotic NO production from nitrite media raises questions on whether low- N_2O producers among fungi truly reduce nitrite over NO to N_2O.

This is supported by a comparison of nitrite usage and N_2O-N production in our study, which showed that except Fusarium strains producing high amounts of N_2O and used nitrite efficiently, all stains decreased nitrite at levels also found in the sterile medium control (Figure 17). Thus low level N_2O producers might not use nitrite at all and response to the presence of NO by detoxifying it to N_2O. Altogether, it will be inevitable in future culturing studies to thoroughly test the nitrite media used for abiotic NO production as well as measuring NO in the headspace during incubation to exclude possible error sources.

Abiotic NO release from the medium under anoxic conditions is probably caused by the versatile chemical nature of nitrite (Nelson and Bremner, 1969; 1970b; Van Cleemput and Samater, 1995). Knowledge about the behaviour of nitrite in solutions and its chemical reaction to NO and N_2O is scarce. Chemodenitrification, a source of abiotic NO and N_2O production appearing at low pH, could be excluded in our study since pH 7 was maintained throughout the entire experiment by a buffered culture medium (Pilegaard, 2013). However, this process can also be induced in the presence of Fe^{2+}, which is a component of Czapeck-Dox broth we used (Nelson and Bremner, 1969; Kampschreur *et al.*, 2011). Under these conditions, the thermodynamically unfavourable red-ox reaction of nitrite reduction to NO and coupled iron oxidation is catalyzed under anoxia by a biological reduction of the built-up Fe^{3+}. Ferric iron reduction by fungi has been related to nitrate reducing strains, the same group of fungi we chose for our study (Ottow and Klopotek, 1969). However, NO production as we observed in the sterile media under anoxia cannot be explained by an iron-coupled reaction which would require the presence of a biologically active organism.

Physiological effects of NO on fungi are ambiguous. Low concentrations of NO promote cell survival and proliferation in higher organisms (Thomas *et al.*, 2008). At higher concentrations (> 1 μM) NO can react with oxygen species, thiol-containing proteins and metaloproteins causing nitrosative stress to organisms (Tillmann *et al.*, 2011). Nitrosative stress on fungi was investigated in the context of host-pathogen interactions, where yeasts showed a response to NO concentrations (1 – 2 μM) similar to peak levels reached in our study (0.3 – 2 μM in the headspace corresponding to 0.2 – 1.3 μM in the liquid for non-*Fusarium* strains) (Liu *et al.*, 2000; Ullmann *et al.*, 2004). All fungi in our study were able to deal with the nitrosative stress under anoxia derived from abiotic NO release from the medium (12 nmol h^{-1} $vial^{-1}$). An efficient NO reduction under anoxia in *Fusarium* strains was expected since NO reductase P450nor has been well described in this group (Shoun *et al.*, 2012). Here, we observed the lowest NO concentrations in the headspace of culture vials throughout incubation, which

confirms the presence of an active NO reductase (Figure 16; Figure S 5). All other tested strains allowed accumulation of NO at higher concentrations before they decreased again. This accumulation and decrease of NO was observed several times for non-*Fusarium* strains, resulting in wave-shaped NO curves. NO curves appeared to be almost identical among five of the tested strains (02_*Aspergillus creber, 27_Penicillium canescens, 28_Talaromyces rugulosus* realted*, 32_Talaromyces purpurogenus* related*, 23_Talaromyces purpureogenus*). In a comparison of the phylogenetic relationships between all tested strains, these 5 candidates were found to be closely related representing the *Eurotiales* order (Figure S 4). A similar pattern in NO concentrations over approximately 210 hours of anoxic culturing among phylogenetically closely related strains could point to a common defense system against NO stress.

Sequenced amplicons of P450nor and nirK amplicons could not be linked to N_2O production or nitrite reduction in this study. Although nirK was present in 02_*Aspergillus creber* we could not see a efficient reduction of nitrite of this strain compared to decrease of nitrite in sterile medium controls. Also for 18_*Paraphoma chrysanthemicola* and 30_*Pyrenochaeta cava* where P450nor sequences could be identified no N_2O production originated from the fungus can be confirmed. These results together with the partly unspecific amplification of the current primers (Figure S 8) suggest that we need to improve primers detecting fungal nitrogen reducing gene sequences. The successful amplification and identification of both genes in the two positive controls, but not in the two also N_2O producing Fusarium strains indicate that primers might be too specific to the sequences now available. Sequences of nirK and P450nor genes of efficient N_2O producing fungi need to be identified in order to improve primer sequences for their detection. However, the lack of P450nor involved in fungal denitrification suggests that the observed NO reduction by the non-*Fusarium* strains might not be based on P450nor activity alone, but also distinct enzymatic pathways partly producing N_2O.

Globin-like proteins, widespread in living organisms, possess a heme centre as prosthetic group that can bind various gases such as CO, NO and O_2, thus playing an important role in NO formation and decay (Tejero and Gladwin, 2014). We lack information about their functional role under anoxia for many of these proteins (Barker *et al.*, 2012; Hillmann *et al.*, 2014). NO detoxification by flavohemoglobin has been intensively studied in oxic conditions, where it acts as a nitric oxide dioxygenase in bacteria (P. R. Gardner *et al.*, 1998; P. R. Gardner, 2005). Nevertheless, in anoxia flavohemoglobin can mediate the reduction of NO to N_2O in E.coli, even though reduction rates were found to be approximately 1% compared to oxic reduction (S. O. Kim *et al.*, 1999; Forrester and Foster, 2012). This anoxic feature of flavohemoglobin was found to be essential in *Bacillus subtilis* for long-term survival under anoxic conditions (Nakano, 2006). Flavohemoglobin was also found to detoxify NO in phylogenetically distinct fungi (Liu *et al.*, 2000; de Jesús-Berríos *et al.*, 2003; Ullmann *et al.*, 2004; Shengmin Zhou *et al.*, 2009; Biesebeke *et al.*, 2010). Flavohemoglobin coding sequences were found in fully sequenced genomes available for *Aspergillus creber*, *Nectria heamatococca* and *Penicillium canescens* as well as *Fusarium oxysporum*.

Besides flavohemoglobin, flavorubredoxin reduces NO to N_2O under anoxia in bacteria at similar rates as determined from purified enzyme essays as heme b_3-Fe_B nor from *Paracoccus denitrificans* (A. M. Gardner *et al.*, 2002; Gomes *et al.*, 2002). However, it has as yet not been described in fungi and BLAST searches we carried out found rubredoxin motifs conserved in bacteria. It should be mentioned that P450nor was upregulated in response to NO-stress *in Histoplasma capsulatum*, a human pathogen (Nittler *et al.*, 2005; Chao *et al.*, 2008) showing that this enzyme is also used to detoxify NO by fungi instead of being involved in an energy generating denitrification process.

All non-*Fusarium* strains in this study could scavenge abiotically produced NO from the medium over approximately 210 h of anoxic incubation. If we assume no NO production by

an active nitrite reductase, NO to N_2O conversion efficiency was 12 - 90% for non-*Fusarium* strains. Efficiency in N_2O production from NO by *Solicoccozyma aeria* calculated this way was 35±5% (Table 2), ratios we also observed for *Solicoccozyma aeria* after NO injection (20-35%) (Figure 19b). The genome of this strain has yet to be sequenced to confirm the presence of candidate genes that mediate N_2O production. A distinct behavior in NO reduction in the screening experiment (Figure S 5) as well as N_2O production at significantly lower rates after NO injection compared to *Fusarium lichenicola* (CBS 483.96) but higher than sterile controls (Table 3; Figure S 7) suggest a NO reduction distinct from the P450nor system. However, this still needs to be confirmed by molecular methods and further tests.

In conclusion, our data showed an unexpected, abiotic NO production from Czapeck-Dox broth in anoxia amended with nitrite at high concentrations as is often used in fungal screening studies. Abiotic NO production in anoxia was also induced when O_2 was consumed by fungi, which was confirmed by injection of cycloheximide in cultures. Injecting NO in *Solicoccozyma aeria* culture resulted in a partial conversion to N_2O. Efficient reduction of nitrite and production of N_2O could be confirmed for all four *Fusarium* strains tested, while low concentrations of N_2O measured in non-*Fusarium* vials is most likely derived from an anoxic NO defense mechanism against abiotic NO produced from the medium. Similarity and comparability of experimental design and of ranges of detected N_2O levels with previous studies suggest that we might have overestimated the number of nitrite reducing, N_2O producing fungi by including low level N_2O producers identified in nitrite medium.

Chapter 3: Bacterial and fungal response to organic matter addition of distinct carbon chemistries

Abstract

Nitrous-oxide (N_2O) gas concentrations are currently increasing in the atmosphere and are an environmental concern because of their contribution to global warming through the degradation of the ozone layer. Soil microbes, such as bacteria and fungi, were found to potentially produce this greenhouse gas, leading to elevated emissions. The contribution of fungi to N_2O emissions from soils remains unclear, but inhibition experiments suggested their importance. We hypothesized that fungi play an indirect role in N_2O production processes by providing nutrients through organic matter decomposition for nitrogen cycling bacterial communities. We incubated soil in microcosms with different organic matter additions (paper pulp, compost and sewage sludge) for 30 days, analyzed bacterial and fungal community development by sampling a time series of metagenomes and metatranscriptomes and quantified ammonium and nitrate concentrations as well as N_2O, CO_2 and CH_4 in the headspace of the microcosm bottles. We observed distinct responses of bacterial and fungal communities to different treatments and could link carbon degrading and nitrogen cycling activity to fungal and bacterial community members. N_2O production after organic matter addition was inhibited by the suppression of fungal activity. Altogether, our data suggests and indirect involvement of fungi via the carbon cycle to N_2O emissions rather than a direct contribution to N-cycling related processes.

Introduction

In chapter 2 we suggested that the number of N_2O producing fungi might have been overestimated. Furthermore, the N_2O production rates we found were comparable to previous studies (Mothapo *et al.*, 2015), which were orders of magnitude lower than those reported for bacteria (I. C. Anderson and Levine, 1986; Zumft, 1997) and so far, no study could show a correlation between N_2O production potential and fungal denitrification activity through molecular approaches (H. Chen *et al.*, 2015; Higgins *et al.*, 2016). However, several studies have shown that inhibiting fungal communities caused a decrease in N_2O emitted from soil (Crenshaw *et al.*, 2007; Laughlin *et al.*, 2009; Marusenko *et al.*, 2013; Wei *et al.*, 2014; H. Chen, Mothapo, and Shi, 2014a; 2014b), which fuels the discussion on the participation of fungi in these processes.

Fungi and bacteria respond differently to various environmental factors including pH (Pennanen *et al.*, 1998; Bååth and T. H. Anderson, 2003), substrate composition (Bittman *et al.*, 2005; Boer *et al.*, 2005; Georgieva *et al.*, 2005; Engelking *et al.*, 2007; Rousk and Bååth, 2007; Barreiro *et al.*, 2016), salinity (Sardinha *et al.*, 2003; Rasul *et al.*, 2006), temperature (Lipson *et al.*, 2002; Schadt *et al.*, 2003; Pietikäinen *et al.*, 2005), heavy metals and pollutants (Ley and Schmidt, 2002; Rajapaksha *et al.*, 2004; Fernández-Calviño and Bååth, 2016). Also, fungi and bacteria were shown to degrade organic matter differently (Strickland and Rousk, 2010). Generally, as recalcitrance of organic matter increases, fungal dominance in decomposition processes is expected to increase. Carbon input to natural soil ecosystems is mainly comprised of dead plant material, thus difficult to break down polysaccharides such as cellulose, hemi-cellulose, lignin and pectin (Northcote, 1972; Keegstra, 2010). In addition, the application of organic material on agricultural soil to recycle nutrients previously removed from the system by crop production constitutes a widely used practice (Tilman, 1999;

Diacono and Montemurro, 2010). Consequently, the chemistry of the organic matter applied might influence the selection for distinct microbial communities.

There is growing evidence on the co-occurrence and co-dependence of specific fungi and bacteria in soil (Boer *et al.*, 2005; Kohlmeier *et al.*, 2005; Artursson *et al.*, 2006; Nazir *et al.*, 2010; Frey-Klett *et al.*, 2011). For example, fungi were shown to excrete low molecular carbon molecules that can be used by bacteria that then proliferate in the immediate vicinity of fungal hyphae (Warmink and van Elsas, 2008; Warmink *et al.*, 2009). These findings suggest that in order to understand microbial processes in soil knowledge of complex food webs and interactions between various communities rather than simple dose-response models is required.

Based on the concept of interspecies co-dependence combined with distinct strategies to access nutrients from organic matter by bacteria and fungi, we hypothesized that bacterial nitrogen cycling communities are dependent on nutrients provided by an organic matter degrading fungal community. This could explain the discrepancy between the observed N_2O emission reduction through fungal inhibition in soil microcosm experiments and the lack of high N_2O production rates found in fungal pure cultures.

To test the relationships between fungal and bacterial communities, three types of organic matter (OM) with distinct C:N ratios and carbon chemistries (paper pulp, green compost and sewage sludge) were used as soil amendments to the same agricultural soil in a microcosm set-up. We sampled 8 times during an incubation period of 30 days to investigate development and response of communities to OM addition. Metatranscriptomic data derived from total RNA and poly-A-tail isolated mRNA provided insights on activity of organisms at distinct time points and resulted in taxonomic and functional information. By comparing metagenomic data derived from genomic DNA, we were able to see changes due to OM addition at the DNA level. Additionally, gas samples were taken from the headspace of

microcosms and analyzed for N_2O, CO_2 and CH_4 concentrations. Ammonium, nitrate and nitrite concentrations were also quantified in the soil. Controls included 1) no addition of organic material and 2) added fungicides to the various treatments to inhibit fungal activity.

Material and Methods

Soil microcosm set-up

Soil microcosm bottles (330 mL) were filled with 80 g of dry soil (sandy loam from Wageningen – Netherlands for details see (Ho *et al.*, 2015)). 8 mL of deionized water per microcosm was added to bring water content back to levels at the time of sampling (~10 % w/w). In order to inhibit fungal communities, cycloheximide, nystatin and captan were mixed with dry soil at 2, 2 and 4 mg $g^{-1}_{dry\ soil,}$ respectively, before being distributed to the respective microcosms. Microcosms were then closed with butyl-rubber stoppers and incubated at 20 °C for 20 days to ensure comparable conditions before the addition of organic matter and start of the actual experiment. During this time, microcosms were aerated every two days by opening butyl-rubber stoppers for 2 minutes.

Paper pulp (PP), compost (C) and sewage sludge (SS) were chosen as organic material (OM) for addition. Paper pulp, a residue from paper producing industries, and compost were provided by Paul Bodelier's group at the Netherlands Institute of Ecology and described in (Ho *et al.*, 2015). Sewage sludge was collected from an anaerobic digester after sludge thickening from a wastewater treatment plant in Lyon (La Feyssine, Villeurbanne, France). Chemical properties of the used materials are summarized in Table S 4. Paper pulp and compost were ground and sieved at 2 mm to ensure equal distribution of different amendments when mixed with soil. Sewage sludge was added directly. For microcosms with added fungicides, OMs were sprayed with captan dissolved in deionized water and air-dried again to ensure inhibition of fungal communities on the additives.

At the start of the incubation experiment, organic residues were mixed with soil at a ratio corresponding to 20 tons ha^{-1} typically used in agriculture amendments (Diacono and Montemurro, 2010). Control microcosms where no OM was added were also mixed to ensure similar conditions in all treatments. Microcosm bottles were closed gas-tight with butyl-

rubber stoppers and incubated at 20 °C for subsequent sampling. Aerobic conditions were ensured throughout the experiment by aerating the microcosms every 2 days.

Soil sampling and nucleic acid extractions

Destructive sampling was carried out to avoid bias by mechanical disturbance of the soil ecosystem through repeated sampling of the same microcosm. Microcosms with no fungicides added were sampled after 20 days of equilibration and before addition of organic residues and 0.25, 1, 2, 6, 12, 20, 30 and 55 days after addition. Samples from treatments with added fungicides were taken before addition, then 6 and 30 days after addition of substrates. Soil in microcosms was mixed thoroughly immediately before sampling and 2 g of soil were transferred to a clean 2 mL reaction tube, snap-frozen in liquid nitrogen and stored at -80 °C to preserve RNA molecules until nucleic acid extraction. Two times 1 g of soil were transferred to 15 mL reaction tubes for extraction of ammonium, nitrite and nitrate, and remaining soil was stored in plastic bags at -20 °C for further chemical analysis.

RNA and DNA were extracted from the same frozen soil using the RNA PowerSoil® Total RNA Isolation Kit together with the RNA PowerSoil® DNA Elution Accessory Kit (MO BIO Laboratories, Inc; Carlsbad, CA). Concentrations of DNA and RNA were quantified directly after extraction with a Qubit® Fluorometer using Qubit® dsDNA BR Assay Kit and Qubit® RNA HS Assay Kit respectively (Invitrogen™, Life Technologies). DNA samples were subsequently stored at -20 °C for further analysis. Following quantification, RNA samples were treated with DNase Max® Kit according to the manufacturer's protocol to digest co-extracted DNA (MO BIO Laboratories, Inc; Carlsbad, CA). Instead of using the resin from the DNase Max® Kit to remove the enzyme and tRNAs, DNase digestion reactions were cleaned up using the RNeasy MinElute Cleanup Kit and eluted in 60 µL of RNase free H_2O (QIAGEN, Redwood City, CA). Absence of DNA in RNA samples was tested by PCR targeting bacterial 16S rRNA genes (primers used: 341F/534R (Ferris *et al.*, 1996; Watanabe

et al., 2001)). Samples showing a band on agarose gel were treated again for DNA removal and purified as described above until no amplification from RNA samples was achieved by PCR. RNase inhibitor Murein (60 units) was added to the extracted and purified RNA samples and stored at -80 °C for subsequent analysis (New England BioLabs®Inc.).

Chemical analysis of soil samples

All extractions for chemical analysis were carried out directly after sampling of the microcosms. Nitrite measurements were performed immediately after extraction, quantification of ammonium and nitrate was done at the end of the experiment with soil samples stored at -20 °C. Approximately 4 g of wet soil per sample was transferred to a weighing tray and dried at 60 °C in a soil drying oven to determine water content of soil at sampling time point. Two times 1 g of wet soil was transferred to 15 mL reaction tubes and 6 and 5 mL 1M KCl solution and deionized water were then added, respectively. After initial shaking by hand of the soil suspension, reaction tubes were put on a rotating wheel for 20 min to extract ammonium, nitrate and nitrite from the soil samples. Soil suspensions were centrifuged (2000 rpm, 10 min) and 2 mL of supernatant was transferred to 2 mL reaction tubes. Standard solutions were prepared in 1M KCl and deionized water from $NaNO_3$, $NaNO_2$ and NH_4Cl salts and further diluted to generate standard curves for quantification (Sigma-Aldrich®). Colorimetric quantification of extracted nitrogen ions was performed as previously described (Hood-Nowotny *et al.*, 2010).

Sequencing library preparation

Sequencing libraries of isolated genomic DNA and RNA were prepared following the protocols for NEBNext® Ultra™ II DNA Library Prep Kit for Illumina® and NEBNext® Ultra™ Directional RNA Library Prep Kit for Illumina®, respectively (New England BioLabs®Inc.). For isolation of eukaryotic mRNAs, a poly-A-tail capture approach using magnetic beads was used prior to cDNA library preparation (NEBNext® Poly(A) mRNA

Magnetic Isolation Module; New England BioLabs®Inc.). Size selection steps during the library preparation were performed using Agencourt® AMPure® XP beads with conditions retaining insert sizes between 400 and 500 bp, as suggested in the user manual. For indexing, NEBNext® Multiplex Oligos for Illumina® (Dual Index Primers Set 1) were used. After 6 cycles of PCR with the indexed primers, sequencing libraries of individual samples were run on an Agilent 2100 Bioanalyzer system to determine size distribution curves of samples. Samples were pooled at equimolar concentration based on the area of bioanalyzer curves between 400 and 500 bp region and subsequently run on a 1.5% agarose gel. DNA between 400 and 500 bp was excised from the gel and purified for a more stringent size selection (illustra GFX PCR DNA and Gel Band Purification Kit; GE Healthcare Life Sciences). Indexed and size selected library pool was loaded on a Illumina® flowcell for 618 cycles of paired-end sequencing on a MiSeq platform using MiSeq reagent kit v3 (Illumina® Inc.).

Sequence analysis

Adapter sequences of paired-end sequence reads were trimmed using the MiSeq built in program for demultiplexing and fastq-file generation. Forward and reverse reads were overlapped using pandaseq (Masella *et al.*, 2012) with a minimum overlap of 10 bp and otherwise default settings and both assembled and unassembled reads were combined in one file. Quality filtering was carried out by running prinseq perl scripts (PRINSEQ-lite version 0.20.4) (Schmieder and Edwards, 2011) to remove sequences with mean quality scores below 20, more than 5 ambiguous bases and all but one exact duplicate per sample. Ribosomal RNA derived sequences were taxonomically assigned by MEGAN analysis of blastn files against a database of SSU and LSU sequences downloaded from SILVA (parameters: minimum bit score, 150; minimum support, 1; top percent, 10) (Quast *et al.*, 2013; Huson *et al.*, 2016). Sequences with bit scores < 100 were treated as putative mRNAs in further analysis. Putative mRNAs were functionally assigned by MEGAN analysis (parameters: minimum bit score, 50; minimum support, 1; best blast hit only) of diamond files against a custom database

containing protein sequences coding for carbohydrate transforming and nitrogen cycling involved enzymes (Buchfink *et al.*, 2014). Protein sequences of the carbohydrate active enzyme database (CAZy) and sequences classified in the GO term "GO:0071941 nitrogen cycling metabolic processes" were downloaded from the NCBI protein database and dereplicated by running prinseq perl scripts to get a non-redundant database (Binns *et al.*, 2009; Lombard *et al.*, 2013). Analysis of carbohydrate degrading and nitrogen cycling functional signatures was carried out with STAMP profiles exported from the INTERPRO2GO classification system available in MEGAN.

Results

Soil pH and nitrogen chemistry in microcosms

Changes in pH after addition of organic materials were measured over the incubation period (Table 4). In all three treatments where OM was added, an increase in pH was measured, in contrast to the control, where pH was stable over the whole incubation period. Increase in pH was found to be highest in the sewage sludge microcosms, followed by compost and paper pulp amended soil. In microcosms where fungicides were added to the control and paper pulp treatment, pH also stayed constant over 30 days of incubation. In soil amended with compost, we found a slightly higher pH than in the no-fungicide incubations after 30 days. Sewage sludge amended soil with added fungicide also showed an increase in pH, but this was found to be lower than in the no-fungicide microcosms.

Extractable inorganic nitrogen forms were also quantified for sampled time points during incubation (Table 4). No ammonium could be measured before the addition of any OM when no fungicide was added. In soil with inhibitors, ammonium could be detected after the 20 days of the equilibrium phase and before addition of OM. Of all treatments, ammonium concentrations were found to be lowest in the paper pulp microcosms and were within the range of control values when detectable. Higher ammonia levels were observed following the addition of compost, in which the highest values were measured right after the addition of compost followed by a decline until 12 and 20 days after incubation, when ammonium concentrations increased again. Overall, the highest concentrations of ammonium in soil extracts were measured after the addition of sewage sludge to microcosms. Values changed between 50 and 578 µg N $g^{-1}_{dry\ soil}$ over the incubation period, with peaks at 2, 12 and 55 days after start of the experiment. Microcosms with added fungicide were found to be generally higher in extractable ammonium than the no-fungicide treatment with the exception of the

Table 4: Summarized data of soil microcosms over the incubation period. Values show the mean and standard deviation (n=3).

	Time after addition [days]	pH $_{KCl}$	pH $_{H2O}$	Ammonium [µg N $g^{-1}_{dry\ soil}$]	Nitrate [µg N $g^{-1}_{dry\ soil}$]	Nitrite [µg N $g^{-1}_{dry\ soil}$]	RNA [µg $g^{-1}_{dry\ soil}$]	DNA [µg $g^{-1}_{dry\ soil}$]
	BA	5.6 ± 0.03	6.3 ± 0.03	nd	26.9 ± 3.92	0.2 ± 0.04	1.0 ± 0.36	5.1 ± 1.00
	0.25	5.7 ± 0.01	6.5 ± 0.08	0.1 ± 0.79	26.7 ± 0.74	0.2 ± 0.03	1.1 ± 0.08	4.4 ± 0.28
	1	5.7 ± 0.02	6.4 ± 0.02	1.1 ± 0.51	31.1 ± 3.7	0.1 ± 0.01	1.2 ± 0.21	4.6 ± 1.14
	2	5.7 ± 0.02	6.5 ± 0.15	nd	26.8 ± 2.58	nd	0.8 ± 0.32	2.8 ± 1.01
PP	6	5.8 ± 0.01	6.7 ± 0.12	0.7 ± 0.48	nd	0.1 ± 0.01	1.3 ± 0.15	5.5 ± 0.40
	12	5.8 ± 0.03	6.6 ± 0.02	nd	nd	0.1 ± 0.01	0.7 ± 0.70	5.9 ± 0.42
	20	5.8 ± 0.03	6.8 ± 0.13	0.6 ± 0.41	nd	0.1 ± 0.01	0.8 ± 0.40	6.1 ± 0.63
	30	5.8 ± 0.02	6.7 ± 0.08	0.7 ± 1.25	nd	0.0 ± 0.02	0.4 ± 0.24	4.6 ± 1.06
	55	5.7 ± 0.02	6.5 ± 0.07	1.1 ± 1.44	nd	0.2 ± 0.02	0.8 ± 0.05	4.0 ± 1.76
	BA	5.6 ± 0.03	6.3 ± 0.03	nd	26.9 ± 3.92	0.2 ± 0.04	1.0 ± 0.36	5.1 ± 1.00
	0.25	5.8 ± 0.02	6.5 ± 0.02	8.1 ± 0.55	30.2 ± 4.77	0.2 ± 0.06	2.5 ± 1.55	4.6 ± 1.19
	1	5.8 ± 0.01	6.4 ± 0.02	6.3 ± 3.11	30.4 ± 3.50	0.1 ± 0.01	1.6 ± 0.28	5.2 ± 0.54
	2	5.8 ± 0.02	6.3 ± 0.03	4.1 ± 1.45	33.7 ± 1.50	0.1 ± 0.02	1.6 ± 0.40	4.8 ± 2.62
C	6	5.8 ± 0.02	6.3 ± 0.02	1.7 ± 2.07	41.3 ± 3.24	0.3 ± 0.37	1.5 ± 0.26	5.4 ± 0.04
	12	5.8 ± 0.03	6.4 ± 0.06	3.1 ± 0.65	39.8 ± 2.47	0.1 ± 0.04	1.1 ± 0.85	6.3 ± 1.18
	20	5.9 ± 0.02	6.5 ± 0.05	4.8 ± 2.42	34.9 ± 3.64	0.1 ± 0.02	1.0 ± 0.04	4.4 ± 0.36
	30	5.9 ± 0.02	6.4 ± 0.03	1.9 ± 1.40	38.5 ± 7.05	0.0 ± 0.01	0.9 ± 0.22	3.5 ± 0.97
	55	5.8 ± 0.03	6.4 ± 0.04	1.7 ± 1.20	43.2 ± 4.03	0.2 ± 0.01	1.5 ± 0.25	6.3 ± 1.28
	BA	5.6 ± 0.03	6.3 ± 0.03	nd	26.9 ± 3.92	0.2 ± 0.04	1.0 ± 0.36	5.1 ± 1.00
	0.25	6.4 ± 0.04	7.2 ± 0.05	50.8 ± 6.45	26.3 ± 1.10	0.5 ± 0.09	2.2 ± 0.15	4.2 ± 0.01
	1	6.6 ± 0.03	7.5 ± 0.08	68.4 ± 9.23	25.3 ± 2.50	0.5 ± 0.06	3.4 ± 0.64	5.3 ± 0.30
	2	6.7 ± 0.24	7.7 ± 0.02	345.5 ± 31.74	2.2 ± 0.36	0.2 ± 0.01	3.8 ± 0.14	5.9 ± 0.81
SS	6	7.1 ± 0.03	7.8 ± 0.14	72.9 ± 6.56	nd	0.3 ± 0.03	4.5 ± 0.30	6.7 ± 0.32
	12	7.3 ± 0.05	8.2 ± 0.03	573.7 ± 18.6	nd	0.3 ± 0.06	>5.2*	9.9 ± 1.24
	20	7.6 ± 0.01	8.5 ± 0.09	79.0 ± 1.23	nd	0.3 ± 0.03	1.7 ± 1.38	15.3 ± 1.07
	30	7.5 ± 0.01	8.5 ± 0.01	67.5 ± 1.23	13.7 ± 4.27	2.7 ± 0.34	>5.2*	16.7 ± 3.99
	55	6.5 ± 0.17	7.2 ± 0.23	506.3 ± 62.81	68.8 ± 25.82	13.2 ± 4.1	4.6 ± 0.29	17.3 ± 2.00
	BA	5.6 ± 0.03	6.3 ± 0.03	nd	26.9 ± 3.92	0.2 ± 0.04	1.0 ± 0.36	5.1 ± 1.00
	0.25	5.6 ± 0.02	6.3 ± 0.08	1.3 ± 1.27	35.1 ± 3.74	0.2 ± 0.02	0.8 ± 0.02	3.5 ± 0.26
	1	5.6 ± 0.00	6.3 ± 0.06	0.7 ± 0.39	24.3 ± 1.46	0.1 ± 0.00	1.2 ± 0.15	5.4 ± 0.78
	2	5.6 ± 0.01	6.2 ± 0.03	0.4 ± 1.15	29.1 ± 1.77	0.1 ± 0.03	1.3 ± 0.56	5.7 ± 0.94
CON	6	5.6 ± 0.00	6.2 ± 0.05	0.6 ± 0.09	31.0 ± 1.89	0.1 ± 0.00	1.0 ± 0.11	4.7 ± 0.10
	12	5.6 ± 0.00	6.3 ± 0.02	0.7 ± 0.24	32.8 ± 1.92	0.1 ± 0.04	0.9 ± 0.34	5.2 ± 0.27
	20	5.6 ± 0.01	6.3 ± 0.03	2.5 ± 0.78	37.7 ± 3.33	0.0 ± 0.01	0.5 ± 0.03	3.3 ± 0.77
	30	5.6 ± 0.02	6.3 ± 0.05	1.7 ± 0.71	40.6 ± 4.65	0.0 ± 0.01	0.6 ± 0.25	3.2 ± 0.49
	55	5.6 ± 0.01	6.2 ± 0.02	nd	45.1 ± 3.98	0.2 ± 0.01	0.9 ± 0.13	4.1 ± 0.85
					Fungicide Treatment			
	BA	5.8 ± 0.01	6.5 ± 0.02	10.1 ± 1.01	3.4 ± 0.28	0.1 ± 0.02	0.9 ± 0.11	2.7 ± 0.55
PP	6	5.8 ± 0.02	6.7 ± 0.09	13.6 ± 0.60	3.9 ± 0.68	0.1 ± 0.03	0.5 ± 0.30	1.3 ± 1.15
	30	5.8 ± 0.01	6.6 ± 0.08	17.3 ± 3.68	4.0 ± 0.92	0.2 ± 0.33	0.4 ± 0.05	2.8 ± 0.03
	BA	5.8 ± 0.01	6.5 ± 0.02	10.1 ± 1.01	3.4 ± 0.28	0.1 ± 0.02	0.9 ± 0.11	2.7 ± 0.55
C	6	6.0 ± 0.01	6.8 ± 0.05	16.3 ± 5.84	2.9 ± 0.30	0.1 ± 0.08	1.0 ± 0.08	2.4 ± 0.83
	30	6.0 ± 0.01	6.6 ± 0.03	27.1 ± 3.98	2.9 ± 1.47	0.0 ± 0.03	1.0 ± 0.19	4.1 ± 0.17
	BA	5.8 ± 0.01	6.5 ± 0.02	10.1 ± 1.01	3.4 ± 0.28	0.1 ± 0.02	0.9 ± 0.11	2.7 ± 0.55
SS	6	6.7 ± 0.06	7.5 ± 0.03	47.8 ± 4.57	0.4 ± 0.70	0.3 ± 0.03	3.9 ± 0.28	6.0 ± 0.57
	30	6.8 ± 0.06	7.6 ± 0.07	44.5 ± 1.85	nd	0.1 ± 0.02	3.0 ± 0.15	3.3 ± 0.40
	BA	5.8 ± 0.01	6.5 ± 0.02	10.1 ± 1.01	3.4 ± 0.28	0.1 ± 0.02	0.9 ± 0.11	2.7 ± 0.55
CON	6	5.8 ± 0.01	6.5 ± 0.02	11.5 ± 1.93	3.0 ± 0.78	nd	0.4 ± 0.15	1.9 ± 0.39
	30	5.8 ± 0.01	6.4 ± 0.03	15.2 ± 2.62	2.7 ± 0.62	0.0 ± 0.02	0.5 ± 0.05	2.4 ± 0.33

pH_{KCl} / pH_{H2O}: pH measured in 1M KCl extract (1:5) and H_2O extract (1:6) of 1 g amendment respectively
Organic matter added to microcosms: SS: sewage sludge; PP: paper pulp; C: compost; CON: no addition
BA: before addition; nd: not detectable; *obtained values over detection limit of method

sewage sludge amended soil. Ammonium in paper pulp, compost and control soils with added fungicide increased over 30 days, in contrast to no-fungicide incubations, where ammonium was found to decrease. Ammonium concentrations as high as those detected in the sewage sludge amended soil were not found in the fungicide treatment.

Nitrate could be measured in soil extracts before addition of OM. Compost amended microcosms showed similar values as the control, with a slight increase in nitrate towards the end of the incubation. Nitrate in the paper pulp treatment was found to be stable during the first 2 days of the experiment, but could not be detected in any of the later time points. Sewage sludge amended microcosms showed a similar behavior in nitrate concentrations at the beginning of the incubation, although nitrate concentrations decreased after one day. After no nitrate was detected in samples of day 6, 12 and 20, we measured it again at 30 and 55 days. In contrast to ammonium, nitrate was found to be lower in soil where fungicides were added before the addition of OM. In the presence of fungal inhibitors, nitrate levels stayed constant over 30 days for paper pulp, compost and control microcosms, but decreased in the sewage sludge amended soil.

Nitrite could be measured at low concentrations in all OM and control microcosms with the exception of day 30 and 55 of the sewage sludge treatment, where an increase in nitrite was observed. Low concentrations of nitrite were also found in all samples derived from microcosms with added fungicide.

Concentrations of extracted RNA and DNA over the incubation period

Nucleic acid concentrations were measured right after extraction from soil samples (Table 4). RNA concentrations of the paper pulp treatment resembled those obtained from the control as they stayed constant with small increases and decreases over the incubation period. Neither an increase nor a decrease in DNA was observed for the control as well as the paper pulp amended microcosms. Compost amended microcosms showed an increase in extractable

RNA right after addition, which declined again and reached initial levels after 12 days of incubation. DNA concentrations for this treatment were found to be similar over the duration of the experiment. An increase in extractable RNA was measured in the sewage sludge amended microcosms. RNA increased constantly over 12 days, was found to be lower after 20 days and increased again at days 30 and 55 of the experiment. DNA concentrations for this treatment were found to be comparable over the first 2 days of incubation, followed by an increase in samples from day 6 and 12 and reached a plateau at days 20, 30 and 55, with the highest concentrations of DNA measured of all samples. Overall, RNA and DNA concentrations were found to increase 4.5 and 3 times respectively in this treatment.

Nucleic acid concentrations in soil with added fungicides were generally found to be lower than in no-fungicide ones. Before addition of OM, RNA concentrations were in the same range as no-fungicide samples, but DNA concentrations were found to decrease by about 50% after addition of fungicides. Extractable RNA decreased over 30 days in the paper pulp and control soils, whereas DNA levels stayed constant. In soil amended with compost and added fungicide, RNA levels stayed constant over 30 days and resembled no-fungicide incubations. DNA from these samples was found to be higher than at the beginning and resembled concentrations of no-fungicide treatments after 30 days of incubation. Microcosms amended with sewage sludge and added fungicide showed an increase in extractable RNA relative to the no-fungicide treatment (approximately 3 times). DNA also doubled when fungicide was present after 6 days and decreased again after 30 days to initial levels. DNA concentrations measured after 30 days were 5 times lower in the fungicide treatment than in the no-fungicide one.

Gas measurements in headspace of microcosms

Carbon dioxide, methane and nitrous oxide were measured in the headspace of the soil microcosms (Table 5). Carbon dioxide production was higher in all OM amended soils than in the control. Compost amended soil showed the lowest production of CO_2 among treatments, followed by paper pulp and sewage sludge. When fungicide was added, we observed a decrease in CO_2 production of 90, 50 and 50% for paper pulp, compost and sewage sludge amended soil respectively, whereas CO_2 production in control vials showed similar values than in the no-fungicide treatment.

Nitrous-oxide in headspace of paper pulp treatments was not found to be higher than control concentrations, but soil amended with compost showed an elevated production of N_2O. Soil amended with sewage sludge showed the highest concentrations of N_2O, where concentrations increased right after addition of the amendment and stayed constant over the incubation period. The addition of fungicides decreased N_2O production in the paper pulp and control to 27 and 41 % of levels reached in the no-fungicide treatments. For compost and sewage sludge treatments, these values were only found to be 2 and 7 % respectively.

In contrast to N_2O, which increased in compost amended soils, methane was found to resemble the values from the controls. This was not the case for paper pulp addition, where we measured the highest concentrations of methane (8.1 ppm) of all treatments after 30 days of incubation. In the sewage sludge amended microcosms, CH_4 production was higher than in the control and resembled values derived from the paper pulp treatments. The addition of fungicide to the microcosms with added OM decreased CH_4 production between 5 (compost and paper pulp) and 25 % (sewage sludge). We observed a 60% decrease in CH_4 production in the control soils when fungicide was added.

Table 5: Cumulative concentrations of measured gases in headspace of microcosms with and without addition of fungicides over 30 days of incubation. Mean values and standard deviation were calculated from triplicate vials (n=3).

	Time after addition	without fungicide			with fungicide		
		CH_4	CO_2	N_2O	CH_4	CO_2	N_2O
	[days]	ppm	‰	ppm	ppm	‰	ppm
PP	2	1.1 ± 0.1	18.0 ± 1.4	0.6 ± 0.3	0.9 ± 0.5	15.0 ± 0.7	0.0 ± 0.0
	6	1.2 ± 0.1	189.6 ± 18.1	1.7 ± 0.8	2.2 ± 0.8	33.4 ± 1.0	0.4 ± 0.1
	12	2.2 ± 0.1	423.4 ± 16.5	1.8 ± 0.8	3.7 ± 0.8	53.7 ± 2.9	0.6 ± 0.3
	16	2.9 ± 0.3	528.0 ± 16.7	1.8 ± 0.8	4.7 ± 0.8	64.5 ± 3.9	0.8 ± 0.7
	20	3.7 ± 0.7	606.6 ± 17.6	1.8 ± 0.8	5.8 ± 1.1	73.3 ± 4.5	0.8 ± 0.7
	23	4.5 ± 1.1	665.1 ± 18.7	1.8 ± 0.8	6.5 ± 0.9	80.1 ± 4.8	0.8 ± 0.7
	27	6.2 ± 1.4	728.7 ± 21.2	1.9 ± 0.8	7.2 ± 1.1	87.8 ± 5.1	0.9 ± 0.7
	30	8.1 ± 1.6	781.3 ± 23.5	2.2 ± 0.5	7.7 ± 1.5	92.4 ± 5.1	0.9 ± 0.7
C	2	0.5 ± 0.2	30.1 ± 2.6	1.2 ± 0.3	0.1 ± 0.1	25.7 ± 1.7	0.0 ± 0.0
	6	0.7 ± 0.4	70.1 ± 7.7	2.3 ± 0.2	0.6 ± 0.3	54.0 ± 6.1	0.2 ± 0.1
	12	1.5 ± 0.7	124.7 ± 13.3	4.6 ± 0.6	1.1 ± 0.8	79.0 ± 6.2	0.3 ± 0.1
	16	1.8 ± 1.0	155.7 ± 15.8	6.5 ± 1.9	1.6 ± 0.9	90.9 ± 6.5	0.3 ± 0.1
	20	2.4 ± 0.8	183.8 ± 18.8	9.3 ± 3.3	1.7 ± 1.0	100.4 ± 7.0	0.3 ± 0.1
	23	2.4 ± 0.8	204.3 ± 21.1	12.1 ± 4.2	2.3 ± 0.8	106.6 ± 7.8	0.3 ± 0.1
	27	2.4 ± 0.8	224.4 ± 22.7	16.0 ± 4.9	2.3 ± 0.9	113.7 ± 8.0	0.3 ± 0.1
	30	2.4 ± 0.8	238.5 ± 23.1	20.0 ± 5.2	2.3 ± 0.9	117.9 ± 8.4	0.3 ± 0.1
SS	2	0.6 ± 0.3	198.5 ± 3.0	3879.4 ± 474.1	1.1 ± 0.3	161.6 ± 29.1	0.1 ± 0.2
	6	0.9 ± 0.4	421.7 ± 2.4	3879.4 ± 474.1	2.6 ± 1.5	358.6 ± 37.7	254.5 ± 255.1
	12	2.9 ± 0.6	650.2 ± 3.9	3879.4 ± 474.1	3.3 ± 1.7	528.1 ± 67.8	267.3 ± 274.4
	16	4.5 ± 0.2	836.0 ± 6.7	3879.4 ± 474.1	3.9 ± 1.6	592.0 ± 73.7	268.6 ± 275.0
	20	5.4 ± 0.2	1016.6 ± 9.1	3879.4 ± 474.1	4.0 ± 1.7	640.1 ± 74.8	268.8 ± 275.0
	23	6.0 ± 0.4	1192.2 ± 10.5	3879.4 ± 474.1	4.4 ± 1.8	676.6 ± 75.0	269.0 ± 275.0
	27	6.2 ± 0.4	1363.7 ± 11.4	3879.4 ± 474.1	4.7 ± 1.9	709.9 ± 73.7	269.3 ± 274.8
	30	6.4 ± 0.5	1485.8 ± 16.5	3971.5 ± 480.1	4.7 ± 1.9	730.5 ± 72.5	269.4 ± 274.8
CON	2	0.5 ± 0.3	6.7 ± 1.0	0.2 ± 0.0	0.1 ± 0.0	10.1 ± 1.6	0.0 ± 0.0
	6	0.7 ± 0.3	15.1 ± 2.0	0.6 ± 0.0	0.4 ± 0.0	23.1 ± 4.0	0.1 ± 0.0
	12	1.3 ± 0.3	26.7 ± 3.8	1.2 ± 0.6	0.7 ± 0.2	35.5 ± 4.6	0.2 ± 0.1
	16	1.4 ± 0.3	33.2 ± 4.3	1.3 ± 0.6	0.9 ± 0.2	42.0 ± 4.8	0.4 ± 0.3
	20	2.1 ± 0.4	39.4 ± 4.8	1.4 ± 0.6	0.9 ± 0.2	46.8 ± 5.3	0.4 ± 0.3
	23	2.4 ± 0.8	44.4 ± 6.0	1.4 ± 0.6	0.9 ± 0.2	49.9 ± 5.2	0.4 ± 0.3
	27	2.4 ± 0.8	48.9 ± 6.6	1.5 ± 0.6	0.9 ± 0.2	53.6 ± 5.7	0.4 ± 0.3
	30	2.4 ± 0.8	51.8 ± 7.0	1.5 ± 0.6	0.9 ± 0.2	55.4 ± 5.8	0.4 ± 0.3

Organic matter added to microcosms: PP: paper pulp; C: compost; SS: sewage sludge; CON: no addition

Fungal and bacterial response to OM addition

In order to quantify the stimulation of fungi and bacteria by the addition of organic matter of distinct qualities, we compared the change in relative abundance of rRNA molecules extracted from soil (Figure 20). Control soils showed no change in abundance of fungal or bacterial sequences, as the ratio between the two groups was found to be comparable over the incubation period. This was also the case for soil where compost was added. Different

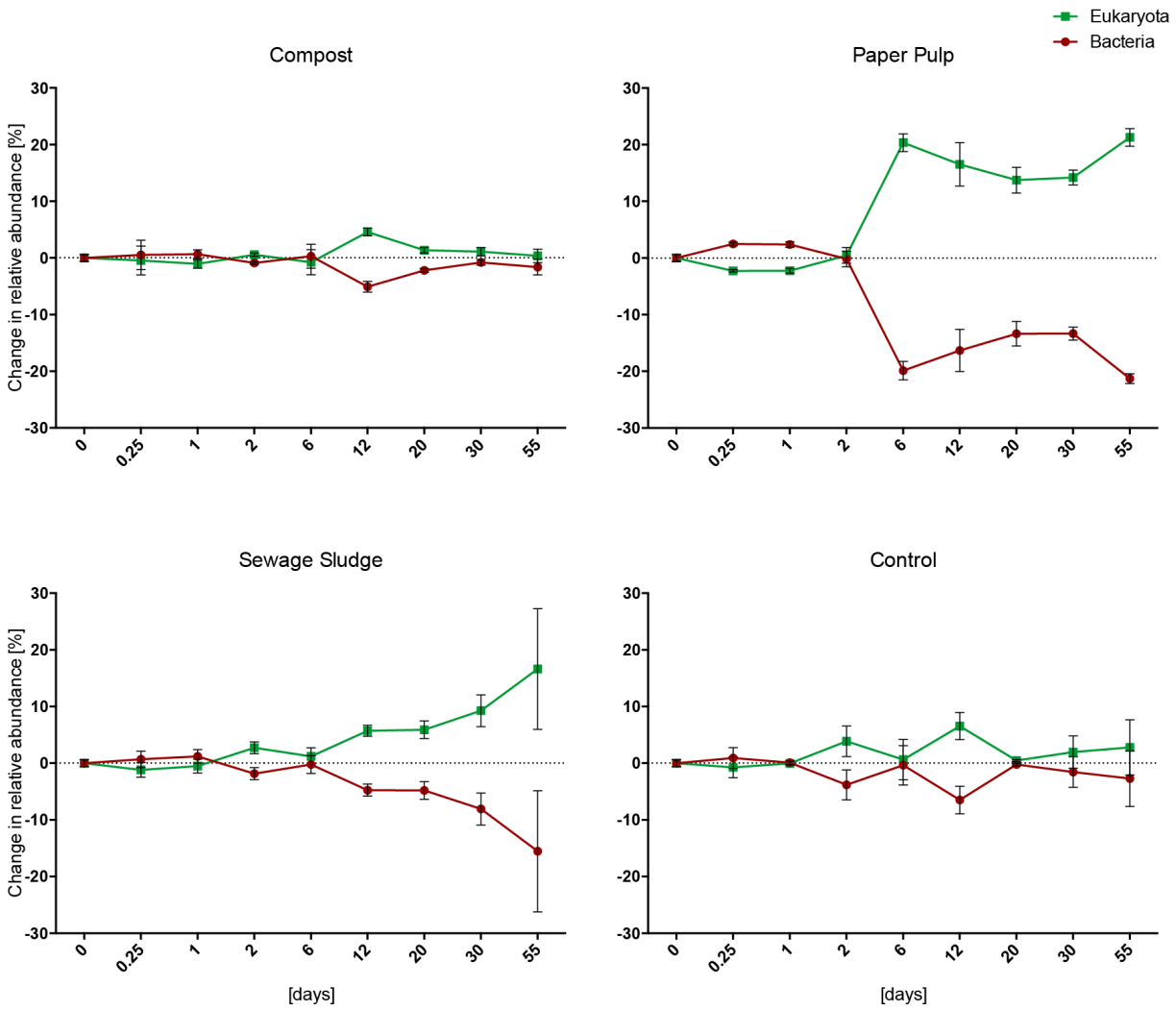

Figure 20: Change in relative abundance of assigned bacterial and fungal reads of cDNA hits against SILVA database over incubation of 55 days. Data points show the mean, error bars the standard deviation of the mean (n=3).

patterns were found in the paper pulp and sewage sludge treatment. After addition of paper pulp, we observed an immediate response (~3 % increase in relative abundance) of bacterial sequences over the first 2 days, which was followed by an increase in fungal derived rRNA sequences (up to 20 % increase in relative abundance) that stayed constant until the end of the experiment. Following the addition of sewage sludge, fungal derived rRNA sequences increased in relative abundance after 6 days and continued to increase over the duration of the experiment, resulting in a 15 % higher relative abundance of fungal rRNAs than at the beginning of the incubation.

Community development after OM addition

Metagenomes derived from extracted DNA of time points 0.25, 6 and 30 days after addition of OM were compared in order to identify the development of distinct microbial communities over the incubation period. Genus assigned sequences were clustered to group similar metagenomic profiles (Figure 21). Metagenomes of samples with added fungicide were separated from the no-fungicide soils, regardless of the time point sampled.

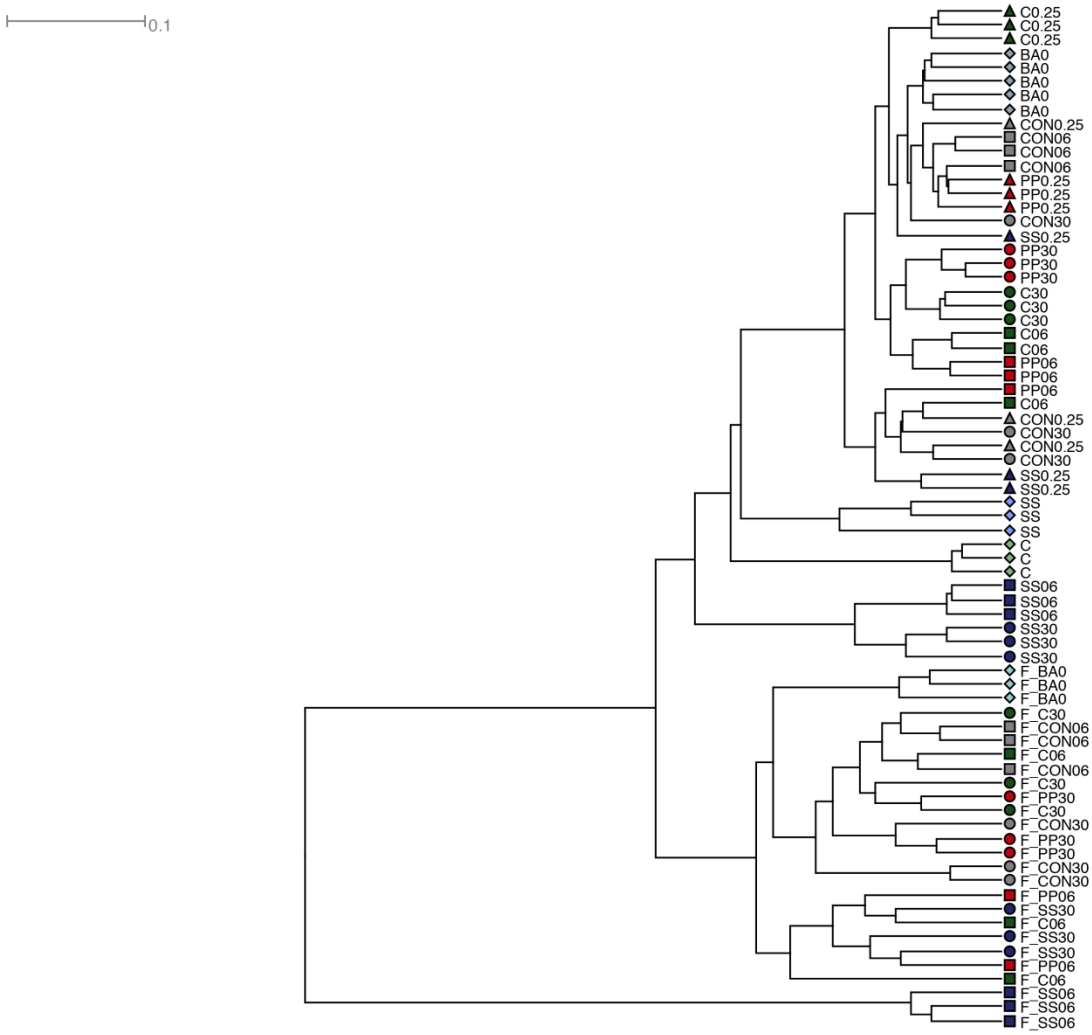

Figure 21: UPDMA tree based on DNA of soil microcosms sampled before addition, 0.25, 6 and 30 days after incubation. Sequences were blasted against NCBI_nt database and annotated in MEGAN. Colors indicate different treatments: blue (SS), sewage sludge; red (PP), paper pulp; green (C), compost; grey (CON), control – no addition of organic matter; light blue (S), pure sewage sludge; light green (C), pure compost. Shapes of symbols indicated timepoint of sampling: ◇, before addition of organic matter or pure organic matter; △, 0.25 days; □, 6 days; ◯, 30 days after incubation. F: microcosms treated with fungicide.

Metagenomes after 30 days of incubation clustered for treatments where paper pulp, compost and sewage sludge were added. In contrast, control samples after 30 days of incubation were distributed over the no-fungicide part of the tree. Metagenomes sampled 6 days after OM addition clustered for the sewage sludge treatment, but paper pulp and compost samples could not be distinguished clearly. In microcosms with added fungicide, metagenomic profiles could not be distinguished by clustering for addition of different OM materials.

Carbon degradation and N-cycling signatures of metagenomes

Functional assignment of sequences derived from metatranscriptomes and metagenomes was used to identify occurrence of carbon degradation and nitrogen transformation signatures over the incubation period (Figure 22 and Figure 23). In analyzed metagenomes (Figure 22), we could not see changes in relative proportions of sequences assigned to glycoside hydrolases or nitrogen cycle processes for distinct treatments except where sewage sludge was added. Here, an increase in polysaccharide degrading signatures was observed while nitrogen cycle related sequences decreased in the isolated metagenomes. In microcosms with added paper pulp, an increase in glycoside hydrolase assigned sequences was observed after 6 days of incubation, but decreased again after 30 days. Other signatures related to carbon and nitrogen cycling did not change over the incubation period except in the sewage sludge treatment. Sequences assigned to nitrate transport of bacteria and archaea (represented by IPR005890 Nitrate transport ATP-binding subunit C/D) declined in this treatment, while peptidase assigned sequences increased (GO:0008233 peptidase activity). Other marker signatures (IPR016288 1,4-beta cellobiohydrolase, IPR023644 nitrous-oxide reductase and IPR001287 nitrite reductase, copper-type) were not found to change in relative proportion in the metagenomes.

Carbon degradation and N-cycling signatures of metatranscriptomes

RNA sequences extracted from microcosms (with and without the addition of fungicides) as well as sequenced polyA-tail isolated RNA was assigned to carbon degrading and nitrogen

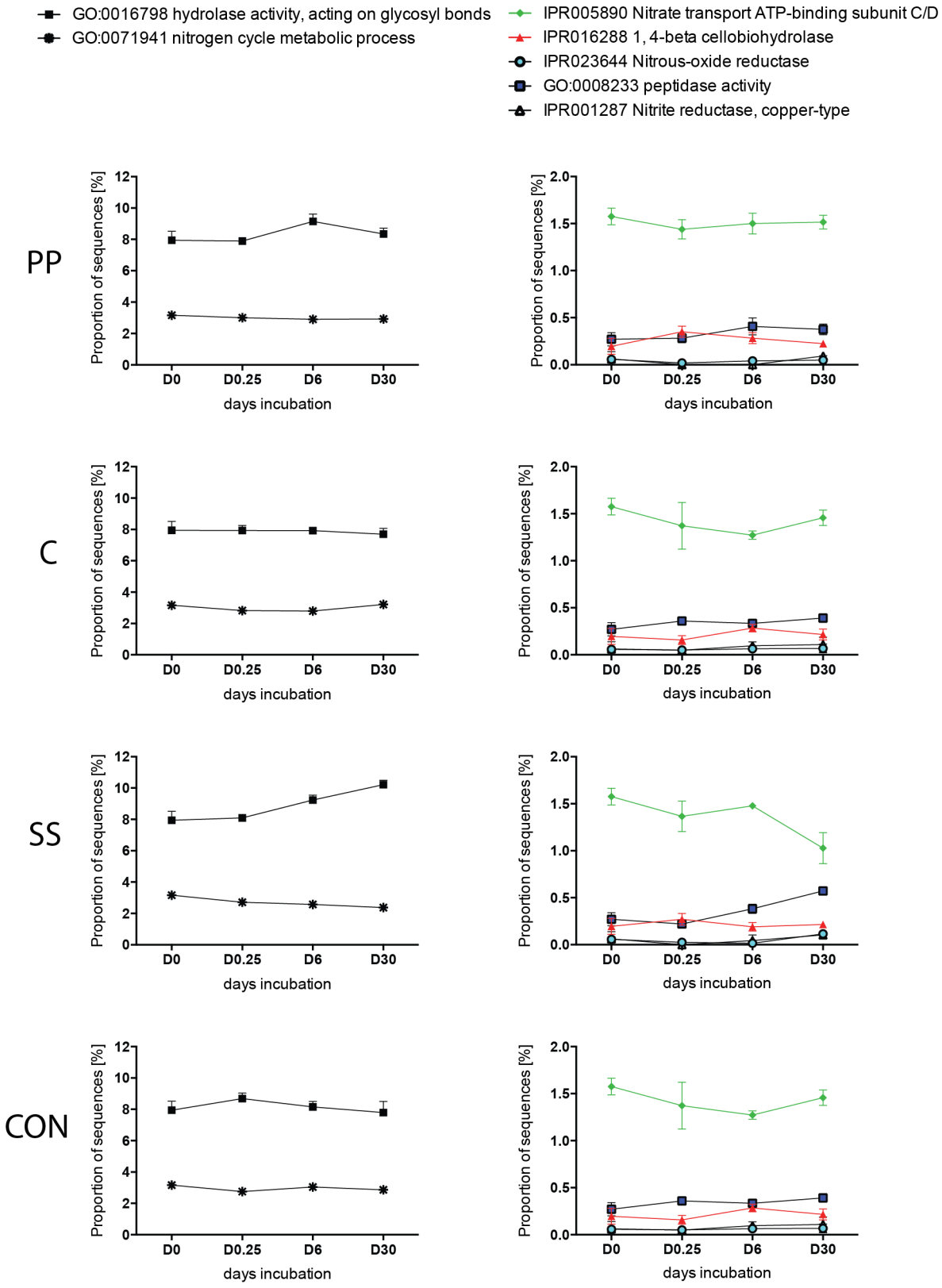

Figure 22: Proportion of sequences based on sequenced metagenomes assigned to polysaccharide degradation and nitrogen cycling related gene ontology terms and InterPro classes by MEGAN for different OM additions and control over 30 days. PP: paper pulp; C: compost; SS: sewage sludge; CON: no addition control. Sequences were assigned based on diamond searches versus a custom database including protein sequences from the CAZy database (carbohydrate active enzymes) and nitrogen cycling related entries from InterPro2Go. Data points and error bars show the mean and standard deviation (n=3).

cycling protein classes (Figure 23). When no OM was added to the microcosms, relative proportions of transcripts assigned to glycoside hydrolases represented between 0 and 0.5 % of the sequences. Slightly higher levels were found in the sewage sludge treatment, but these decreased 6 days after incubation. For the paper pulp and compost treatment, these signatures were found to be higher in relative proportion over the entire incubation period.

We could identify different patterns of nitrogen cycling related mRNAs for the OM treatments. The relative proportion of N-cycling assigned sequences represented between 0 and 0.5 % in the control treatments. The addition of paper pulp led to an increase in the relative abundance of these genes and two peaks were observed, the first at 1 day and the second at 12 days. This behavior was found to differ from the compost treatment, where an increase in N-cycling transcripts was detected after 6 days of incubation. The addition of sewage sludge led to an initial decrease of this marker for the first 6 days of incubation and a subsequent recovery to initial expression levels for the rest of the incubation.

Nucleic acids were extracted from microcosms with added fungicides before addition, then 6 and 30 days after addition of OM. Here, transcripts assigned to glycoside hydrolases decreased in all treatments after the first 6 days. In the compost and control treatment, relative proportions of these transcripts increased again after 30 days, whereas levels were constant in the sewage sludge and paper pulp treatment with added fungicide. Nitrogen cycle assigned transcripts were detected for all OM treatments when fungicide was added, but never reached the peak values (~1.5 % rel. proportion) observed in the no-fungicide microcosms.

We sequenced and assigned poly-A-tail isolated mRNAs of 4 time points throughout the incubation to identify eukaryotic transcriptome signatures. Glycoside hydrolase

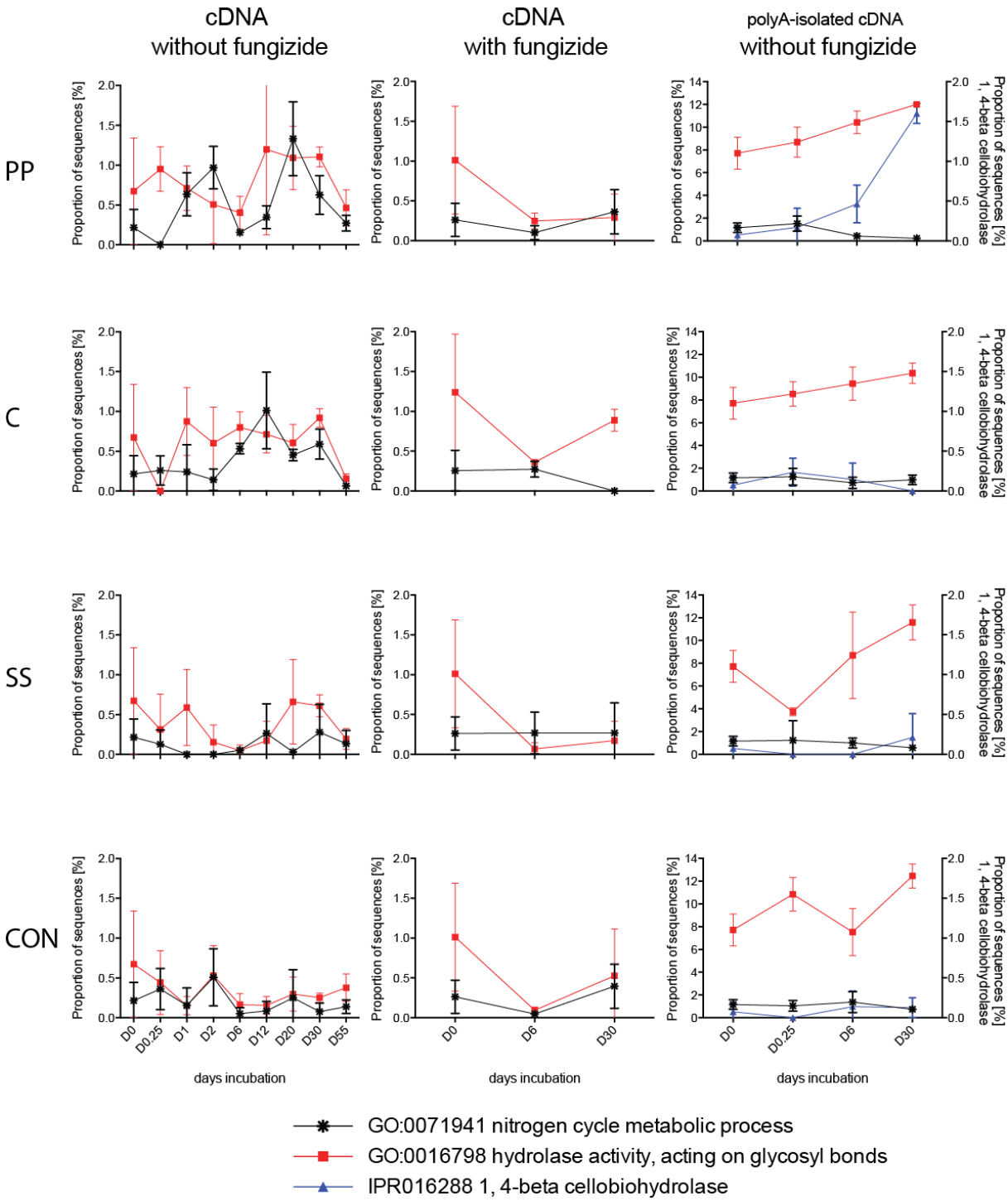

Figure 23: Proportion of sequences based on sequenced metatranscriptomes assigned to polysaccharide degradation and nitrogen cycling related gene ontology terms and InterPro classes by MEGAN for different OM additions and control over 30 days. Glycoside hydrolases (red) and nitrogen cycling related transcripts (black) are plotted on the left axis, β- 1,4 cellobiohydrolase transcripts are plotted on the right axis. PP: paper pulp; C: compost; SS: sewage sludge; CON: no addition control. Sequences were assigned based on diamond searches versus a custom database including protein sequences from the CAZy database (http://www.cazy.org) and nitrogen cycling related entries from InterPro2Go. Data points and error bars show the mean and standard deviation (n=3).

assigned transcripts increased in relative proportion for all treatments and also in the control. In the paper pulp and compost treatment, a constant increase was observed, and sewage sludge addition led to an initial decrease 0.25 days after OM addition followed by an increase.

No addition of OM also led to an increase in polysaccharide degrading eukaryotic transcripts over the incubation period. Nitrogen cycling related eukaryotic transcript levels were found constant for the compost, sewage sludge and control microcosms, but decreased 6 days after paper pulp addition. Additionally, we looked for transcripts encoding 1,4-beta cellobiohydrolases in poly-A-tail isolated RNA. While we could not observe a response in the control, sewage sludge and compost treatment for this protein family, the addition of paper pulp triggered an increase of transcripts coding for cellulose degrading enzymes during incubation.

Discussion

In this experiment, we added three different types of organic matter residues from various industrial processes that can be used as carbon and nitrogen additives for soil environments. We expected that fungal communities would respond faster than bacteria to the addition of OM with high C:N ratios , and that bacteria would outcompete fungi if low C:N substrates were available. Furthermore, we hypothesized that fungi are primary degraders of organic materials, thus providing substrates for a nitrogen cycling bacterial community and thereby fulfilling an indirect role in N_2O production. We tested this by analyzing metatranscriptomic data in a time series of 30 days after the addition of OM. Metatranscriptomes from total isolated RNA and poly-A-tail isolated mRNA were sequenced to get information on a) the functional response of the complete soil biome and on b) the eukaryotic members of the biome. In the following paragraphs, the impact of the distinct additives on soil communities and changes in soil chemical parameters are discussed in order of decreasing C:N ratio of the additive.

Addition of paper pulp

We expected that the addition of paper pulp would provide the most advantageous conditions for fungal communities since this organic material is considered the most recalcitrant among those chosen for this experiment. Indeed, this treatment showed the strongest shift towards fungal rRNAs among all treatments and this shift happened abruptly between 2 and 6 days after the start of the experiment (Figure 20). This might be due to hyphal growth of fungi towards the additive at this time point to benefit from available nutrients. After 6 days of incubation, we could see an increase in transcripts of glycosidic hydrolases in total RNA transcripts, which stayed elevated for about 20 days. In the poly-A-tail isolated transcripts, we could see a transcriptional response in this class of enzymes as they increased constantly during the experiment (Figure 23). A constant increase in eukaryotic transcripts related to the

cleavage of carbohydrate bonds suggests that fungal members degrading OM were active throughout the experiment and might increase in relative abundance. This is supported by an increasing activity of 1,4-beta cellobiohydrolases throughout incubation in the eukaryotic signatures, which is a key enzyme in the degradation of cellulose (Bischof *et al.*, 2016). Altogether, this supports our hypothesis that fungi are dominating the OM degradation in this treatment.

Data on inorganic nitrogen extracted from this treatment also showed a change around 6 days after addition (Table 4). The addition of paper pulp provided low amounts of available ammonium and nitrate (Table S 4). Nitrate concentrations in the microcosms stayed constant for 2 to 6 days, after which nitrate could no longer be detected for the duration of the incubation. This suggests that fungal growth and activity in the initial phase were supported by available nitrate before the breakdown of organic matter occurred to provide further nutrients. The availability of nitrogen forms at the beginning of the experiment might also explain the increase in nitrogen cycling transcripts within the first 6 days, which then later decreased to initial levels after day 6 (Figure 20). A second peak of transcripts assigned to nitrogen cycling processes was observed between 12 and 30 days of incubation and followed the increase observed for glycoside hydrolase transcripts. At the same time, nitrogen cycling signatures in the poly-A-tail isolated mRNAs were found to decrease compared to initial levels. Altogether, metatranscriptomic data corroborates our hypothesis that bacterial nitrogen cycling communities might be dependent on organic matter degrading fungal members. However, no elevated N_2O emissions were observed for the addition of paper pulp.

Addition of compost

A preferential use of OM by bacteria or fungi following the addition of compost was not apparent from the relative proportions of rRNA transcripts sequenced over the incubation

period (Figure 20). Nevertheless, in this treatment we observed sequential transcription of carbon degrading and nitrogen cycling genes over time in the metatranscriptomes of total mRNA, while in poly-A-tail isolated mRNAs, carbon degradation increased and nitrogen cycling related transcripts stayed constant for 30 days. As was observed with the addition of paper pulp, this suggests activity of a fungal carbon degrading community throughout the entire sampling period, while a nitrogen cycling related transcriptional response can be seen in total RNA derived data. Therefore, nitrogen cycling processes can be mainly assigned to bacterial activity. Surprisingly, almost no transcripts assigned to glycoside hydrolases could be detected after just 0.25 days of addition, which was not the case for any other treatment or control microcosms. The compost we used had undergone a controlled decomposition process, thus it might already contain low molecular weight carbon molecules (Benito *et al.*, 2003). If this is the case, then there is no need in degrading more complex carbon structures directly after addition. The breakdown of polysaccharides is considered to be energy intensive, thus it is expected to be tightly regulated in organisms depending on it (Leger and R. M. Cooper, 1986; Aro *et al.*, 2005; van den Brink and R. P. de Vries, 2011a).

Data on extracted ammonium and nitrate concentrations support the findings from the metatranscriptomic analysis. Compost provided the highest concentrations of available ammonium right after addition, which decreased within the first 6 days (Table S 4). After that, when we observed an increase in nitrogen cycling transcripts, we could also see an increase in ammonium. This could point to the release of nitrogen by polymer degradation or to a transformation of nitrogen towards ammonium through dissimilatory nitrogen reduction to ammonium (DNRA), since nitrate concentrations simultaneously decreased. However, a further analysis of isolated transcripts needs to be carried out to identify contributing nitrogen cycling pathways.

Only the addition of compost triggered the emission of considerable amounts of N_2O among the tested organic materials (Table 5). N_2O production after compost addition has already been shown before in sandy soils (Zhu-Barker *et al.*, 2015). N_2O emission rates measured were higher after 12 days of incubation when initial readily available ammonium was used up. Thus, the production of this greenhouse gas can be linked to the period where carbon degrading fungi and nitrogen cycling bacteria were found to be active. The addition of fungicides has been shown to reduce, or as in our case, even completely inhibit N_2O emissions (Seo and DeLaune, 2010; Wei *et al.*, 2014; H. Chen, Mothapo, and Shi, 2014b). Since we saw similar responses in the functional signatures of the compost and paper pulp treatment, we were interested in which fungal members were active. **Figure 24** shows a comparison of assigned rRNAs of metatranscriptomes of the two treatments. The PCA plot shows that, over the entire incubation period, active fungal communities from compost and paper pulp addition could be distinguished. Already 6 hours after the addition, the two treatments could be distinguished from one another and this was also the case for all other time points. The y-axis representing differences between OM treatments in the plot accounts for only 8 % of the total inertia, while the x-axis that represents changes over time, explains 72 %. This suggests that the communities were less different between each other and that they changed more significantly over time during the 55 days of incubation. This could mean that shifts in community structure are driven by the same members in both communities, but also that some distinct fungi able to respond specifically to the added type of organic material were active throughout. Figure 24 b shows active fungal genera that were found to be different in relative abundance in the two treatments throughout the experiment. Genera present in the compost treatment and not in paper pulp will serve as a basis for further analysis to explore their potential involvement in processes leading to N_2O emissions as detected after compost, but not paper pulp addition.

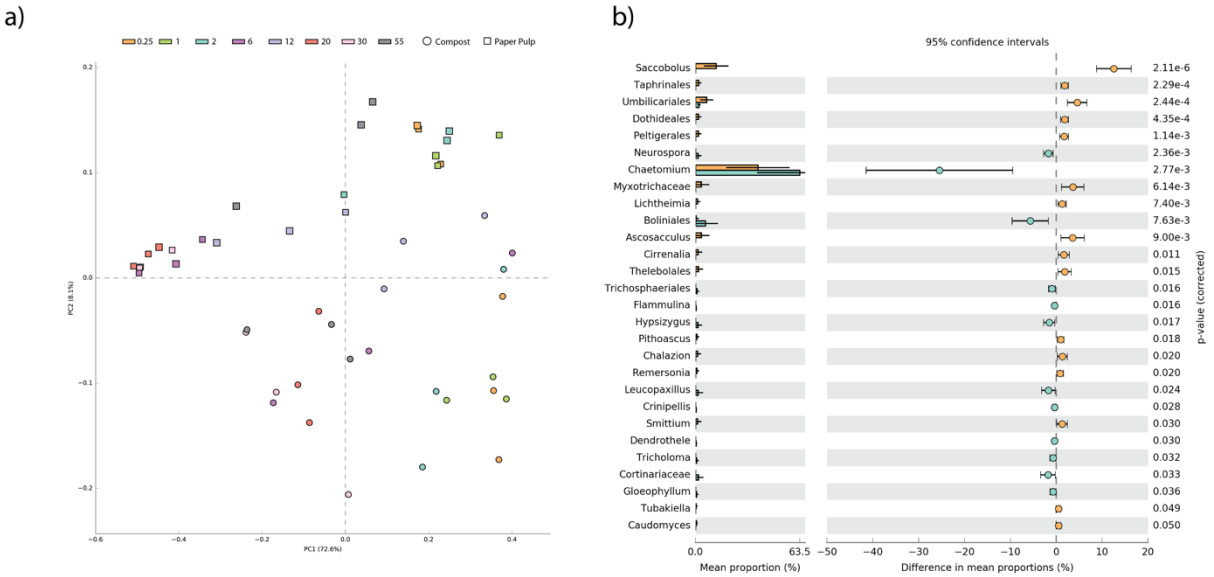

Figure 24: Active fungal communities of compost and paper pulp treatment based on assigned metatranscriptomes in MEGAN. (a) PCA of samples from both treatments coloured according to sample time after addition. (b) Differences in assigned active fungal genera calculated from all sampled timpoints of compost and paper pulp treatments. Graphs plotted in STAMP from profile files exported from metatranscriptome comparison in MEGAN.

However, the disappearance of N_2O together with transcriptomic data of eukaryotic and total communities corroborates our hypothesis that fungi do not contribute directly, but indirectly to N_2O emissions from soils via nutrient provision.

Addition of sewage sludge

We found the strongest response in biological activity after the addition of sewage sludge. This can be seen by the 3 to 5-fold increase in extractable DNA and RNA and the highest respiration measured by CO_2 produced in the headspace of microcosms as compared to all other treatments. This might be related to the physical nature of sewage sludge. Since it was the finest material with respect to grain size among the tested substrates, it might also be more easily accessible due to scale reasons. Regardless of the physical nature of sewage sludge, we expected that this amendment would be preferentially used by bacteria given that it had the lowest C:N ratio. However, we could not confirm a preferential use of this substrate by

bacteria by comparing relative proportions of fungal and eukaryotic rRNAs in the metatranscriptomes and instead observed a steady increase towards fungal derived rRNAs. Due to the easily accessible nutrient source, we expected no time shifted occurrence in carbon degrading and nitrogen cycling transcripts in this treatment. This was confirmed by the metatranscriptomic data, where carbon degradation and nitrogen cycling activities stayed constant over the incubation period.

However, the addition of sewage sludge had a big effect on soil communities, inducing the biggest shifts in metagenomic and metatranscriptomic signatures (Figure 21). This suggests the presence of an easily accessible nutrient source that only certain members of the community able to outgrow their competitive rivals can use. In the first 6 days of incubation, *Bacillus* species were found to respond strongly to this treatment, but a shift to a dominance (> 50 % in relative abundance) of *Arthrobacter* species in the active community was observed by the end of incubation. We also observed the highest dynamics in ammonium and nitrate concentrations in this treatment, which highlights the need for investigating the nitrogen cycling pathways more closely in order to conclude on activity of distinct nitrogen cycling communities.

Since CO_2 production in these microcosms was found to be constant during incubation, the high N_2O concentrations detected might be caused by interference from a compound derived from sewage sludge that can interfere with the N_2O peak during gas-chromatography measurements. Consequently, these values have to be interpreted with care and no conclusive interpretation of N_2O production was obtained from this treatment.

Consequences of the addition of fungicides

Eukaryotic sequences were found to account for between 10 and 40 % of the rRNAs in no-fungicide treatments. This value decreased to less than 1 % in the fungicide treatments over

30 days, which suggests that we successfully inhibited eukaryotic community members in our experiment. Therefore, we can exclude an active fungal contribution to the processes investigated in these treatments.

We compared rRNA sequences assigned at the order level of metatranscriptomes from the same organic matter treatments with and without added fungicide (Figure S 1). In all treatments and in the control, we found that *Pseudomonadales* dominated in the presence of fungicides while other members of the community decreased in relative abundance. The use of inhibitor addition in determining contribution ratios of soil communities to specific biochemical processes is a widely use practice (Land *et al.*, 1993; Velvis, 1997; Castaldi and Smith, 1998; Susyan *et al.*, 2005; Rousk, Demoling, and Bååth, 2008; Rousk, Demoling, Bahr, *et al.*, 2008). As a consequence of the inhibition, the biomass of the inhibited organisms might become an easily available substrate for the remaining community. *Pseudomonas* strains are among the bacteria which were found to degrade and grow on fungal cell wall material (Lim *et al.*, 1991; Chernin *et al.*, 1995; Tolonen *et al.*, 2014). The dominance of *Pseudomonadales* assigned sequences in the fungicide treatment could be a consequence of fungal biomass decay by this bacterial order. Samples from microcosms with added fungicides before the addition of organic material (20 days of incubation before the start of the experiment) already showed an increase in active *Pseudomonadales*, supporting the hypothesis that we unintentionally provide substrates for bacterial communities by inhibiting eukaryotic ones. Another possible reason for the dominance of this order could be the use of the inhibitor itself as a substrate by these organisms. A study using streptomycin and cycloheximide as inhibitors concluded that the initial killed community was used as substrate by the survivors before they started to use the biocidal molecules as energy and nutrient source themselves (Badalucco *et al.*, 1994).

The addition of fungicides led to an accumulation of ammonium in all treatments (Table 4). This has already been observed when cycloheximide was added to soil (Ingham and Coleman, 1984). The inhibitory effect of cycloheximide on ammonia oxidizing archaea might be an explanation for the increase in ammonia, since its oxidation would be prevented or at least slowed down (Vajrala *et al.*, 2014).

Another effect of fungicide addition was observed by comparing the development of soil communities over the experiment. When distinct organic materials were applied to the same soil, metagenomic signatures could be distinguished from each other after 30 days of incubation (Figure 21). Metagenomes from added communities of organic materials did not cluster with metagenomes 30 days after addition. This suggests that the material and not the added communities determined the development of community structure in the soil and thus might also have consequences on functions carried out. However, in the presence of fungicides, metagenomic signatures could not be clearly distinguished after 30 days. One reason for this is the dominance of *Pseudomonadales,* which also increased in relative abundance in extracted DNA as discussed previously. However, it might also point to the importance of fungal members for community development and adaptability

Conclusions

Fungal and bacterial communities responded differently to the addition of different types of OM as observed by shifts in the relative abundance of active organisms and the timing of the response. Changes in extracted ammonium and nitrate concentrations over the incubation period could be linked to the occurrence of nitrogen cycling related transcripts in metatranscriptomes derived from total mRNA in the paper pulp and compost treatment. Furthermore, nitrogen cycling activity was found in transcripts of total mRNA but not in poly-A-tail isolated transcripts, suggesting that bacteria are dominating these processes. Conversely, carbon degrading activity was linked to fungal communities, which supports our hypothesis that nitrogen cycling bacteria are dependent on nutrients provided by a fungal community. The addition of fungicides had effects in all measured biological and chemical parameters and inhibited N_2O production in the compost treatment. Although a successful inactivation of fungal members could be confirmed by transcriptomic analysis, conclusions on functional potentials in this treatment have to be drawn with care, since the inhibition of an important member of the soil community might also cause perturbations in the food web since their biomass becomes available as nutrients for survivors. However, the lack of N_2O production after inhibition confirms once more the importance of fungi in processes leading to N_2O emissions. Our data suggests that their role might be an indirect one, through the degradation of carbon rather than acting on nitrogen molecules directly themselves.

General conclusions and perspectives

Nitous-oxide is currently accumulating in the atmosphere due to modern agriculture practices. Relative to this, the need for producing crops to feed an increasing world population stands against the impact of a trace gas on climate, which might seem irrelevant. However, a changing climate would lead to a loss in arable land and thus increase the problem of sufficient nutrition for humanity to a probably unmanageable dimension. Therefore, we have to understand biological processes leading to elevated N_2O production observed in soil in order to develop targeted and feasible mitigation strategies.

The purpose to this thesis was to determine the role of bacteria and fungi in nitrogen cycling and N_2O emissions. Nitrification, denitrification and N_2O reducing potentials were found to be present throughout the soil and no micro environment could be specifically linked to a process. This could indicate that these processes occur in soils independent of location and thus no specific hotspot for the various processes involved in nitrogen cycling exists. That would mean that denitrification inside of an aggregate is as likely to happen as on surfaces of soil in pristine soils. This could be different in fertilized soils where nutrient inputs initially occur by transport and diffusion processes in water films. When trying to clarify the role of fungi in N cycling, we found that direct contribution to N_2O production by fungi seems unlikely, since we did not measure high production rates even in strains that can take up nitrogen as NH_4^+ and NO_3^- . Findings of an abiotic NO production by nitrite media generally used in these screening studies could lead to reinvestigations of fungi for which low N_2O production was reported, since its biological origin now seems questionable. In the discussion on whether nitrogen reduction in fungi is used for energy generation or as a detoxification mechanism, our results point to the latter. Sequencing the full genomes of the strains tested in this study would support our hypothesis that NO reduction mediated by NOR-activity distinct from P450nor in fungi is widespread. Based on our results, the suggested contribution of

fungi to N_2O production in soils might be more related to their activity as decomposers in the carbon cycle. Fungal communities present in soil aggregates and on the surface of soil were found to differ in contrast to bacteria, suggesting that certain members find preferred conditions in different locations within soil. The dominating members found were described as having distinct strategies in carbohydrate usage. This might be an indication that carbohydrates are not equally distributed in soil. When exploring the role of carbon in more detail, we showed that the response of fungal and bacterial communities after organic matter addition to soil differs and that nitrogen cycling bacteria might be dependent on the decomposing function of fungi. This implies that we could influence nitrogen cyclers with the organic matter qualities that we add. A possible mitigation strategy for N_2O emissions from agricultural soils would be management practices that promote an increased N_2O reducing community in soils, since these bacteria are the only organisms known so far to reduce N_2O further to N_2. Studies on the mycorrhizal impact on bacterial communities and data presented in this thesis suggest that one way to influence bacterial communities could be through favoring specific fungal communities that support N_2O reducing bacteria that are dependent on them. Potentially, organic matter addition could be a useful tool to achieve this. For example, a combination of organic matter addition and simultaneous use of fertilizer could be a way to ensure high yields and reduce ecosystem contamination by N_2O at the same time. Another strategy to follow would be the implementation of these findings in crop breeding programs. Breeds which favor the symbiosis of mycorrhiza that show symbiotic relationships with N_2O reducers could help to reduce negative effects of nitrogen fertilization. To achieve this goal, more research is needed to gain a deeper understanding of fungal-bacterial interactions. Targeted laboratory experiments with artificial communities combined with transcriptomic methods could be a feasible tool and the use of stable isotopes could help us to follow nutrient streams in these processes. Generally, a more integrated view of soil ecology

that includes the complete biome is needed in order to make a step towards unraveling mechanisms behind unbalanced biogeochemical cycling.

Appendix

Supplemental Figures and Tables

Chapter 1

Table S 1: Summary of qPCR primers for SSU rRNA and N-cycling marker gene quantification used in this study.

Target gene	Names of primers	Sequence (5'-3')	Reference
16S rRNA bacteria	341F 534R	CCTACGGGAGGCAGCAG ATTACCGCGGCTGCTGGCA	(Watanabe *et al.*, 2001) (Ferris *et al.*, 1996)
16S rRNA archaea	Crenar771F Crenar975R	ACGGTGAGGGATGAAAGCT CGGCGTTGACTCCAATTG	(Wessén *et al.*, 2011)
18S rRNA fungi	FR1 FF390	AICCATTCAATCGGTAIT CGATAACGAACGAGACCT	(Chemidlin Prévost-Bouré *et al.*, 2011)
amoA archaea	crenamoA23F crenamoA616R	ATCGTCTGGCTWAGACG GCCATCCATCTGTATGTCCA	(Nicol *et al.*, 2008)
amoA bacteria	amoA1F amoA2R	GGGGTTTCTACTGGTGGT CCCCTCKGSAAAGCCTTCTTC	(Nicol *et al.*, 2008)
nirK	nirK876F nirK1040R	ATYGGCGGVCAYGGCGA GCCTCGATCAGRTTRTGGTT	(Henry *et al.*, 2004)
nirS	nirS4QF nirS6QR	GTSAACGYSAAGGARACSGG GASTTCGGRTGSGTCTTSAYGAA	(Kandeler *et al.*, 2006)
nosZ clade 1	nosZ 1840F nosZ 2090R	CGCRACGGCAASAAGGTSMSSGT CAKRTGCAKSGCRTGGCAGAA	(Henry *et al.*, 2006)
nosZ clade 2	1153_nosZ8F 1888_nosZ29R	CTIGGICCIYTKCAYAC GCIGAICARAAITCBGTRC	(Jones *et al.*, 2013)

Table S 2 Summary of physical and chemical characteristics for bulk soil and particle size fractions of Rothamsted Park Grass soil. pH_w was measured in supernatants of fractions and bulk soil after fractionation with distilled water. Ammonium and nitrate concentrations were measured after extraction with 1 M KCl solution.

	Mass [1] [%]	pH_w	d_{50} [µm]	C_u	Tot. C_{org} [g C kg^{-1}_{dw}]	Tot. N_{org} [g N kg^{-1}_{dw}]	NH_4^+ [mg N kg^{-1}_{dw}]	NO_3^- [mg N kg^{-1}_{dw}]
>250 µm	46.03	5.84 ± 0.11	425.6	13.3	64.9 ± 3.5	4.77 ± 0.2	19.5 ± 3.2	0.01 ± 0.03
250-63 µm	9.50	5.85 ± 0.13	119.7	2.3	86.5 ± 11.5	6.40 ± 0.8	35.7 ± 10.2	0.11 ± 0.21
63-20 µm	25.87	5.95 ± 0.02	32.8	2.2	15.6 ± 0.8	1.19 ± 0.1	7.9 ± 1.7	0.00 ± 0.00
20-2 µm	16.21	6.01 ± 0.08	9.5	4.3	53.5 ± 1.8	4.73 ± 0.0	32.8 ± 1.8	0.47 ± 0.95
<2 µm	2.39	6.21 ± 0.15	3.1	3.3	67.1 ± 0.7	7.30 ± 0.0	224.6 ± 127.0	0.16 ± 0.31
Bulk	100.00	5.59 ± 0.01	285.7	16.7	52.2 ± 0.7	4.10 ± 0.1	25.6 ± 1.3	4.60 ± 0.74
Sum fractions [a]	-	5.91 [b] ± -	-	-	52.4 [b] ± -	4.05 [b] ± -	25.1 [b] ± -	0.10 ± -

Major cation	Al [mg g^{-1}]	Ca [mg g^{-1}]	Fe [mg g^{-1}]	K [mg g^{-1}]	Mg [mg g^{-1}]	Mn [mg g^{-1}]	Na [mg g^{-1}]	Ti [mg g^{-1}]
>250 µm	24.39 ± 12.5	0.80 ± 0.25	30.50 ± 1.32	6.38 ± 3.20	0.51 ± 0.66	0.89 ± 0.03	2.58 ± 0.43	5.00 ± 0.12
250-63 µm	30.31 ± 6.5	0.96 ± 0.12	31.96 ± 0.34	6.02 ± 0.91	0.54 ± 0.51	1.16 ± 0.10	1.62 ± 0.05	4.26 ± 0.19
63-20 µm	13.79 ± 0.6	0.43 ± 0.05	10.49 ± 0.33	6.35 ± 0.93	0.08 ± 0.00	0.21 ± 0.01	3.16 ± 0.25	4.66 ± 0.04
20-2 µm	37.58 ± 6.7	1.09 ± 0.11	33.60 ± 2.68	9.24 ± 1.37	0.41 ± 0.38	0.47 ± 0.06	3.19 ± 0.52	6.15 ± 0.01
<2 µm	49.39 ± 2.3	1.05 ± 0.00	55.41 ± 1.31	5.92 ± 0.04	0.23 ± 0.04	0.89 ± 0.23	1.03 ± 0.14	5.11 ± 0.44
Bulk	27.20 ± 1.5	0.71 ± 0.04	28.54 ± 0.80	6.87 ± 0.68	0.36 ± 0.10	0.68 ± 0.01	2.70 ± 0.04	5.01 ± 0.01
Sum fractions [a]	24.95 [b] ± -	0.77 [b] ± -	26.56 [b] ± -	6.79 [b] ± -	0.38 [b] ± -	0.67 [b] ± -	2.70 [b] ± -	5.03 [b] ± -

Trace elements	As [µg g^{-1}]	B [µg g^{-1}]	Ba [µg g^{-1}]	Co [µg g^{-1}]	Cr [µg g^{-1}]	Cu [µg g^{-1}]	Ni [µg g^{-1}]	Pb [µg g^{-1}]	Sn [µg g^{-1}]	Sr [µg g^{-1}]	Tl [µg g^{-1}]	Zn [µg g^{-1}]
>250 µm	9.4 ± 0.6	92.1± 2.3	81.7 ± 73.8	11.2 ± 0.4	65.4 ± 2.5	26.9 ± 0.8	66.3 ± 58.9	71.7 ± 13.3	5.4 ± 1.4	11.6 ± 10.6	13.5 ± 0.3	118.2 ± 8.9
250-63 µm	9.8 ± 0.4	79.7 ± 2.2	79.2 ± 66.2	13.7 ± 0.9	57.8 ± 1.4	45.7 ± 2.9	88.5 ± 11.1	86.2 ± 19.8	4.1	11.0 ± 6.8	11.2 ± 0.3	136.5 ± 6.2
63-20 µm	3.8 ± 0.0	79.6 ± 2.6	162.5 ± 11.3	3.6 ± 0.1	47.6 ± 0.1	16.5 ± 0.2	19.4 ± 5.5	37.0 ± 1.1	nd	15.9 ± 0.8	14.0 ± 0.2	43.6 ± 1.5
20-2 µm	8.8 ± 0.0	93.9 ± 3.0	56.2 ± 19.6	7.9 ± 0.7	71.4 ± 1.2	42.7 ± 0.7	26.5 ± 0.6	55.6 ± 9.9	3.3 ± 0.1	11.1 ± 0.9	16.8 ± 0.1	114.1 ± 8.9
<2 µm	15.1 ± 0.9	110.3 ± 4.1	62.9 ± 12.1	13.1 ± 1.6	102.8 ± 1.4	64.7 ± 2.8	50.2 ± 19.4	82.7 ± 9.8	6.2 ± 0.3	10.5 ± 1.0	13.8 ± 0.7	199.3 ± 7.5
Bulk	8.1 ± 0.2	97.5 ± 6.5	60.6 ± 1.9	8.8 ± 0.3	61.1 ± 0.5	28.5 ± 0.4	21.7 ± 0.9	61.5 ± 2.4	2.3	8.9 ± 0.1	13.9 ± 0.4	121.2 ± 23.6
Sum fractions [a]	8.0 [b] ± -	88.4 [b] ± -	97.8 ± -	9.0 [b] ± -	62.0 [b] ± -	29.5 [b] ± -	49.4 ± -	61.8 [b] ± -	3.6 ± -	12.55 ± -	13.95 [b] ± -	101.91 ± -

a: Sum of all fractions (> 250, 250-63, 63-20, 20-2 and < 2 µm) according to their mass contribution of bulk soil (1)
b: values included in PCA on chemical properties of soil fractions (Figure 1); sum of fractions (a) represent 90 -110% of the analyte found in bulk soil samples
C_u: coefficient of uniformity - d_{60}/d_{10}
nd: not detectable

Table S 3: Summary of cation and anion concentrations in supernatant of different particel size fractions and bulk soil after fractionation with distilled water

	Al^{3+} [mg L^{-1}]	Ca^{2+} [mg L^{-1}]	Fe^{2+} [mg L^{-1}]	K^{+} [mg L^{-1}]	Mg^{2+} [mg L^{-1}]	Mn [mg L^{-1}]	Na+ [mg L^{-1}]	Ti^{4+} [mg L^{-1}]
>250 µm	nd	nd	nd	nd	nd	nd	nd	nd
250-63 µm	nd	nd	nd	nd	nd	nd	nd	nd
63-20 µm	nd	nd	nd	nd	nd	nd	nd	nd
20-2 µm	nd	nd	nd	nd	nd	nd	nd	nd
<2 µm	nd	nd	nd	nd	nd	nd	nd	nd
Bulk soil	1.04 ± 0.04	2.13 ± 0.23	0.76 ± 0.01	4.59 ± 1.36	0.38 ± 0.05	nd	2.78 ± 0.02	nd

	F^{-} [mg L^{-1}]	Cl^{-} [mg L^{-1}]	NO_3^{-} [mg L^{-1}]	PO_4^{2-} [mg L^{-1}]	SO_4^{2-} [mg L^{-1}]
>250 µm	0.05	0.74 ± 0.20	nd	nd	nd
250-63 µm	0.05	0.41 ± 0.16	nd	nd	nd
63-20 µm	nd	1.21 ± 0.85	nd	nd	nd
20-2 µm	0.16 ± 0.00	0.66 ± 0.56	0.11	nd	0.21
<2 µm	0.07	0.52 ± 0.42	nd	nd	nd
Bulk soil	0.12 ± 0.02	5.13 ± 1.59	4.08 ± 1.02	1.21 ± 1.44	5.43 ± 1.04

nd: not detectable

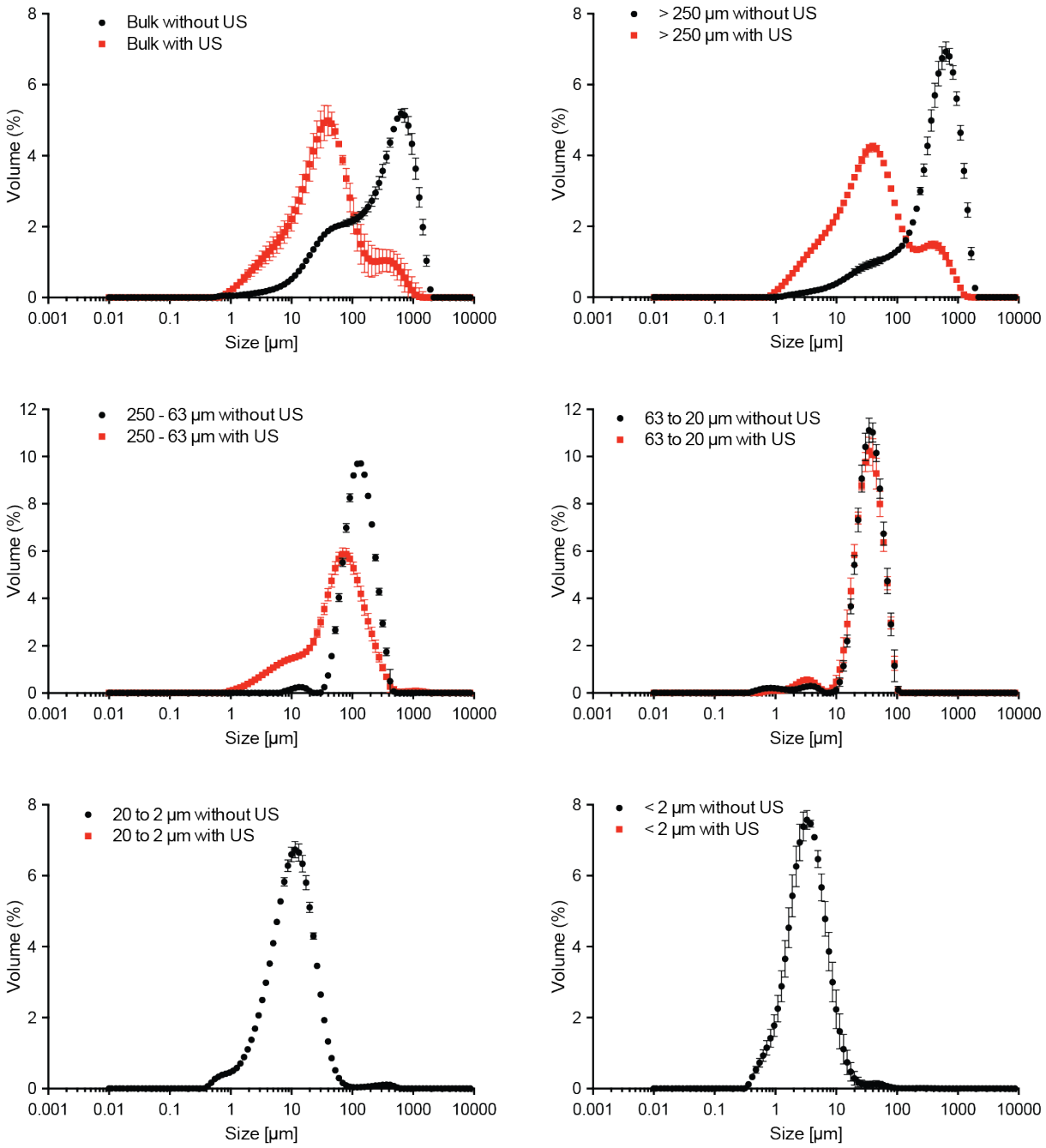

Figure S 1: Particle size distribution of Rothamsted Park Grass soil fractions and bulk soil obtained by laser granulometry (Mastersizer 2000, Malvern) with (red dots) and without (black dots) ultra-sonication. Data points represent the mean, error bars the standard deviation of the mean.

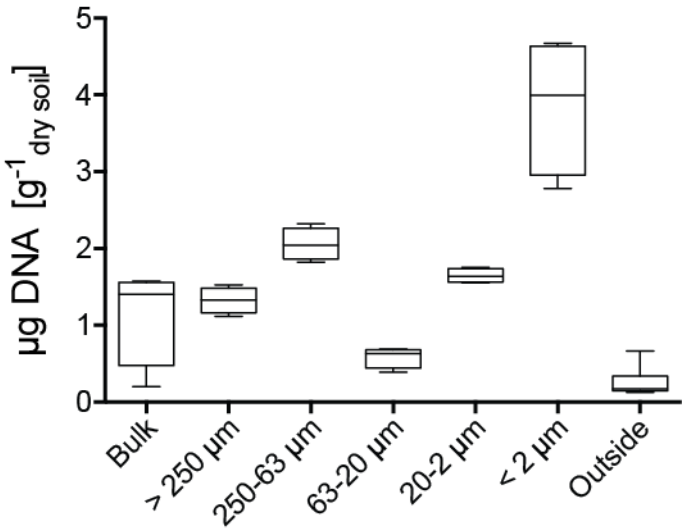

Figure S 2: Extracted DNA from Rothamsted Park Grass soil fractions (n=6).

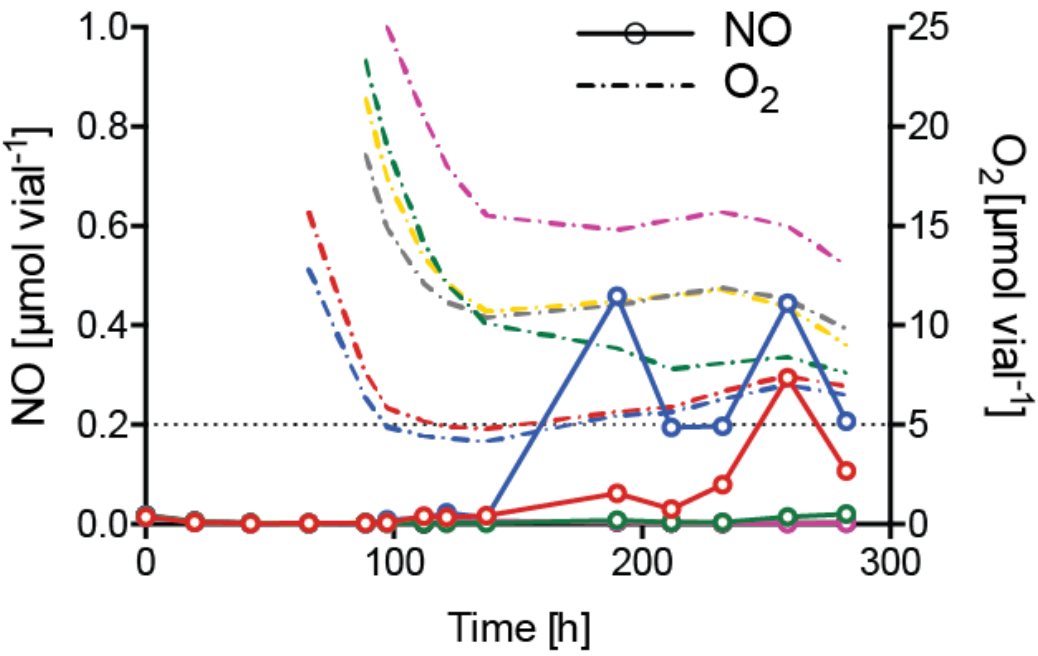

Figure S 3: O_2 threshold concentration at which an abiotic NO production from culture medium could be expected. Butyl-rubber sealed vials (120 mL) containing 50 mL sterile, He-washed Czapeck-Dox medium (3mM ammonium; 10mM nitrite; 50 mM phosphate buffer (pH 7); 3 % O_2 in headspace of vials) were inoculated with 1 mL of pre-cultures and subsequently incubated at 27°C for 270 h for headspace gas sampling. Dotted lines show O_2, open symbols NO concentrations in headspace of single vials (n=3); same color indicates data from the same vial) of *05_Solicoccozyma terricola* and 38_*Oidiodendron cerealis*. Vials where O_2 was consumed to concentrations below 5 µmol O_2 $vial^{-1}$ showed increase in NO concentrations. Consequently, this O_2 concentration was chosen as threshold value for estimation of abiotic NO production in all other cultures incubated at same conditions.

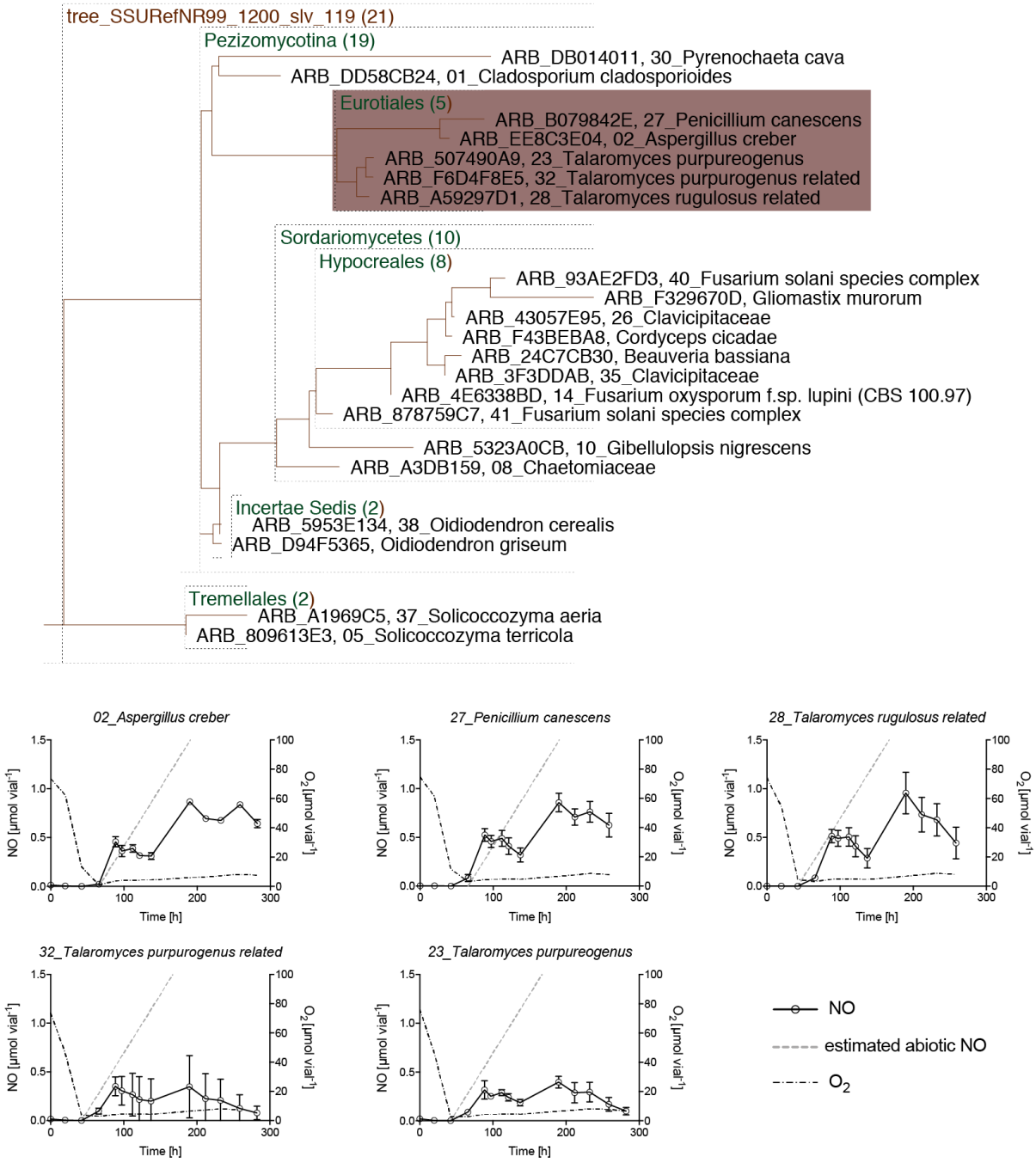

Figure S 4: Phylogenetic tree of tested strains within SSU rRNA based tree dowloaded from SILVA database (Quast *et al.*, 2013) and NO reduction of *Eurotiales* related strains. Representative sequences of tested strains were chosen based on names from SILVA database, strains which could not be found in the database were replaced by a close relative to include the phylogenetic group in the graph. Bottom graphs show the NO curves throughout incubation of *Eurotiales* related strains. Butyl-rubber sealed vials (120 mL) containing 50 mL sterile, He-washed Czapeck-Dox medium (3mM ammonium; 10mM nitrite; 50 mM phosphate buffer (pH 7); 3 % O_2 in headspace of vials) were inoculated with 1 mL of pre-cultures and subsequently incubated at 27°C for 270 h for headspace gas sampling. Grey dotted lines show estimated abiotic NO (12 nmol h^{-1} $vial^{-1}$) and N_2O-N (2.5 mol h^{-1} $vial^{-1}$) production when vials get anoxic (O_2 < 5 µmol $vial^{-1}$); black dotted lines show O_2 concentrations measured in headspace; open symbols show NO concentrations in headspace. Data points show mean of replicates (n=3), error bars standard deviation of mean.

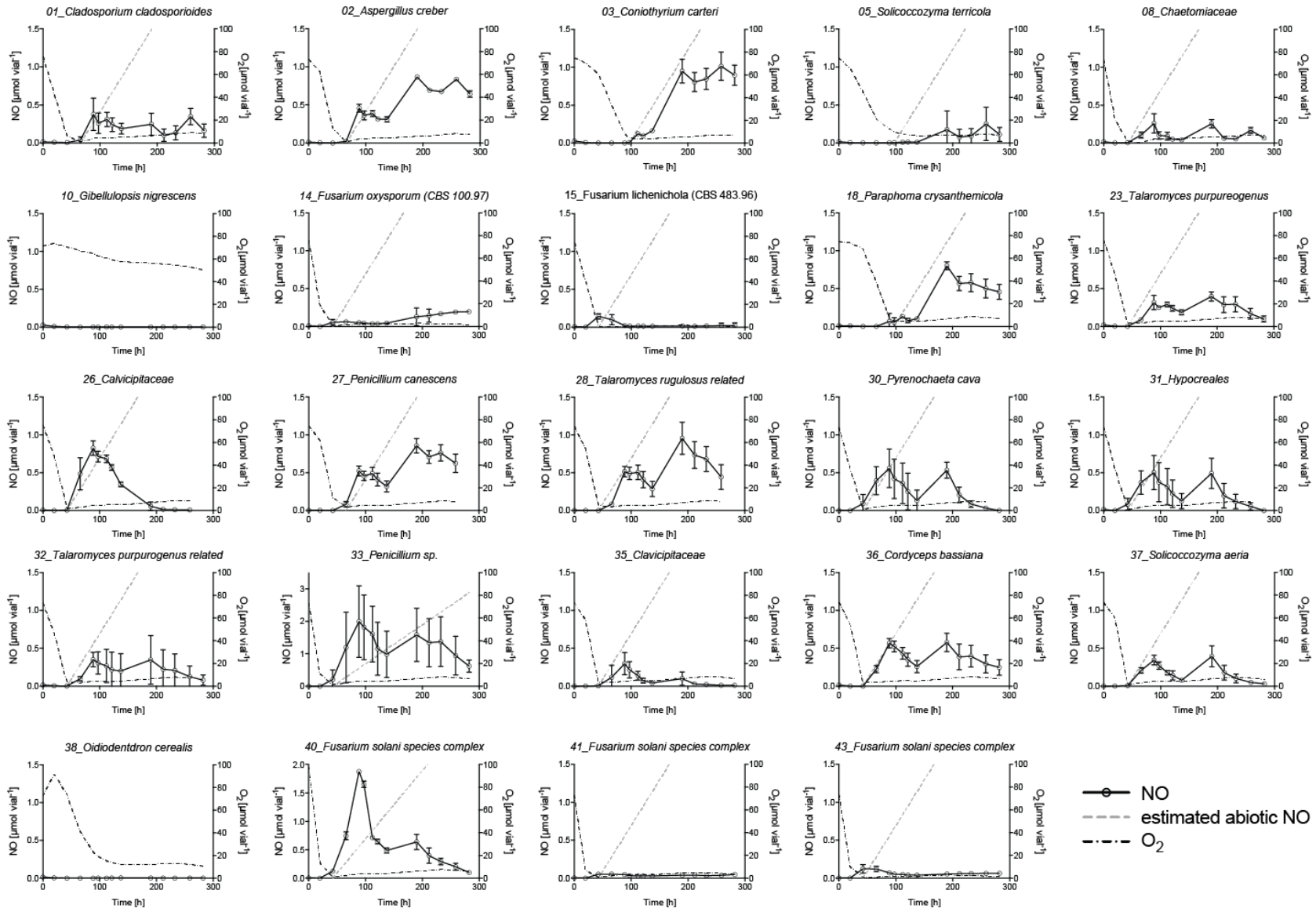

Figure S 5: NO concentrations in headspace of 24 tested fungal strains throughout incubation in Czapeck-Dox medium). Butyl-rubber sealed vials (120 mL) containing 50 mL sterile, He-washed Czapeck-Dox medium (3mM ammonium; 10mM nitrite; 50 mM phosphate buffer (pH 7); 3 % O_2 in headspace of vials) were inoculated with 1 mL of pre-cultures and subsequently incubated at 27°C for 270 h for headspace gas sampling.Grey dotted lines show estimated abiotic NO (12 nmol h^{-1} $vial^{-1}$) production when vials get anoxic (O_2 < 5 µmol $vial^{-1}$); black dotted line indicates O_2 concentrations in headspace of vials; open symbols show NO concentrations in headspace. Data points show mean of replicates (n=3), error bars standard deviation of mean.

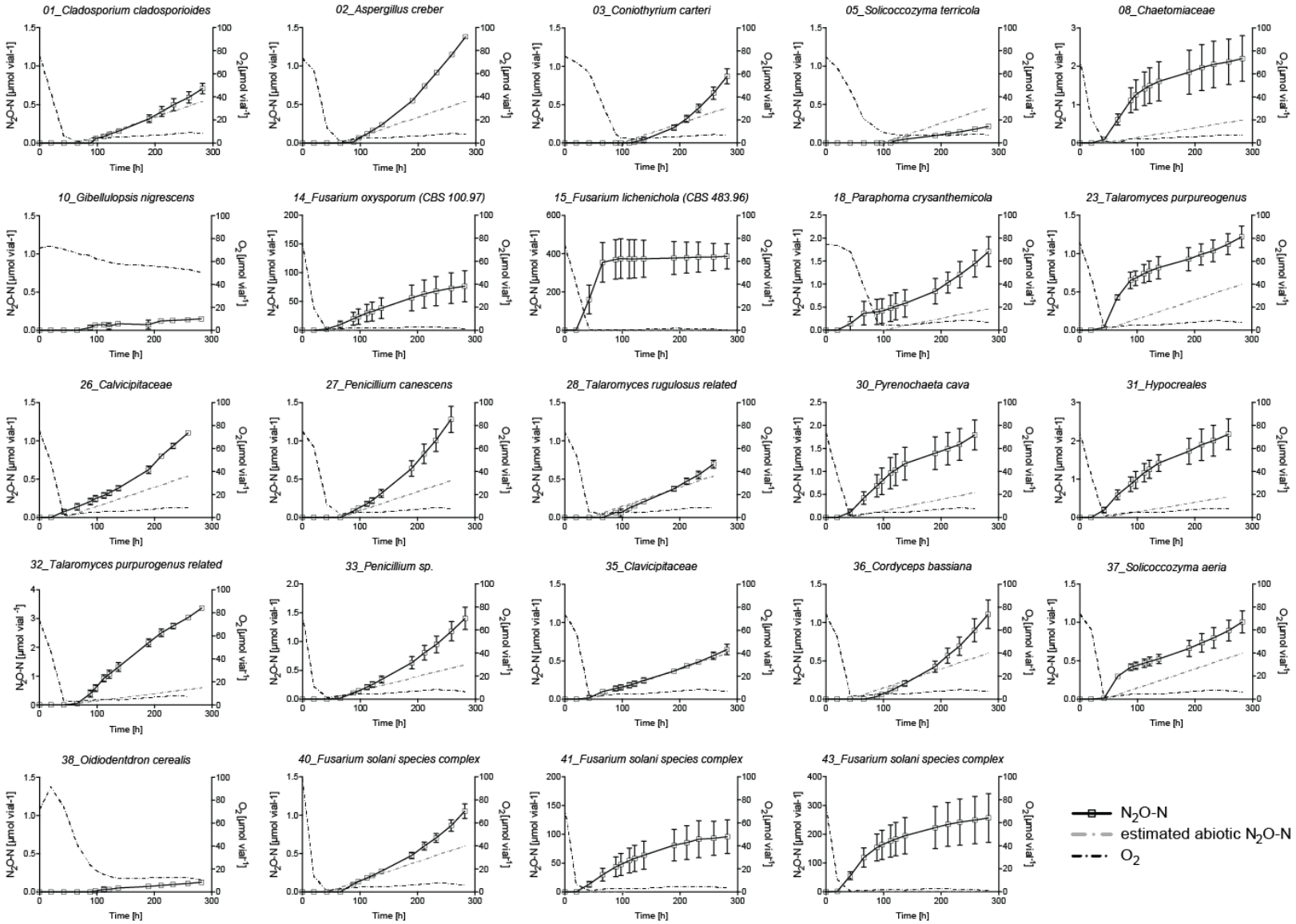

Figure S 6: N_2O-N concentrations in headspace of 24 tested fungal strains throughout incubation in Czapeck-Dox medium. Butyl-rubber sealed vials (120 mL) containing 50 mL sterile, He-washed Czapeck-Dox medium (3mM ammonium; 10mM nitrite; 50 mM phosphate buffer (pH 7); 3 % O_2 in headspace of vials) were inoculated with 1 mL of pre-cultures and subsequently incubated at 27°C for 270 h for headspace gas sampling. Grey dotted lines show estimated abiotic N_2O-N (2.5 nmol h^{-1} $vial^{-1}$) production when vials get anoxic (O_2 < 5 µmol $vial^{-1}$); black dotted line indicates O_2 concentrations in headspace of vials; open symbols show NO concentrations in headspace. Data points show mean of replicates (n=3), error bars standard deviation of mean.

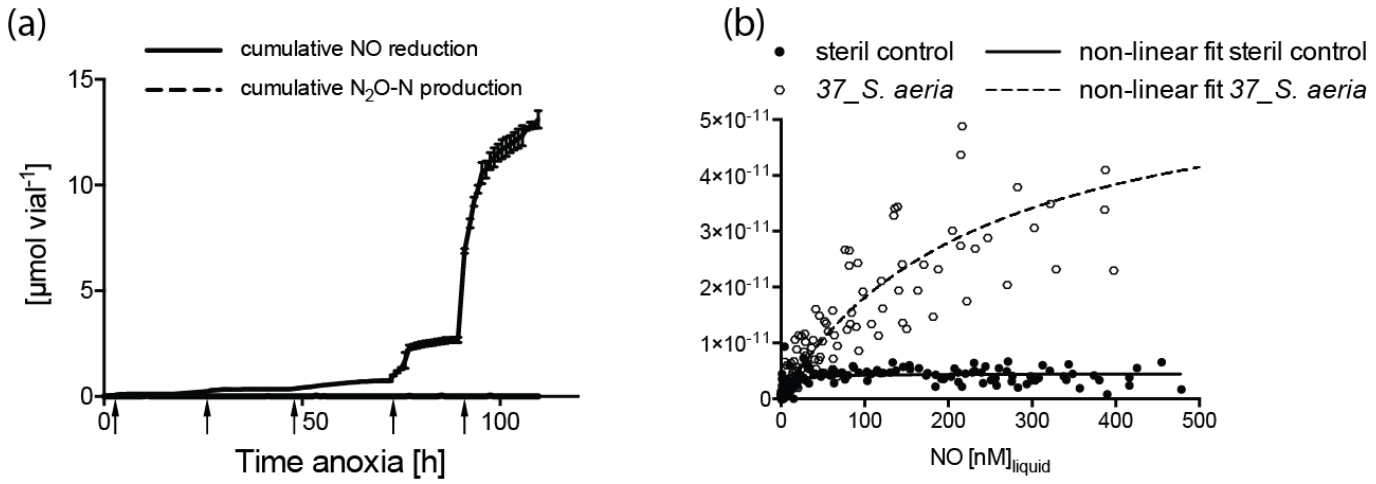

Figure S 7: Cumulative NO reduction vs. N_2O-N production (a) and NO reduction rates (b) of sterile Czapeck-Dox medium control in anoxia after NO injection. Butyl-rubber sealed vials (120 mL) containing 50 mL sterile, He-washed Czapeck-Dox medium (3 mM ammonium; 2 mM nitrite; 50 mM phosphate buffer (pH 7); 3 % O_2 in headspace of vials, 10mM nitrite) were inoculated with 1 mL of pre-culture of tested strain and subsequently incubated at 27°C for for 110 hours for headspace gas sampling.(a): NO to N_2O-N concentrations in headspace plotted as cumulative reduction of NO and cumulative production of N_2O-N in vials. Arrows indicate time points of NO injections of increasing concentrations. Lines show mean of replicates, error bars the standard deviation. (b) show Michaelis-Menten curve fit to NO reduction rates calculated from NO injections in 3 vials (Table 2). NO concentrations in liquid phase were calculated based on measured headspace concentrations.

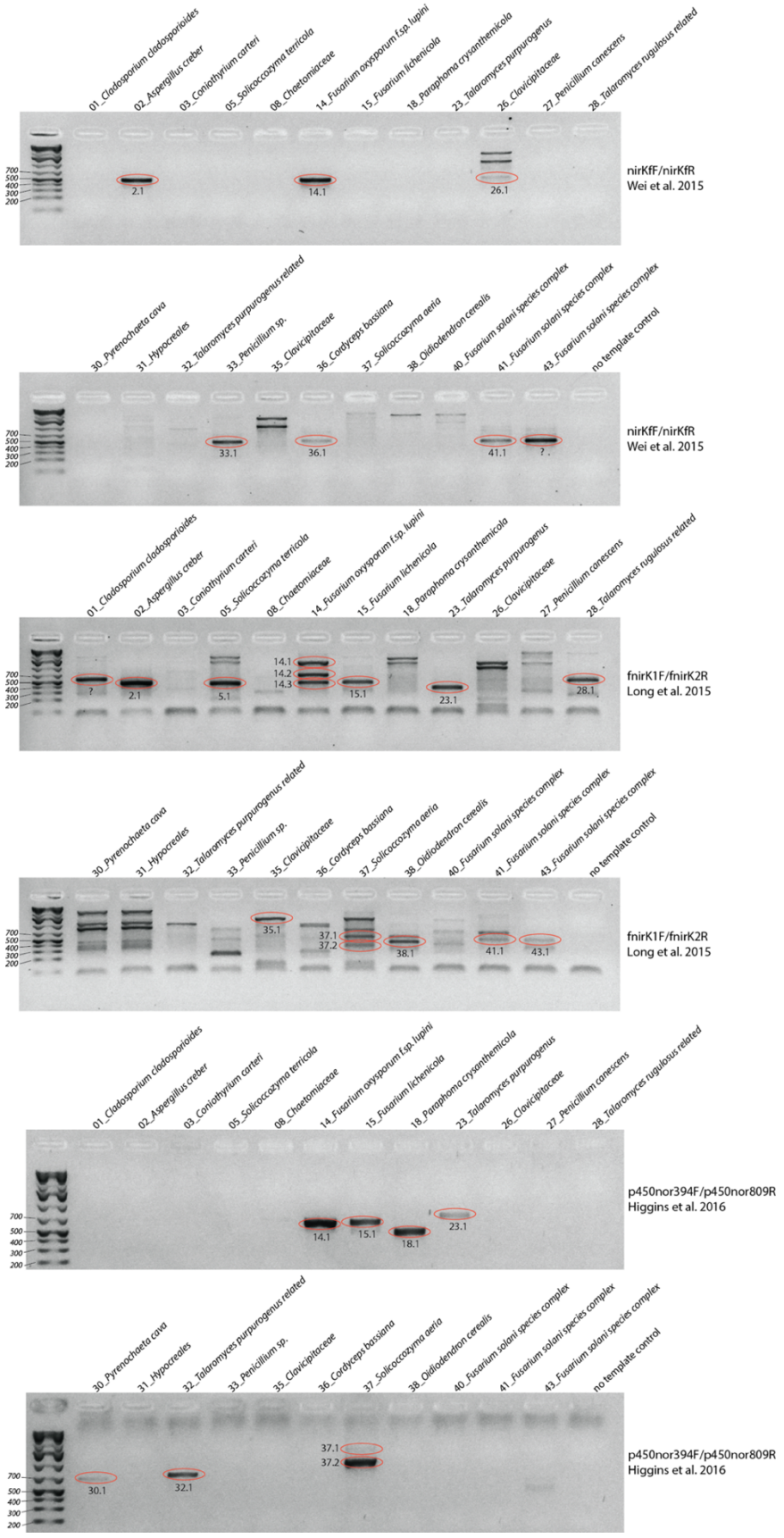

Figure S 8: Gel bands of amplified nirK and P450nor gene sequences from genomic DNA of tested fungal isolates. Red marks indicate bands which were send out for Sanger sequencing.

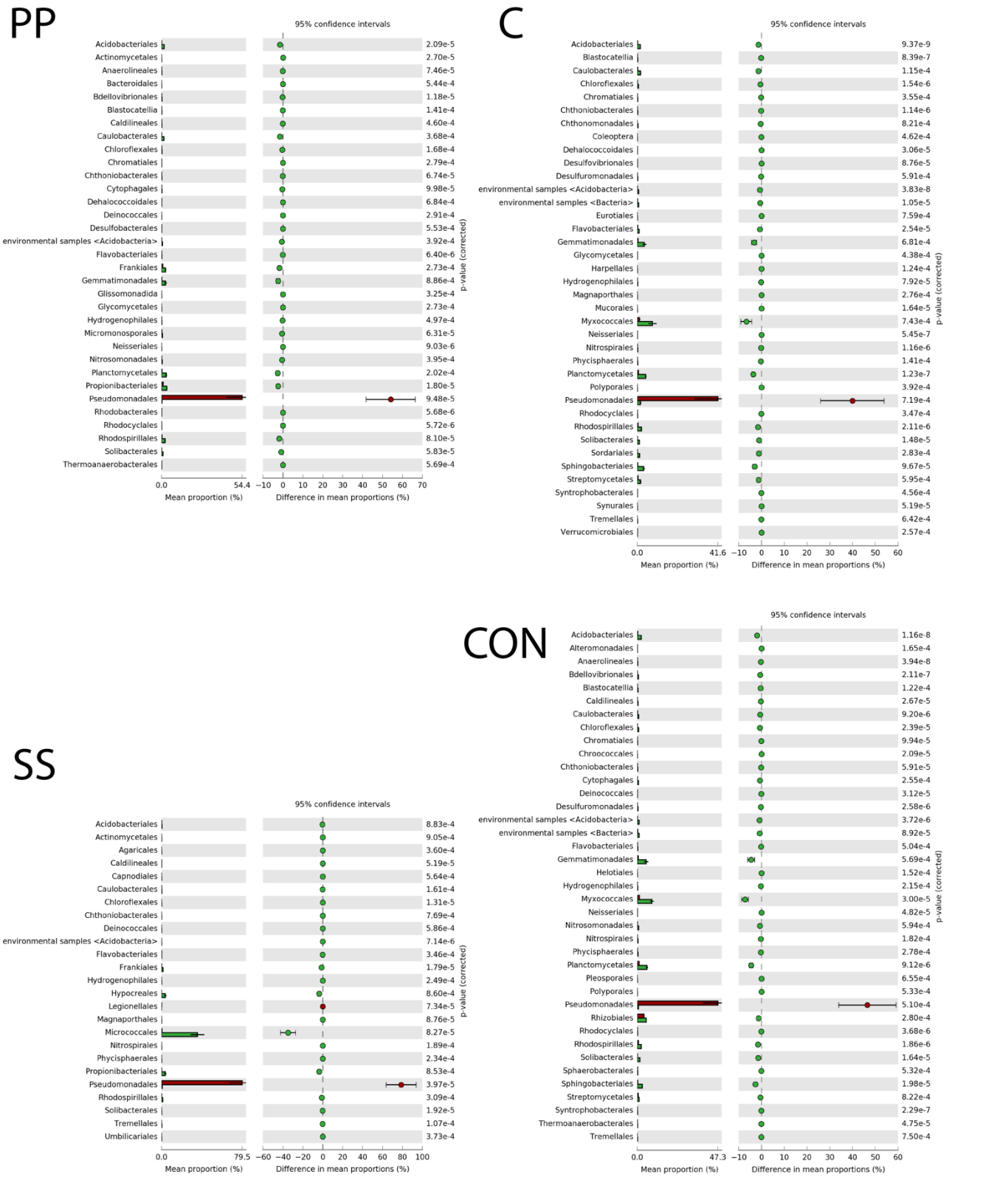

Figure S 9: Comparison between active orders of metatranscriptomes from microcosms with (red) and without (green) added fungicides. C, compost; PP, paper pulp; SS, sewage sludge; CON, control. Graphs produced by STAMP after importing profiles from compared metatranscriptomes in MEGAN. Samples from 6 and 30 days after addition of various organic materials are compared together with and without added fungizdes. P-values from Welch's t-test in STAMP (n=6).

Table S 4: Summarized data of different organic matter classed added to the microcosms. Values show the mean and standard deviation (n=3).

	pH_{KCl}	pH_{H2O}	Ammonium [µg N g^{-1}_{DM}]	Nitrate [µg N g^{-1}_{DM}]	Nitrite [µg N g^{-1}_{DM}]	RNA* [µg g^{-1}_{DM}]	DNA [µg g^{-1}_{DM}]
SS	7.1 ± 0.03	7.6 ± 0.05	0.3 ± 0.12	nd	0.4 ± 0.06	2.0 ± 0.29	1.8 ± 0.09
PP	6.6 ± 0.03	7.3 ± 0.09	7.9 ± 4.03	0.7 ± 0.19	0.2 ± 0.03	nd	0.6 ± 0.07
C	7.1 ± 0.02	7.5 ± 0.06	71.3 ± 6.51	0.0 ± 0.22	0.1 ± 0.01	5.2 ± 1.98	9.4 ± 3.62

pH_{KCl} / pH_{H2O}: pH measured in 1M KCl extract (1:5) and H_2O extract (1:6) of 1 g amendment respectively
PP: paper pulp; C: compost; SS: sewage sludge;DM: dry matter
*RNA measured after 2 days incubation of pure amendments under same conditions as microcosms
nd: not detectable

Bibliography

Ali, M. and Okabe, S. (2015) Anammox-based technologies for nitrogen removal: Advances in process start-up and remaining issues. *Chemosphere* **141**: 144–153.

Anderson, I.C. and Levine, J.S. (1986) Relative rates of nitric oxide and nitrous oxide production by nitrifiers, denitrifiers, and nitrate respirers. *Appl. Environ. Microbiol.* **51**: 938–945.

Aro, N., Pakula, T., and Penttilä, M. (2005) Transcriptional regulation of plant cell wall degradation by filamentous fungi. *FEMS Microbiology Reviews* **29**: 719–739.

Artursson, V., Finlay, R.D., and Jansson, J.K. (2006) Interactions between arbuscular mycorrhizal fungi and bacteria and their potential for stimulating plant growth. *Environmental Microbiology* **8**: 1–10.

Aschenbrenner, I.A., Cernava, T., Berg, G., and Grube, M. (2016) Understanding Microbial Multi-Species Symbioses. *Front Microbiol* **7**: 143–9.

Badalucco, L., Pomare, F., Grego, S., Landi, L., and Nannipieri, P. (1994) Activity and degradation of streptomycin and cycloheximide in soil. *Biol Fertil Soils* **18**: 334–340.

Bailey, Bilskis, Fansler, McCue, Smith, Konopka (2012) Measurements of microbial community activities in individual soil macroaggregates. *Soil Biology and Biochemistry* **48**: 4–4.

Bailey, V.L., Fansler, S.J., Stegen, J.C., and McCue, L.A. (2013) Linking microbial community structure to β-glucosidic function in soil aggregates. *The ISME Journal* **7**: 2044–2053.

Bakken, L.R. (1985) Separation and Purification of Bacteria from Soil. *Appl. Environ. Microbiol.* **49**: 1482–1487.

Bakken, L.R., Bergaust, L., Liu, B., and Frostegård, Å. (2012) Regulation of denitrification at the cellular level: a clue to the understanding of N2O emissions from soils. *Phil. Trans. R. Soc. B* **367**: 1226–1234.

Bakker, M.G., Schlatter, D.C., Otto-Hanson, L., and Kinkel, L.L. (2014) Diffuse symbioses: roles of plant-plant, plant-microbe and microbe-microbe interactions in structuring the soil microbiome. *Mol Ecol* **23**: 1571–1583.

Bardgett, R., Usher, M., and Hopkins, D. (2005) Biological Diversity and Function in Soils Cambridge University Press.

Barker, B.M., Kroll, K., Vödisch, M., Mazurie, A., Kniemeyer, O., and Cramer, R.A. (2012) Transcriptomic and proteomic analyses of the Aspergillus fumigatus hypoxia response using an oxygen-controlled fermenter. *BMC Genomics* **13**: 62.

Barreiro, A., Bååth, E., and Díaz-Raviña, M. (2016) Bacterial and fungal growth in burnt acid soils amended with different high C/N mulch materials. *Soil Biology and Biochemistry* **97**: 102–111.

Bateman, E.J. and Baggs, E.M. (2005) Contributions of nitrification and denitrification to N2O emissions from soils at different water-filled pore space. *Biol Fertil Soils* **41**: 379–388.

Battaglia, E., Benoit, I., van den Brink, J., Wiebenga, A., Coutinho, P.M., Henrissat, B., and de Vries, R.P. (2011) Carbohydrate-active enzymes from the zygomycete fungus Rhizopus oryzae: a highly specialized approach to carbohydrate degradation depicted at genome level. *BMC Genomics* **12**: 38.

Bååth, E. and Anderson, T.H. (2003) Comparison of soil fungal/bacterial ratios in a pH gradient using physiological and PLFA-based techniques. *Soil Biology and Biochemistry* **35**: 955–963.

Beare, M.H., Hu, S., Coleman, D.C., and Hendrix, P.F. (1996) Influences of mycelial fungi on soil aggregation and organic matter storage in conventional and no-tillage soils. *Applied Soil Ecology* **5**: 211–219.

Bell, M.J., Hinton, N., Cloy, J.M., Topp, C.F.E., Rees, R.M., Cardenas, L., et al. (2015) Nitrous oxide emissions from fertilised UK arable soils: Fluxes, emission factors and mitigation. *"Agriculture, Ecosystems and Environment"* **212**: 134–147.

Bender, S.F., Plantenga, F., Neftel, A., Jocher, M., Oberholzer, H.-R., hl, L.K.O., et al. (2013) Symbiotic relationships between soil fungi and plants reduce N2O emissions from soil. *The ISME Journal* **8**: 1336–1345.

Benito, M., Masaguer, A., Moliner, A., and Arrigo, N. (2003) Chemical and microbiological parameters for the characterisation of the stability and maturity of pruning waste compost. *Biol Fertil Soils* **37**: 184–189.

Berger, H., Basheer, A., Böck, S., Reyes-Dominguez, Y., Dalik, T., Altmann, F., and Strauss, J. (2008) Dissecting individual steps of nitrogen transcription factor cooperation in the Aspergillus nidulansnitrate cluster. *Molecular Microbiology* **69**: 1385–1398.

Berry, D. and Widder, S. (2014) Deciphering microbial interactions and detecting keystone species with co-occurrence networks. *Front Microbiol* **5**: 1–14.

Betlach, M.R. and Tiedje, J.M. (1981) Kinetic explanation for accumulation of nitrite, nitric oxide, and nitrous oxide during bacterial denitrification. *Appl. Environ. Microbiol.* **42**: 1074–1084.

Biesebeke, te, R., Levasseur, A., Boussier, A., Record, E., van den Hondel, C.A.M.J.J., and Punt, P.J. (2010) Phylogeny of fungal hemoglobins and expression analysis of the Aspergillus oryzae flavohemoglobin gene fhbA during hyphal growth. *Mycological Research* **114**: 135–143.

Billen, G., Garnier, J., and Lassaletta, L. (2013) The nitrogen cascade from agricultural soils to the sea: modelling nitrogen transfers at regional watershed and global scales. *Phil. Trans. R. Soc. B* **368**: 20130123.

Binns, D., Dimmer, E., Huntley, R., Barrell, D., O'Donovan, C., and Apweiler, R. (2009) QuickGO: a web-based tool for Gene Ontology searching. *Bioinformatics* **25**: 3045–3046.

Bischof, R.H., Ramoni, J., and Seiboth, B. (2016) Cellulases and beyond: the first 70 years of the enzyme producer Trichoderma reesei. *Microb Cell Fact* **15**: 24–14.

Bittman, S., Forge, T.A., and Kowalenko, C.G. (2005) Responses of the bacterial and fungal biomass in a grassland soil to multi-year applications of dairy manure slurry and fertilizer. *Soil Biology and Biochemistry* **37**: 613–623.

Blasco, F., Guigliarelli, B., Magalon, A., Asso, M., Giordano, G., and Rothery, R.A. (2001) The coordination and function of the redox centres of the membrane-bound nitrate reductases. *Cell. Mol. Life Sci.* **58**: 179–193.

Bleakley, B.H.B. and Tiedje, J.M.J. (1982) Nitrous oxide production by organisms other than nitrifiers or denitrifiers. *Appl. Environ. Microbiol.* **44**: 1342–1348.

Boer, W. de, Folman, L.B., Summerbell, R.C., and Boddy, L. (2005) Living in a fungal world: impact of fungi on soil bacterial niche development. *FEMS Microbiology Reviews* **29**: 795–811.

Bokulich, N.A., Bokulich, N.A., Mills, D.A., and Mills, D.A. (2013) Improved Selection of Internal Transcribed Spacer-Specific Primers Enables Quantitative, Ultra-High-Throughput Profiling of Fungal Communities. *Appl. Environ. Microbiol.* **79**: 2519–2526.

Briar, Fonte, Park, Six, Scow, Ferris (2011) The distribution of nematodes and soil microbial communities across soil aggregate fractions and farm management systems. *Soil Biology and Biochemistry* **43**: 10–10.

Bronick, C.J. and Lal, R. (2005) Soil structure and management: a review. *Geoderma* **124**: 3–22.

Bru, D., Ramette, A., Saby, N.P.A., Dequiedt, S., Ranjard, L., Jolivet, C., et al. (2011) Determinants of the distribution of nitrogen-cycling microbial communities at the landscape scale. *The ISME Journal* **5**: 532–542.

Buchfink, B., Xie, C., and Huson, D.H. (2014) Fast and sensitive protein alignment using DIAMOND. *Nat Meth* **12**: 59–60.

Bugg, T.D.H., Ahmad, M., Hardiman, E.M., and Rahmanpour, R. (2011) Pathways for degradation of lignin in bacteria and fungi. *Nat Prod Rep* **28**: 1883–1896.

Caddick, M.X., Peters, D., and Platt, A. (1994) Nitrogen regulation in fungi. *Antonie van Leeuwenhoek* **65**: 169–177.

Caesar-TonThat, T.C. and Cochran, V.L. (2001) Role of saprophytic basidiomycete soil fungus in aggregate stabilization. *Sustaining the Global Farm* 575–579.

Caporaso, J.G., Kuczynski, J., Stombaugh, J., Bittinger, K., Bushman, F.D., Costello, E.K., et al. (2010) QIIME allows analysis of high-throughput community sequencing data. *Nat Meth* **7**: 335–336.

Castaldi, S. and Smith, K.A. (1998) Effect of cycloheximide on N_2O and NO_3^- production in a forest and an agricultural soil. *Biol Fertil Soils* **27**: 27–34.

Chao, L.Y., Rine, J., and Marletta, M.A. (2008) Spectroscopic and kinetic studies of Nor1, a cytochrome P450 nitric oxide reductase from the fungal pathogen Histoplasma capsulatum. *Archives of Biochemistry and Biophysics* **480**: 132–137.

Chemidlin Prévost-Bouré, N., Christen, R., Dequiedt, S., Mougel, C., Lelièvre, M., Jolivet, C., et al. (2011) Validation and Application of a PCR Primer Set to Quantify Fungal Communities in the Soil Environment by Real-Time Quantitative PCR. *PLoS ONE* **6**: e24166.

Chen, H., Mothapo, N.V., and Shi, W. (2015) Fungal and bacterial N2O production regulated by soil amendments of simple and complex substrates. *Soil Biology and Biochemistry* **84**: 116–126.

Chen, H., Mothapo, N.V., and Shi, W. (2014a) Soil Moisture and pH Control Relative Contributions of Fungi and Bacteria to N2O Production. *Microb Ecol* **69**: 180–191.

Chen, H., Mothapo, N.V., and Shi, W. (2014b) The significant contribution of fungi to soil N 2 O production across diverse ecosystems. *Applied Soil Ecology* **73**: 70–77.

Chen, Z., Wang, C., Gschwendtner, S., Willibald, G., Unteregelsbacher, S., Lu, H., et al. (2015) Relationships between denitrification gene expression, dissimilatory nitrate reduction to ammonium and nitrous oxide and dinitrogen production in montane grassland soils. *Soil Biology and Biochemistry* **87**: 67–77.

Chernin, L., Ismailov, Z., Haran, S., and Chet, I. (1995) Chitinolytic Enterobacter agglomerans Antagonistic to Fungal Plant Pathogens. *Appl. Environ. Microbiol.* **61**: 1720–1726.

Chotte, J.L., Monrozier, L.J., Villemin, G., and Albrecht, A. (1993) Soil microhabitats and the importance of the fractionation method.

Coby, A.J. and Picardal, F.W. (2005) Inhibition of NO_3^- and NO_2^- reduction by microbial Fe(III) reduction: evidence of a reaction between NO_2^- and cell surface-bound Fe_2^+. *Appl. Environ. Microbiol.* **71**: 5267–5274.

Cole, J. (1996) Nitrate reduction to ammonia by enteric bacteria: redundancy, or a strategy for survival during oxygen starvation? *FEMS Microbiol Lett* **136**: 1–11.

Cooper, D.C. and Picardal, F.W. (2003) Chemical and biological interactions during nitrate and goethite reduction by Shewanella putrefaciens 200. *Appl. Environ. Microbiol.* **69**: 3517–3525.

Coutinho, P.M., Andersen, M.R., Kolenova, K., vanKuyk, P.A., Benoit, I., Gruben, B.S., et al. (2009) Post-genomic insights into the plant polysaccharide degradation potential of Aspergillus nidulans and comparison to Aspergillus niger and Aspergillus oryzae. *Fungal Genetics and Biology* **46**: S161–S169.

Cox, R.D. (1980) Determination of nitrate and nitrite at the parts per billion level by chemiluminescence. *Anal. Chem.* **52**: 332–335.

Cragg, S.M., Beckham, G.T., Bruce, N.C., Bugg, T.D.H., Distel, D.L., Dupree, P., et al. (2015) Lignocellulose degradation mechanisms across the Tree of Life. *Current Opinion in Chemical Biology* **29**: 108–119.

Crawford, N.M. and Arst, H.N. (1993) The molecular genetics of nitrate assimilation in fungi and plants. *Annu. Rev. Genet.* **27**: 115–146.

Crenshaw, C.L., Lauber, C., Sinsabaugh, R.L., and Stavely, L.K. (2007) Fungal control of nitrous oxide production in semiarid grassland. *Biogeochemistry* **87**: 17–27.

Cuhel, J., Simek, M., Laughlin, R.J., Bru, D., Cheneby, D., Watson, C.J., and Philippot, L. (2010) Insights into the Effect of Soil pH on N2O and N2 Emissions and Denitrifier Community Size and Activity. *Appl. Environ. Microbiol.* **76**: 1870–1878.

Črešnar, B. and Petrič, Š. (2011) Cytochrome P450 enzymes in the fungal kingdom. *Biochim Biophys Acta* **1814**: 29–35.

Daims, H., Lebedeva, E.V., Pjevac, P., Han, P., Herbold, C., Albertsen, M., et al. (2015) Complete nitrification by Nitrospira bacteria. *Nature* **528**: 504–509.

Dance, A. (2008) Soil ecology: What lies beneath. *Nature* **455**: 724–725.

Darwin, A., Tormay, P., Page, L., Griffiths, L., and Cole, J. (1993) Identification of the formate dehydrogenases and genetic determinants of formate-dependent nitrite reduction by Escherichia coli K12. *J Gen Microbiol* **139**: 1829–1840.

Davinic, M., Fultz, L.M., and Acosta-Martínez, V. (2012) Pyrosequencing and mid-infrared spectroscopy reveal distinct aggregate stratification of soil bacterial communities and organic matter composition. *Soil Biology and Biochemistry* **46**: 63–72.

Davis, G.J. and Sinnott, M.L. (2008) Sorting the diverse: The sequence-based classification of carbohydrate-active enzymes. *Biochemical Journal Classic Papers* 26–32.

de Gonzalo, G., Colpa, D.I., Habib, M.H.M., and Fraaije, M.W. (2016) Bacterial enzymes involved in lignin degradation. *Journal of Biotechnology* **236**: 110–119.

de Jesús-Berríos, M., Liu, L., Nussbaum, J.C., Cox, G.M., Stamler, J.S., and Heitman, J. (2003) Enzymes that counteract nitrosative stress promote fungal virulence. *Current Biology* **13**: 1963–1968.

Di, H.J., Cameron, K.C., Podolyan, A., and Robinson, A. (2014) Effect of soil moisture status and a nitrification inhibitor, dicyandiamide, on ammonia oxidizer and denitrifier growth and nitrous oxide emissions in a grassland soil. *Soil Biology and Biochemistry* **73**: 59–68.

Diacono, M. and Montemurro, F. (2010) Long-term effects of organic amendments on soil fertility. A review. *Agron. Sustain. Dev.* **30**: 401–422.

Eastwood, D.C., Floudas, D., Binder, M., Majcherczyk, A., Schneider, P., Aerts, A., et al. (2011) The Plant Cell Wall–Decomposing Machinery Underlies the Functional Diversity of Forest Fungi. *Science* **333**: 762–765.

Einsle, O., Messerschmidt, A., Stach, P., Bourenkov, G.P., Bartunik, H.D., Huber, R., and Kroneck, P.M. (1999) Structure of cytochrome c nitrite reductase. *Nature* **400**: 476–480.

Ellington, M.J.K., Fosdike, W.L.J., Sawers, R.G., Richardson, D.J., and Ferguson, S.J. (2005) Regulation of the nap operon encoding the periplasmic nitrate reductase of Paracoccus pantotrophus: delineation of DNA sequences required for redox control. *Archives of Microbiology* **184**: 298–304.

Elliott, E.T. and Cambardella, C.A. (1991) Physical separation of soil organic matter. *Agriculture* **34**: 407–419.

Elmholt, S. and Kjøller, A. (1987) Measurement of the length of fungal hyphae by the membrane filter technique as a method for comparing fungal occurrence in cultivated field soils. *Soil Biology and Biochemistry* **19**: 679–682.

Engelking, B., Flessa, H., and Joergensen, R.G. (2007) Shifts in amino sugar and ergosterol contents after addition of sucrose and cellulose to soil. *Soil Biology and Biochemistry* **39**: 2111–2118.

Enwall, K., Philippot, L., and Hallin, S. (2005) Activity and Composition of the Denitrifying Bacterial Community Respond Differently to Long-Term Fertilization. *Appl. Environ. Microbiol.* **71**: 8335–8343.

Enwall, K., Throbäck, I.N., Stenberg, M., Söderström, M., and Hallin, S. (2010) Soil resources influence spatial patterns of denitrifying communities at scales compatible with land management. *Appl. Environ. Microbiol.* **76**: 2243–2250.

Erisman, J.W., Galloway, J., Seitzinger, S., Bleeker, A., and Butterbach-Bahl, K. (2011) Reactive nitrogen in the environment and its effect on climate change. *Current Opinion in Environmental Sustainability* **3**: 281–290.

Faust, K. and Raes, J. (2012) Microbial interactions: from networks to models. *Nature Publishing Group* **10**: 538–550.

Fernández-Calviño, D. and Bååth, E. (2016) Interaction between pH and Cu toxicity on fungal and bacterial performance in soil. *Soil Biology and Biochemistry* **96**: 20–29.

Ferris, M.J., Muyzer, G., and Ward, D.M. (1996) Denaturing gradient gel electrophoresis profiles of 16S rRNA-defined populations inhabiting a hot spring microbial mat community. *Appl. Environ. Microbiol.* **62**: 340–346.

Folwell, B.D., McGenity, T.J., and Whitby, C. (2016) Biofilm and Planktonic Bacterial and Fungal Communities Transforming High-Molecular-Weight Polycyclic Aromatic Hydrocarbons. *Appl. Environ. Microbiol.* **82**: 2288–2299.

Forrester, M.T. and Foster, M.W. (2012) Protection from nitrosative stress: A central role for microbial flavohemoglobin. *Free Radical Biology and Medicine* **52**: 1620–1633.

Forster, P., Ramaswamy, V., and Artaxo, P. (2007) Changes in atmospheric constituents and in radiative forcing. In, *Climate Change The Physical Science Basis. Contribution of Working Group I to the Fourth Assessment Report of the Intergovernmental Panel on Climate Change*. IPCC Localised.

Fowler, D., Coyle, M., Skiba, U., Sutton, M.A., Cape, J.N., Reis, S., et al. (2013) The global nitrogen cycle in the twenty-first century. *Phil. Trans. R. Soc. B* **368**: 20130164.

Frey-Klett, P., Burlinson, P., Deveau, A., Barret, M., Tarkka, M., and Sarniguet, A. (2011) Bacterial-Fungal Interactions: Hyphens between Agricultural, Clinical, Environmental, and Food Microbiologists. *Microbiol. Mol. Biol. Rev.* **75**: 583–609.

Frey-Klett, P., Garbaye, J., and Tarkka, M. (2007) The mycorrhiza helper bacteria revisited. *New Phytologist* **176**: 22–36.

Galloway, J.N. (2003) The global nitrogen cycle. In, *Treatise on Geochemistry*. Elsevier, pp. 557–583.

Galloway, J.N., Aber, J.D., Erisman, J.W., Seitzinger, S.P., Howarth, R.W., Cowling, E.B., and Cosby, B.J. (2003) The Nitrogen Cascade. *BioScience* **53**: 341–356.

Gans, J., Wolinsky, M., and Dunbar, J. (2005) Computational improvements reveal great bacterial diversity and high metal toxicity in soil. *Science* **309**: 1387–1390.

Garbaye, J. (1994) Tansley Review No. 76 Helper bacteria: a new dimension to the mycorrhizal symbiosis. *New Phytologist* **128**: 197–210.

Gardner, A.M., Helmick, R.A., and Gardner, P.R. (2002) Flavorubredoxin, an Inducible Catalyst for Nitric Oxide Reduction and Detoxification in Escherichia coli. *J. Biol. Chem.* **277**: 8172–8177.

Gardner, P.R. (2005) Nitric oxide dioxygenase function and mechanism of flavohemoglobin, hemoglobin, myoglobin and their associated reductases. *J. Inorg. Biochem.* **99**: 247–266.

Gardner, P.R., Gardner, A.M., Martin, L.A., and Salzman, A.L. (1998) Nitric oxide dioxygenase: an enzymic function for flavohemoglobin. *Proc Natl Acad Sci U S A* **95**: 10378–10383.

Georgieva, S., Christensen, S., Petersen, H., Gjelstrup, P., and Thorup-Kristensen, K. (2005) Early decomposer assemblages of soil organisms in litterbags with vetch and rye roots. *Soil Biology and Biochemistry* **37**: 1145–1155.

Glaser, K., Hackl, E., Inselsbacher, E., Strauss, J., Wanek, W., Zechmeister-Boltenstern, S., and Sessitsch, A. (2010) Dynamics of ammonia-oxidizing communities in barley-planted bulk soil and rhizosphere following nitrate and ammonium fertilizer amendment. *FEMS Microbiol Ecol* **74**: 575–591.

Gomes, C.M., Giuffrè, A., Forte, E., Vicente, J.B., Saraiva, L.M., Brunori, M., and Teixeira, M. (2002) A novel type of nitric-oxide reductase. Escherichia coli flavorubredoxin. *J. Biol. Chem.* **277**: 25273–25276.

Gorfer, M., Blumhoff, M., Klaubauf, S., Urban, A., Inselsbacher, E., Bandian, D., et al. (2011) Community profiling and gene expression of fungal assimilatory nitrate reductases in agricultural soil. *The ISME Journal* **5**: 1771–1783.

Green, J. and Bohannan, B.J.M. (2006) Spatial scaling of microbial biodiversity. *Trends in Ecology & Evolution* **21**: 501–507.

Guerrero, M.G., Vega, J.M., and Losada, M. (1981) The assimilatory nitrate-reducing system and its regulation. *Annual review of plant physiology* **32**: 169–204.

Haber, F. and Le Rossignol, R. (1913) Über die technische Darstellung von Ammoniak aus den Elementen. *Zeitschrift für Elektrochemie und angewandte physikalische Chemie* **19**: 53–72.

Hallin, S., Jones, C.M., Schloter, M., and Philippot, L. (2009) Relationship between N-cycling communities and ecosystem functioning in a 50-year-old fertilization experiment. *The ISME Journal* **3**: 597–605.

Hassan, J., Bergaust, L.L., Molstad, L., de Vries, S., and Bakken, L.R. (2015) Homeostatic control of NO at nanomolar concentrations in denitrifying bacteria - modelling and experimental determination of nitric oxide reductase kinetics in vivo in Paracoccus denitrificans. *Environmental Microbiology* 1–15.

Hayatsu, M., Tago, K., and Saito, M. (2008) Various players in the nitrogen cycle: Diversity and functions of the microorganisms involved in nitrification and denitrification. *Soil Science and Plant Nutrition* **54**: 33–45.

Hendriks, J., Oubrie, A., Castresana, J., Urbani, A., Gemeinhardt, S., and Saraste, M. (2000) Nitric oxide reductases in bacteria. *Biochim Biophys Acta* **1459**: 266–273.

Henrissat, B. (1991) A classification of glycosyl hydrolases based on amino acid sequence similarities. *Biochemical Journal* **280**: 309–316.

Henry, S., Baudoin, E., López-Gutiérrez, J.C., Martin-Laurent, F., Brauman, A., and Philippot, L. (2004) Quantification of denitrifying bacteria in soils by nirK gene targeted real-time PCR. *Journal of Microbiological Methods* **59**: 327–335.

Henry, S., Bru, D., Stres, B., Hallet, S., and Philippot, L. (2006) Quantitative detection of the nosZ gene, encoding nitrous oxide reductase, and comparison of the abundances of 16S rRNA, narG, nirK, and nosZ genes in soils. *Appl. Environ. Microbiol.* **72**: 5181–5189.

Henry, S., Texier, S., Hallet, S., Bru, D., Dambreville, C., Cheneby, D., et al. (2008) Disentangling the rhizosphere effect on nitrate reducers and denitrifiers: insight into the role of root exudates. *Environmental Microbiology* **10**: 3082–3092.

Higgins, S.A., Welsh, A., Orellana, L.H., Konstantinidis, K.T., Chee-Sanford, J.C., Sanford, R.A., et al. (2016) Detection and Diversity of Fungal Nitric Oxide Reductase Genes (p450nor) in Agricultural Soils. *Appl. Environ. Microbiol.* **82**: 2919–2928.

Hillmann, F., Linde, J., Beckmann, N., Cyrulies, M., Strassburger, M., Heinekamp, T., et al. (2014) The novel globin protein fungoglobin is involved in low oxygen adaptation of Aspergillus fumigatus. *Molecular Microbiology* **93**: 539–553.

Ho, A., Reim, A., Kim, S.Y., Meima-Franke, M., Termorshuizen, A., de Boer, W., et al. (2015) Unexpected stimulation of soil methane uptake as emergent property of agricultural soils following bio-based residue application. *Glob Change Biol* **21**: 3864–3879.

Hood-Nowotny, R., Umana, N.H.-N., Inselbacher, E., Oswald- Lachouani, P., and Wanek, W. (2010) Alternative Methods for Measuring Inorganic, Organic, and Total Dissolved Nitrogen in Soil. *Soil. Sci. Soc. Am. J.* **74**: 1018.

Howarth, R.W. (2008) Coastal nitrogen pollution: A review of sources and trends globally and regionally. *Harmful Algae* **8**: 14–20.

Humbert, S., Tarnawski, S., Fromin, N., Mallet, M.-P., Aragno, M., and Zopfi, J. (2009) Molecular detection of anammox bacteria in terrestrial ecosystems: distribution and diversity. *ISME J* **4**: 450–454.

Huse, S.M., Dethlefsen, L., Huber, J.A., Welch, D.M., Relman, D.A., and Sogin, M.L. (2008) Exploring Microbial Diversity and Taxonomy Using SSU rRNA Hypervariable Tag Sequencing. *PLoS Genet* **4**: e1000255–10.

Huson, D.H., Beier, S., Flade, I., Górska, A., El-Hadidi, M., Mitra, S., et al. (2016) MEGAN Community Edition - Interactive Exploration and Analysis of Large-Scale Microbiome Sequencing Data. *PLoS Comput. Biol.* **12**: e1004957.

Ingham, E.R. and Coleman, D.C. (1984) Effects of streptomycin, cycloheximide, Fungizone, captan, carbofuran, cygon, and PCNB on soil microorganisms. *Microb Ecol* **10**: 345–358.

Inselsbacher, E., Ripka, K., Klaubauf, S., Fedosoyenko, D., Hackl, E., Gorfer, M., et al. (2008) A cost-effective high-throughput microcosm system for studying nitrogen dynamics at the plant-microbe-soil interface. *Plant Soil* **317**: 293–307.

Jeffries, T.W., Grigoriev, I.V., Grimwood, J., Laplaza, J.M., Aerts, A., Salamov, A., et al. (2007) Genome sequence of the lignocellulose-bioconverting and xylose-fermenting yeast Pichia stipitis. *Nature Biotechnology* **25**: 319–326.

Jennings, D.H. (1987) Translocation of solutes in fungi. *Biological Reviews* **112**: 2046–2051.

Jirout, J., Šimek, M., and Elhottová, D. (2012) Fungal contribution to nitrous oxide emissions from cattle impacted soils. *Chemosphere* **90**: 565–572.

Joergensen, R.G. and Wichern, F. (2008) Quantitative assessment of the fungal contribution to microbial tissue in soil. *Soil Biology and Biochemistry* **40**: 2977–2991.

Johansen, K.S. (2016) Lytic Polysaccharide Monooxygenases: The Microbial Power Tool for Lignocellulose Degradation. *Trends in Plant Science* **21**: 926–936.

Johansson, J.F., Paul, L.R., and Finlay, R.D. (2004) Microbial interactions in the mycorrhizosphere and their significance for sustainable agriculture. *FEMS Microbiol Ecol* **48**: 1–13.

Jones, C.M., Graf, D.R.H., Bru, D., and Philippot, L. (2013) The unaccounted yet abundant nitrous oxide-reducing microbial community: a potential nitrous oxide sink. *ISME J* **7**: 417–426.

Jones, C.M., Spor, A., Brennan, F.P., Breuil, M.-C., Bru, D., Lemanceau, P., et al. (2014) Recently identified microbial guild mediates soil N2O sink capacity. *Nature Climate change* **4**: 801–805.

Kampschreur, M.J., Kleerebezem, R., de Vet, W.W.J.M., and van Loosdrecht, M.C.M. (2011) Reduced iron induced nitric oxide and nitrous oxide emission. *Water Research* **45**: 5945–5952.

Kandeler, E., Deiglmayr, K., Tscherko, D., Bru, D., and Philippot, L. (2006) Abundance of narG, nirS, nirK, and nosZ genes of denitrifying bacteria during primary successions of a glacier foreland. *Appl. Environ. Microbiol.* **72**: 5957–5962.

Kartal, B., Kuypers, M.M.M., Lavik, G., Schalk, J., Op den Camp, H.J.M., Jetten, M.S.M., and Strous, M. (2007) Anammox bacteria disguised as denitrifiers: nitrate reduction to dinitrogen gas via nitrite and ammonium. *Environmental Microbiology* **9**: 635–642.

Keegstra, K. (2010) Plant cell walls. *Plant Physiol.* **154**: 483–486.

Keil, D., Meyer, A., Berner, D., Poll, C., Schützenmeister, A., Piepho, H.-P., et al. (2011) Influence of land-use intensity on the spatial distribution of N-cycling microorganisms in grassland soils. *FEMS Microbiol Ecol* **77**: 95–106.

Kim, S.-W., Fushinobu, S., Zhou, S., Wakagi, T., and Shoun, H. (2009) Eukaryotic nirK Genes Encoding Copper-Containing Nitrite Reductase: Originating from the Protomitochondrion? *Appl. Environ. Microbiol.* **75**: 2652–2658.

Kim, S.-W., Fushinobu, S., Zhou, S., Wakagi, T., and Shoun, H. (2010) The possible involvement of copper-containing nitrite reductase (NirK) and flavohemoglobin in denitrification by the fungus Cylindrocarpon tonkinense. *Biosci Biotechnol Biochem* **74**: 1403–1407.

Kim, S.O., Orii, Y., Lloyd, D., Hughes, M.N., and Poole, R.K. (1999) Anoxic function for the Escherichia coli flavohaemoglobin (Hmp): reversible binding of nitric oxide and reduction to nitrous oxide. *FEBS Lett* **445**: 389–394.

Klotz, M.G. and Stein, L.Y. (2008) Nitrifier genomics and evolution of the nitrogen cycle. *FEMS Microbiol Lett* **278**: 146–156.

Kobayashi, M., Matsuo, Y., Takimoto, A., Suzuki, S., Maruo, F., and Shoun, H. (1996) Denitrification, a novel type of respiratory metabolism in fungal mitochondrion. *J. Biol. Chem.* **271**: 16263–16267.

Kohlmeier, S., Smits, T.H.M., Ford, R.M., Keel, C., Harms, H., and Wick, L.Y. (2005) Taking the Fungal Highway: Mobilization of Pollutant-Degrading Bacteria by Fungi. *Environ. Sci. Technol.* **39**: 4640–4646.

Kong, A.Y.Y., Scow, K.M., Córdova-Kreylos, A.L., Holmes, W.E., and Six, J. (2011) Microbial community composition and carbon cycling within soil microenvironments of conventional, low-input, and organic cropping systems. *Soil Biology and Biochemistry* **43**: 20–30.

Kracher, D., Scheiblbrandner, S., Felice, A.K.G., Breslmayr, E., Preims, M., Ludwicka, K., et al. (2016) Extracellular electron transfer systems fuel cellulose oxidative degradation. *Science* **352**: 1098–1101.

Kraft, B., Strous, M., and Tegetmeyer, H.E. (2011) Microbial nitrate respiration - Genes, enzymes and environmental distribution. *Journal of Biotechnology* **155**: 104–117.

Krapp, A. (2015) Plant nitrogen assimilation and its regulation: a complex puzzle with missing pieces. *Current Opinion in Plant Biology* **25**: 115–122.

Land, L., Badalucco, L., Pomare, F., and Nannipieri, P. (1993) Effectiveness of antibiotics to distinguish the contributions of fungi and bacteria to net nitrogen mineralization, nitrification and respiration. *Soil Biol. Biochem.* **25**: 1771–1778.

Lang, C., Seven, J., and Polle, A. (2010) Host preferences and differential contributions of deciduous tree species shape mycorrhizal species richness in a mixed Central European forest. *Mycorrhiza* **21**: 297–308.

Lary, D.J. (1997) Catalytic destruction of stratospheric ozone. *Journal of Gephysical Research* **102**: 21515–21526.

Laughlin, R.J., Rütting, T., Müller, C., Watson, C.J., and Stevens, R.J. (2009) Effect of acetate on soil respiration, N_2O emissions and gross N transformations related to fungi and bacteria in a grassland soil. *Applied Soil Ecology* **42**: 25–30.

Leger, R.S. and Cooper, R.M. (1986) Cuticle-degrading enzymes of entomopathogenic fungi: regulation of production of chitinolytic enzymes. *Microbiology* **132**: 1509–1517.

Lehmann, J. and Kleber, M. (2015) The contentious nature of soil organic matter. *Nature* **528**: 60–68.

Leigh, J., Fitter, A.H., and Hodge, A. (2011) Growth and symbiotic effectiveness of an arbuscular mycorrhizal fungus in organic matter in competition with soil bacteria. *FEMS Microbiol Ecol* **76**: 428–438.

Leininger, S., Urich, T., Schloter, M., Schwark, L., Qi, J., Nicol, G.W., et al. (2006) Archaea predominate among ammonia-oxidizing prokaryotes in soils. *Nature* **442**: 806–809.

Levasseur, A., Drula, E., Lombard, V., Coutinho, P.M., and Henrissat, B. (2013) Expansion of the enzymatic repertoire of the CAZy database to integrate auxiliary redox enzymes. *Biotechnology for Biofuels* **6**: 1–1.

Levičnik-Höfferle, Š., Nicol, G.W., Ausec, L., Mandić-Mulec, I., and Prosser, J.I. (2012) Stimulation of thaumarchaeal ammonia oxidation by ammonia derived from organic nitrogen but not added inorganic nitrogen. *FEMS Microbiol Ecol* **80**: 114–123.

Ley, R.E. and Schmidt, S.K. (2002) Fungal and bacterial responses to phenolic compounds and amino acids in high altitude barren soils. *Soil Biology and Biochemistry* **34**: 989–995.

Lê, S., Josse, J., and Husson, F. (2008) FactoMineR: an R package for multivariate analysis. *Journal of statistical software* **25**: 1–18.

Li, X., Sørensen, P., Olesen, J.E., and Petersen, S.O. (2016) Evidence for denitrification as main source of N2O emission from residue-amended soil. *Soil Biology and Biochemistry* **92**: 153–160.

Lim, H.-S., Kim, Y.-S., and Kim, S.-D. (1991) Pseudomonas stutzeri YPL-1 Genetic Transformation and Antifungal Mechanism against Fusarium solani, an Agent of Plant Root Rot. *Appl. Environ. Microbiol.* **57**: 510–516.

Lipson, D.A., Schadt, C.W., and Schmidt, S.K. (2002) Changes in Soil Microbial Community Structure and Function in an Alpine Dry Meadow Following Spring Snow Melt. *Microb Ecol* **43**: 307–314.

Liti, G., Carter, D.M., Moses, A.M., Warringer, J., Parts, L., James, S.A., et al. (2009) Population genomics of domestic and wild yeasts. *Nature* **458**: 337–341.

Liu, L., Zeng, M., Hausladen, A., Heitman, J., and Stamler, J.S. (2000) Protection from nitrosative stress by yeast flavohemoglobin. *Proc Natl Acad Sci U S A* **97**: 4672–4676.

Lombard, V., Golaconda Ramulu, H., Drula, E., Coutinho, P.M., and Henrissat, B. (2013) The carbohydrate-active enzymes database (CAZy) in 2013. *Nucleic Acids Research* **42**: D490–D495.

Long, A., Song, B., Fridey, K., and Silva, A. (2015) Detection and diversity of copper containing nitrite reductase genes (nirK) in prokaryotic and fungal communities of agricultural soils. *FEMS Microbiol Ecol* **91**: 1–9.

Loque, D. and Wiren, von, N. (2004) Regulatory levels for the transport of ammonium in plant roots. *J. Exp. Bot.* **55**: 1293–1305.

MacArthur, P.H., Shiva, S., and Gladwin, M.T. (2007) Measurement of circulating nitrite and S-nitrosothiols by reductive chemiluminescence. *Journal of Chromatography B* **851**: 93–105.

Maeda, K., Spor, A., Edel-Hermann, V., Heraud, C., Breuil, M.-C., Bizouard, F., et al. (2015) N2O production, a widespread trait in fungi. *Sci. Rep.* **5**: 9697–7.

Mahne, I. and Tiedje, J.M. (1995) Criteria and methodology for identifying respiratory denitrifiers. *Appl. Environ. Microbiol.* **61**: 1110–1115.

Marti, E., Jofre, J., and Balcazar, J.L. (2013) Prevalence of Antibiotic Resistance Genes and Bacterial Community Composition in a River Influenced by a Wastewater Treatment Plant. *PLoS ONE* **8**: e78906–8.

Marusenko, Y., Huber, D.P., and Hall, S.J. (2013) Fungi mediate nitrous oxide production but not ammonia oxidation in aridland soils of the southwestern US. *Soil Biology and Biochemistry* **63**: 24–36.

Marzluf, G.A. (1997) Genetic regulation of nitrogen metabolism in the fungi. *Microbiol. Mol. Biol. Rev.* **61**: 17–32.

Masella, A.P., Bartram, A.K., Truszkowski, J.M., Brown, D.G., and Neufeld, J.D. (2012) PANDAseq: PAired-eND Assembler for Illumina sequences. *BMC Bioinformatics* **13**: 31.

McSwiney, C.P. and Robertson, G.P. (2005) Nonlinear response of N2O flux to incremental fertilizer addition in a continuous maize (Zea mays L.) cropping system. *Glob Change Biol* **11**: 1712–1719.

Megonigal, J.P., Hines, M.E., and Visscher, P.T. (2003) Anaerobic Metabolism: Linkages to Trace Gases and Aerobic Processes. In, *Treatise on Geochemistry*. Elsevier, pp. 317–424.

Mohan, S.B. and Cole, J.A. (2007) The dissimilatory reduction of nitrate to ammonia by anaerobic bacteria. In, *Biology of the Nitrogen Cycle*.

Molstad, L., Dörsch, P., and Bakken, L.R. (2007) Robotized incubation system for monitoring gases (O_2, NO, N_2O N_2) in denitrifying cultures. *Journal of Microbiological Methods* **71**: 202–211.

Moni, C., Derrien, D., Hatton, P.J., Zeller, B., and Kleber, M. (2012) Density fractions versus size separates: does physical fractionation isolate functional soil compartments? *Biogeosciences* **9**: 5181–5197.

Monrozier, L.J., Ladd, J.N., Fitzpatrick, R.W., Foster, R.C., and Rapauch, M. (1990) Components and microbial biomass content of size fractions in soils of contrasting aggregation. *Geoderma* **50**: 37–62.

Mosier, A.R., Duxbury, J.M., Freney, J.R., Heinemeyer, O., and Minami, K. (1998) Assessing and Mitigating N2O Emissions from Agricultural Soils. *Climatic Change* **40**: 7–38.

Mothapo, N., Chen, H., Cubeta, M.A., Grossman, J.M., Fuller, F., and Shi, W. (2015) Phylogenetic, taxonomic and functional diversity of fungal denitrifiers and associated N_2O production efficacy. *Soil Biology and Biochemistry* **83**: 160–175.

Mothapo, N.V., Chen, H., Cubeta, M.A., and Shi, W. (2013) Nitrous oxide producing activity of diverse fungi from distinct agroecosystems. *Soil Biology and Biochemistry* **66**: 94–101.

Mouginot, C., Kawamura, R., Matulich, K.L., Berlemont, R., Allison, S.D., Amend, A.S., and Martiny, A.C. (2014) Elemental stoichiometry of Fungi and Bacteria strains from grassland leaf litter. *Soil Biology and Biochemistry* **76**: 278–285.

Mummey, D., Holben, W., Six, J., and Stahl, P. (2006) Spatial Stratification of Soil Bacterial Populations in Aggregates of Diverse Soils. *Microb Ecol* **51**: 404–411.

Müller, C., Laughlin, R.J., Spott, O., and Rütting, T. (2014) Quantification of N2O emission pathways via a 15N tracing model. *Soil Biology and Biochemistry* **72**: 44–54.

Nakano, M.M. (2006) Essential Role of Flavohemoglobin in Long-Term Anaerobic Survival of Bacillus subtilis. *J Bacteriol* **188**: 6415–6418.

Navel, A. and Martins, J.M.F. (2014) Effect of long term organic amendments and vegetation of vineyard soils on the microscale distribution and biogeochemistry of copper. *Sci. Total Environ.* **466-467**: 681–689.

Nazir, R., Warmink, J.A., Boersma, H., and van Elsas, J.D. (2010) Mechanisms that promote bacterial fitness in fungal-affected soil microhabitats. *FEMS Microbiol Ecol* **71**: 169–185.

Nelson, D.W. and Bremner, J.M. (1969) Factors affecting chemical transformations of nitrite in soils. *Soil Biology and Biochemistry* **1**: 229–239.

Nelson, D.W. and Bremner, J.M. (1970a) Gaseous products of nitrite decomposition in soils. *Soil Biology and Biochemistry* **2**: 203–215.

Nelson, D.W. and Bremner, J.M. (1970b) Role of soil minerals and metallic cations in nitrite decomposition and chemodenitrification in soils. *Soil Biology and Biochemistry* **2**: 1–8.

Neumann, D., Heuer, A., Hemkemeyer, M., Martens, R., and Tebbe, C.C. (2013) Response of microbial communities to long-term fertilization depends on their microhabitat. *FEMS Microbiol Ecol* **86**: 71–84.

Németh, D.D., Wagner-Riddle, C., and Dunfield, K.E. (2014) Abundance and gene expression in nitrifier and denitrifier communities associated with a field scale spring thaw N2O flux event. *Soil Biology and Biochemistry* **73**: 1–9.

Nicol, G.W., Leininger, S., Schleper, C., and Prosser, J.I. (2008) The influence of soil pH on the diversity, abundance and transcriptional activity of ammonia oxidizing archaea and bacteria. *Environmental Microbiology* **10**: 2966–2978.

Nielsen, U.N., Ayres, E., and Wall, D.H. (2011) Soil biodiversity and carbon cycling: a review and synthesis of studies examining diversity–function relationships. *European Journal of Soil Science* **62**: 105–116.

Nittler, M.P., Hocking-Murray, D., Foo, C.K., and Sil, A. (2005) Identification of Histoplasma capsulatum transcripts induced in response to reactive nitrogen species. *Mol. Biol. Cell* **16**: 4792–4813.

Northcote, D.H. (1972) Chemistry of the plant cell wall. *Annual review of plant physiology* **23**: 113–132.

O'Brien, J.A., Vega, A., Bouguyon, E., Krouk, G., Gojon, A., Coruzzi, G., and Gutiérrez, R.A. (2016) Nitrate Transport, Sensing, and Responses in Plants. *Molecular Plant* **9**: 837–856.

Oades, J.M. (1984) Soil organic matter and structural stability: mechanisms and implications for management. *Plant Soil* **76**: 319–337.

Oades, J.M. and Waters, A.G. (1991) Aggregate hierarchy in soils. *Soil Res.* **29**: 815–828.

Ohm, R.A., Riley, R., Salamov, A., Min, B., Choi, I.-G., and Grigoriev, I.V. (2014) Genomics of wood-degrading fungi. *Fungal Genetics and Biology* **72**: 82–90.

Ottow, J.C. and Klopotek, Von, A. (1969) Enzymatic reduction of iron oxide by fungi. *Appl Microbiol* **18**: 41–43.

Park, S., Croteau, P., Boering, K.A., Etheridge, D.M., Ferretti, D., Fraser, P.J., et al. (2012) Trends and seasonal cycles in the isotopic composition of nitrous oxide since 1940. *Nature Geoscience* **5**: 261–265.

Pawłowska, J., Aleksandrzak-Piekarczyk, T., Banach, A., Kiersztyn, B., Muszewska, A., Serewa, L., et al. (2016) Preliminary studies on the evolution of carbon assimilation abilities within Mucorales. *Fungal Biology* **120**: 752–763.

Payne, C.M., Knott, B.C., Mayes, H.B., Hansson, H., Himmel, M.E., Sandgren, M., et al. (2015) Fungal Cellulases. *Chem. Rev.* **115**: 1308–1448.

Peinemann, N., Amiotti, N.M., and Zalba, P. (2000) Effect of clay minerals and organic matter on the cation exchange capacity of silt fractions. *J. Plant Nutr. Soil Sci.* **163**: 47–52.

Pennanen, T., Fritze, H., Vanhala, P., Kiikkila, O., Neuvonen, S., and Bååth, E. (1998) Structure of a microbial community in soil after prolonged addition of low levels of simulated acid rain. *Appl. Environ. Microbiol.* **64**: 2173–2180.

Penton, C.R., Devol, A.H., and Tiedje, J.M. (2006) Molecular Evidence for the Broad Distribution of Anaerobic Ammonium-Oxidizing Bacteria in Freshwater and Marine Sediments. *Appl. Environ. Microbiol.* **72**: 6829–6832.

Philippot, L. (2002) Denitrifying genes in bacterial and Archaeal genomes. *Biochim Biophys Acta* **1577**: 355–376.

Pietikäinen, J., Pettersson, M., and Bååth, E. (2005) Comparison of temperature effects on soil respiration and bacterial and fungal growth rates. *FEMS Microbiol Ecol* **52**: 49–58.

Pihlatie, M., Syväsalo, E., Simojoki, A., Esala, M., and Regina, K. (2004) Contribution of nitrification and denitrification to N_2O production in peat, clay and loamy sand soils under different soil moisture conditions. *Nutr Cycl Agroecosyst* **70**: 135–141.

Pilegaard, K. (2013) Processes regulating nitric oxide emissions from soils. *Phil. Trans. R. Soc. B* **368**: 20130126.

Portmann, R.W., Daniel, J.S., and Ravishankara, A.R. (2012) Stratospheric ozone depletion due to nitrous oxide: influences of other gases. *Phil. Trans. R. Soc. B* **367**: 1256–1264.

Prather, M.J., Hsu, J., and DeLuca, N.M. (2015) Measuring and modeling the lifetime of nitrous oxide including its variability. *Journal of Geophysical Research: Atmospheres (1984–2012)* **120**: 5693–5705.

Pulford, I.D. (2007) The Chemistry of the Solid Earth. In, Harrison,R.M. (ed), *Principles of Environmental Chemistry*. Royal Society of Chemistry, Cambridge, pp. 234–278.

Quast, C., Pruesse, E., Yilmaz, P., Gerken, J., Schweer, T., Yarza, P., et al. (2013) The SILVA ribosomal RNA gene database project: improved data processing and web-based tools. *Nucleic Acids Research* **41**: D590–6.

R Core Team (2015) R: A language and environment for statistical computing. R Foundation for Statistical Computing, Vienna, Austria. Version 3.1. 1 Available at www. R-project. org.

Rajapaksha, R.M.C.P., Tobor-Kaplon, M.A., and Bååth, E. (2004) Metal Toxicity Affects Fungal and Bacterial Activities in Soil Differently. *Appl. Environ. Microbiol.* **70**: 2966–2973.

Ranjard, L., Brothier, E., and Nazaret, S. (2000) Sequencing bands of ribosomal intergenic spacer analysis fingerprints for characterization and microscale distribution of soil bacterium populations responding to mercury spiking. *Appl. Environ. Microbiol.* **66**: 5334–5339.

Rasul, G., Appuhn, A., Müller, T., and Joergensen, R.G. (2006) Salinity-induced changes in the microbial use of sugarcane filter cake added to soil. *Applied Soil Ecology* **31**: 1–10.

Ravishankara, A.R., Daniel, J.S., and Portmann, R.W. (2009) Nitrous oxide (N2O): the dominant ozone-depleting substance emitted in the 21st century. *Science* **326**: 123–125.

Rennenberg, H., Dannenmann, M., Gessler, A., Kreuzwieser, J., Simon, J., and Papen, H. (2009) Nitrogen balance in forest soils: nutritional limitation of plants under climate change stresses. *Plant Biology* **11**: 4–23.

Richardson, M. (2009a) The ecology of the Zygomycetes and its impact on environmental exposure. *Clinical Microbiology and Infection* **15**: 2–9.

Richardson, M. (2009b) The ecology of the Zygomycetes and its impact on environmental exposure. *Clinical Microbiology and Infection* **15**: 2–9.

Rileya, R., Salamova, A.A., and Brownb, D.W. (2014) Extensive sampling of basidiomycete genomes demonstrates inadequacy of the white-rot/brown-rot paradigm for wood decay fungi. *Proceedings of the National Academy of Sciences* **111**: 9923–9928.

Roesch, L.F.W., Fulthorpe, R.R., Riva, A., Casella, G., Hadwin, A.K.M., Kent, A.D., et al. (2007) Pyrosequencing enumerates and contrasts soil microbial diversity. *ISME J* **1**: 283–290.

Rousk, J. and Bååth, E. (2007) Fungal and bacterial growth in soil with plant materials of different C/N ratios. *FEMS Microbiol Ecol* **62**: 258–267.

Rousk, J., Demoling, L.A., and Bååth, E. (2008) Contrasting Short-Term Antibiotic Effects on Respiration and Bacterial Growth Compromises the Validity of the Selective Respiratory Inhibition Technique to Distinguish Fungi and Bacteria. *Microb Ecol* **58**: 75–85.

Rousk, J., Demoling, L.A., Bahr, A., and Bååth, E. (2008) Examining the fungal and bacterial niche overlap using selective inhibitors in soil. *FEMS Microbiol Ecol* **63**: 350–358.

Saggar, S., Jha, N., Deslippe, J., Bolan, N.S., Luo, J., Giltrap, D.L., et al. (2013) Denitrification and N2O:N2 production in temperate grasslands: Processes, measurements, modelling and mitigating negative impacts. *Science of the Total Environment* **465**: 173–195.

Sanford, R.A., Wagner, D.D., Wu, Q., Chee-Sanford, J.C., Thomas, S.H., Cruz-García, C., et al. (2012) Unexpected nondenitrifier nitrous oxide reductase gene diversity and abundance in soils. *Proc Natl Acad Sci U S A* **109**: 19709–19714.

Sardinha, M., Müller, T., Schmeisky, H., and Joergensen, R.G. (2003) Microbial performance in soils along a salinity gradient under acidic conditions. *Applied Soil Ecology* **23**: 237–244.

Schadt, C.W., Martin, A.P., Lipson, D.A., and Schmidt, S.K. (2003) Seasonal dynamics of previously unknown fungal lineages in tundra soils. *Science* **301**: 1359–1361.

Schimel, J.P. and Schaeffer, S.M. (2012) Microbial control over carbon cycling in soil. *Front Microbiol* **3**: 348.

Schmidt, S.K., Naff, C.S., and Lynch, R.C. (2012) Fungal communities at the edge: Ecological lessons from high alpine fungi. *Fungal Ecology* **5**: 443–452.

Schmieder, R. and Edwards, R. (2011) Quality control and preprocessing of metagenomic datasets. *Bioinformatics* **27**: 863–864.

Seo, D.C. and DeLaune, R.D. (2010) Fungal and bacterial mediated denitrification in wetlands: Influence of sediment redox condition. *Water Research* **44**: 2441–2450.

Sexstone, A.J. and Revsbech, N.P. (1985) Direct measurement of oxygen profiles and denitrification rates in soil aggregates. *Soil. Sci. Soc. Am. J.* **49**: 549–559.

Shcherbak, I., Millar, N., and Robertson, G.P. (2014a) Global metaanalysis of the nonlinear response of soil nitrous oxide (N_2O) emissions to fertilizer nitrogen. *Proceedings of the National Academy of Sciences* **111**: 9199–9204.

Shcherbak, I., Millar, N., and Robertson, G.P. (2014b) Global metaanalysis of the nonlinear response of soil nitrous oxide (N2O) emissions to fertilizer nitrogen. *Proc Natl Acad Sci U S A* **111**: 9199–9204.

Shoun, H. and Tanimoto, T. (1991) Denitrification by the fungus Fusarium oxysporum and involvement of cytochrome P-450 in the respiratory nitrite reduction. *J. Biol. Chem.* **266**: 11078–11082.

Shoun, H., Fushinobu, S., Jiang, L., Kim, S.W., and Wakagi, T. (2012) Fungal denitrification and nitric oxide reductase cytochrome P450nor. *Phil. Trans. R. Soc. B* **367**: 1186–1194.

Simon, J. (2002) Enzymology and bioenergetics of respiratory nitrite ammonification. *FEMS Microbiology Reviews* **26**: 285–309.

Simon, J., Sänger, M., Schuster, S.C., and Gross, R. (2003) Electron transport to periplasmic nitrate reductase (NapA) of Wolinella succinogenes is independent of a NapC protein. *Molecular Microbiology* **49**: 69–79.

Simon, J., van Spanning, R.J.M., and Richardson, D.J. (2008) The organisation of proton motive and non-proton motive redox loops in prokaryotic respiratory systems. *Biochim Biophys Acta* **1777**: 1480–1490.

Six, J. and Paustian, K. (2014) Aggregate-associated soil organic matter as an ecosystem property and a measurement tool. *Soil Biology and Biochemistry* **68**: A4–A9.

Six, J., Bossuyt, H., Degryze, S., and Denef, K. (2004) A history of research on the link between (micro)aggregates, soil biota, and soil organic matter dynamics. *Soil & Tillage Research* **79**: 7–31.

Six, J., Elliott, E.T., and Paustian, K. (2000) Soil macroaggregate turnover and microaggregate formation: a mechanism for C sequestration under no-tillage agriculture. *Soil Biology and Biochemistry* **32**: 2099–2103.

Slot, J.C. and Hibbett, D.S. (2007) Horizontal Transfer of a Nitrate Assimilation Gene Cluster and Ecological Transitions in Fungi: A Phylogenetic Study. *PLoS ONE* **2**: e1097–8.

Smith, K.A. and Conen, F. (2004) Impacts of land management on fluxes of trace greenhouse gases. *Soil Use and Management* **20**: 255–263.

Snider, D.M., Venkiteswaran, J.J., Schiff, S.L., and Spoelstra, J. (2015) From the Ground Up: Global Nitrous Oxide Sources are Constrained by Stable Isotope Values. *PLoS ONE* **10**: e0118954.

Sogin, M.L., Morrison, H.G., Huber, J.A., Welch, D.M., Huse, S.M., Neal, P.R., et al. (2006) Microbial diversity in the deep sea and the underexplored "rare biosphere". *Proc Natl Acad Sci U S A* **103**: 12115–12120.

Stocker, T.F., Qin, D., Plattner, G.K., Tignor, M., and Allen, S.K. (2013) IPCC, 2013: Climat Change 2013: The Physical Science Basis. Contribution of Working Group I to the fifth assessment report of the Intergovernmental Panel on Climate Change IPCC Localised.

Stockmann, U., Adams, M.A., Crawford, J.W., Field, D.J., Henakaarchchi, N., Jenkins, M., et al. (2013) The knowns, known unknowns and unknowns of sequestration of soil organic carbon. *"Agriculture, Ecosystems and Environment"* **164**: 80–99.

Stremińska, M.A., Felgate, H., Rowley, G., Richardson, D.J., and Baggs, E.M. (2011) Nitrous oxide production in soil isolates of nitrate-ammonifying bacteria. *Environmental Microbiology Reports* **4**: 66–71.

Strickland, M.S. and Rousk, J. (2010) Considering fungal: bacterial dominance in soils–methods, controls, and ecosystem implications. *Soil Biology and Biochemistry* **42**: 1385–1395.

Strous, M., Fuerst, J.A., Kramer, E., and Logemann, S. (1999) Missing lithotroph identified as new planctomycete. *Nature* **400**: 446–449.

Suharti and de Vries, S. (2005) Membrane-bound denitrification in the Gram-positive bacterium Bacillus azotoformans. *Biochm. Soc. Trans.* **33**: 130–133.

Susyan, E.A., Ananyeva, N.D., and Blagodatskaya, E.V. (2005) The Antibiotic-Aided Distinguishing of Fungal and Bacterial Substrate-Induced Respiration in Various Soil Ecosystems. *Microbiology* **74**: 336–342.

Takaya, N. (2002) Dissimilatory nitrate reduction metabolisms and their control in fungi. *Journal of Bioscience and Bioengineering* **94**: 506–510.

Tavares, P., Pereira, A.S., Moura, J.J.G., and Moura, I. (2006) Metalloenzymes of the denitrification pathway. *J. Inorg. Biochem.* **100**: 2087–2100.

Tejero, J. and Gladwin, M.T. (2014) The globin superfamily: functions in nitric oxide formation and decay. *Biological Chemistry* **395**: 1–10.

Thomas, D.D., Ridnour, L.A., Isenberg, J.S., Flores-Santana, W., Switzer, C.H., Donzelli, S., et al. (2008) The chemical biology of nitric oxide: Implications in cellular signaling. *Free Radical Biology and Medicine* **45**: 18–31.

Thornton, P.E., Lamarque, J.-F., Rosenbloom, N.A., and Mahowald, N.M. (2007) Influence of carbon-nitrogen cycle coupling on land model response to CO_2 fertilization and climate variability. *Global Biogeochemical Cycles* **21**: 1–15.

Tillmann, A., Gow, N.A.R., and Brown, A.J.P. (2011) Nitric oxide and nitrosative stress tolerance in yeast. *Biochm. Soc. Trans.* **39**: 219–223.

Tilman, D. (1999) Global environmental impacts of agricultural expansion: the need for sustainable and efficient practices. *Proc Natl Acad Sci U S A* **96**: 5995–6000.

Tisdall, J.M. (1994) Possible role of soil microorganisms in aggregation in soils. *Plant Soil* **4**: 85–98.

Tisdall, J.M. and Oades, J.M. (1982) Organic matter and water-stable aggregates in soils. *European Journal of Soil Science* **33**: 141–163.

Tisserant, E., Malbreil, M., Kuo, A., Kohler, A., Symeonidi, A., Balestrini, R., et al. (2013) Genome of an arbuscular mycorrhizal fungus provides insight into the oldest plant symbiosis. *Proc Natl Acad Sci U S A* **110**: 20117–20122.

Toljander, J.F., Artursson, V., Paul, L.R., Jansson, J.K., and Finlay, R.D. (2006) Attachment of different soil bacteria to arbuscular mycorrhizal fungal extraradical hyphae is determined by hyphal vitality and fungal species. *FEMS Microbiol Lett* **254**: 34–40.

Tolonen, A.C., Cerisy, T., El-Sayyed, H., Boutard, M., Salanoubat, M., and Church, G.M. (2014) Fungal lysis by a soil bacterium fermenting cellulose. *Environmental Microbiology* **17**: 2618–2627.

Turpault, M.P., Bonnaud, P., Fighter, J., Ranger, J., and Dambrine, E. (1996) Distribution of cation exchange capacity between organic matter and mineral fractions in acid forest soils (Vosges mountains, France). *European Journal of Soil Science* **47**: 545–556.

Ullmann, B.D., Myers, H., Chiranand, W., Lazzell, A.L., Zhao, Q., Vega, L.A., et al. (2004) Inducible defense mechanism against nitric oxide in Candida albicans. *Eukaryotic Cell* **3**: 715–723.

Vajrala, N., Bottomley, P.J., Stahl, D.A., Arp, D.J., and Sayavedra-Soto, L.A. (2014) Cycloheximide prevents the de novopolypeptide synthesis required to recover from acetylene inhibition in Nitrosopumilus maritimus. *FEMS Microbiol Ecol* **88**: 495–502.

Vallee, B.L. and Williams, R.J. (1968) Metalloenzymes: the entatic nature of their active sites. *Proc Natl Acad Sci U S A* **59**: 498–505.

Van Cleemput, O. and Samater, A.H. (1995) Nitrite in soils: accumulation and role in the formation of gaseous N compounds. *Fertilizer Research* **45**: 81–89.

Van den Brink, J. and de Vries, R.P. (2011a) Fungal enzyme sets for plant polysaccharide degradation. *Appl Microbiol Biotechnol* **91**: 1477–1492.

Van den Brink, J. and de Vries, R.P. (2011b) Fungal enzyme sets for plant polysaccharide degradation. *Appl Microbiol Biotechnol* **91**: 1477–1492.

Van der Heijden, M.G., de Bruin, S., Luckerhoff, L., van Logtestijn, R.S., and Schlaeppi, K. (2015) A widespread plant-fungal-bacterial symbiosis promotes plant biodiversity, plant nutrition and seedling recruitment. *ISME J* **10**: 389–399.

Van der Heijden, M.G.A., Martin, F.M., Selosse, M.-A., and Sanders, I.R. (2015) Mycorrhizal ecology and evolution: the past, the present, and the future. *New Phytologist* **205**: 1406–1423.

Van Dorst, J., Bissett, A., Palmer, A.S., Brown, M., Snape, I., Stark, J.S., et al. (2014) Community fingerprinting in a sequencing world. *FEMS Microbiol Ecol* **89**: 316–330.

Van Spanning, R.J.M., Richardson, D.J., and Ferguson, S.J. (2007) Introduction to the Biochemistry and Molecular Biology of Denitrification. In, *Biology of the Nitrogen Cycle*, Biology of the Nitrogen Cycle. Elsevier, Amsterdam, pp. 3–20.

Velvis, H. (1997) Evaluation of the selective respiratory inhibition method for measuring the ratio of fungal:bacterial activity in acid agricultural soils. *Biol Fertil Soils* **25**: 354–360.

Verhamme, D.T., Prosser, J.I., and Nicol, G.W. (2011) Ammonia concentration determines differential growth of ammonia-oxidising archaea and bacteria in soil microcosms. *ISME J* **5**: 1067–1071.

Voloshin, R.A. and Rodionova, M.V. (2016) Review: Biofuel production from plant and algal biomass. *International Journal of Hydrogen Energy* **41**: 17257–17273.

Vos, M. and Velicer, G.J. (2006) Genetic population structure of the soil bacterium Myxococcus xanthus at the centimeter scale. *Appl. Environ. Microbiol.* **72**: 3615–3625.

Vos, M., Wolf, A.B., Jennings, S.J., and Kowalchuk, G.A. (2013) Micro-scale determinants of bacterial diversity in soil. *FEMS Microbiology Reviews* **37**: 936–954.

Wagg, C., Bender, S.F., Widmer, F., and van der Heijden, M.G.A. (2014) Soil biodiversity and soil community composition determine ecosystem multifunctionality. *Proceedings of the National Academy of Sciences* **111**: 5266–5270.

Waldron, K.J. and Robinson, N.J. (2009) How do bacterial cells ensure that metalloproteins get the correct metal? *Nature Reviews Microbiology* **7**: 25–35.

Walther, G., Garnica, S., and Weiss, M. (2005) The systematic relevance of conidiogenesis modes in the gilled Agaricales. *Mycological Research* **109**: 525–544.

Wardle, D.A. (2006) The influence of biotic interactions on soil biodiversity. *Ecol Lett* **9**: 870–886.

Warmink, J.A. and van Elsas, J.D. (2008) Selection of bacterial populations in the mycosphere of Laccaria proxima: is type III secretion involved? *ISME J* **2**: 887–900.

Warmink, J.A., Nazir, R., and Van Elsas, J.D. (2009) Universal and species-specific bacterial “fungiphiles” in the mycospheres of different basidiomycetous fungi. *Environmental Microbiology* **11**: 300–312.

Watanabe, K., Kodama, Y., and Harayama, S. (2001) Design and evaluation of PCR primers to amplify bacterial 16S ribosomal DNA fragments used for community fingerprinting. *Journal of Microbiological Methods* **44**: 253–262.

Watsuji, T.-O., Takaya, N., Nakamura, A., and Shoun, H. (2003) Denitrification of nitrate by the fungus Cylindrocarpon tonkinense. *Biosci Biotechnol Biochem* **67**: 1115–1120.

Webster, F.A. and Hopkins, D.W. (1996) Contributions from different microbial processes to N2O emission from soil under different moisture regimes. *Biol Fertil Soils* **22**: 331–335.

Wei, W., Isobe, K., Shiratori, Y., Nishizawa, T., Ohte, N., Ise, Y., et al. (2015) Development of PCR primers targeting fungal nirK to study fungal denitrification in the environment. *Soil Biology and Biochemistry* **81**: 282–286.

Wei, W., Isobe, K., Shiratori, Y., Nishizawa, T., Ohte, N., Otsuka, S., and Senoo, K. (2014) N2O emission from cropland field soil through fungal denitrification after surface applications of organic fertilizer. *Soil Biology and Biochemistry* **69**: 157–167.

Wessén, E., Söderström, M., Stenberg, M., Bru, D., Hellman, M., Welsh, A., et al. (2011) Spatial distribution of ammonia-oxidizing bacteria and archaea across a 44-hectare farm related to ecosystem functioning. *The ISME Journal* **5**: 1213–1225.

Willför, S., Pranovich, A., Tamminen, T., Puls, J., Laine, C., Suurnäkki, A., et al. (2009) Carbohydrate analysis of plant materials with uronic acid-containing polysaccharides–A comparison between different hydrolysis and subsequent chromatographic analytical techniques. *Industrial Crops and Products* **29**: 571–580.

Wrage, N., Velthof, G.L., and Van Beusichem, M.L. (2001) Role of nitrifier denitrification in the production of nitrous oxide. *Soil Biology and Biochemistry* **33**: 1723–1732.

Zehr, J.P., Jenkins, B.D., Short, S.M., and Steward, G.F. (2003) Nitrogenase gene diversity and microbial community structure: a cross-system comparison. *Environmental Microbiology* **5**: 539–554.

Zelitch, I. (1975) Pathways of carbon fixation in green plants. *Annu. Rev. Biochem.* **44**: 123–145.

Zhou, Shengmin, Fushinobu, S., Nakanishi, Y., Kim, S.-W., Wakagi, T., and Shoun, H. (2009) Cloning and characterization of two flavohemoglobins from Aspergillus oryzae. *Biochemical and Biophysical Research Communications* **381**: 7–11.

Zhou, Zhemin, Takaya, N., Sakairi, M.A.C., and Shoun, H. (2001) Oxygen requirement for denitrification by the fungus Fusarium oxysporum. *Archives of Microbiology* **175**: 19–25.

Zhou, Zhifeng, Shi, X., Zheng, Y., Qin, Z., Xie, D., Li, Z., and Guo, T. (2014) European Journal of Soil Biology. *European Journal of Soil Biology* **60**: 24–33.

Zhu-Barker, X., Doane, T.A., and Horwath, W.R. (2015) Role of green waste compost in the production of N2O from agricultural soils. *Soil Biology and Biochemistry* **83**: 57–65.

Zumft, W.G. (1997) Cell biology and molecular basis of denitrification. *Microbiol. Mol. Biol. Rev.* **61**: 533–616.

Zumft, W.G. and Kroneck, P.M.H. (2007) Respiratory transformation of nitrous oxide (N_2O) to dinitrogen by Bacteria and Archaea. *Adv Microb Physiol* **52**: 107–227.